

Lack of knowledge on ecological determinants and cryptic lifestyles hinder our understanding of *Terfezia* diversity

Celeste Santos-Silva¹, Rogério Louro¹, Bruno Natário¹, Tânia Nobre²

1 *Biology Department, Macromycology Laboratory, MED - Mediterranean Institute for Agriculture, Environment and Development, University of Évora, Évora, Portugal* **2** *MED–Mediterranean Institute for Agriculture, Environment and Development, University of Évora, 7000-083 Évora, Portugal*

Corresponding author: Celeste Santos-Silva (css@uevora.pt)

Academic editor: F. D. Grande | Received 10 July 2021 | Accepted 15 September 2021 | Published 18 October 2021

Citation: Santos-Silva C, Louro R, Natário B, Nobre T (2021) Lack of knowledge on ecological determinants and cryptic lifestyles hinder our understanding of *Terfezia* diversity. MycoKeys 84: 1–14. <https://doi.org/10.3897/mycokeys.84.71372>

Abstract

Developing below the soil surface desert, truffles are hard to find. Within *Terfezia* genus, at least 18 species are described and many are endemic to the Mediterranean basin. Ecological and geographic information are key factors for species diagnosis, and so far *Terfezia* species are believed to be linked to either acidic or basic soils or to specific plant hosts. Thus, we have looked at *Terfezia* diversity within a relatively homogeneous geographical area in Portugal that is suitable for these species and that covered different soils and different dominant host species. We analyzed the observed intraspecific variability within the context of species ecological preferences (e. g. edaphic and putative host). One of our major findings was the discovery of *T. grisea* in acid soils in association with *Tuberaria guttata*, a puzzling information since, until now, this species was only found in alkaline soils. We also report on the linkage of different *Terfezia* lineages within species and ecologic parameters such as soil texture, soil pH and plant host. Additionally, by placing the collected specimens on the most recent genus phylogeny based on the ITS region, we also updated the number of known *Terfezia* species occurring in Portugal from three to ten. *Terfezia dunensis* is here reported for the first time for Portugal. Overall, our results show that the exploration of undersampled sites reveals itself as a good strategy to disclose unknown aspects of desert truffle diversity and ecology. These aspects are of prime importance when considering the economic value of the desert truffles for rural populations in the Mediterranean basin.

Keywords

Desert truffles, host plants, phylogeny, soil properties, taxonomy

Introduction

Desert truffles produce macroscopic fruitbodies partially or completely embedded in soil. These hypogeous *Ascomycota* encompass several genera within the *Pezizaceae* family. *Terfezia* Tul. & Tul. is the most diverse genera of desert truffle with 18 species described, typically found in arid and semi-arid areas throughout the world (Morte et al. 2009; Navarro-Ródenas et al. 2011; Moreno et al. 2014; Louro et al. 2019). Many of the *Terfezia* spp. are endemic to the Mediterranean basin and they play an essential role in soil conservation – preventing erosion and desertification – of Mediterranean shrublands and xerophytic grasslands (Honrubia et al. 1992).

The interest in understanding diversity and the molecular phylogeny of fungi, in particular of desert truffles, has increased in recent years following up from the increasing importance of biotechnology and plant nutrition. In addition, and for *Terfezia*, the interest is even higher as the demand for ascocarp availability/production increased. *Terfezia* products are continuously gaining in relevance as exquisite components of the Mediterranean diet.

Early attempts at *Terfezia* classification relied on morphological characteristics, such as spore and peridium morphology, gleba colour, and chemical features (Bordallo and Rodriguez 2014). Yet, these features alone showed to be problematic to distinguish species. In many hypogeous genera, *Terfezia* included, the evolution for mycophagy and reduction of water loss translated in convergent morphological characteristics and homoplasy (Thiers 1984; Bruns et al. 1989; Diez et al. 2002). The result was an array of species names in which many were synonyms of previously described ones (Alsheikh 1994) and others were lacking useful diagnostic features or were rarely cited after the first time (Zitouni-Haouar et al. 2018). With advances in molecular technology scientists have re-examined herbarium specimens and personal collections of *Terfezia* around the world for their sequences of the Internal transcribed spacer (ITS), the primary fungal barcode. These efforts have revealed inaccurate generic assignments, misidentifications at the genus and species level and, overall, were able to remove ambiguity around several taxonomic statuses involving this genus (Zitouni-Haouar et al. 2018; Louro et al. 2019). This given clarity was not without its inherent difficulties.

The first step in linking diversity to its geographic and ecological determinants is to know the diversity that we are dealing with. Considered as separated species in pre-molecular era, *Terfezia leptoderma* (Tul. & C. Tul.) Tul. & C. Tul. and *T. fanfani* Mat. tir. are now regarded as one taxa (*T. fanfani*) since phylogenetic studies show a clear nesting of these species sequences in a well-supported monophyletic group (Bordallo et al. 2013, 2015; Louro et al. 2019). Furthermore, *T. leptoderma* and *Terfezia olbiensis* (Tul. & C. Tul.) Sacc. were by some authors regarded as the same species, being that *T. olbiensis* was considered an immature stage of *T. leptoderma* (Moreno et al. 1986; Diez et al. 2002; Bordallo et al. 2013). Recent studies, however, propose *T. olbiensis* as a unique taxa and absolved *T. leptoderma* from the previously assigned sequences (Montecchi and Sarasini 2000; Louro et al. 2019), with the exception of one sequence (GenBank AF396864) that remains unassigned (Louro et al. 2019, 2020). The spiny

spored *Terfezia* complex harbors further phylogenetic difficulties, for example *T. cistophila* Ant. Rodr., Bordallo, Kaounas, & Morte was suggested as a later synonym of *Terfezia trappei* (R. Galán & G. Moreno) A. Paz & Lavoise (Paz et al. 2017), after suffering a taxonomic change at the genus level from *Elaphomyces* Nees to *Terfezia* (Paz et al. 2017). Later, we showed that *T. cistophila* and *T. trappei* formed two distinct and well-supported clades (Louro et al. 2019). The sequences describing *T. trappei* were recently re-considered as either *T. fanfani* (Vizzini et al. 2019) or as the newly described *Terfezia solaris-libera* Louro, Nobre, Santos-Silva (Louro et al. 2020) suggesting that *T. trappei* might not be a valid taxon.

Despite all the above contributions, the genus *Terfezia* is still undergoing frequent taxonomic reevaluations. It now seems clear that combined efforts are needed: classic taxonomy, molecular biology and ecology have to be worked synergistically. The lack of available sequences regarding the most cryptic species and the lack of a clear description of its ecological and geographic preferences are still obstacles hindering our understanding of the genus diversity.

As with all other truffles, *Terfezia* species are obligate symbionts of specific host plants, mainly members of the *Cistaceae* (Alsheikh 1994; Morte et al. 2009) including different annual and perennial species of the genus *Helianthemum* and *Cistus*, but also with members of the *Fagaceae* and *Pinaceae* (i.e. oaks and pines) (Alsheikh 1994; Diez et al. 2002; Kagan-Zur and Roth-Bejerano 2008; Morte et al. 2009). These plants and their associated *Terfezia* can be found in soils ranging from acidic to basic in their characteristics (Gutiérrez et al. 2003; Morte and Andrino 2014; Bordallo et al. 2015; Dafri and Beddiar 2017). Given their symbiotic nature, host specialization and edaphic tolerances have been hypothesized to have played significant roles in *Terfezia* adaptive evolution (Diez et al. 2002). Therefore, ecologic and geographic information are indisputably key factors for *Terfezia* species diagnosis; many species are thought to occur only in acidic or basic soils or in association with specific host plants (Gutiérrez et al. 2003; Morte and Andrino 2014; Bordallo et al. 2015; Dafri and Beddiar 2017). It is surprising that little to no geographic and ecological information is available for many of the deposited sequences of *Terfezia* in the most popular nucleotide databases. Even when that information does exist, it often seems incongruent, leading to worrying misidentification errors when crossing molecular analysis and ecological information. This seems to be the case with a sequence of an uncultured *Pezizaceae* (GenBank FJ013087) supposedly associated with *Pinus pinaster* Aiton, which corresponds to *T. cistophila* according to the phylogenetic reconstitution from Louro et al. (2019). However, this last finding opposes the initial description that *T. cistophila* lives solely associated with *Cistus* spp. (Bordallo et al. 2015). Another example (discussed in Louro et al. 2019) refers to two sequences given as *T. olbiensis* and associated to *Tuberaria guttata* (L.) Fourr. as putative host plant. *T. olbiensis* is by all accounts associated with *Pinus* spp. and *Quercus* spp. (Bordallo et al. 2013), and the published sequences nest inside *Terfezia albida* Ant. Rodr., Muñoz-Mohedano & Bordallo clade (Louro et al. 2019).

At this point it seems that only through a multidisciplinary approach encompassing molecular, morphological and ecological features will we be able to broaden our

understanding of *Terfezia* diversity. This especially applies in undersampled regions where the probability of discovering new species is favored due to the cryptic lifestyle of *Terfezia*. Adhering to these these stipulations, we have developed a case study in Portugal, where until 2018 *Terfezia* richness was greatly overlooked, with only three species documented. Since then, five more *Terfezia* species have been recorded *T. cistophila*, *T. extremadurensis*, *T. lusitanica*, *T. pini* and *T. solaris-libera* (Bordallo et al. 2018; Louro 2020; Louro et al. 2020, 2021) and the soil main features and putative host plant were registered. In the present work we reassess the diversity of this genus and characterize *Terfezia* ecology within the framework of ecological preferences, while also probing the intraspecific variability of the *Terfezia* taxa in analysis.

Methods

Surveys

The sampling took place between 2013 and 2020 from February to June, in the most favorable months for desert truffle growth. The surveys occurred within the framework of two projects (Santos-Silva 2015, 2020) aiming to develop the technology necessary to produce the two most economically important desert truffles in Portugal, namely, *Terfezia arenaria* (Moris) Trappe and *T. fanfani*. The specimens were collected in a wide range of habitats within the relatively homogeneous geographical area that is favorable to *Terfezia*. Hence, several areas with documented occurrence of desert truffle were surveyed and all the desert truffle specimens encountered were collected. The putative plant host was registered. Soil samples (50 mm diameter, 150 mm depth) were collected in each sampling site. A compose sample of 6 soil samples replicas per site was analyzed at the Laboratório Químico Agrícola Rebelo da Silva (INIAV/LQARS) for particle size and subsequent soil textural classification and water pH measurements. Throughout the collection period, the fresh ascocarps were brought to the laboratory for morphological and molecular characterization. Fragments of each specimen were frozen at -20 °C for DNA amplification and the remaining specimens were dried at 40 °C and stored in sealed plastic bags, labeled with collection details. All samples are deposited at the Herbarium of the Évora University Herbarium (UEVH-FUNGI), Portugal.

ITS sequences

DNA extraction from the analyzed specimens was performed by CTAB method, following the protocol described in Nobre et al. (2018). All extraction products were stored at -20 °C and later used directly in the PCR. The Internal Transcribed Spacer (ITS) region of the rDNA, including the 5.8S ribosomal gene, was amplified using the ITS5 and ITS4 primers (White et al. 1990). PCR reactions were conducted using 1 µl of the extracted DNA in a standard 25 µl reaction, with 0.5 pmol/µl of each primer,

1.5 mM MgCl₂, 0.5 mM dNTPs and 0.04 U/ml Taq DNA polymerase. PCR reactions were performed using a Mastercycler Gradient thermocycler (Eppendorf, Hamburg, Germany) with the following cycling parameters: an initial denaturalization step for 3 min at 95 °C, followed by 35 cycles consisting of: 30 s at 95 °C, 30 s at 55 °C (annealing temperature), 1 min at 72 °C, and a final extension at 72 °C for 10 min. All the PCR products were purified using the NZYGelpure kit (from NZYTech, Lda) and sequencing was done commercially (STAB VIDA, Lda.).

Phylogenetic reconstruction

Based on the most recent published phylogenetic reconstruction using UNITE curate sequences (Louro et al. 2019) we have selected 42 sequences covering each of the well supported clades. The same three known non-*Terfezia* sequences were selected as putative outgroups: *Tirmania* Chatin (GenBank JF908769.1), *Cazia* Trappe (GenBank AY830852.1) and *Peziza* Dill. Ex Fr. (GenBank JX414200.1). These sequences were aligned with the dataset of newly generated sequences from this work (216 sequences), using the E-INS-i strategy of the online MAFFT version 7 (Katoh et al. 2017). The phylogenetic reconstruction analysis based on the above sequences was performed in BEAST v.4.2.8 software (Drummond and Rambaut 2007), allowing the software to estimate the evolutionary model. All other settings were left as default. The output of BEAST was analyzed in the software Tracer v.1.6 to determine chain convergence and burnin. Trees were combined using the software TreeAnnotator v.2.4.8 to produce the single tree that best represents the posterior distribution, considering a burn-in of 10% (first 1000 trees were removed).

Results

An ITS amplified fragment with gaps of 721 bp was aligned, comprising 67 bp of the partial sequence of the 18S ribosomal RNA gene; 228 bp internal transcribed spacer 1; 156 bp of the 5.8S ribosomal RNA gene; 221 bp of the internal transcribed spacer 2; and 49 bp of the 28S ribosomal RNA gene. The reconstructed phylogeny amply supports the existence of 18 distinct clades representing well supported monophyletic groups (Fig. 1). Concerning the position of the newly collected specimens, the phylogenetic analysis successfully assigned them to 9 separate clades, namely to *T. arenaria*, *T. cistophila*, *T. dunensis*, *T. extremadurensis*, *T. fanfani*, *T. grisea*, *T. lusitanica*, *T. pini* and *T. solaris-libera* clades. Overall, the total number of registered *Terfezia* in Portugal expanded to 10 species.

Concerning species distribution and representativeness, *T. arenaria* and *T. fanfani* were the most widespread and commonly found *Terfezia* species, being in abundance at every sampling site. All other 7 species seemed to have narrower distribution ranges, however, their stochastic appearance throughout the sampling period made it impossible to confirm their distribution and fructification patterns.

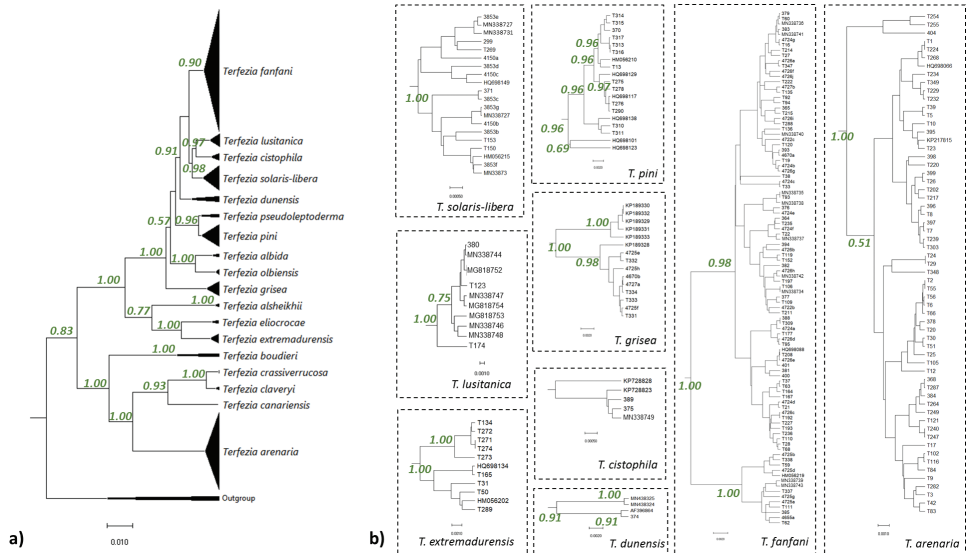


Figure 1. a Phylogenetic relationship between *Terfezia* species. The reconstructed phylogeny corresponds to the majority rule consensus tree higher than 0.50 of trees sampled in a Bayesian analysis, and the posterior probability values are shown for main nodes b clades with new sequenced specimens collected within the present study.

Regarding soil texture, *Terfezia* species occupied areas dominated by loamy sand soils (lSs) (51%) or sandy loam soils (sLs) (42%), and less frequently pure sandy soils (Ss) (7%). As to the soil pH, values varied from 5.1 to 7.3, with 5.6 the most frequent value, and half of the areas sampled showed pH values between 5.6 and 6.0. In other words, the sampled *Terfezia* specimens occupy strongly acidic to neutral soils, ranging from sandy to loamy soils (Table 1, Suppl. material 1: Table S1).

Despite the observed spatial heterogeneity of the different sampling sites, and the multiple putative plant hosts available, which in some sites included annual plants, *Cistus* shrubs and either *Quercus* or *Pinus* trees, the most frequent putative plant host was *Tuberaria guttata* (91%) (Suppl. material 1: Table S1).

While checking for possible relations between the specimens' position in the reconstructed phylogenetic tree and the recorded ecological parameters, we found that proximity of sampling locations was not an influencing factor to explain the multiple lineages (i.e. subgroups) seen within each clade, since specimens from different locations were often grouped together in almost all the subgroups of a given clade. For instance, *T. pini* intraspecific variability, as shown by well supported branches in the reconstructed phylogeny (Fig. 1), comprises specimens collected in Spain and different locations in Portugal in each subgroup. On the other hand, some patterns and tendencies were observed between different *Terfezia* lineages within each clade and ecologic parameters such as soil texture, soil pH and putative plant host (Table 1, Suppl. material 1: Table S1, Fig. 2).

Table 1. *Terfezia* preferences relating to host plant and soil (see more details in Suppl. material 1: Table S1). *Tuberaria guttata* – Tg; *Cistus salvifolius* – Cs; *Cistus ladanifer* – Cl; *Quercus* spp. – Q; *Pinus* spp – P.

Species	Host plant	Soil type	Soil pH
<i>T. arenaria</i>	Tg	Loamy sand, Sandy loam	5.2–7.3
<i>T. cistophila</i>	Cs, Cl	Loamy sand	5.5–5.6
<i>T. dunensis</i>	Cs, P	Loamy sand	6.1
<i>T. extremadurensis</i>	Tg	Sandy loam	5.3–6.0
<i>T. fanfani</i>	Tg	Loamy sand, Sandy loam, Sandy	5.1–6.4
<i>T. grisea</i>	Tg	Loamy sand, Sandy	5.7–6.1
<i>T. lusitanica</i>	Tg	Loamy sand, Sandy	5.5–6.2
<i>T. pini</i>	Q, P	Sandy loam	5.3–6.0
<i>T. solaris-libera</i>	Tg	Sandy loam	6.0

T. arenaria occupies strongly acid to neutral sandy or loamy soils and its putative host is only *T. guttata*. In *T. arenaria* intraspecific reconstructed phylogenetic variability (Fig. 1) three groups were formed which seem to show, from top to bottom, a decrease in preference for more neutral and sandier soils. Represented at the top, a small group separates from the others, and these specimens were all collected in ISs with pH higher than 7.0. The second group shows, on average, different preferences to the third, with 77% collected in ISs (pH from 5.2 to 7.3) against 59% ISs (pH from 5.1 to 6.2). Summing up, it seems that there is a tendency in the reconstructed phylogenetic groups to relate with soil characteristics (Fig. 2a).

T. fanfani showed a larger range of soil textures and narrow pH soil preferences (Table 1) and is always associated with *T. guttata*. No differences in soil pH ranges can be linked to the intraspecific groups observed in the reconstructed phylogeny. However, soil texture preferences are slightly different in both clades, with one group including 65% specimens collected in sandy soils (ISs and Ss) and the other group with a higher preference value (77%) for this type of soils. Overall, *T. fanfani* seems to prefer slightly, to strongly, acid soils and, as for *T. arenaria*, a diversity linkage to sandier or loamier soil preferences is suggested (Fig. 2b). *T. extremadurensis* occurs in strongly to moderate acid loamy soils (Table 1), mainly with *T. guttata* (only in one Spanish record, GenBank HQ698134) *Cistus albidus* is considered as putative host). The first group integrates specimens collected in the same region and no pattern is apparent concerning soil features.

This is the first report of *T. grisea* in this region. More interesting, *T. grisea* was considered exclusively an alkaline soil species until the present work. We have shown *T. grisea* presence in moderately to slightly acidic soils, mainly sandy soils and in association to *T. guttata* (Table 1). The two reconstructed groups (Fig. 2c) suggest a separation between variants, one associated with alkaline soils and hosted by *Pinus* spp. and the other associated with acid soils and linked to *T. guttata*. This separation is not clear-cut, however, as two samples collected in Burgos (Spain; GenBank KP189328 and GenBank KP189333) are nested in separate groups and are reported as collected in alkaline soil and on *Helianthemum* sp. host.

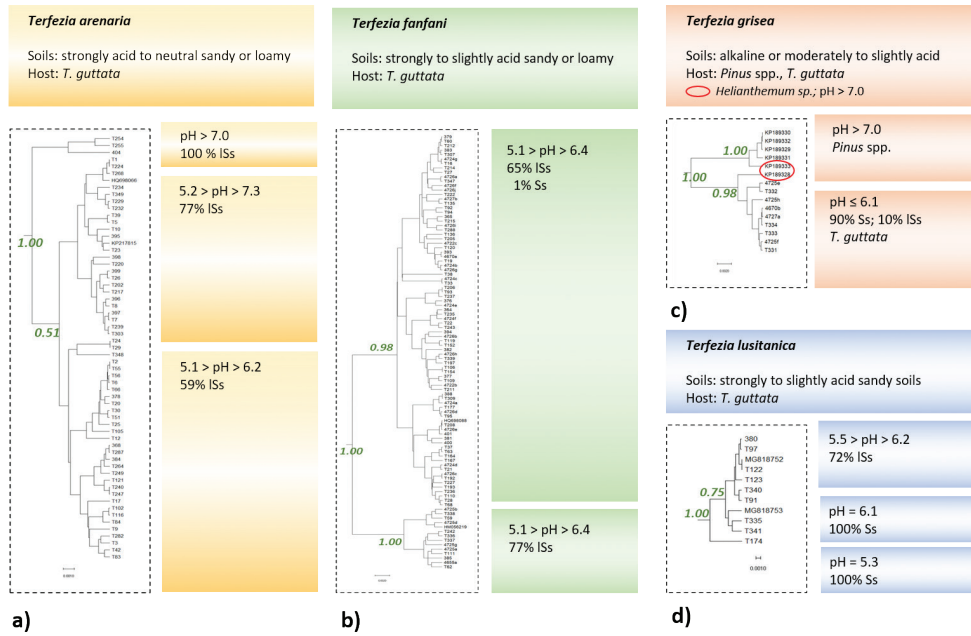


Figure 2. Phylogenetic reconstruction of intra-species diversity (Fig. 1) linking to soil properties and putative host plant **a** *T. arenaria* **b** *T. fanfani* **c** *T. grisea* [specimens in the circle represent deviations from the ecological grouping, see text for details] **d** *T. lusitanica*. The other species are identified and their relation to soil and host plant are presented in the main text.

T. lusitanica occurs in strongly to slightly acidic sandy soils exclusively with *T. guttata* (Table 1). The reconstructed intraspecific phylogeny suggests three well supported groups, albeit with few representatives (Fig. 2d). The group with the highest number of specimens were mainly collected in ISs (72%) with a wide pH range (5.5 to 6.2), which separates them from the rest of the specimens, which were collected in Ss and at the higher range of the soil pH scale registered for this species (6.1). A single specimen was encountered on Ss at lower pH.

T. pini occurs in strongly to moderate acid loamy soils associated with *Quercus spp.* and *Pinus spp* (Table 1). The two first reconstructed intraspecific groups (Fig. 1) integrate specimens associated with both *Quercus* and *Pinus*, the first with a pH range from 5.3 to 6.0 and the second in soils with the same pH value (5.4). The remaining groups comprise specimens collected in association with *Quercus*. No tendency is apparent on both putative hosts and soil pH that could be linked to the intraspecific variability observed.

The recently described *T. solaris-libera* occurs in moderate acid loamy soils associated with *T. guttata* (Table 1), and this is consistent for all specimens regardless of their geographic origin. *T. cistophila* occurs in strongly to moderate acid sandy soils associated with *Cistus spp.* (Table 1). This is consistent with all samples but one (GenBank KP728828), which does not group with the others and it is originated from Greece

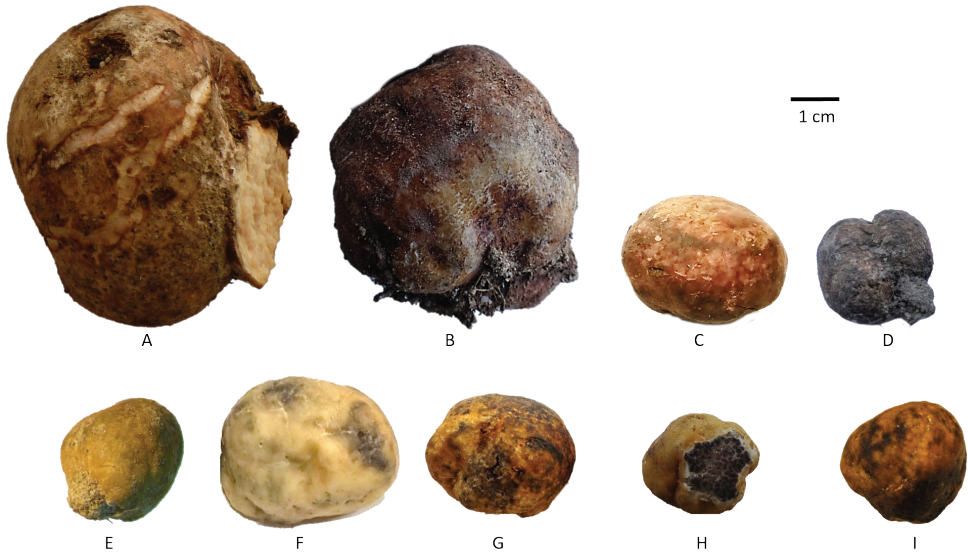


Figure 3. *Terfezia* species collected in the present work **A** *T. arenaria* **B** *T. fanfani* **C** *T. cistophila* **D** *T. grisea* **E** *T. dunensis* **F** *T. extremadurensis* **G** *T. lusitanica* **H** *T. pini* **I** *T. solaris-libera*.

and associated with *C. monspeliensis* and *C. creticus* (and no information on soil type is available). The remaining specimens are from Portugal and Spain and are linked to *C. salviifolius* and *C. ladanifer*. *T. dunensis* is so far represented by four specimens and only one with soil features information (Table 1). The two samples from Huelva (Spain) cluster together and are linked to *Cistaceae*. The other two samples are the “unclassifiable” GenBank AF396864 (Louro et al. 2019) and a sample from South Portugal that is either associated with *Cistus* or *Pinus*.

The nine *Terfezia* species collected in the present work are illustrated in Fig. 3.

Discussion

The introduction of the newly collected *Terfezia* samples on the most recent published phylogenetic reconstruction of the genus (Louro et al. 2019) reinforces the existence of 18 well supported clades. Yet, GenBank AF396864, which at the time did not cluster with any of the other taxa, now fell under the newly described *T. dunensis* clade. This suggests that we might be closer to solving the identity of this previously unassigned sequenced if its position within the *T. dunensis* clade is to be sustained in subsequent studies with new data. The primary fungal barcode ITS remains the most informative DNA fragment available, and the great majority of available sequence data is based on this region. Although it is widely accepted as a standard molecular marker, some issues remain unresolved and other types of markers (e.g. microsatellites or, ideally genome wide data) might be needed to shed light on inter-species diversity and evolutionary patterns.

The comprehensive sampling along eight consecutive years, allowed us to update the existing knowledge on *Terfezia* species diversity in the region, and expand the number of species occurring in the country to 10 species (i.e. *T. alsheikhii*, *T. arenaria*, *T. cistophila*, *T. extremadurensis*, *T. fanfani*, *T. grisea*, *T. lusitanica*, *T. pini*, *T. olbiensis* and *T. solaris-libera* sp. nov.). Though *Terfezia alsheikhii* was only registered once for Portugal (Bordallo et al. 2013), we were unable to find any specimen of this species and thus to confirm its presence. *Terfezia dunensis* and *T. grisea*, on the other hand, had never been registered in Portugal and therefore the present work represents the first record of their presence. The significance of these findings go beyond the scope of national or regional species checklist as they prove undoubtedly that the Iberian Peninsula, as a whole, is a diversity hotspot for the genus *Terfezia* given that every one of the eighteen accepted species occur in the territory. This documented outstanding diversity can be explained by the abundance of different putative hosts occurring on the Peninsula, as host specialization and edaphic tolerances likely played significant roles in *Terfezia* adaptive evolution (Diez et al. 2002; Bordallo and Rodriguez 2004).

More importantly, the present work examined the observed intraspecific variability within the context of soil and host preferences. The here achieved better understanding of the edaphic preference and host specificity of the analyzed *Terfezia* species is of the utmost importance in the framework of desert truffle cultivation. Although we found that the sampling area was not an influencing factor to explain the multiple lineages seen within each clade, we were able to identify some tendencies linking different *Terfezia* lineages within species to ecological parameters such as soil texture, soil pH and host plant.

As such, the finding of *T. grisea* in acid soils is puzzling and contradicts the original species description. Our reconstructed phylogeny suggests a separation between two variants, one associated with alkaline soils and hosted by *Pinus* spp. and the other with acid soils and linked to *T. guttata*. Yet, this separation is not clear-cut, since the two existing Spanish sequences associated with *Helianthemum* spp. were represented in both sub-clades. Further sampling of this species is still needed in order to clarify if this clade represents a group of cryptic species, a single species that is undergoing speciation or a single species that has a wide edaphic tolerance and low host specificity.

The other two species with clear intra-species variability are *Terfezia arenaria* and *T. fanfani*, both associated with a higher number of samples. These two species seem to be much more abundant but are also much more conspicuous because of their size. Whether the observed intra-species diversity can be linked to clear ecological preferences remains unknown. For *T. arenaria* we could observe a grouping tendency based on pH and soil type tolerance. For *T. fanfani*, differential preferences were also observed on these variables, albeit less defined. In both cases, the intra-specific diversity found in these species calls for a more detailed study including a set of meaningful ecological variables, forest and land management options. Concerning the last, it is reported that macrofungal richness, particularly for mycorrhizal *taxa*, are shaped by tree canopy density (Santos-Silva et al. 2011) and negatively affected by severe soil tillage and intensive grazing (Santos-Silva and Louro 2016; Pinto-Correia et al. 2018).

Understanding *Terfezia* diversity and its ecological constraints is highly relevant when considering the economic value of the desert truffles for rural populations on the Mediterranean basin. Desert truffles are a potentially important food source that is highly valued in local markets. A shift from expert collector to cultivation would enhance the socio-economic development of rural and/or local populations. To efficiently mass produce *Terfezia* one needs to explore the best genotype-host species combination but also learn the growing determinants that lead to a more efficient growth and fruitbodies production. *T. arenaria* and *T. fanfani* are by their abundance and size the most promising for cultivation purposes. In fact, most of the other *Terfezia* species have small size, do not fructify every year and are even harder to find. The attempt to describe its ecology is thus of utmost importance to confirm their identity, distribution and fructification patterns.

Conclusion

The present work attempts, to the best of our knowledge for the first time, to systematically associate the diversity of *Terfezia* species with soil type, pH and with a putative host plant in a geographically limited sampling area. By doing so, it contributes to our knowledge of the species in the region, increasing the number of species to ten, opening the cultivation possibilities to other species, other host plants and to a wider range of soil types. To notice the first reference of *T. grisea* in acidic soils. No doubt *T. arenaria* and *T. fanfani* are the most found *Terfezia* species, either by their size, by their abundance or by a combination of both. We need to increase our knowledge on the crucial ecological determinants affecting desert truffles if we want to understand their diversity and cultivation potential.

Acknowledgements

The authors acknowledge National Funds through FCT - Foundation for Science and Technology under the Project UIDB/05183/2020. This work was supported by the projects PRODER, PA 46134 Produção de Túberas, and Alentejo 2020, ALT-20-03-0145-FEDER-000006 Micorrização de *Cistus* spp. com *Terfezia arenaria* (Moris) Trappe e sua aplicação na produção de túberas. TN acknowledges the support by “Fundação para a Ciência e Tecnologia”, FCT Portugal (PTDC/ASP-PLA/30650/2017).

References

- Alsheikh AM (1994) Taxonomy and mycorrhizal ecology of the desert truffles in the genus *Terfezia*. PhD Thesis, Oregon State University, Corvallis.
- Bordallo JJ, Rodriguez A (2014) Cryptic and new species. In: Kagan-Zur V, Roth-Bejerano N, Sitrit Y, Morte A (Eds) Desert Truffles, phylogeny, physiology, distribution and domestication. Springer, Berlin, 39–53.

- Bordallo JJ, Rodríguez A, Muñoz-Mohedano JM, Suz LM, Honrubia M, Morte A (2013) Morphological and molecular characterization of five new *Terfezia* species from the Iberian Peninsula. *Mycotaxon* 124: 189–208. <https://doi.org/10.5248/124.189>
- Bordallo JJ, Rodríguez A, Kaounas V, Camello F, Honrubia M (2015) Two new *Terfezia* species from Southern Europe. *Phytotaxa* 230(3): 239–249. <https://doi.org/10.11646/phytotaxa.230.3.2>
- Bordallo JJ, Rodríguez A, Santos-Silva C, Louro R, Muñoz-Mohedano JM, Morte A (2018) *Terfezia lusitanica*, a new mycorrhizal species associated to *Tuberaria guttata* (Cistaceae). *Phytotaxa* 357(2): 141–147. <https://doi.org/10.11646/phytotaxa.357.2.7>
- Bruns TD, Fogel, R, White TJ, Palmer JD (1989) Accelerated evolution of a false-truffle from a mushroom ancestor. *Nature* 339: 140–142. <https://doi.org/10.1038/339140a0>
- Dafri A, Beddiar A (2017) Desert truffles from northeastern Algerian coastal dunes: Ecology, identification and symbiosis. *Journal of Fundamental and Applied Sciences* 9(1): 153–169. <https://doi.org/10.4314/jfas.v9i1.11>
- Diez J, Manjon JL, Martin F (2002) Molecular phylogeny of the mycorrhizal desert truffles (*Terfezia* and *Tirmania*), host specificity and edaphic tolerance. *Mycologia* 94: 247–259. <https://doi.org/10.2307/3761801>
- Drummond A, Rambaut A (2007) BEAST: bayesian evolutionary analysis by sampling trees. *BMC Evolutionary Biology* 7: e214. <https://doi.org/10.1186/1471-2148-7-214>
- Gutiérrez A, Morte A, Honrubia M (2003) Morphological characterization of the mycorrhiza formed by *Helianthemum almeriense* Pau with *Terfezia claveryi* Chatin and *Picoa lefebvrei* (Pat.) Maire. *Mycorrhiza* 13: 299–307. <https://doi.org/10.1007/s00572-003-0236-7>
- Honrubia M, Cano A, Molina-Ninirola C (1992) Hypogeous fungi from Southern Spanish semiarid lands. *Persoonia* 14(4): 647–653.
- Kagan-Zur V, Roth-Bejerano N (2008) Studying the brown desert truffles of Israel. *Israel Journal of Plant Sciences* 56(4): 309–314. <https://doi.org/10.1560/IJPS.56.4.309>
- Katoh K, Rozewicki J, Yamada KD (2017) MAFFT online service: multiple sequence alignment, interactive sequence choice and visualization. *Briefings in Bioinformatics* bbx118: 1–7.
- Louro R (2020) *Terfezia* diversity in southern Portugal and their mycorrhizal associations with *Cistus* L.: a study towards the viable production of desert truffles on acid soils. PhD Thesis, University of Évora, Évora.
- Louro R, Santos-Silva C, Nobre T (2019) What is in a name? *Terfezia* classification revisited. *Fungal Biology* 123(4): 267–273. <https://doi.org/10.1016/j.funbio.2019.01.003>
- Louro R, Nobre T, Santos-Silva C (2020) *Terfezia solaris-libera* sp. nov., A new mycorrhizal species within the spiny-spored lineages. *Journal of Mycology & Mycological Sciences* 3(2): 1–13. <https://doi.org/10.23880/OAJMMS-16000121>
- Louro R, Natário B, Santos-Silva C (2021) Morphological characterization of the in vitro mycorrhizae formed between four *Terfezia* species (Pezizaceae) with *Cistus salviifolius* and *Cistus ladanifer* –Towards desert truffles production in acid soils. *Journal of Fungi* 7(1): e35. <https://doi.org/10.3390/jof7010035>
- Montecchi A, Sarasini M (2000) *Funghi Ipogei d'Europa*. AMB Fondazione Centro Studi Micologici, Trento.

- Moreno G, Galan R, Ortega A (1986) Hypogeous fungi from continental Spain I. Cryptogamie Mycologie 7(3): 201–229.
- Moreno G, Alvarado P, Manjón JP (2014) Hypogeous desert fungi. In: Kagan-Zur V, Roth-Bejerano N, Sitrit Y, Morte A (Eds) Desert Truffles, phylogeny, physiology, distribution and domestication. Springer, Berlin, 3–20. https://doi.org/10.1007/978-3-642-40096-4_1
- Morte A, Andriano A (2014) Domestication: Preparation of mycorrhizal seedlings. In: Kagan-Zur V, Roth-Bejerano N, Sitrit Y, Morte A (Eds) Desert Truffles, phylogeny, physiology, distribution and domestication. Springer, Berlin, 343–365. https://doi.org/10.1007/978-3-642-40096-4_21
- Morte A, Zamora M, Gutiérrez A, Honrubia M (2009) Desert truffle cultivation in semiarid Mediterranean areas. In: Azcon-Aguilar C, Barea JM, Gianinazzi S, Gianinazzi-Pearson V (Eds) Mycorrhizas: Functional Processes and Ecological Impact. Springer, Berlin, 221–234. https://doi.org/10.1007/978-3-540-87978-7_15
- Navarro-Ródenas A, Lozano-Carrillo MC, Pérez-Gilabert M, Morte A (2011) Effect of water stress on in vitro mycelium cultures of two mycorrhizal desert truffles. Mycorrhiza 21: 247–253. <https://doi.org/10.1007/s00572-010-0329-z>
- Nobre T, Gomes L, Rei F (2018) Uncovered variability in olive moth (*Prays oleae*) questions species monophyly. PLoS ONE 13(11): 1–12. <https://doi.org/10.1371/journal.pone.0207716>
- Paz A, Bellanger JM, Lavoise C, Molia A, Ławrynowicz M, Larsson E, Ibarguren IO, Jeppson M, Læssøe T, Sauve M, Richard F, Moreau PA (2017) The genus *Elaphomyces* (*Ascomycota*, *Eurotiales*): a ribosomal DNA-based phylogeny and revised systematics of European “deer truffles”. Persoonia 38: 197–239. <https://doi.org/10.3767/003158517X697309>
- Pinto-Correia T, Guiomar N, Ferraz-de-Oliveira MI, Sales-Baptista E, Rabaça J, Godinho C, Ribeiro N, Sousa PS, Santos P, Santos-Silva C, Simões MP (2018) Progress in identifying high nature value montados: Impacts of grazing on hardwood rangeland biodiversity. Rangeland Ecology and Management 71(5): 612–625. <https://doi.org/10.1016/j.rama.2018.01.004>
- Santos-Silva C (2015) Produção de Túberas (Desert truffles production) Final report. Project PRODER, ref. PA 46134.
- Santos-Silva C (2020) Micorrização de *Cistus* spp. com *Terfezia arenaria* (Moris) Trappe e sua aplicação na produção de túberas (*Cistus* ssp. mycorrhization with *Terfezia arenaria* (Moris) Trappe and its application in desert truffles production) Final report. Project Alentejo 2020, ref. ALT20-03-0145-FEDER-000006.
- Santos-Silva C, Louro R (2016) Assessment of the diversity of epigeous Basidiomycota under different soil-management systems in a Montado ecosystem: a case study conducted in Alentejo. Agroforestry Systems 90: 117–126. <https://doi.org/10.1007/s10457-015-9800-3>
- Santos-Silva C, Gonçalves A, Louro R (2011) Canopy cover influence on macrofungal richness and sporocarp production in montado ecosystems. Agroforestry Systems 82: 149–159. <https://doi.org/10.1007/s10457-011-9374-7>
- Thiers HD (1984) The secotioid syndrome. Mycologia 76: 1–8. <https://doi.org/10.2307/3792830>
- Vizzini A, Arenas F, Rodríguez A, Mello A, Lainé P, Muñoz-Mohedano JM, Morte A (2019) Typification of *Terfezia fanfani* (*Ascomycota*, *Pezizaceae*). Phytotaxa 387(1): 73–76. <https://doi.org/10.11646/phytotaxa.387.1.7>

- White T, Bruns T, Lee S, Taylor J (1990) Amplification and direct sequencing of fungal ribosomal RNA genes for phylogenetics. In: Innis MA, Gelfand DH, Sninsky JJ, White TJ (Eds) PCR protocols: a guide to methods and applications. Academic Press, New York, 315–322. <https://doi.org/10.1016/B978-0-12-372180-8.50042-1>
- Zitouni-Haouar F, Carlavilla JR, Moreno G, Manjon JL, Fortas Z (2018) Genetic diversity of the genus *Terfezia* (*Pezizaceae*, *Pezizales*): new species and new record from North Africa. *Phytotaxa* 334(2): 183–194. <https://doi.org/10.11646/phytotaxa.334.2.7>

Supplementary material I

Table S1

Authors: Celeste Santos-Silva, Rogério Louro, Bruno Natário, Tânia Nobre

Data type: Taxonomic, geographical and ecological information

Explanation note: This file discloses all *Terfezia* sequences falling within each clade on the phylogenetic analysis generated in this work (including the 45 sequences selected from the most recent genus phylogenetic reconstruction and the 216 newly generated sequences from this work) and their respective accession numbers and bibliographic references. A collection/sampling number is also provided for each one of the new sequences pertaining to the samples deposited at the Évora University Herbarium (UEVH-FUNGI).

Copyright notice: This dataset is made available under the Open Database License (<http://opendatacommons.org/licenses/odbl/1.0/>). The Open Database License (ODbL) is a license agreement intended to allow users to freely share, modify, and use this Dataset while maintaining this same freedom for others, provided that the original source and author(s) are credited.

Link: <https://doi.org/10.3897/mycokeys.84.71372.suppl1>

Characterization of *Diaporthe* species on *Camellia oleifera* in Hunan Province, with descriptions of two new species

Qin Yang^{1,2}, Jie Tang¹, Guo Y. Zhou^{1,2}

1 Forestry Biotechnology Hunan Key Laboratories, Central South University of Forestry and Technology, Changsha 410004, China **2** The Key Laboratory for Non-Wood Forest Cultivation and Conservation of the Ministry of Education, Central South University of Forestry and Technology, Changsha 410004, China

Corresponding author: Guo Y. Zhou (zgyingqq@163.com)

Academic editor: R. Phookamsak | Received 16 July 2021 | Accepted 14 September 2021 | Published 18 October 2021

Citation: Yang Q, Tang J, Zhou GY (2021) Characterization of *Diaporthe* species on *Camellia oleifera* in Hunan Province, with descriptions of two new species. MycoKeys 84: 15–33. <https://doi.org/10.3897/mycokeys.84.71701>

Abstract

Tea-oil tree (*Camellia oleifera* Abel.) is an important edible oil woody plant with a planting area over 3,800,000 hectares in southern China. Species of *Diaporthe* inhabit a wide range of plant hosts as plant pathogens, endophytes and saprobes. At present, relatively little is known about the taxonomy and genetic diversity of *Diaporthe* on *C. oleifera*. Here, we conducted an extensive field survey in Hunan Province in China to identify and characterise *Diaporthe* species associated with tea-oil leaf spots. As a result, eleven isolates of *Diaporthe* were obtained from symptomatic *C. oleifera* leaves. These isolates were studied by applying a polyphasic approach including morphological and phylogenetic analyses of partial ITS, *cal*, *his3*, *tef1* and *tub2* gene regions. Two new *Diaporthe* species (*D. camelliae-oleiferae* and *D. hunanensis*) were proposed and described herein, and *C. oleifera* was revealed to be new host records of *D. hubeiensis* and *D. sojiae*. This study indicated there is a potential of more undiscovered *Diaporthe* species from *C. oleifera* in China.

Keywords

Camellia oleifera, DNA phylogeny, systematics, taxonomy, two new taxa

Introduction

Tea-oil tree, *Camellia oleifera* Abel., is a unique woody edible oil species in China, mainly distributed in the Qinling-Huaihe River area. It has a long history of cultivation and utilization for more than 2300 years since ancient China (Zhuang 2008). Camellia oil, obtained from *C. oleifera* seeds, is rich in unsaturated fatty acids and unique flavors, and has become a rising high-quality edible vegetable oil in China. The edible of tea-oil is also conducive to preventing cardiovascular sclerosis, anti-tumor, lowering blood lipid, protecting liver and enhancing human immunity (Wang et al. 2007). Hunan Province leads the country in *C. oleifera* production with the average of 3.3–40,000 hm² to expand the cultivation area every year (Tan et al. 2018). By the end of 2017, the cultivation area of *C. oleifera* reached 1.4 million hm², tea oil 290100 tons, and output value of 35 billion yuan (Tan et al. 2018). Thus, the development of *C. oleifera* industry is of great significance for the economic development of Hunan Province and the poverty alleviation of local farmers.

Diseases are a major constraint to *C. oleifera* production. Anthracnose disease caused by *Colletotrichum* species is one of the foremost diseases in southern China, which can infect leaves and fruits of *C. oleifera*, causing up to 40% fruit drop and up to 40% camellia seeds loss (Wang et al. 2020). During July and August of 2020, new leaf spots were detected on tea-oil tree with irregular, brownish-grey lesions, often associated with leaf margins. Infected leaves cultured on medium had dark pycnidia producing ellipsoid guttulate conidia, similar to that of *Diaporthe* species (Yang et al. 2020, 2021). *Diaporthe* species are responsible for diseases on a wide range of plant hosts, including agricultural crops, forest trees and ornamentals, some of which can cause substantial yield losses (Santos et al. 2011; Gomes et al. 2013; Udayanga et al. 2015; Gao et al. 2016; Guarnaccia and Crous 2017, 2018; Yang et al. 2018, 2020, 2021). For instance, *D. ampelina*, the causal agent of Phomopsis cane and leaf spot, is known as a severe pathogen of grapevines (Hewitt and Pearson 1988), infecting all green tissues and causing yield reductions of up to 30% in temperate regions (Erincik et al. 2001). *Diaporthe citri* is another well-known pathogen exclusively found on *Citrus* spp. causing melanose, stem-end rot and gummosis in all the citrus production area except Europe (Mondal et al. 2007; Udayanga et al. 2014a; Guarnaccia and Crous 2017, 2018).

Species identification criteria in *Diaporthe* has mainly relied on host association, morphology and culture characteristics (Mostert et al. 2001; Santos and Phillips 2009; Udayanga et al. 2011), which resulted in the description of over 200 species. Some species of *Diaporthe* were reported to colonise a single host plant, while other species were found to be associated with different host plants (Santos and Phillips 2009; Diogo et al. 2010; Santos et al. 2011; Gomes et al. 2013). In addition, considerable variability of the phenotypic characters was found to be present within a species (Rehner and Uecker 1994; Mostert et al. 2001; Udayanga et al. 2011). During the past decade, a polyphasic approach, based on multi-locus DNA data, morphological, phytopathological and phylogenetical analyses, has been employed for species boundaries in the

genus *Diaporthe* (Huang et al. 2015; Gao et al. 2016, 2017; Guarnaccia and Crous 2017; Guarnaccia et al. 2018; Yang et al. 2018, 2020, 2021).

The classification of *Diaporthe* has been ongoing; however, little is known about species able to infect *C. oleifera*. Thus, the objective of the present study was to identify the prevalence of *Diaporthe* spp. associated with tea-oil tree leaf spot in the major plantations in Hunan Province based on morphological and phylogenetic features.

Materials and methods

Fungal isolation

Leaves of *C. oleifera* with typical symptoms of leaf spots were collected from the main tea-oil camellia production fields in Hunan Province. Small sections (3 × 3 mm) were cut from the margins of infected tissues, and surface-sterilised in 75% ethanol for 30 s, then sterilised in 5% sodium hypochlorite for 1 min, followed by three rinses with sterilised water and finally dried on sterilised filter paper. The sections were then plated on to PDA plates and incubated at 25 °C. Fungal growth was examined daily for up to 7 d. Isolates were then transferred aseptically to fresh PDA and purified by single-spore culturing. All fungal isolates were placed on PDA slants and stored at 4 °C. Specimens and axenic cultures are maintained in the Central South University of Forestry and Technology (CSUFT).

Morphological and cultural characterization

Agar plugs (6 mm diam.) were taken from the edge of actively growing cultures on PDA and transferred on to the centre of 9 cm diam. Petri dishes containing 2% tap water agar supplemented with sterile pine needles (PNA; Smith et al. 1996) and potato dextrose agar (PDA), and incubated at 25 °C under a 12 h near-ultraviolet light/12 h dark cycle to induce sporulation as described in recent studies (Gomes et al. 2013; Lombard et al. 2014). Colony characters and pigment production on PNA and PDA were noted after 10 d. Colony colours were rated according to Rayner (1970). Cultures were examined periodically for the development of ascomata and conidiomata. The morphological characteristics were examined by mounting fungal structures in clear lactic acid and 30 measurements at ×1000 magnification were determined for each isolate using a Leica compound microscope (DM 2500) with interference contrast (DIC) optics. Descriptions, nomenclature and illustrations of taxonomic novelties are deposited in MycoBank (Crous et al. 2004a).

DNA extraction, PCR amplification and sequencing

Genomic DNA was extracted from colonies grown on cellophane-covered PDA using a CTAB [cetyltrimethylammonium bromide] method (Doyle and Doyle 1990).

DNA was estimated by electrophoresis in 1% agarose gel, and the quality was measured using the NanoDrop 2000 (Thermo Scientific, Waltham, MA, USA), following the user manual (Desjardins et al. 2009). PCR amplifications were performed in a DNA Engine Peltier Thermal Cycler (PTC-200; Bio-Rad Laboratories, Hercules, CA, USA). The primer set ITS1/ITS4 (White et al. 1990) was used to amplify the ITS region. The primer pair CAL228F/CAL737R (Carbone and Kohn 1999) was used to amplify the calmodulin gene (*cal*), and the primers CYLH4F (Crous et al. 2004b) and H3-1b (Glass and Donaldson 1995) were used to amplify part of the histone H3 (*his3*) gene. The primer pair EF1-728F/EF1-986R (Carbone and Kohn 1999) was used to amplify a partial fragment of the translation elongation factor 1- α gene (*tef1*). The primer set T1 (O'Donnell and Cigelnik 1997) and Bt2b (Glass and Donaldson 1995) was used to amplify the beta-tubulin gene (*tub2*); the additional combination of Bt2a/Bt2b (Glass and Donaldson 1995) was used in case of amplification failure of the T1/Bt2b primer pair. The PCR amplifications of the genomic DNA with the phylogenetic markers were done using the same primer pairs and conditions as in Yang et al. (2018). PCR amplification products were assayed via electrophoresis in 2% agarose gels. DNA sequencing was performed using an ABI PRISM 3730XL DNA Analyzer with a BigDye Terminator Kit v.3.1 (Invitrogen, USA) at the Shanghai Invitrogen Biological Technology Company Limited (Beijing, China).

Phylogenetic analyses

The quality of the amplified nucleotide sequences was checked and combined using SeqMan v.7.1.0 and reference sequences were retrieved from the National Center for Biotechnology Information (NCBI), based on recent publications on the genus *Diaporthe* (Guarnaccia et al. 2018; Yang et al. 2018, 2020, 2021). Sequences were aligned using MAFFT v. 6 (Katoh and Toh 2010) and corrected manually using Bioedit 7.0.9.0 (Hall 1999). The best-fit nucleotide substitution models for each gene were selected using jModelTest v. 2.1.7 (Darriba et al. 2012) under the Akaike Information Criterion.

The phylogenetic analyses of the combined gene regions were performed using Maximum Likelihood (ML) and Bayesian Inference (BI) methods. ML was conducted using PhyML v. 3.0 (Guindon et al. 2010), with 1000 bootstrap replicates while BI was performed using a Markov Chain Monte Carlo (MCMC) algorithm in MrBayes v. 3.0 (Ronquist et al. 2003). Two MCMC chains, started from random trees for 1,000,000 generations and trees, were sampled every 100th generation, resulting in a total of 10,000 trees. The first 25% of trees were discarded as burn-in of each analysis. Branches with significant Bayesian Posterior Probabilities (BPP) were estimated in the remaining 7500 trees. Phylogenetic trees were viewed with FigTree v.1.3.1 (Rambaut and Drummond 2010) and processed by Adobe Illustrator CS5. The nucleotide sequence data of the new taxa were deposited in GenBank (Table 1). The multilocus sequence alignments were deposited in TreeBASE (www.treebase.org) as accession S28703 and S22703.

Table 1. Isolates and GenBank accession numbers used in the phylogenetic analyses of *Diaporthe*.

Species	Isolate	Host	Location	GenBank accession numbers				
				ITS	<i>cal</i>	<i>bis3</i>	<i>tef1</i>	<i>tub2</i>
<i>D. acericola</i>	MFLUCC 17-0956	<i>Acer negundo</i>	Italy	KY964224	KY964137	NA	KY964180	KY964074
<i>D. acerigena</i>	CFCC 52554	<i>Acer tataricum</i>	China	MH121489	MH121413	MH121449	MH121531	NA
<i>D. alangii</i>	CFCC 52556	<i>Alangium kurzii</i>	China	MH121491	MH121415	MH121451	MH121533	MH121573
<i>D. alnea</i>	CBS 146.46	<i>Alnus</i> sp.	Netherlands	KC343008	KC343250	KC343492	KC343734	KC343976
<i>D. amygdali</i>	CBS 126679	<i>Prunus dulcis</i>	Portugal	KC343022	KC343264	KC343506	AY343748	KC343990
<i>D. angelicae</i>	CBS 111592	<i>Heracleum sphondylium</i>	Austria	KC343027	KC343269	KC343511	KC343753	KC343995
<i>D. apiculatum</i>	CGMCC 3.17533	<i>Camellia sinensis</i>	China	KP267896	NA	NA	KP267970	KP293476
<i>D. arecae</i>	CBS 161.64	<i>Areca catechu</i>	India	KC343032	KC343274	KC343516	KC343758	KC344000
<i>D. arengae</i>	CBS 114979	<i>Arenga enngleri</i>	Hong Kong	KC343034	KC343276	KC343518	KC343760	KC344002
<i>D. aseana</i>	MFLUCC 12-0299	Unknown dead leaf	Thailand	KT459414	KT459464	NA	KT459448	KT459432
<i>D. biguttulata</i>	CGMCC 3.17248	<i>Citrus limon</i>	China	KJ490582	NA	KJ490524	KJ490461	KJ490403
	CFCC 52584	<i>Juglans regia</i>	China	MH121519	MH121437	MH121477	MH121561	MH121598
<i>D. camelliae-oleiferae</i>	HNZZ027	<i>Camellia oleifera</i>	China	MZ509555	MZ504685	MZ504696	MZ504702	MZ504718
	HNZZ030	<i>Camellia oleifera</i>	China	MZ509556	MZ504686	MZ504697	MZ504708	MZ504719
	HNZZ032	<i>Camellia oleifera</i>	China	MZ509557	MZ504687	MZ504698	MZ504709	MZ504720
<i>D. celeris</i>	CPC 28262	<i>Vitis vinifera</i>	Czech Republic	MG281017	MG281712	MG281363	MG281538	MG281190
<i>D. celastrina</i>	CBS 139.27	<i>Celastrus</i> sp.	USA	KC343047	KC343289	KC343531	KC343773	KC344015
<i>D. cercidis</i>	CFCC 52565	<i>Cercis chinensis</i>	China	MH121500	MH121424	MH121460	MH121542	MH121582
<i>D. charlesworthii</i>	BRIP 54884m	<i>Rapistrum rugostrum</i>	Australia	KJ197288	NA	NA	KJ197250	KJ197268
<i>D. chrysalidocarpi</i>	SAUCC194.35	<i>Chrysalidocarpus lutescens</i>	China	MT822563	MT855646	MT855532	MT855876	MT855760
<i>D. cinnamomi</i>	CFCC 52569	<i>Cinnamomum</i> sp.	China	MH121504	NA	MH121464	MH121546	MH121586
<i>D. citriasiana</i>	CGMCC 3.15224	<i>Citrus unshiu</i>	China	JQ954645	KC357491	KJ490515	JQ954663	KC357459
<i>D. citrichinensis</i>	CGMCC 3.15225	<i>Citrus</i> sp.	China	JQ954648	KC357494	NA	JQ954666	NA
<i>D. collariana</i>	MFLU 17-2770	<i>Magnolia champaca</i>	Thailand	MG806115	MG783042	NA	MG783040	MG783041
<i>D. conica</i>	CFCC 52571	<i>Alangium chinense</i>	China	MH121506	MH121428	MH121466	MH121548	MH121588
<i>D. cucurbitae</i>	CBS 136.25	<i>Arctium</i> sp.	Unknown	KC343031	KC343273	KC343515	KC343757	KC343999
<i>D. cuppatea</i>	CBS 117499	<i>Aspalathus linearis</i>	South Africa	KC343057	KC343299	KC343541	KC343783	KC344025
<i>D. discoidispora</i>	ZJUD89	<i>Citrus unshiu</i>	China	KJ490624	NA	KJ490566	KJ490503	KJ490445
<i>D. dreuthii</i>	BRIP 66524	<i>Macadamia</i> sp.	South Africa	MN708229	NA	NA	MN696526	MN696537
<i>D. endophytica</i>	CBS 133811	<i>Schinus terebinthifolius</i>	Brazil	KC343065	KC343307	KC343549	KC343791	KC343065
<i>D. eres</i>	AR5193	<i>Ulmus</i> sp.	Germany	KJ210529	KJ434999	KJ420850	KJ210550	KJ420799
<i>D. fraxini-angustifoliae</i>	BRIP 54781	<i>Fraxinus angustifolia</i>	Australia	JX862528	NA	NA	JX862534	KF170920
<i>D. fraxinicola</i>	CFCC 52582	<i>Fraxinus chinensis</i>	China	MH121517	MH121435	NA	MH121559	NA
<i>D. fructicola</i>	MAFF 246408	<i>Passiflora edulis</i> × <i>P. edulis</i> f. <i>flavicarpa</i>	Japan	LC342734	LC342738	LC342737	LC342735	LC342736
<i>D. fusicola</i>	CGMCC 3.17087	<i>Lithocarpus glabra</i>	China	KF576281	KF576233	NA	KF576256	KF576305

Species	Isolate	Host	Location	GenBank accession numbers				
				ITS	<i>cal</i>	<i>his3</i>	<i>tefl</i>	<i>tub2</i>
<i>D. ganzhouensis</i>	CFCC 53087	Unknown	China	MK432665	MK442985	MK443010	MK578139	MK578065
<i>D. garethjonesii</i>	MFLUCC 12-0542a	Unknown dead leaf	Thailand	KT459423	KT459470	NA	KT459457	KT459441
<i>D. guangxiensis</i>	JZB320094	<i>Vitis vinifera</i>	China	MK335772	MK736727	NA	MK523566	MK500168
<i>D. helicis</i>	AR5211	<i>Hedera helix</i>	France	KJ210538	KJ435043	KJ420875	KJ210559	KJ420828
<i>D. heterostemmati</i>	SAUCC194.85	<i>Heterostemma grandiflorum</i>	China	MT822613	MT855692	MT855581	MT855925	MT855810
<i>D. hubeiensis</i>	JZB320123	<i>Vitis vinifera</i>	China	MK335809	MK500235	NA	MK523570	MK500148
	HNZZ009	<i>Camellia oleifera</i>	China	MZ509553	MZ504683	MZ504694	MZ504705	MZ504716
	HNZZ019	<i>Camellia oleifera</i>	China	MZ509554	MZ504684	MZ504695	MZ504706	MZ504717
<i>D. hunanensis</i>	HNZZ023	<i>Camellia oleifera</i>	China	MZ509550	MZ504680	MZ504691	MZ504702	MZ504713
	HNZZ025	<i>Camellia oleifera</i>	China	MZ509551	MZ504681	MZ504692	MZ504703	MZ504714
	HNZZ033	<i>Camellia oleifera</i>	China	MZ509552	MZ5046802	MZ504693	MZ504704	MZ504715
<i>D. kadsurae</i>	CFCC 52586	<i>Kadsura longipedunculata</i>	China	MH121521	MH121439	MH121479	MH121563	MH121600
<i>D. litchicola</i>	BRIP 54900	<i>Litchi chinensis</i>	Australia	JX862533	NA	NA	JX862539	KF170925
<i>D. loniceriae</i>	MFLUCC 17-0963	<i>Lonicera</i> sp.	Italy	KY964190	KY964116	NA	KY964146	KY964073
<i>D. masirevicii</i>	BRIP 57892a	<i>Helianthus annuus</i>	Australia	KJ197277	NA	NA	KJ197239	KJ197257
<i>D. miriciae</i>	BRIP 54736j	<i>Helianthus annuus</i>	Australia	KJ197282	NA	NA	KJ197244	KJ197262
<i>D. momicola</i>	MFLUCC 16-0113	<i>Prunus persica</i>	China	KU557563	KU557611	NA	KU557631	KU557578
<i>D. musigena</i>	CBS 129519	<i>Musa</i> sp.	Australia	KC343143	KC343385	KC343627	KC343869	KC344111
<i>D. neilliae</i>	CBS 144.27	<i>Spiraea</i> sp.	USA	KC343144	KC343386	KC343628	KC343870	KC344112
<i>D. nobilis</i>	CBS 113470	<i>Castanea sativa</i>	Korea	KC343146	KC343388	KC343630	KC343872	KC344114
<i>D. oraccinii</i>	CGMCC 3.17531	<i>Camellia sinensis</i>	China	KP267863	NA	KP293517	KP267937	KP293443
<i>D. ovoicicola</i>	CGMCC 3.17093	<i>Citrus</i> sp.	China	KF576265	KF576223	NA	KF576240	KF576289
<i>D. pandanicola</i>	MFLU 18-0006	<i>Pandanus</i> sp.	Thailand	MG646974	NA	NA	NA	MG646930
<i>D. pascoei</i>	BRIP 54847	<i>Persea americana</i>	Australia	JX862532	NA	NA	JX862538	KF170924
<i>D. passifloricola</i>	CBS 141329	<i>Passiflora foetida</i>	Malaysia	KX228292	NA	KX228367	NA	KX228387
<i>D. penetriteum</i>	CGMCC 3.17532	<i>Camellia sinensis</i>	China	KP714505	NA	KP714493	KP714517	KP714529
<i>D. perseae</i>	CBS 151.73	<i>Persea gratissima</i>	Netherlands	KC343173	KC343415	KC343657	KC343899	KC344141
<i>D. pescicola</i>	MFLUCC 16-0105	<i>Prunus persica</i>	China	KU557555	KU557603	NA	KU557623	KU557579
<i>D. pseudomangiferae</i>	CBS 101339	<i>Mangifera indica</i>	Dominican Republic	KC343181	KC343423	KC343665	KC343907	KC344149
<i>D. pseudophoenicicola</i>	CBS 462.69	<i>Phoenix dactylifera</i>	Spain	KC343184	KC343426	KC343668	KC343910	KC344152
<i>D. pulla</i>	CBS 338.89	<i>Hedera helix</i>	Yugoslavia	KC343152	KC343394	KC343636	KC343878	KC344120
<i>D. racemosae</i>	CBS 143770	<i>Euclia racemosa</i>	South Africa	MG600223	MG600219	MG600221	MG600225	MG600227
<i>D. schimae</i>	CFCC 53103	<i>Schima superba</i>	China	MK432640	MK442962	MK442987	MK578116	MK578043
<i>D. schini</i>	CBS 133181	<i>Schinus terebinthifolius</i>	Brazil	KC343191	KC343433	KC343675	KC343917	KC344159
<i>D. schoeni</i>	MFLU 15-1279	<i>Schoenus nigricans</i>	Italy	KY964226	KY964139	NA	KY964182	KY964109
<i>D. searlei</i>	BRIP 66528	<i>Macadamia</i> sp.	South Africa	MN708231	NA	NA	NA	MN696540

Species	Isolate	Host	Location	GenBank accession numbers				
				ITS	<i>cal</i>	<i>his3</i>	<i>tefl</i>	<i>tub2</i>
<i>D. sennicola</i>	CFCC 51634	<i>Senna bicapsularis</i>	China	KY203722	KY228873	KY228879	KY228883	KY228889
<i>D. siamensis</i>	MFLUCC 10-573a	<i>Dasymaschalos</i> sp.	Thailand	JQ619879	NA	NA	JX275393	JX275429
<i>D. sojae</i>	FAU635	<i>Glycine max</i>	USA	KJ590719	KJ612116	KJ659208	KJ590762	KJ610875
	HNZZ008	<i>Camellia oleifera</i>	China	MZ509547	MZ504677	MZ504688	MZ504699	MZ504710
	HNZZ010	<i>Camellia oleifera</i>	China	MZ509548	MZ504678	MZ504689	MZ504700	MZ504711
	HNZZ022	<i>Camellia oleifera</i>	China	MZ509549	MZ504679	MZ504690	MZ504701	MZ504712
<i>D. spinosa</i>	PSCG	<i>Pyrus pyrifolia</i>	China	MK626849	MK691129	MK726156	MK654811	MK691234
<i>D. sterilis</i>	CBS 136969	<i>Vaccinium corymbosum</i>	Italy	KJ160579	KJ160548	MF418350	KJ160611	KJ160528
<i>D. subclavata</i>	ICMP20663	<i>Citrus unshiu</i>	China	KJ490587	NA	KJ490529	KJ490466	KJ490408
<i>D. subellipicola</i>	MFLU 17-1197	on dead wood	China	MG746632	NA	NA	MG746633	MG746634
<i>D. subordinaria</i>	CBS 464.90	<i>Plantago lanceolata</i>	New Zealand	KC343214	KC343456	KC343698	KC343940	KC344182
<i>D. taioicola</i>	MFLUCC 16-0117	<i>Prunus persica</i>	China	KU557567	NA	NA	KU557635	KU557591
<i>D. tectonae</i>	MFLUCC 12-0777	<i>Tectona grandis</i>	Thailand	KU712430	KU749345	NA	KU749359	KU743977
<i>D. tectonendophytica</i>	MFLUCC 13-0471	<i>Tectona grandis</i>	Thailand	KU712439	KU749354	NA	KU749367	KU749354
<i>D. tectonigena</i>	MFLUCC 12-0767	<i>Tectona grandis</i>	Thailand	KU712429	KU749358	NA	KU749371	KU743976
<i>D. terebinthifolii</i>	CBS 133180	<i>Schinus terebinthifolius</i>	Brazil	KC343216	KC343458	KC343700	KC343942	KC344184
<i>D. tibetensis</i>	CFCC 51999	<i>Juglandis regia</i>	China	MF279843	MF279888	MF279828	MF279858	MF279873
<i>D. tulliensis</i>	BRIP 62248a	<i>Theobroma cacao</i>	Australia	KR936130	NA	NA	KR936133	KR936132
<i>D. ukurunduensis</i>	CFCC 52592	<i>Acer ukurunduense</i>	China	MH121527	MH121445	MH121485	MH121569	NA
<i>D. unshiuensis</i>	CGMCC 3.17569	<i>Citrus unshiu</i>	China	KJ490587	NA	KJ490529	KJ490408	KJ490466
	CFCC 52594	<i>Carya ilinoensis</i>	China	MH121529	MH121447	MH121487	MH121571	MH121606
<i>D. viniferae</i>	JZB320071	<i>Vitis vinifera</i>	China	MK341551	MK500107	NA	MK500119	MK500112
<i>D. xishuangbanica</i>	CGMCC 3.18282	<i>Camellia sinensis</i>	China	KX986783	NA	KX999255	KX999175	KX999216
<i>D. yunnanensis</i>	CGMCC 3.18289	<i>Coffea</i> sp.	China	KX986796	KX999290	KX999267	KX999188	KX999228
<i>Diaporthebella corylina</i>	CBS 121124	<i>Corylus</i> sp.	China	KC343004	KC343246	KC343488	KC343730	KC343972

Note: NA, not applicable. Strains in this study are marked in bold.

Results

Phylogenetic analyses

The five-gene sequence dataset (ITS, *cal*, *his3*, *tefl* and *tub2*) was analysed to infer the interspecific relationships within *Diaporthe*. The dataset consisted of 96 sequences including the outgroup taxon, *Diaporthebella corylina* (CBS 121124). A total of 2520 characters including gaps (510 for ITS, 518 for *cal*, 533 for *his3*, 460 for *tefl* and 499 for *tub2*) were included in the phylogenetic analysis. The best nucleotide substitution

model for ITS, *his3* and *tub2* was TrN+I+G, while HKY+I+G was selected for both *cal* and *tef1*. The topologies resulting from ML and BI analyses of the concatenated dataset were congruent (Fig. 1). According to the phylogenetic tree, two known species, *D. hubeiensis* and *D. sojiae*, were part of *Diaporthe*. *Diaporthe camelliae-oleiferae* and *D. hunanensis* are new to science based on the distinct and well-supported molecular phylogenetic placement with their closest described relatives. Phylogenetically, *D. camelliae-oleiferae* clustered together with *D. pandanicola* and *D. viniferae*. *Diaporthe hunanensis* clustered together with *D. chrysalidocarpi* and other species, including *D. drethii*, *D. searlei* and *D. spinosa*.

Taxonomy

Diaporthe camelliae-oleiferae Q. Yang, sp. nov.

Mycobank No: 840451

Figure 2

Diagnosis. Distinguished from the phylogenetically closely-related species, *D. pandanicola* and *D. viniferae* based on DNA sequence data.

Etymology. Named after the host species, *Camellia oleifera*.

Description. Asexual morph: *pycnidia* on PDA 500–660 µm in diam., superficial, scattered on PDA, dark brown to black, globose, solitary, or clustered in groups of 3–5 *pycnidia*. Pale yellow conidial drops exuding from ostioles. *Conidiophores* reduced to conidiogenous cells. *Conidiogenous cells* (7.5–)10–14(–15.5) × 1.5–2.3 µm (n = 30), aseptate, cylindrical, straight, densely aggregated, terminal, slightly tapered toward the apex. *Alpha conidia* 5–6.5(–7.5) × 1.9–2.3 µm (n = 30), aseptate, hyaline, ellipsoidal to fusiform, biguttulate. *Beta conidia* (26.5–)28.5–31(–33) × 0.8–1.2 µm (n = 30), hyaline, aseptate, filiform, sinuous at one end, eguttulate.

Culture characters. Culture incubated on PDA at 25 °C, originally flat with white fluffy aerial mycelium, becoming brown to black in the centre, with yellowish-cream conidial drops exuding from the ostioles after 20 days.

Specimens examined. CHINA. Hunan Province: Zhuzhou City, on leaves of *Camellia oleifera*, 27°2'41"N, 113°19'17"E, 14 Aug. 2020, Q. Yang (holotype CSUFT027; ex-type living culture: HNZZ027; other living cultures: HNZZ030 and HNZZ032).

Notes. Three isolates representing *D. camelliae-oleiferae* cluster in a well-supported clade (ML/BI=100/1) and appear most closely related to *D. pandanicola* on *Pandanus* sp. and *D. viniferae* on *Vitis vinifera*. *Diaporthe camelliae-oleiferae* can be distinguished from *D. pandanicola* based on ITS and *tub2* loci (24/462 in ITS and 11/401 in *tub2*); from *D. viniferae* based on ITS, *cal*, *tef1* and *tub2* loci (13/453 in ITS, 42/448 in *cal*, 7/339 in *tef1* and 26/402 in *tub2*). Morphologically, *D. camelliae-oleiferae* differs from *D. viniferae* in having shorter alpha conidia (5–6.5 µm vs. 5–8.3 µm) (Manawasinghe et al. 2019); from *D. pandanicola* in having narrower alpha conidia (1.9–2.3 µm vs. 2.5–3.2 µm) (Huang et al. 2021).

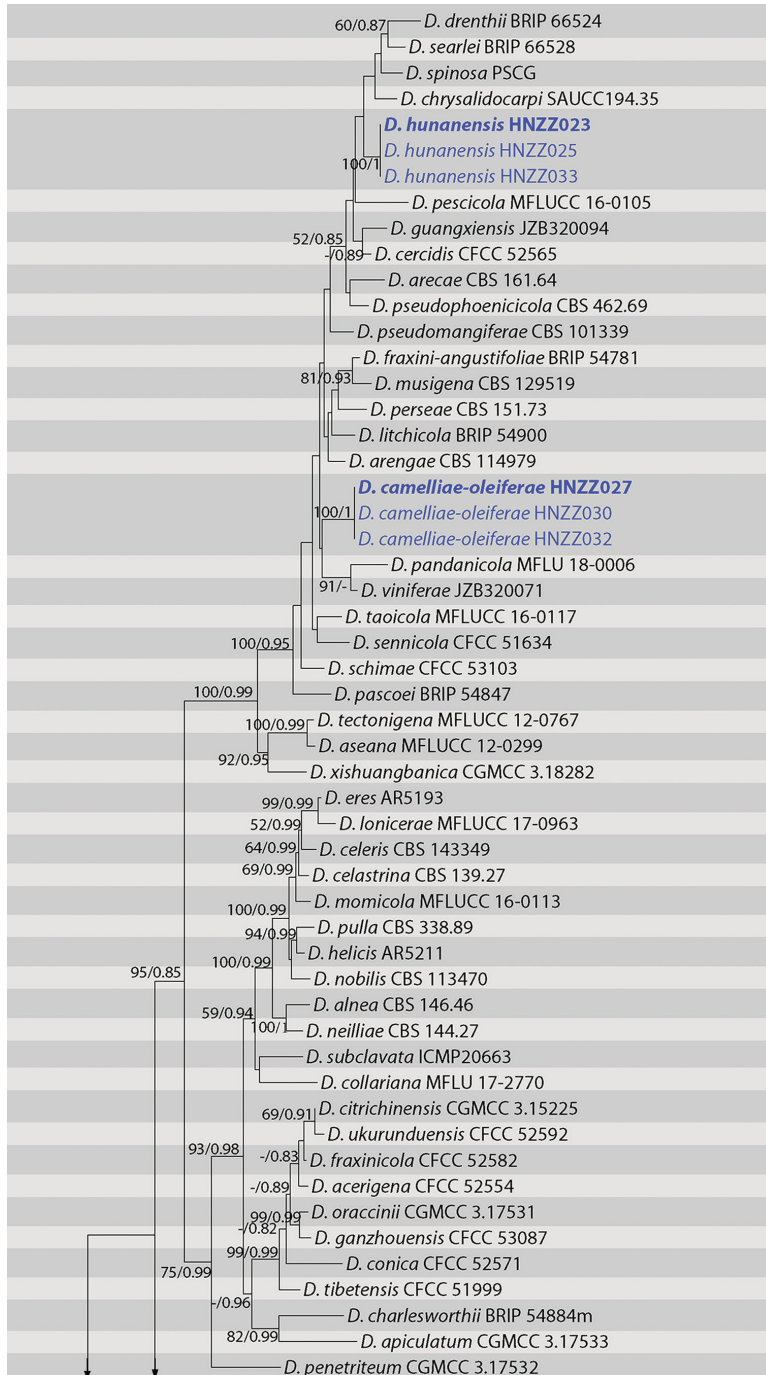


Figure 1. Phylogram of *Diaporthe* resulting from a maximum likelihood analysis based on combined ITS, *cal*, *his3*, *tef1* and *tub2*. Numbers above the branches indicate ML bootstraps (left, ML BS $\geq 50\%$) and Bayesian Posterior Probabilities (right, BPP ≥ 0.75). The tree is rooted with *Diaporthella corylina*. Isolates in current study are in blue. “-” indicates ML BS $< 50\%$ or BI PP < 0.75 .

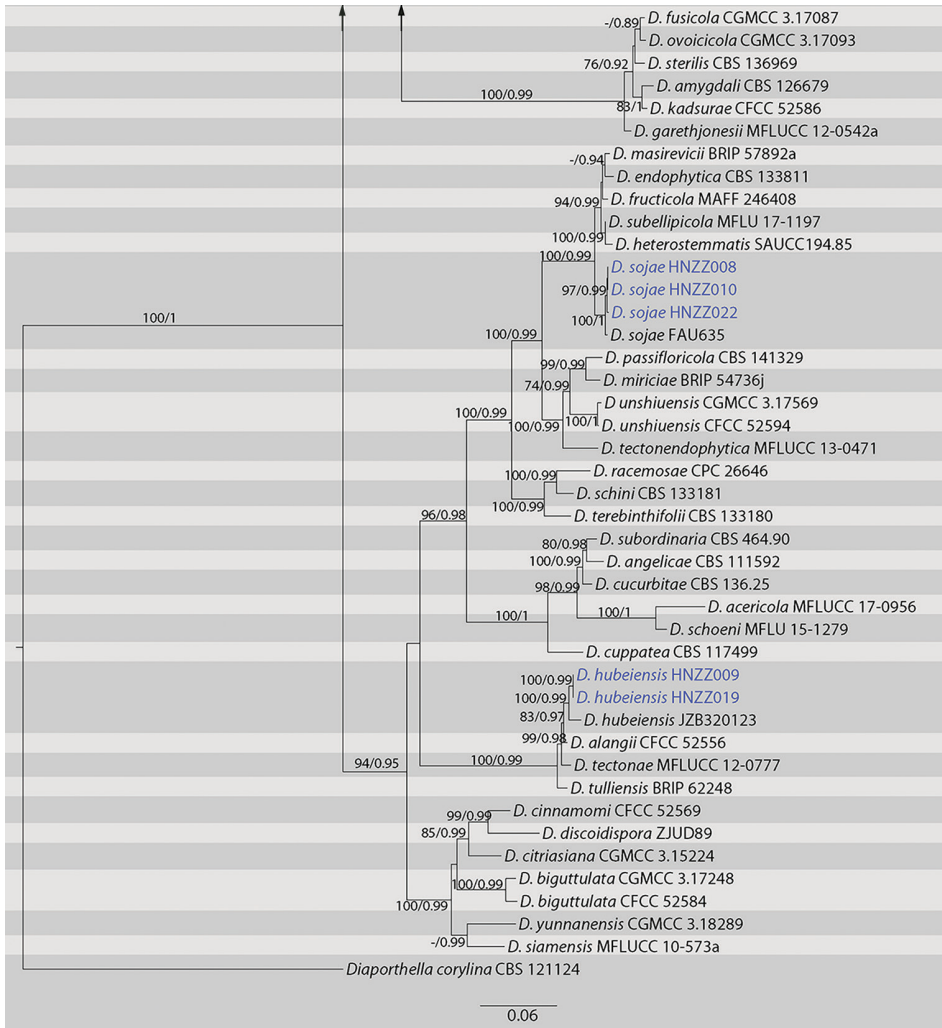


Figure 1. Continued

Diaporthe hubeiensis Dissanayake, X.H. Li & K.D. Hyde

Figure 3

Manawasinghe, Dissanayake, Li, Liu, Wanasinghe, Xu, Zhao, Zhang, Zhou, Hyde, Brooks & Yan, *Frontiers in Microbiology* 10(no. 1936): 20 (2019)

Description. Asexual morph: *pycnidia* on PDA in culture, 700–885 μm in diam., superficial, scattered, dark brown to black, globose or subglobose. *Conidiophores* reduced to conidiogenous cells. *Conidiogenous cells* (6.5–)7–10(–11.5) \times 2–3.5 μm (n = 30), aseptate, cylindrical, phialidic, straight or slightly curved. *Alpha conidia* 5.8–8(–8.5) \times 2.5–3.2 μm (n = 30), aseptate, hyaline, ellipsoidal to cylindrical, biguttulate, blunt at both ends. *Beta conidia* not observed.

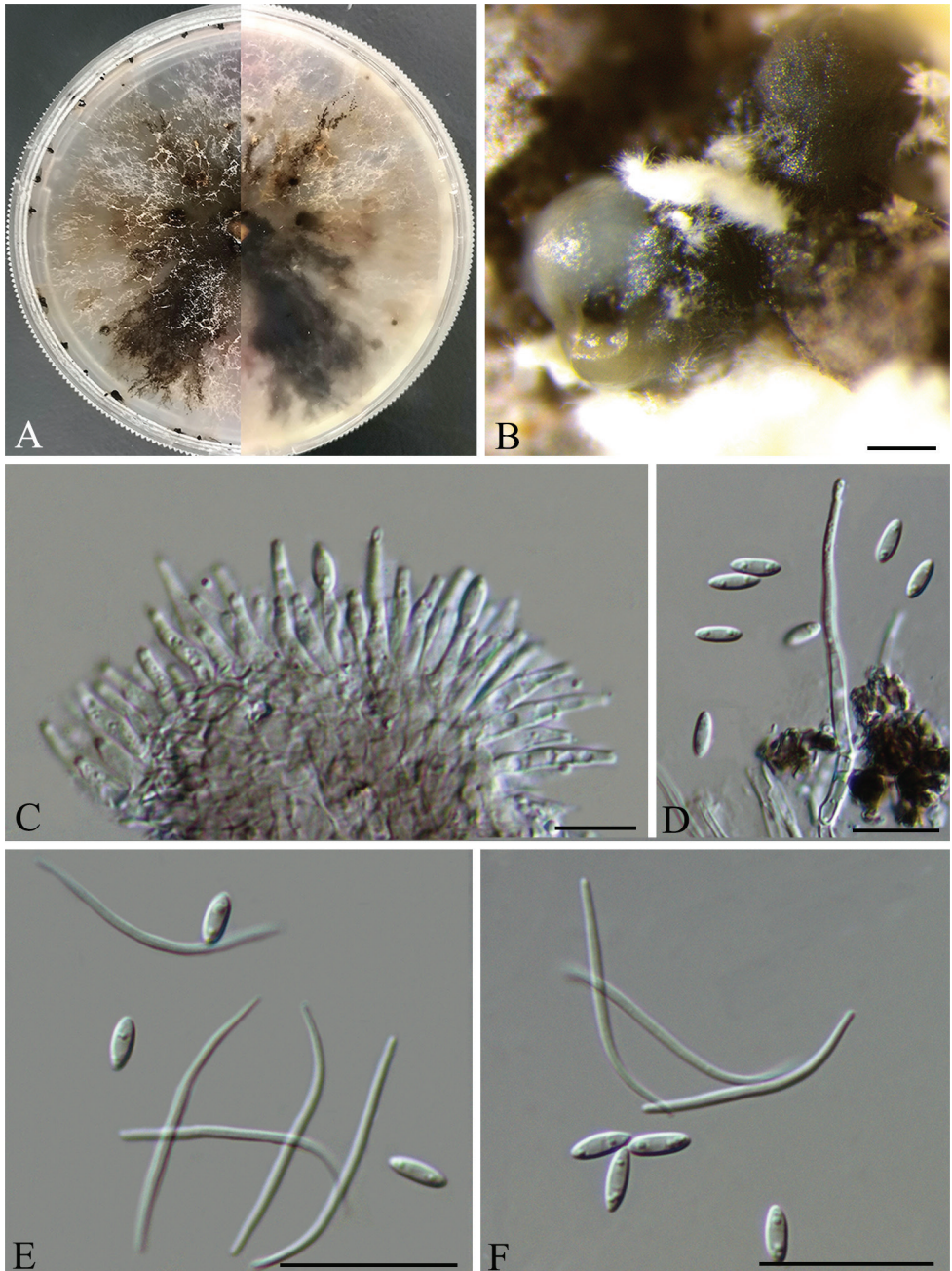


Figure 2. *Diaporthe camelliae-oleiferae* (HNZZ027) **A** Culture on PDA **B** conidiomata **C** conidiogenous cells **D–F** alpha and beta conidia. Scale bars: 200 μm (**B**); 10 μm (**C–D**); 20 μm (**E, F**).

Culture characters. Culture incubated on PDA at 25 °C, originally flat with white felted aerial mycelium, becoming dark brown mycelium due to pigment formation, conidiomata irregularly distributed over agar surface after 20 days.

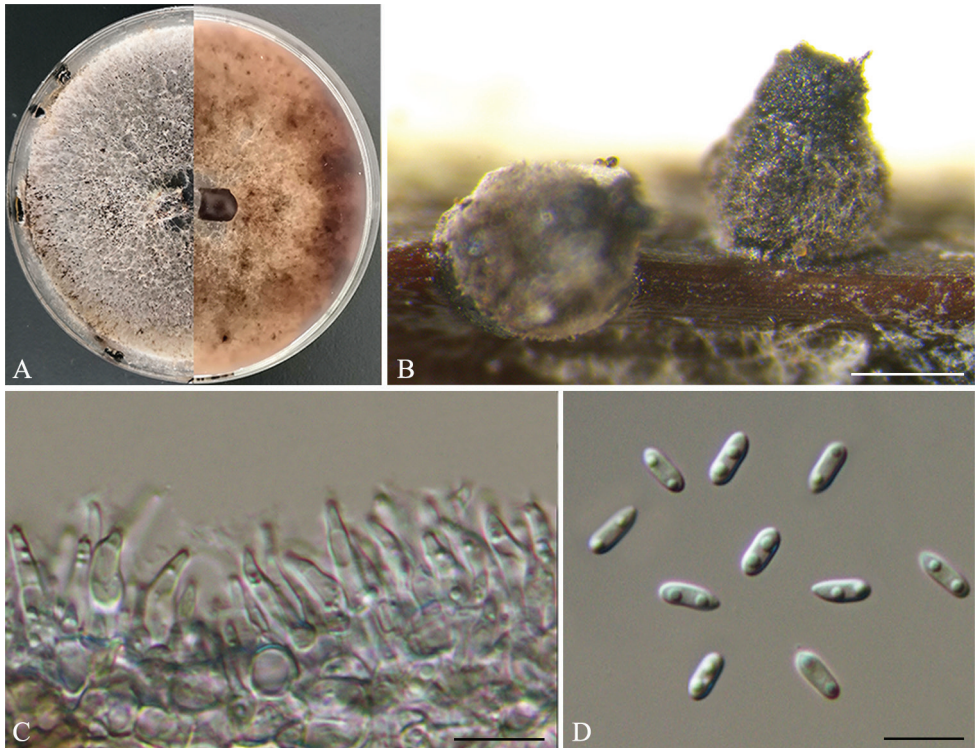


Figure 3. *Diaporthe hubeiensis* (HNZZ019) **A** Culture on PDA **B** conidiomata **C** conidiogenous cells **D** alpha conidia. Scale bars: 500 μm (**B**); 10 μm (**C–D**).

Specimens examined. CHINA. Hunan Province: Zhuzhou City, on leaves of *Cammellia oleifera*, 27°2'35"N, 113°19'20"E, 14 Aug. 2020, Q. Yang (CSUFT019; living cultures: HNZZ019 and HNZZ009).

Notes. *Diaporthe hubeiensis* was originally described as pathogen of grapevines in Hubei Province, China (Manawasinghe et al. 2019). In the present study, two isolates (HNZZ019 and HNZZ009) are closely related to *D. hubeiensis* in the combined phylogenetic tree (Fig. 1). The differences of nucleotides in the concatenated alignment (1/460 in ITS, 3/458 in *cal*, 1/320 in *his3* and 3/433 in *tub2*) are minor. Morphological comparison indicated that the isolates were similar to *D. hubeiensis* by the size of alpha conidia. We therefore identify the isolates as belonging to *D. hubeiensis*.

***Diaporthe hunanensis* Q. Yang, sp. nov.**

Mycobank No: 840452

Figure 4

Diagnosis. Distinguished from its phylogenetically closely-related species, *D. chrysalidocarpi*, *D. drenthii*, *D. searlei* and *D. spinosa* based on DNA sequence data.

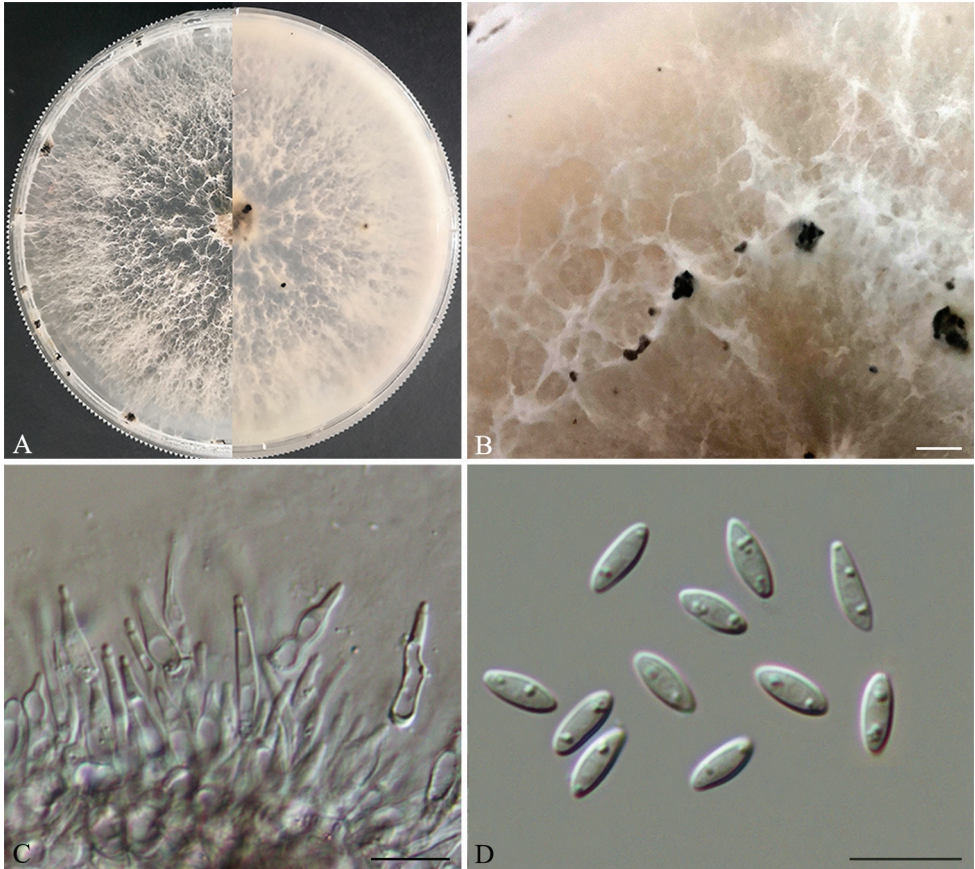


Figure 4. *Diaporthe hunanensis* (HNZZ023) **A** Culture on PDA **B** conidiomata **C** conidiogenous cells **D** alpha conidia. Scale bars: 500 μ m (**B**); 10 μ m (**C–D**).

Etymology. In reference to the Hunan province, from where the fungus was first collected.

Description. Asexual morph: *pycnidia* on PDA 180–300 μ m in diam., superficial, scattered, black, globose, solitary in most. *Conidiophores* reduced to conidiogenous cells. *Conidiogenous cells* (8–)9–15(–16.5) \times 1.7–2.1 μ m ($n = 30$), aseptate, cylindrical, phialidic, straight or slightly curved. *Alpha conidia* 6.5–7.5(–8.5) \times 2.4–2.9 μ m ($n = 30$), aseptate, hyaline, ellipsoidal, biguttulate, both ends obtuse. *Beta conidia* not observed.

Culture characters. Culture incubated on PDA at 25 $^{\circ}$ C, originally flat with white fluffy aerial mycelium, becoming pale brown with age, with visible solitary conidiomata at maturity after 18 days.

Specimens examined. CHINA. Hunan Province: Zhuzhou City, on leaves of *Camellia oleifera*, 27 $^{\circ}$ 2'41"N, 113 $^{\circ}$ 19'17"E, 14 Aug. 2020, Q. Yang (holotype CSUFT 023; ex-type living culture: HNZZ023; living cultures: HNZZ025 and HNZZ033).

Notes. Three isolates representing *D. hunanensis* cluster in a well-supported clade (ML/Bi=100/1) and appear most closely related to *D. chrysalidocarpi* on *Chrysalidocarpus lutescens*, *D. drenthii* and *D. searlei* on *Macadamia* sp., and *D. spinosa* on *P. pyrifolia* cv. Cuiguan. *Diaporthe hunanensis* can be distinguished from *D. chrysalidocarpi* based on ITS, *cal*, *his3* and *tub2* loci (7/457 in ITS, 28/448 in *cal*, 8/455 in *his3* and 5/401 in *tub2*); from *D. drenthii* based on ITS, *tef1* and *tub2* loci (9/457 in ITS, 13/328 in *tef1* and 23/401 in *tub2*); from *D. searlei* based on ITS and *tub2* loci (10/457 in ITS and 12/401 in *tub2*); from *D. spinosa* based on ITS, *cal*, *his3*, *tef1* and *tub2* loci (8/458 in ITS, 31/448 in *cal*, 5/455 in *his3*, 8/328 in *tef1* and 19/401 in *tub2*). Morphologically, *D. chrysalidocarpi* produces only beta conidia, while *D. hunanensis* produces alpha conidia (Huang et al. 2021); *D. hunanensis* differs from *D. drenthii* and *D. searlei* in wider alpha conidia (2.4–2.9 µm in *D. hunanensis* vs. 1.5–2.5 µm in *D. drenthii* vs. 1.5–2 µm in *D. searlei*) (Wrona et al. 2020); from *D. spinosa* in shorter alpha conidia (6.5–7.5 × 2.4–2.9 µm vs. 5.5–8 × 2–3.5 µm) (Guo et al. 2020). Therefore, we establish this fungus as a novel species.

***Diaporthe sojae* Lehman, Ann. Mo. bot. Gdn 10: 128 (1923)**

Figure 5

Description. Sexual morph: *perithecia* on pine needles in culture, black, globose, 250–500 µm in diam., densely clustered in groups, deeply immersed with elongated, tapering perithecial necks protruding through substrata, 525–800 µm. *Asci* unitunicate, 8-spored, sessile, elongate to clavate, (35–)37–42(–44.5) × (8–)10–11.5 µm (n = 30). *Ascospores* hyaline, two-celled, often 4-guttulate, with larger guttules at centre and smaller one at ends, elongated to elliptical, slightly or not constricted at septum, (9–)9.5–11.5 × 2.7–4 µm (n = 30). Asexual morph not observed.

Culture characters. Culture incubated on PNA at 25 °C, originally white, fluffy aerial mycelium, reverse yellowish pigmentation developing in centre, later becoming dark brown, with yellowish-cream drops exuding from the perithecia after 15 days.

Specimens examined. CHINA. Hunan Province: Zhuzhou City, on leaves of *Camellia oleifera*, 27°2'41"N, 113°19'17"E, 14 Aug. 2020, Q. Yang (USUFT 022; living cultures: HNZZ022, HNZZ008 and HNZZ010).

Notes. *Diaporthe sojae* was first reported on pods and stems of soybean, and subsequently reported on a wide range of hosts (Dissanayake et al. 2015; Udayanga et al. 2015; Guo et al. 2020). It was also reported on some fruit trees in China, such as *Vitis* spp. (Dissanayake et al. 2015) and *Citrus* spp. (Huang et al. 2015). In the present, three isolates (HNZZ008, HNZZ010 and HNZZ022) are closely related to *D. sojae* in the combined phylogenetic tree (Fig. 1). The differences of nucleotides in the concatenated alignment (1/460 in ITS, 3/458 in *cal*, 1/320 in *his3* and 3/433 in *tub2*) are minor. Compared with the description of the ex-type isolate FAU635, the isolate has wider asci (10–11.5 µm vs. 7–9 µm) (Udayanga et al. 2015). We therefore identify the isolates as belonging to *D. sojae*.

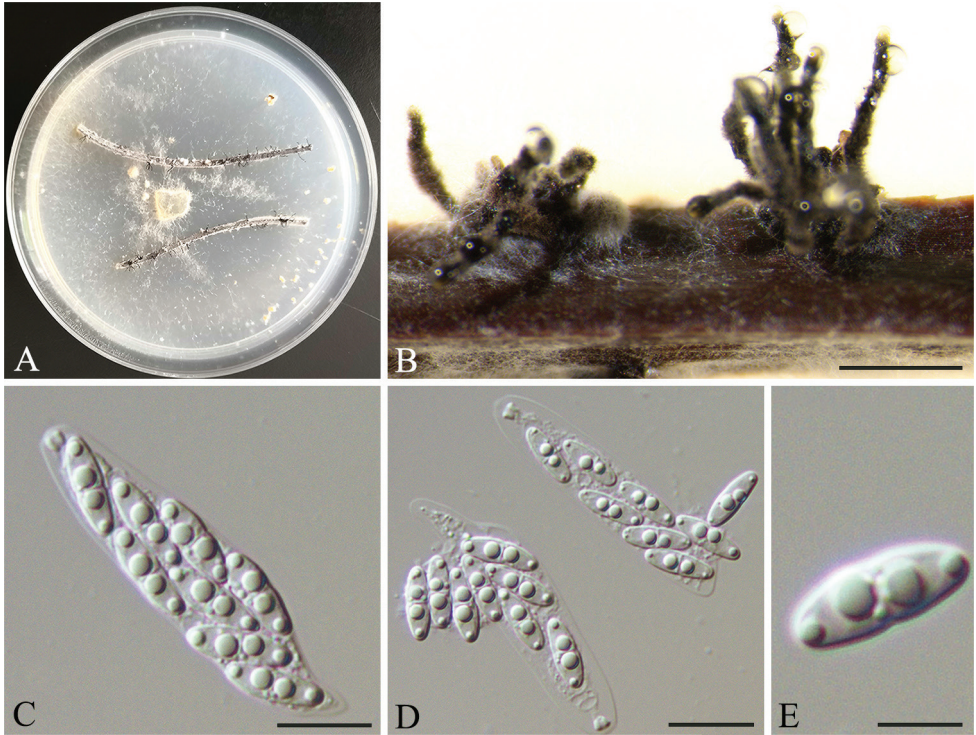


Figure 5. *Diaporthe sojae* (HNZZ022) **A** Culture on PNA **B** ascomata **C–E** asci and ascospores. Scale bars: 500 μm (**B**); 10 μm (**C–E**).

Discussion

In this study, an important oil-tea tree species, *Camellia oleifera* was investigated and *Camellia* leaf disease was found as a common disease in plantations in Hunan Province. Identification of our collections was conducted, based on isolates from symptomatic leaves of *C. oleifera* using five combined loci (ITS, *cal*, *his3*, *tef1* and *tub2*), as well as morphological characters. It includes *D. hubeiensis*, *D. sojae*, as well as two new species named *D. camelliae-oleiferae* and *D. hunanensis*.

The expanding cultivation of *C. oleifera* over the last several decades has attracted increasing attention from plant pathologists to infectious diseases on this crop. Therein, diseases caused by *Diaporthe* species have becoming the emerging *Camellia* leaf diseases in southern China (Gao et al. 2016; Guarnaccia et al. 2018; Yang et al. 2018; Zhou and Hou 2019). Understanding the diversity of *Diaporthe* species and the genetic variation within pathogen populations could help in developing sustainable disease management strategies.

According to the USDA Fungal–host interaction database, there are two records of *Diaporthe* species associated with *C. oleifera* (<https://nt.ars-grin.gov/fungal-databases/fungushost/fungushost.cfm>) (accessed 9 September 2021). These records are related

to the following two *Diaporthe* species: *D. eres* and *D. huangshanensis* (Zhou and Hou 2019). *Diaporthe eres*, the type species of the genus, was described by Nitschke (1870) on *Ulmus* sp. collected in Germany, which has a widespread distribution and a broad host range as pathogens, endophytes or saprobes (Udayanga et al. 2014b). *Diaporthe eres* differs from *D. camelliae-oleiferae* and *D. hunanensis* in having wider alpha conidia (3–4 µm in *D. eres* vs. 1.9–2.3 µm in *D. camelliae-oleiferae* vs. 2.4–2.9 µm in *D. hunanensis*) (Gomes et al. 2003); *D. huangshanensis* differs from *D. camelliae-oleiferae* in having larger alpha conidia (5.7–8.4 × 2.7–4.5 µm vs. 5–6.5 × 1.9–2.3 µm); from *D. hunanensis* in having wider alpha conidia (2.7–4.5 µm vs. 2.4–2.9 µm) and longer conidiophores (12.1–23.5 µm vs. 9–15 µm) (Zhou and Hou 2019).

As the species concept of *Diaporthe* has been improved a lot by using molecular data (Huang et al. 2015; Gao et al. 2016, 2017; Guarnaccia and Crous 2017; Guarnaccia et al. 2018; Yang et al. 2018, 2020, 2021; Manawasinghe et al. 2019; Guo et al. 2020), many new species have been discovered and reported in recent years. In this study, the *Diaporthe* isolates from *C. oleifera* were identified based on sequence analysis and morphological characteristics. Future studies should focus on pathogenicity, epidemiology and fungicide sensitivity of the important plant fungal pathogen to develop effective management of *C. oleifera* disease and on the pathogenic molecular mechanism.

Acknowledgements

This study is financed by the Research Foundation of Education Bureau of Hunan Province, China (Project No.: 19B608) and the introduction of talent research start-up fund project of CSUFT (Project No.: 2019YJ025).

References

- Carbone I, Kohn LM (1999) A method for designing primer sets for speciation studies in filamentous ascomycetes. *Mycologia* 3: 553–556. <https://doi.org/10.2307/3761358>
- Crous PW, Gams W, Stalpers JA, Robert V, Stegehuis G (2004a) MycoBank: an online initiative to launch mycology into the 21st century. *Studies in Mycology* 50: 19–22.
- Crous PW, Groenewald JZ, Risède JM, Simoneau P, Hywel-Jones NL (2004b) *Calonectria* species and their *Cylindrocladium* anamorphs: species with sphaeropedunculate vesicles. *Studies in Mycology* 50: 415–430.
- Darriba D, Taboada GL, Doallo R, Posada D (2012) jModelTest 2: more models, new heuristics and parallel computing. *Nature Methods* 9: 772–772. <https://doi.org/10.1038/nmeth.2109>
- Desjardins P, Hansen JB, Allen M (2009) Microvolume protein concentration determination using the NanoDrop 2000c spectrophotometer. *Journal of Visualized Experiments: JoVE* 33: 1–3. <https://doi.org/10.3791/1610>
- Diogo E, Santos JM, Phillips AJ (2010) Phylogeny, morphology and pathogenicity of *Diaporthe* and *Phomopsis* species on almond in Portugal. *Fungal Diversity* 44: 107–115. <https://doi.org/10.1007/s13225-010-0057-x>

- Doyle JJ, Doyle JL (1990) Isolation of plant DNA from fresh tissue. *Focus* 12: 13–15. <https://doi.org/10.2307/2419362>
- Erincik O, Madden L, Ferree D, Ellis M (2001) Effect of growth stage on susceptibility of grape berry and rachis tissues to infection by *Phomopsis viticola*. *Plant Disease* 85: 517–520. <https://doi.org/10.1094/PDIS.2001.85.5.517>
- Gao YH, Liu F, Cai L (2016) Unravelling *Diaporthe* species associated with *Camellia*. *Systematics and Biodiversity* 14: 102–117. <https://doi.org/10.1080/14772000.2015.1101027>
- Gao YH, Liu F, Duan W, Crous PW, Cai L (2017) *Diaporthe* is paraphyletic. *IMA Fungus* 8: 153–187. <https://doi.org/10.5598/imafungus.2017.08.01.11>
- Gomes RR, Glienke C, Videira SIR, Lombard L, Groenewald JZ, Crous PW (2013) *Diaporthe*: a genus of endophytic, saprobic and plant pathogenic fungi. *Persoonia* 31: 1–41. <https://doi.org/10.3767/003158513X666844>
- Guarnaccia V, Crous PW (2017) Emerging citrus diseases in Europe caused by species of *Diaporthe*. *IMA Fungus* 8: 317–334. <https://doi.org/10.5598/imafungus.2017.08.02.07>
- Guarnaccia V, Crous PW (2018) Species of *Diaporthe* on *Camellia* and *Citrus* in the Azores Islands. *Phytopathologia Mediterranea* 57: 307–319.
- Guarnaccia V, Groenewald JZ, Woodhall J, Armengol J, Cinelli T, Eichmeier A, Ezra D, Fontaine F, Gramaje D, Gutierrez-Aguirregabiria A, Kaliterna J, Kiss L, Laignon P, Luque J, Mugnai L, Naor V, Raposo R, Sándor E, Váczy KZ, Crous PW (2018) *Diaporthe* diversity and pathogenicity revealed from a broad survey of grapevine diseases in Europe. *Persoonia* 40: 135–153. <https://doi.org/10.3767/persoonia.2018.40.06>
- Guindon S, Dufayard JF, Lefort V, Anisimova M, Hordijk W, Gascuel O (2010) New algorithms and methods to estimate maximum-likelihood phylogenies: assessing the performance of PhyML 3.0. *Systematic Biology* 59: 307–321. <https://doi.org/10.1093/sysbio/syq010>
- Guo YS, Crous PW, Bai Q, Fu M, Yang MM, Wang XH, Du YM, Hong N, Xu WX, Wang GP (2020) High diversity of *Diaporthe* species associated with pear shoot canker in China. *Persoonia* 45: 132–162. <https://doi.org/10.3767/persoonia.2020.45.05>
- Hall T (1999) BioEdit: a user-friendly biological sequence alignment editor and analysis program for Windows 95/98/NT. *Nucleic Acids Symposium Series* 41: 95–98.
- Hewitt W, Pearson R (1988) *Phomopsis* cane and leaf spot. *Compendium of grape diseases*: 17–18. APS Press, St Paul, Minnesota.
- Huang F, Udayanga D, Wang X, Hou X, Mei X, Fu Y, Hyde KD, Li HY (2015) Endophytic *Diaporthe* associated with *Citrus*: A phylogenetic reassessment with seven new species from China. *Fungal Biology* 119: 331–347. <https://doi.org/10.1016/j.funbio.2015.02.006>
- Huang ST, Xia JW, Zhang XG, Sun WX (2021) Morphological and phylogenetic analyses reveal three new species of *Diaporthe* from Yunnan, China. *Mycology* 78: 49–77. <https://doi.org/10.3897/mycokeys.78.60878>
- Katoh K, Toh H (2010) Parallelization of the MAFFT multiple sequence alignment program. *Bioinformatics* 26: 1899–1900. <https://doi.org/10.1093/bioinformatics/btq224>
- Li H, Zhu XD, Liu JA, Xu JP (2014) Population genetic structure of *Colletotrichum gloeosporioides* causing anthracnose of *Camellia oleifera* in China. *Acta Phytopathologica Sinica* 44: 620–628.
- Lombard L, Van Leeuwen GCM, Guarnaccia V, Polizzi G, Van Rijswijk PC, Karin Rosendahl KC, Gabler J, Crous PW (2014) *Diaporthe* species associated with *Vaccinium*, with specific reference to Europe. *Phytopathologia Mediterranea* 53: 287–299.

- Manawasinghe IS, Dissanayake AJ, Li X, Liu M, Wanasinghe DN, Xu J, Zhao W, Zhang W, Zhou Y, Hyde KD, Brooks S, Yan J (2019) High genetic diversity and species complexity of *Diaporthe* associated with grapevine dieback in China. *Frontiers in Microbiology* 10: e1936. <https://doi.org/10.3389/fmicb.2019.01936>
- Mondal SN, Vincent A, Reis RF, Timmer LW (2007) Saprophytic colonization of citrus twigs by *Diaporthe citri* and factors affecting pycnidial production and conidial survival. *Plant Disease* 91: 387–392. <https://doi.org/10.1094/PDIS-91-4-0387>
- Mostert L, Crous PW, Kang JC, Phillips AJ (2001) Species of *Phomopsis* and a *Libertella* sp. occurring on grapevines with specific reference to South Africa: morphological, cultural, molecular and pathological characterization. *Mycologia* 93: 146–167. <https://doi.org/10.2307/3761612>
- O'Donnell K, Cigelnik E (1997) Two divergent intragenomic rDNA ITS2 types within a monophyletic lineage of the fungus *Fusarium* are nonorthologous. *Molecular Phylogenetics and Evolution* 7: 103–116. <https://doi.org/10.1006/mpev.1996.0376>
- Rambaut A, Drummond A (2010) FigTree v.1.3.1. Institute of Evolutionary Biology, University of Edinburgh, Edinburgh.
- Rayner RW (1970) A mycological colour chart. Commonwealth Mycological Institute, Kew.
- Rehner SA, Uecker FA (1994) Nuclear ribosomal internal transcribed spacer phylogeny and host diversity in the coelomycete *Phomopsis*. *Canadian Journal of Botany* 72: 1666–1674. <https://doi.org/10.1139/b94-204>
- Ronquist F, Huelsenbeck JP (2003) MrBayes 3: Bayesian phylogenetic inference under mixed models. *Bioinformatics* 19: 1572–1574. <https://doi.org/10.1093/bioinformatics/btg180>
- Santos JM, Phillips AJL (2009) Resolving the complex of *Diaporthe* (*Phomopsis*) species occurring on *Foeniculum vulgare* in Portugal. *Fungal Diversity* 34: 111–125.
- Santos JM, Vrandečić K, Čosić J, Duvnjak T, Phillips AJL (2011) Resolving the *Diaporthe* species occurring on soybean in Croatia. *Persoonia* 27: 9–19. <https://doi.org/10.3767/003158511X603719>
- Smith H, Wingfeld MJ, Coutinho TA, Crous PW (1996) *Sphaeropsis sapinea* and *Botryosphaeria dothidea* endophytic in *Pinus* spp. and *Eucalyptus* spp. in South Africa. *South African Journal of Botany* 62: 86–88. [https://doi.org/10.1016/S0254-6299\(15\)30596-2](https://doi.org/10.1016/S0254-6299(15)30596-2)
- Tan XF, Guan TQ, Yuan J (2018) Report on upgrading output value of oil-tea industry to 100 billion RMB in Hunan. *Non-wood Forest Research* 36: 1–4.
- Tibpromma S, Hyde KD, Bhat JD, Mortimer PE, Xu J, Promputtha I, Doilom M, Yang JB, Tang AMC, Karunaratna SC (2018) Identification of endophytic fungi from leaves of Pandanaceae based on their morphotypes and DNA sequence data from southern Thailand. *MycKeys* 33: 25–67. <https://doi.org/10.3897/mycokeys.33.23670>
- Udayanga D, Castlebury LA, Rossman AY, Chukeatirote E, Hyde KD (2014b) Insights into the genus *Diaporthe*: phylogenetic species delimitation in the *D. eres* species complex. *Fungal Diversity* 67: 203–229. <https://doi.org/10.1007/s13225-014-0297-2>
- Udayanga D, Castlebury LA, Rossman AY, Chukeatirote E, Hyde KD (2015) The *Diaporthe sojae* species complex: Phylogenetic re-assessment of pathogens associated with soybean, cucurbits and other field crops. *Fungal Biology* 119: 383–407. <https://doi.org/10.1016/j.funbio.2014.10.009>

- Udayanga D, Castlebury LA, Rossman AY, Hyde KD (2014a) Species limits in *Diaporthe*: molecular re-assessment of *D. citri*, *D. cytospora*, *D. foeniculina* and *D. rudis*. *Persoonia* 32: 83–101. <https://doi.org/10.3767/003158514X679984>
- Udayanga D, Liu X, McKenzie EH, Chukeatirote E, Bahkali AH, Hyde KD (2011) The genus *Phomopsis*: biology, applications, species concepts and names of common phytopathogens. *Fungal Diversity* 50: 189–225. <https://doi.org/10.1007/s13225-011-0126-9>
- Wang WJ, Chen CG, Cheng J (2007) The medicinal active role of tea oil in health care. *Food and Nutrition in China* 9: 48–51.
- Wang Y, Chen JY, Xu XW, Cheng JY, Zheng L, Huang JB, Li DW (2020) Identification and characterization of *Colletotrichum* species associated with anthracnose disease of *Camellia oleifera* in China. *Plant Disease* 104: 474–482. <https://doi.org/10.1094/PDIS-11-18-1955-RE>
- White TJ, Bruns T, Lee S, Taylor J (1990) Amplification and direct sequencing of fungal ribosomal RNA genes for phylogenetics. *PCR Protocols: A Guide to Methods and Applications* 18: 315–322. <https://doi.org/10.1016/B978-0-12-372180-8.50042-1>
- Wrona CJ, Mohankumar V, Schoeman MH, Tan YP, Shivas RG, Jeff-Ego OS, Akinsanmi OA (2020) Phomopsis husk rot of macadamia in Australia and South Africa caused by novel *Diaporthe* species. *Plant Pathology* 69: 911–921. <https://doi.org/10.1111/ppa.13170>
- Yang Q, Fan XL, Guarnaccia V, Tian CM (2018) High diversity of *Diaporthe* species associated with dieback diseases in China, with twelve new species described. *MycKeys* 39: 97–149. <https://doi.org/10.3897/mycokeys.39.26914>
- Yang Q, Jiang N, Tian CM (2020) Three new *Diaporthe* species from Shaanxi Province, China. *MycKeys* 67: 1–18. <https://doi.org/10.3897/mycokeys.67.49483>
- Yang Q, Jiang N, Tian CM (2021) New species and records of *Diaporthe* from Jiangxi Province, China. *MycKeys* 77: 41–64. <https://doi.org/10.3897/mycokeys.77.59999>
- Zhou H, Hou CL (2019) Three new species of *Diaporthe* from China based on morphological characters and DNA sequence data analyses. *Phytotaxa* 422: 157–174. <https://doi.org/10.11646/phytotaxa.422.2.3>
- Zhuang RL (2008) *Camellia oleifera*. 2nd Edn. China Forestry Press, Beijing.

Two new calcicolous caloplacoid lichens from South Korea, with a taxonomic key to the species of *Huriella* and *Squamulea*

Beeyoung Gun Lee¹, Jae-Seoun Hur²

1 Baekdudaegan National Arboretum, Bonghwa 36209, Republic of Korea **2** Korean Lichen Research Institute, Suncheon National University, Suncheon 57922, Republic of Korea

Corresponding author: Beeyoung Gun Lee (gitanoblue@koagi.or.kr)

Academic editor: Gerhard Rambold | Received 7 July 2021 | Accepted 20 September 2021 | Published 01 November 2021

Citation: Lee BG, Hur J-S (2021) Two new calcicolous caloplacoid lichens from South Korea, with a taxonomic key to the species of *Huriella* and *Squamulea*. MycoKeys 84: 35–55. <https://doi.org/10.3897/mycokeys.84.71227>

Abstract

Pyrenodesmia rugosa Lee & Hur and *Huriella aeruginosa* Lee & Hur are described as new lichen-forming fungi from a calcareous mountain of South Korea. *Pyrenodesmia rugosa* is distinguishable from *Pyrenodesmia micromontana* (Frolov, Wilk & Vondrák) Hafellner & Türk, the most similar species, by thicker thallus, rugose areoles, larger apothecia, shorter hymenium, shorter hypothecium and narrower tip cells of paraphyses. *Huriella aeruginosa*, the second new species, differs from '*Squamulea*' *chelonina* Bungartz & Søchting by dark greenish-grey to grey thallus without pruina, gold to yellow-brown epihymenium, larger ascospores and thallus K– and KC– reaction. Molecular analyses employing internal transcribed spacer (ITS), mitochondrial small subunit (mtSSU) and nuclear large subunit ribosomal RNA (LSU) sequences strongly support the two caloplacoid species to be distinct in their genera. A surrogate key is provided to assist in the identification of all 20 taxa in *Huriella* and *Squamulea*.

Keywords

Biodiversity, phylogeny, saxicolous, taxonomy, Teloschistaceae

Introduction

Many lichens are only detected in calcareous areas, particularly for crustaceous lichens, as many plants are never found, except on calcareous rocks and soils (Watson 1918; Kossowska 2008; Pykälä et al. 2017). Caloplacoid lichens have been discovered in calcareous areas, such as *Pyrenodesmia albopustulata* (Khodos. & S.Y. Kondr.) I.V. Frolov & Vondrák, *P. badioreagens* (Tretiach & Muggia) Søchting, Arup & Frödén, *P. concreticola* (Vondrák & Khodos.) Søchting, Arup & Frödén, *P. erodens* (Tretiach, Pinna & Grube) Søchting, Arup & Frödén, '*Squamulea*' *chelonina*, *Squamulea galactophylla* (Tuck.) Arup, Søchting & Frödén, '*Squamulea*' *humboldtiana* Bungartz & Søchting, *Squamulea parviloba* (Wetmore) Arup, Søchting & Frödén and *S. subsoluta* (Nyl.) Arup, Søchting & Frödén (Khodosovtsev et al. 2002; Tretiach et al. 2003; Wetmore 2003; Tretiach and Muggia 2006; Vondrák 2008; Arup 2013; Bungartz et al. 2020). Many lichens have been introduced from the calcareous areas in Korea, such as *Anema decipiens* (A. Massal.) Forssell, *Astrolacla loekoesiania* S.Y. Kondr., Farkas, J.J. Woo & Hur, *Caeruleum heppii* (Nägeli ex Körb.) K. Knudsen & Arcadia, *Clauzadea metzleri* (Körb.) Clauzade & Cl. Roux, *Clauzadea monticola* (Ach.) Hafellner & Bellem., *Collema auriforme* (With.) Coppins & J.R. Laundon, *C. cristatum* (L.) Weber ex F.H. Wigg., *Endocarpon pallidum* Ach., *Halecania pakistanica* van den Boom & Elix, *Heppia adglutinata* A. Massal., *Ionaspis epulotica* (Ach.) Blomb. & Forssell, *Lecania turicensis* (Hepp) Müll. Arg., *Lecanora albescens* (Hoffm.) Branth & Rostr., *L. semipallida* H. Magn., *Lemmopsis arnoldiana* (Hepp) Zahlbr., *Lichinella cribellifera* (Nyl.) P.P. Moreno & Egea, *L. stipatula* Nyl., *Placynthium tantaleum* (Hepp) Hue, *Porina fluminea* P.M. McCarthy & P.N. Johnson, *Psorotichia frustulosa* Anzi, *P. schaeereri* (A. Massal.) Arnold, *Pterygiopsis affinis* (A. Massal.) Henssen, *Pyrenocarpon* aff. *thelostomum* (Ach. ex J. Harriman) Coppins & Aptroot, *Rufoplaca aesanensis* S.Y. Kondr. & Hur, *Staurothele frustulenta* Vain., *Synalissa ramulosa* (Hoffm.) Körb., *Thyrea confusa* Henssen, *Toninia poeltiana* S.Y. Kondr., Lökös & Hur, *T. tristis* (Th. Fr.) Th. Fr. and *Verrucaria muralis* Ach. (van den Boom and Elix 2005; Joshi et al. 2009; Schultz and Moon 2011; Aptroot and Moon 2014, 2015, Kondratyuk et al. 2016a, 2016b, 2017a, 2020). Although calcicolous caloplacoid lichens were little reported from Korea in the past, for example, *Rufoplaca aesanensis*, it is assumed that diverse caloplacoid lichens inhabit calcareous rocks and soils which were previously reported from just rock or soil without specifying specific rock or soil types.

This study describes two new calcicolous caloplacoid lichens in the genera *Pyrenodesmia* and *Huriella*. Qualified field surveys for the lichen diversity on the Baekdudaegan Mountains, the main mountain range stretching across the entire Korean Peninsula, were accomplished during the summer of 2020 and a few dozen specimens of caloplacoid lichens were collected in Mt. Seokbyung, a calcareous mountain (Fig. 1). We describe them as two new species, *Pyrenodesmia rugosa* and *Huriella aeruginosa*. The specimens are deposited in the herbarium of the Baekdudaegan National Arboretum (KBA), South Korea.



Figure 1. Specific collection site for two new species, representing the habitat/landscape and the location (black star mark).

Materials and methods

Morphological and chemical analyses

Hand-cut sections were prepared with a razor blade under a stereomicroscope (Olympus optical SZ51; Olympus, Tokyo, Japan), examined under a compound microscope (Nikon Eclipse E400; Nikon, Tokyo, Japan) and imaged using a software programme (NIS-Elements D; Nikon, Tokyo, Japan) and a DS-Fi3 camera (Nikon, Tokyo, Japan), mounted on a Nikon Eclipse Ni-U microscope (Nikon, Tokyo, Japan). The ascospores were investigated at 1000 \times magnification in water. The length and width of the ascospores were measured and the range of spore sizes was shown with average, standard deviation and number of measured spores. Thin-layer chromatography (TLC) was performed using solvent systems A and C according to standard methods (Orange et al. 2001).

Isolation, DNA extraction, amplification and sequencing

Hand-cut sections of ascomata or thallus from all collected specimens were prepared for DNA isolation and DNA was extracted with a NucleoSpin Plant II Kit in line with the manufacturer's instructions (Macherey-Nagel, Düren, Germany). PCR amplification for the internal transcribed spacer region (ITS1-5.8S-ITS2 rDNA), the mitochondrial

small subunit and the nuclear large subunit ribosomal RNA genes was achieved using Bioneer's AccuPower PCR Premix (Bioneer, Daejeon, Korea) in 20- μ l tubes and primers ITS5 and ITS4 (White et al. 1990), mrSSU1 and mrSSU3R (Zoller et al. 1999) and LR0R and LR5 (Rehner and Samuels 1994), respectively. The PCR thermal cycling parameters used were 95 °C (15 sec), followed by 35 cycles of 95 °C (45 sec), 54 °C (45 sec) and 72 °C (1 min) and a final extension at 72 °C (7 min), based on Ekman (2001). DNA sequences were generated by the genomic research company Macrogen (Seoul, Korea).

Phylogenetic analyses

All ITS, mtSSU and LSU sequences were aligned and edited manually using ClustalW in Bioedit V.7.2.6.1 (Hall 1999). All missing and ambiguously aligned data and parsimony-uninformative positions were removed and only parsimony-informative regions were finally analysed in MEGA X (Stecher et al. 2020). The final alignment comprised 878 (ITS), 900 (mtSSU) and 1701 (LSU) columns for *Pyrenodesmia*. In them, variable regions were 178 (ITS), 42 (mtSSU) and 618 (LSU). The phylogenetically-informative regions were 356 (ITS), 55 (mtSSU) and 98 (LSU). The final alignment for *Huriella* and *Squamulea* comprised 693 (ITS) columns. In them, variable regions were 78 (ITS). Finally, the phylogenetically-informative region was 246 (ITS). Phylogenetic trees with bootstrap values were obtained in RAxML GUI 2.0 beta (Edler et al. 2019) using the Maximum Likelihood method with a rapid bootstrap with 1000 bootstrap replications and GTR GAMMA for the substitution matrix. The posterior probabilities were obtained in BEAST 2.6.4 (Bouckaert et al. 2019) using the HKY (Hasegawa, Kishino and Yano) model, as the appropriate model for nucleotide substitution, based on the Bayesian Information Criterion (BIC) (Schwarz 1978) as evaluated by bModelTest (Bouckaert and Drummond 2017), empirical base frequencies, gamma for the site heterogeneity model, four categories for gamma and a 10,000,000 Markov Chain Monte Carlo chain length with a 10,000-echo state screening and 1000 log parameters. Then, a consensus tree was constructed in TreeAnnotator 2.6.4 (Bouckaert et al. 2019) with a burn-in of 5000, no posterior probability limit, a maximum clade credibility tree for the target tree type and median node heights. All trees were displayed in FigTree 1.4.2 (Rambaut 2014) and edited in Microsoft Paint. The bootstrapping and Bayesian analyses were repeated three times for the result consistency and no significant differences were shown for the tree shapes and branch values. The phylogenetic trees and DNA sequence alignments are deposited in TreeBASE under the study ID 28190.

Results and discussion

Phylogenetic analyses

Three independent phylogenetic trees for *Pyrenodesmia* and one independent phylogenetic tree for *Squamulea* were produced from 165 sequences (96 for ITS, 37 for mtSSU and 32 for LSU) from GenBank and four new sequences (two for ITS, one for mtSSU

and one for LSU) for the new species (Table 1). *Pyrenodesmia rugosa*, a new species, was positioned in the genus *Pyrenodesmia* in all ITS, mtSSU and LSU trees. The ITS tree described that the new species was solely located without any clade. Several species closely positioned with the new species were *Pyrenodesmia aractina* (Fr.) S.Y. Kondr., *P. bicolor* (H. Magn.) S.Y. Kondr. and *P. haematites* (Chaub. ex St.-Amans) S.Y. Kondr., represented by a bootstrap value of 84 and a posterior probability of 0.73 (not shown) for the branch (Fig. 2). The mtSSU tree showed that the new species was located in a clade with *Pyrenodesmia albopruinosa* (Arnold) S.Y. Kondr. and *P. micromontana*, represented by a bootstrap value of 72 and a posterior probability of 1.0 for the branch (Fig. 3). The LSU tree depicted that the new species was positioned solely without any clade. Several species, such as *Kuettlingeria cretensis* (Zahlbr.) I.V. Frolov & Vondrák, *K. neotaurica* (Vondrák, Khodos., Arup & Söchting) I.V. Frolov, Vondrák & Arup, *Pyrenodesmia albopustulata*, *P. chalybaea* (Fr.) A. Massal., *P. helygeoides* (Vain.) Arnold, *P. microstepposa* (Frolov, Nadyeina, Khodos. & Vondrák) Hafellner & Türk, *P. molariformis* (Frolov, Vondrák, Nadyeina & Khodos.) S.Y. Kondr., *P. pratensis* (Wetmore) Frolov & Vondrák and *P. variabilis* (Pers.) A. Massal. are situated close to the new species (Fig. 4). *Huriella aeruginosa*, the second new species, was located in *Huriella* in the ITS tree. The ITS tree described that the new species was positioned in a clade with '*Squamulea*' *subsolata* and '*Squamulea*' sp., represented by a bootstrap value of 35 (not shown) without a posterior probability as the Maximum Likelihood analysis did not match with the Bayesian Inference for the clade (Fig. 5). Although the two closely located sequences were named for *Squamulea* in the beginning, they are close to *Huriella*, not *Squamulea*. The two sequences are arranged in the genus *Huriella* with the new species. The phylogenetic analyses did not designate any species identical to the two new species in each genus *Pyrenodesmia* and *Huriella*.

Taxonomy

Pyrenodesmia rugosa B.G. Lee & J.-S. Hur, sp. nov.

Mycobank No: 839184

Fig. 6

Diagnosis. *Pyrenodesmia rugosa* differs from *P. micromontana* by thicker thallus (125–200 µm vs. 95–125 µm), rugose areoles (vs. flat areoles), larger apothecia (0.2–0.7 mm diam. vs. 0.2–0.4 mm diam.), shorter hymenium (60–70 µm vs. 80–100 µm), shorter hypothecium (50–55 µm vs. 80–100 µm) and narrower tip cells of paraphyses (3–4.5 µm vs. 5–6 µm).

Type. SOUTH KOREA, Gangwon Province, Gangneung, Okgye-myeon, Mt. Seokbyung (summit), 37°35.21'N, 128°53.87'E, 1,072 m alt., on calcareous rock, 17 June 2020, B.G.Lee & H.J.Lee 2020-000902, with *Athallia* cf. *vitellinula* (Nyl.) Arup, Frödén & Söchting, *Bagliettoa baldensis* (A. Massal.) Vězda, *Catillaria lenticularis* (Ach.) Th. Fr. and *Staurothele* aff. *succedens* (Rehm) Arnold (holotype: BDNA-L-0001102!); same locality, on calcareous rock, 17 June 2020, B.G.Lee & H.J.Lee 2020-000899, with *Athallia* cf. *holocarpa* (Hoffm.) Arup, Frödén & Söchting and *Staurothele* cf. *rupifraga*

Table I. Species list and DNA sequence information employed for phylogenetic analysis.

No	Species	ID (ITS)	ID (mtSSU)	ID (LSU)	Voucher
1	<i>Amundsenia approximata</i>	KJ789965			L08179 (LD)
2	<i>Amundsenia austrocontinentalis</i>	KJ789962			21966 (HO)
3	<i>Athallia holocarpa</i>	MG954144			Vondrak 18072
4	<i>Athallia vitellinula</i>	FJ346556			Arup L03052
5	<i>Caloplaca monacensis</i>	MG773668	MG773679		Malicek 8255
6	<i>Caloplaca</i> sp.	KC611244			CBFS:JV6943
7	<i>Erichansenia sauronii</i>	KC179120			Sochting 7654
8	<i>Huriella aeruginosa</i>	MW832829			BDNA-L-0001072
9	<i>Huriella flakusii</i>	MT967442			Bungartz 4131 (CDS 28162)
10	<i>Huriella flakusii</i>	MT967443			Bungartz 4157 (CDS 28188)
11	<i>Huriella flakusii</i>	MT967444			Aptroot 65261 (CDS 31847)
12	<i>Huriella loekoiesiana</i>	KY614406			KoLRI 15423
13	<i>Huriella loekoiesiana</i>	KY614407			KoLRI 19017
14	<i>Huriella loekoiesiana</i>	KY614408			KoLRI 40141
15	<i>Huriella loekoiesiana</i>	KY614409			KoLRI 40236
16	<i>Huriella loekoiesiana</i>	KY614410			KoLRI 40238
17	<i>Huriella loekoiesiana</i>	MK499351			HKAS 102112
18	<i>Huriella</i> sp.	MN108089			KRAM-L-70242
19	<i>Kuettlingeria albolutescens</i>	KC179423	KC179502	MT952898	Arup L09030 (LD)
20	<i>Kuettlingeria areolata</i>	MN305805	MN305825	MN305847	Vondrak 10843
21	<i>Kuettlingeria atroflava</i>	MH104921	MH100775		Vondrak 8723 (PRA)
22	<i>Kuettlingeria cretensis</i>	MH104925	MH100783	MH100751	Frolov s.n.
23	<i>Kuettlingeria diphyodes</i>	MH104926	MH100785	MH100753	Frolov 1430
24	<i>Kuettlingeria emilii</i>	KC416102	MH100787	MH100754	JV9358
25	<i>Kuettlingeria erythrocarpa</i>	KC179427	KC179506	KC179173	Arup L07109 (LD)
26	<i>Kuettlingeria neotaurica</i>	MN305807	MN305829	MN305849	Vondrak 7213
27	<i>Kuettlingeria perocata</i>	MH104931	MH100794		Vondrak 4634 (PRA)
28	<i>Kuettlingeria soralifera</i>	MN305808	MN305830	MN305850	Vondrak 10813
29	<i>Kuettlingeria aff. soralifera</i>	JN641781			CBFS:JV8325
30	<i>Kuettlingeria teicholyta</i>	MH104935	MH100797	MH100767	Vondrak 6943 (PRA)
31	<i>Kuettlingeria xerica</i>	MN305809	MN305831	MN305851	Vondrak 14544
32	<i>Kuettlingeria aff. xerica</i>	HQ611275			CBFS:JV7618
33	<i>Lendemeriella borealis</i>	MG954129			Vondrak 11073
34	<i>Lendemeriella exsecuta</i>	MG954227			Spribile 24441
35	<i>Lendemeriella nivalis</i>	MG954222			Spribile 29306
36	<i>Lendemeriella reptans</i>	MH104934	MH100796	MH100766	Lendem 48186 (NY)
37	<i>Lendemeriella sorocarpa</i>	MG954132			Vondrak12695
38	<i>Lendemeriella tornoensis</i>	MG954221			Spribile 29473
39	<i>Oleglumia demissa</i>	KT220203	KT220221	KT220212	SK C65
40	<i>Pyrenodesmia aetnensis</i>	EU639590	KT291476		X. Llimona (BCN)
41	<i>Pyrenodesmia alpopruinosa</i>	EF093577	MH100770		TSB 37658
42	<i>Pyrenodesmia alpopustulata</i>	MH104918	MH100771	MH100741	Vondrak 10463 (PRA)
43	<i>Pyrenodesmia alociza</i>	EF090931	MH100772	MH100742	TSB 37735
44	<i>Pyrenodesmia aractina</i>	GU723415			Bornholm 5907
45	<i>Pyrenodesmia aractina</i>	GU723418			Bornholm 6911
46	<i>Pyrenodesmia aractina</i>	MH104919	MH100773		Vondrak 6702 (PRA)
47	<i>Pyrenodesmia atroalba</i>	MH104920	MH100774		Spribile s.n.
48	<i>Pyrenodesmia badioreagens</i>	EF081035	MH100776	MH100745	TSB 36422
49	<i>Pyrenodesmia bicolor</i>	MH104922	MH100777	MH100746	Vondrak 10373 (PRA)

No	Species	ID (ITS)	ID (mtSSU)	ID (LSU)	Voucher
50	<i>Pyrenodesmia ceracea</i>	HQ234603			BM-6656
51	<i>Pyrenodesmia chalybaea</i>	KC884498	MH100779	MH100747	CBFS:JV4059
52	<i>Pyrenodesmia circumalbata</i>	MH104923	MH100780	MH100748	Halicis s.n.
53	<i>Pyrenodesmia concreticola</i>	KC884506	MH100781	MH100749	CBFS:JV9443
54	<i>Pyrenodesmia duplicata</i>	HQ611272			TUR-V-7513
55	<i>Pyrenodesmia erodens</i>	MH104927	MH100788	MH100755	Vondrak 12733 (PRA)
56	<i>Pyrenodesmia haematites</i>	GU723420	MH100789	MH100756	Vondrak 7278 (PRA)
57	<i>Pyrenodesmia haematites</i>	GU723421			JS280
58	<i>Pyrenodesmia haematites</i>	MH104928			Vondrak 7278 (PRA)
59	<i>Pyrenodesmia helygeoides</i>	MH104929	MH100790	MH100757	Frolov 1414
60	<i>Pyrenodesmia micromarina</i>	NR_156257			CBFS:JV8199
61	<i>Pyrenodesmia micromarina</i>		MH100791	MH100758	Vondrak 7236 (PRA)
62	<i>Pyrenodesmia micromontana</i>	NR_158297	MH100792	MH100759	CBFS:JV9467
63	<i>Pyrenodesmia microstepposa</i>	NR_156260		MH100760	CBFS:JV9141
64	<i>Pyrenodesmia molariformis</i>	KC416145	MH100793	MH100761	Nadyeina 132 (KW)
65	<i>Pyrenodesmia obscurella</i>	MH104938		MH100762	Vondrak 7641 (PRA)
66	<i>Pyrenodesmia peliophylla</i>	MG733135			Jason Hollinger:16476
67	<i>Pyrenodesmia pratensis</i>	MH104933	MH100795	MH100765	MIN 891605
68	<i>Pyrenodesmia rugosa</i>	MW832828	MW832825	MW832904	BDNA-L-0001099
69	<i>Pyrenodesmia transcaspica</i>	MH104936	MH100799	MH100768	Vondrak 9430 (PRA)
70	<i>Pyrenodesmia variabilis</i>	KT291466	KT291514	KT291561	Ulf Arup L07196 (LD)
71	<i>Shackletonia buelliae</i>	KC179117			Sochting 7583
72	<i>Shackletonia siphonospora</i>	KC179121			Sochting 7883
73	<i>Squamulea galactophylla</i>	KC179122			Morse 10997 (LD)
74	<i>Squamulea kiamae</i>	KC179123			Kondratyuk 20480 (LD)
75	<i>Squamulea parviloba</i>	KC179124			Wetmore 87830 (LD)
76	<i>Squamulea squamosa</i>	MT967462			Moberg 8782 (UPS)
77	<i>Squamulea squamosa</i>	KC179125			Karnefelt AM960105 (LD)
78	<i>Squamulea</i> 'squamosa'	MT967465			Bungartz 7428 (CDS 37915)
79	<i>Squamulea subsoluta</i>	AF353954			Arup L97072
80	<i>Squamulea subsoluta</i>	DQ173238			Arup L97829
81	<i>Squamulea subsoluta</i>	KJ133480			KoLRI 011067
82	' <i>Squamulea</i> ' <i>chelonina</i>	MT967448			Bungartz 4521 (CDS 28607)
83	' <i>Squamulea</i> ' <i>chelonina</i>	MT967451			Bungartz 9251 (CDS 46069)
84	' <i>Squamulea</i> ' <i>chelonina</i>	MT967452			Bungartz 6146 (CDS 34358)
85	' <i>Squamulea</i> ' <i>humboldtiana</i>	MT967439			Buck 29560 (MIN)
86	' <i>Squamulea</i> ' <i>humboldtiana</i>	MT967440			Bungartz 4711B (CDS 56235)
87	' <i>Squamulea</i> ' <i>humboldtiana</i>	MT967441			Bungartz 9985 (CDS 47354)
88	' <i>Squamulea</i> ' <i>oceanica</i>	MT967445			Yáñez-Ayabaca 2023 (CDS 48373)
89	' <i>Squamulea</i> ' <i>oceanica</i>	MT967446			Bungartz 10152 (CDS 47571)
90	' <i>Squamulea</i> ' <i>oceanica</i>	MT967447			Bungartz 9857 (CDS 47195)
91	' <i>Squamulea</i> ' <i>osseophila</i>	MT967455			Aptroot 65489 (CDS 32078)
92	' <i>Squamulea</i> ' <i>phyllidizans</i>	MT967456			Aptroot 65468 (CDS 32057)

No	Species	ID (ITS)	ID (mtSSU)	ID (LSU)	Voucher
93	<i>'Squamulea' phyllidizans</i>	MT967457			Bungartz 4710 (CDS 28808)
94	<i>'Squamulea' phyllidizans</i>	MT967458			Bungartz 4158 (CDS 28189)
95	<i>'Squamulea' subsoluta</i>	KJ133481			KoLRI 012491
96	<i>'Squamulea' sp.</i>	MG954160			Vondrak 18682
97	<i>Usnochroma carphineum</i>	KC179468	KC179598	KC179259	Roux s.n.
98	<i>Usnochroma scoriophilum</i>	JQ301664	JQ301496	JQ301560	P. & B. v.d. Boom 38386
	Overall	98	38	33	

DNA sequences which were generated in this study, i.e. two new species, such as *Pyrenodesmia rugosa* and *Huriella aeruginosa* are presented in bold. All others were obtained from GenBank. The species names are followed by GenBank accession numbers and voucher information. ITS, internal transcribed spacer; mtSSU, mitochondrial small subunit; LSU, large subunit; Voucher, voucher information.

(A. Massal.) Arnold (paratype: BDNA-L-0001099; GenBank MW832828 for ITS, MW832825 for mtSSU and MW832804 for LSU).

Thallus saxicolous (calcicolous), crustose, mainly areolate or slightly rimose, rugose, greyish-brown to pale brown, often with orange spots, margin indeterminate or determinate when placodioid areoles are arranged around edge, vegetative propagules absent, areoles 0.4–1.0 mm diam., 125–200 µm thick; cortex hyaline with pale brown pigment layer, pale brown pigment K+ purple, 10–40 µm thick, cortical cells granular, 5–10 µm diam., with epinecral layer, 5–7 µm thick; medulla 60–110 µm thick below algal layer or inconspicuous and algal layer shown just above substrate; photobiont coccoid, cells globose to oval, 5–15 µm diam., algal layer 50–70 µm thick. Small crystals present between algal cells, not dissolving in K. Prothallus absent.

Apothecia abundant, scattered or concentrated in centre, rounded, often contiguous or even coalescent when mature, emerging on the surface of thallus, immersed or adnate, slightly constricted at the base, 0.2–0.7 mm diam. Disc flat when young and flat or concave when mature, often white pruinose, black, 200–300 µm thick; zeorine, margin persistent, slightly prominent, generally entire or rarely slightly crenulate, thalline margin paler to disc and showing brown colour, often inconspicuous due to locating below proper margin, proper margin concolorous to disc. Amphithecium present, with small crystals between algal cells, not dissolving in K, 80–130 µm wide laterally, algal layers continuous to the base and underlying the hypothecium, algal cells 5–15 µm diam., cortical layer hyaline with pale brownish pigment at periphery, 10–40 µm thick. Parathecium well-developed, hyaline, but grey with slightly brown pigment concolorous to epihymenium at periphery, 20–40 µm wide laterally and 50–90 µm wide at periphery. Epihymenium grey with slightly brown pigment, K+ purple, tiny granules abundant on surface, not dissolving in K, 5–10 µm high. Hymenium hyaline, 60–70 µm high. Hypothecium hyaline, base open and extending downwards, 50–55 µm high. Oil droplets present in upper hypothecium, but absent in hymenium. Paraphyses septate, often anastomosing, 2–2.5 µm wide, generally simple, but occasionally branched at tips, tips slightly swollen, not pigmented, 3.0–4.5 µm wide. Asci oblong to narrowly clavate, 8-spored, 52–60 × 14–18 µm (n = 5). Ascospores ellipsoid, 1-septate, polarilocular when mature or narrow septum remaining, hyaline

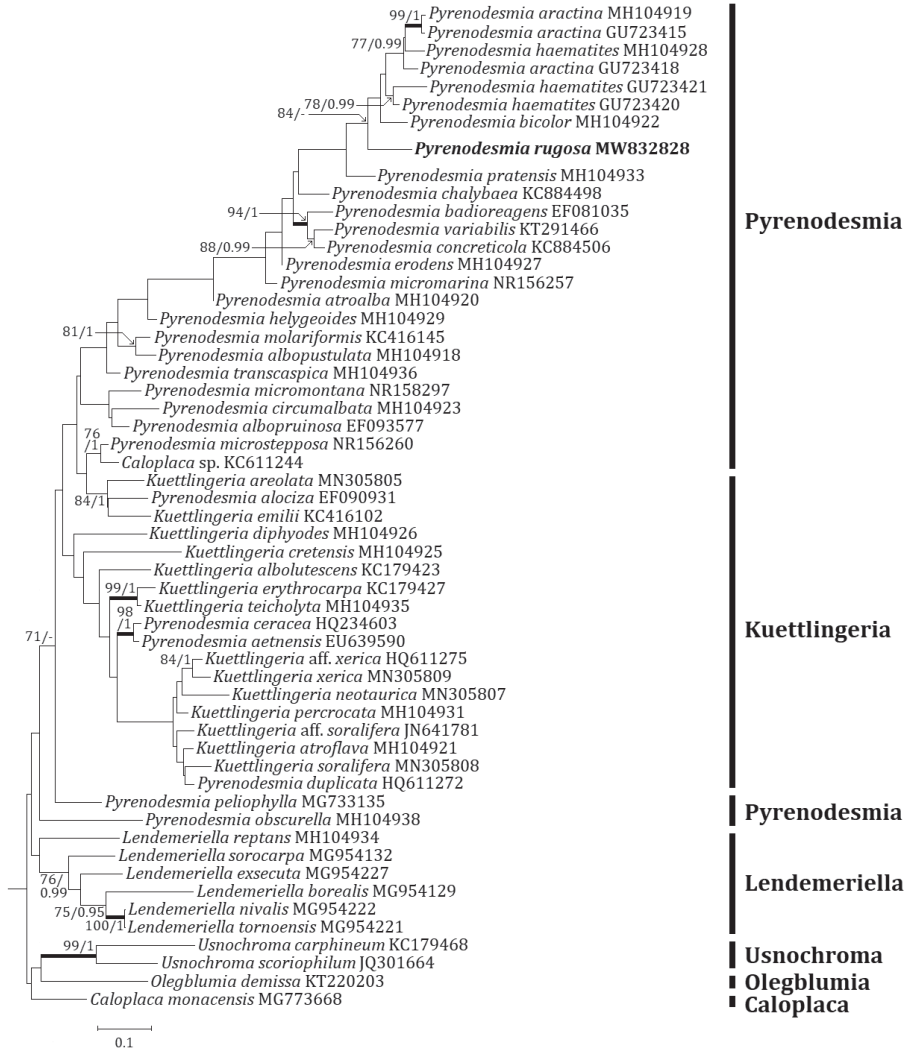


Figure 2. Phylogenetic relationships amongst available species in the genus *Pyrenodesmia*, based on a Maximum Likelihood analysis of the dataset of ITS sequences. The tree was rooted with the sequences of the genera *Caloplaca*, *Lendemerella*, *Olegblumia* and *Usnochroma*. Maximum Likelihood bootstrap values $\geq 70\%$ and posterior probabilities $\geq 95\%$ are shown above internal branches. Branches with bootstrap values $\geq 90\%$ are shown in bold. The new species *Pyrenodesmia rugosa* is presented in bold and all species names are followed by the GenBank accession numbers. Reference Table 1 provides the species related to the specific GenBank accession numbers and voucher information.

permanently, $11\text{--}18 \times 5.5\text{--}11 \mu\text{m}$ (mean = $14.1 \times 7.6 \mu\text{m}$; SD = 1.6(L), 1.0(W); L/W ratio 1.5–2.5, ratio mean = 1.9, ratio SD = 0.3; n = 105), septum 1.5–3.0 μm . Pycnidia not detected.

Chemistry. Thallus K–, KC–, C–, Pd–. Epihymenium K+ purple. Hymenium I+ blue. UV–. No lichen substance was detected by TLC.

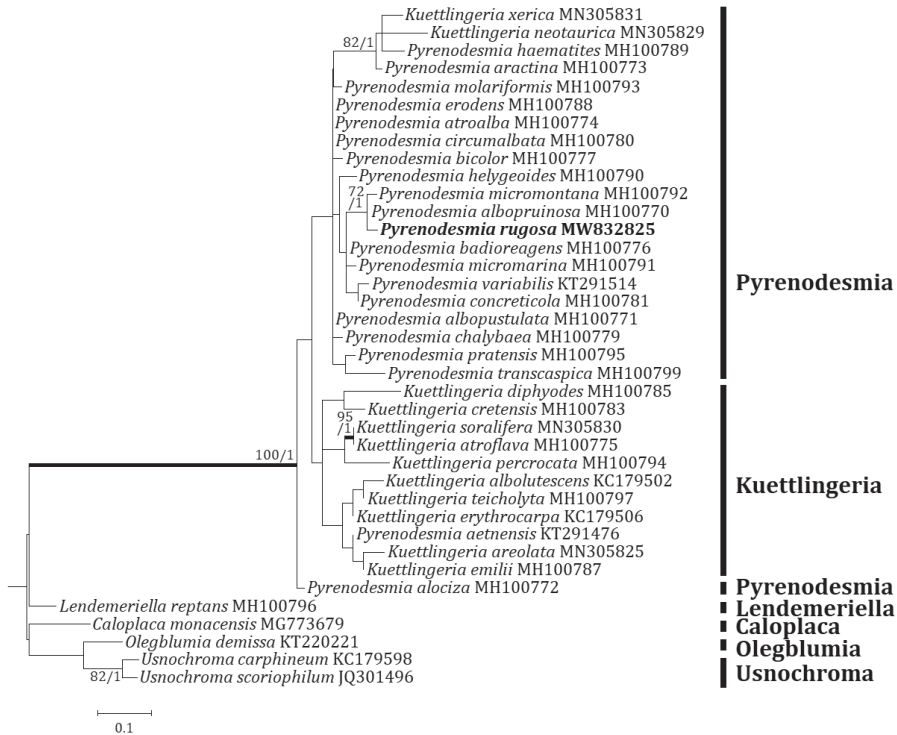


Figure 3. Phylogenetic relationships amongst available species in the genus *Pyrenodesmia*, based on a Maximum Likelihood analysis of the dataset of the mitochondrial small subunit (mtSSU) sequences. The tree was rooted with five sequences of the genera *Caloplaca*, *Lendemerella*, *Olegblumia* and *Usnochroma*. Maximum Likelihood bootstrap values $\geq 70\%$ and posterior probabilities $\geq 95\%$ are shown above internal branches. Branches with bootstrap values $\geq 90\%$ are shown in bold. The new species *Pyrenodesmia rugosa* is presented in bold and all species names are followed by the GenBank accession numbers. Reference Table 1 provides the species related to the specific GenBank accession numbers and voucher information.

Distribution and ecology. The species occurs on the calcareous rock. The species is currently known from the type collections.

Etymology. The species epithet indicates the lichen's thallus texture, rugose or wrinkled, which is the key characteristic distinguished from closely-related calcicolous species in the genus *Pyrenodesmia*.

Notes. The new species is similar to *P. micromontana*, *P. microstepposa* and *Caloplaca micromarina* Frolov, Khodos. & Vondrák in having epilithic thallus without vegetative propagules, small apothecia generally less than 0.5 mm diameter and the substrate preference to calcareous rocks. The new species differs from *P. micromontana* by thicker thallus (125–200 μm vs. 95–125 μm), rugose areoles (vs. flat areoles), larger apothecia (0.2–0.7 mm diam. vs. 0.2–0.4 mm diam.), shorter hymenium (60–70 μm vs. 80–100 μm), shorter hypothecium (50–55 μm vs. 80–100 μm) and narrower tip cells of paraphyses (3–4.5 μm vs. 5–6 μm) (Frolov et al. 2016).

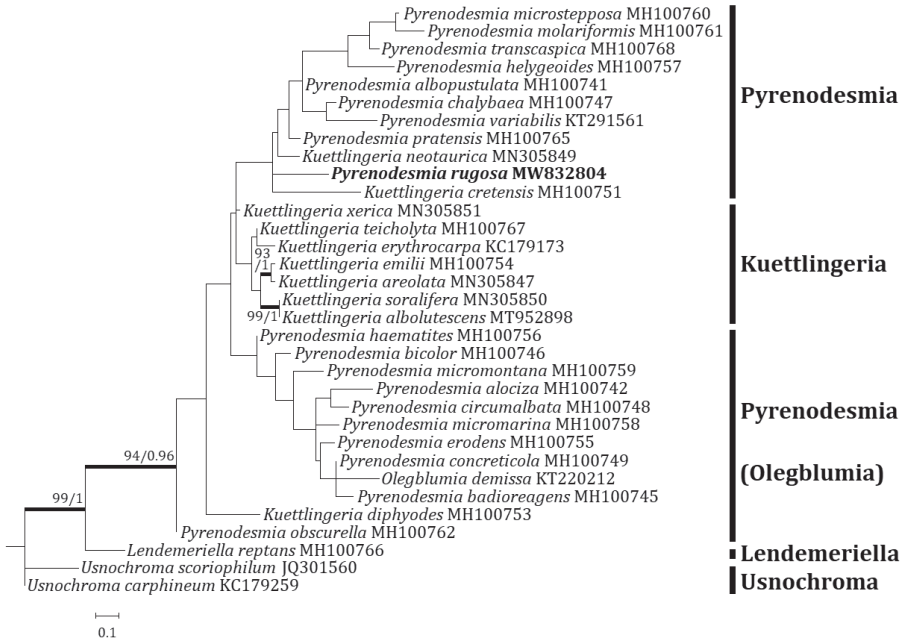


Figure 4. Phylogenetic relationships amongst available species in the genus *Pyrenodesmia*, based on a Maximum Likelihood analysis of the dataset of the nuclear large subunit ribosomal RNA (LSU) sequences. The tree was rooted with three sequences of the genera *Lendemerella* and *Usnochroma*. Maximum Likelihood bootstrap values $\geq 70\%$ and posterior probabilities $\geq 95\%$ are shown above internal branches. Branches with bootstrap values $\geq 90\%$ are shown in bold. The new species *Pyrenodesmia rugosa* is presented in bold and all species names are followed by the GenBank accession numbers. Reference Table 1 provides the species related to the specific GenBank accession numbers and voucher information.

The new species is different from *P. microstepposa* by darker thallus (greyish-brown to pale brown vs. ochre, grey or grey-white), rugose thallus (vs. flat thallus), thinner thallus (125–200 μm vs. 85–370 μm), smaller algal cells (5–15 μm diam. vs. 13.5–20.5 μm diam.), presence of pruina on disc (vs. absence of it), absence of oil droplets in hymenium (vs. presence of it), greyish epihymenium (vs. brownish epihymenium), wider ascospores (11–18 \times 5.5–11 μm with the L/W ratio of 1.5–2.5 vs. 13.6–18.4 \times 6–7.9 μm with the ratio of 1.9–2.9) (Frolov et al. 2016).

The new species is distinguished from *C. micromarina* by darker thallus (greyish-brown to pale brown vs. ochre to grey), rugose thallus (vs. flat thallus), absence of pruina on thallus (vs. presence of it), shorter hymenium (60–70 μm vs. 90–100 μm), shorter septum (1.5–3 μm vs. 2.6–3.4 μm) and the habitat preference to mountain rocks (vs. coastal rocks) (Frolov et al. 2016).

Additional specimens examined: SOUTH KOREA, Gangwon Province, Okgye-myeon, Mt. Seokbyung (summit), 37°35.21'N, 128°53.87'E, 1,072 m alt., on calcareous rock, 17 June 2020, B.G.Lee & H.J.Lee 2020-000889, with *Bagliettoa baldensis*, *Catillaria lenticularis*, *Fulgogasparrea decipiooides* (Arup) S.Y. Kondr., M.H. Jeong,

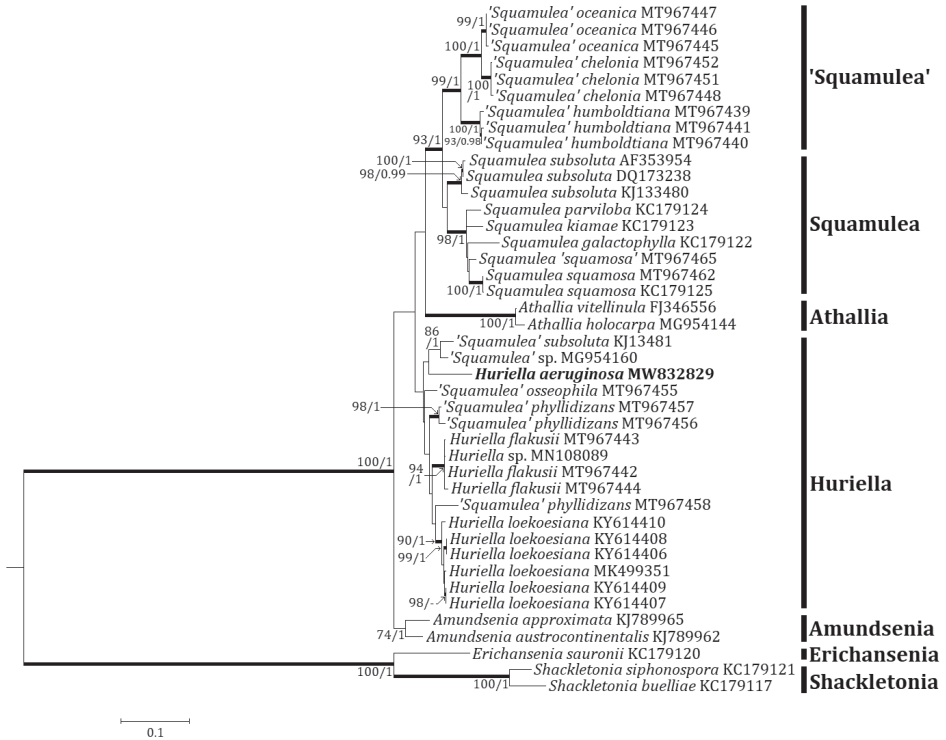


Figure 5. Phylogenetic relationships amongst available species in the genera *Huriella* and *Squamulea*, based on a Maximum Likelihood analysis of the dataset of ITS sequences. The tree was rooted with the sequences of the genera *Amundsenia*, *Erichansenia* and *Shackletonia*. Maximum Likelihood bootstrap values $\geq 70\%$ and posterior probabilities $\geq 95\%$ are shown above internal branches. Branches with bootstrap values $\geq 90\%$ are shown in bold. The new species *Huriella aeruginosa* is presented in bold and all species names are followed by the GenBank accession numbers. Reference Table 1 provides the species related to the specific GenBank accession numbers and voucher information.

Kärnefelt, Elix, A. Thell & Hur and *Laundonia flavovirescens* (Wulfen) S.Y. Kondr., Lökös & Hur (BDNA-L-0001089); same locality, on calcareous rock, 17 June 2020, B.G.Lee & H.J.Lee 2020-000909, with *Bagliettoa baldensis*, *Rusavskia elegans* (Link) S.Y. Kondr. & Kärnefelt and *Verrucaria nigrescens* Pers. (BDNA-L-0001109); same locality, on calcareous rock, 17 June 2020, B.G.Lee & H.J.Lee 2020-000910, with *Bagliettoa baldensis*, *Catillaria lenticularis* and *Laundonia flavovirescens* (BDNA-L-0001110); same locality, on calcareous rock, 17 June 2020, B.G.Lee & H.J.Lee 2020-000911, with *Athallia* cf. *vitellinula*, *Bagliettoa baldensis*, *Lichenella* sp. and *Rusavskia elegans* (BDNA-L-0001111); same locality, on calcareous rock, 17 June 2020, B.G.Lee & H.J.Lee 2020-000913, with *Athallia* cf. *vitellinula*, *Bagliettoa baldensis*, *Endocarpon* sp., *Laundonia flavovirescens*, *Lichenella* sp. and *Rusavskia elegans* (BDNA-L-0001113); same locality, on calcareous rock, 17 June 2020, B.G.Lee & H.J.Lee 2020-000916, with *Caloplaca* sp., *Endocarpon* sp., *Lichenella* sp. and *Rusavskia elegans* (BDNA-L-0001116).

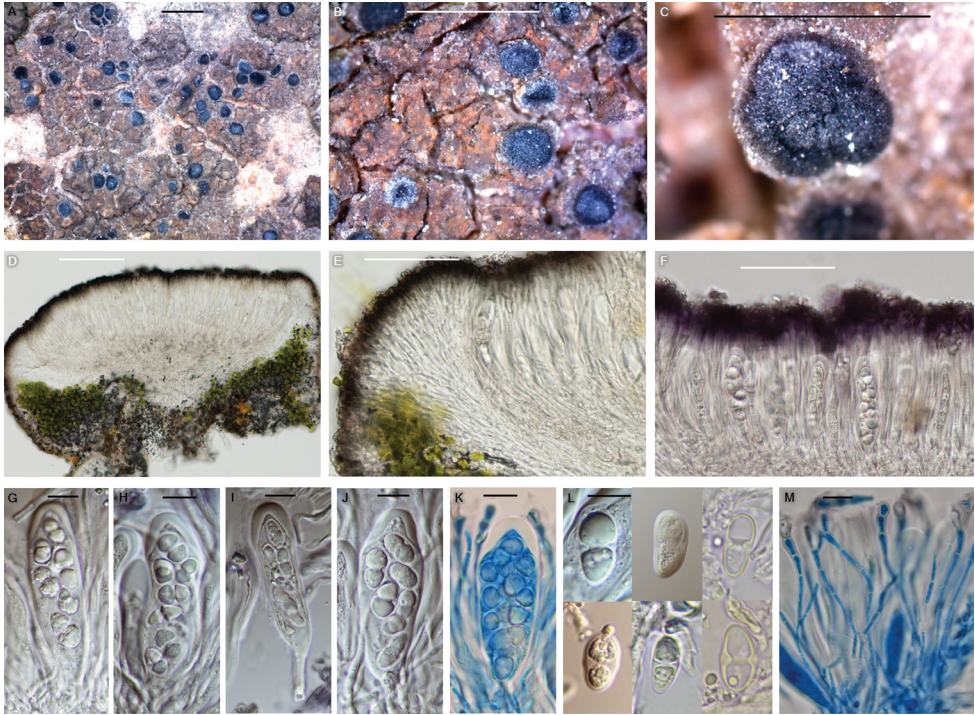


Figure 6. *Pyrenodesmia rugosa* (BDNA-L-0001102, holotype) in morphology **A–C** habitus and apothecia. Rugose thallus brown with orange spots and without pruina, but black apothecia often white pruinose **D–E** zeorine apothecia with well-developed parathecium. Algal layers continue to the base and underlying the hypothecium **F** epihymenium K⁺ purple and tiny granules not dissolving in K **G–K** asci oblong to narrowly clavate with eight spores **K** in the lactophenol cotton blue **L** ascospores simple in the beginning and developed polarilocular at maturity **M** paraphyses anastomosing in lactophenol cotton blue. Paraphysis tips slightly swollen. Scale bars: 1 mm (**A–C**); 100 μ m (**D**); 50 μ m (**E, F**); 10 μ m (**G–M**).

***Huriella aeruginosa* B.G. Lee & J.-S. Hur, sp. nov.**

Mycobank No: 839185

Fig. 7

Diagnosis. *Huriella aeruginosa* differs from '*Squamulea*' *chelonina* by dark greenish-grey to grey thallus without pruina (vs. yellow orange to deep orange thallus with white pruina), gold to yellow-brown epihymenium (vs. orange epihymenium), larger ascospores (7.5–12 \times 4.5–7.5 μ m vs. 8–10.4 \times 4.7–6.0 μ m) and the chemistry (thallus K⁻, KC⁻ and no substance vs. thallus K⁺ purple, KC \pm purplish and the presence of parietin, teloschistin, fallacinal, parietinic acid and emodin).

Type. SOUTH KOREA, Gangwon Province, Gangneung, Okgye-myeon, Mt. Seok-byung (summit), 37°35.21'N, 128°53.87'E, 1,072 m alt., on calcareous rock, 17 June 2020, B.G.Lee & H.J.Lee 2020-000872, with *Bagliettoa baldensis*, *Catillaria lenticularis*, *Endocarpon subramulosum* Y. Joshi & Hur, *Laundonia flavovirescens*, *Rusavskia elegans* and *Verrucaria nigrescens* (holotype: BDNA-L-0001072!; GenBank MW832829 for ITS).

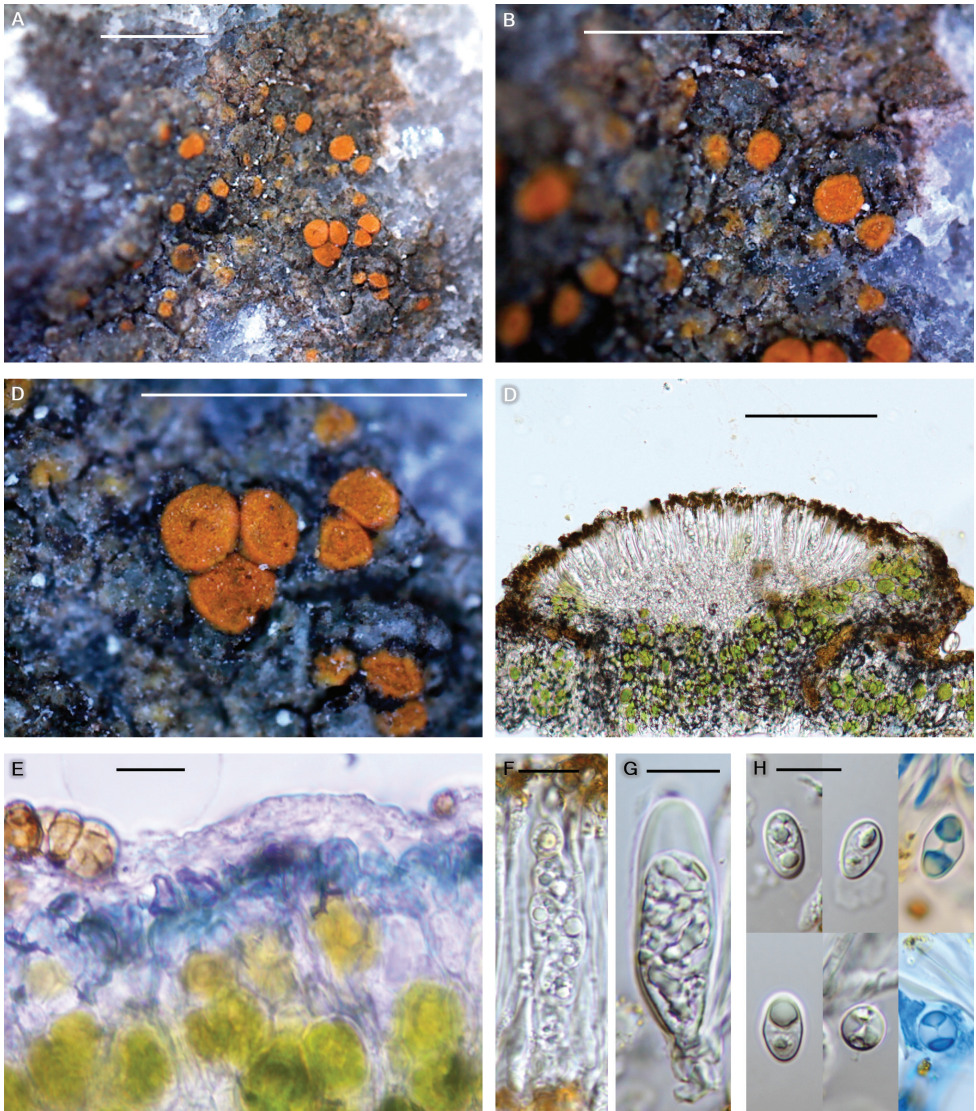


Figure 7. *Huriella aeruginosa* (BDNA-L-0001072, holotype) in morphology **A–C** habitus and apothecia. Thallus dark greenish-grey to grey with no pruina. Thalline margin of apothecia concolorous to disc **D** apothecia adnate or rarely sessile. Amphithecium well-developed, but parathecium inconspicuous. **E** thallus with dark green pigment layer under cortex **F–G** clavate asci containing 8-spores **H** ascospores generally ellipsoid, but occasionally globose, developing polarilocular in both types. Two blue coloured spores in lactophenol cotton blue. Scale bars: 1 mm (**A–C**); 100 μm (**D**); 10 μm (**E–H**).

Thallus saxicolous (calcicolous), crustose, mainly areolate or slightly rimose, placodioid around edge, but without distinct lobes, thin, dark greenish-grey to grey, occasionally pale yellowish-grey when young, margin indeterminate or determinate when placodioid areoles are arranged around edge, vegetative propagules absent, areoles 0.3–0.7 mm diam., 150–200 μm thick; cortex hyaline with dark green pigment

layer, 15–25 µm thick, cortical cells granular, coarsely anticlinally arranged, 5–10 µm diam., with epinecral layer, up to 5 µm thick; medulla 80–100 µm thick, below algal layer, with large crystals (materials of substrate possibly) and brown cells (dead algal cells possibly); photobiont coccoid, cells globose to oval, 5–25 µm. Small crystals in cortex, medulla and between algal cells, dissolving in K. Prothallus absent.

Apothecia abundant, scattered and not concentrated in centre, rounded, often contiguous when mature, emerging on the surface of thallus, immersed, adnate or rarely sessile, constricted at the base, 0.2–0.4 mm diam. Disc flat when young and flat or slightly convex when mature, not pruinose, orange from the beginning, 110–230 µm thick; margin persistent, even to disc or slightly prominent, generally entire or slightly crenulate, thalline margin concolorous to disc, proper margin inconspicuous. Amphithecium well-developed, with small crystals between algal cells, dissolving in K, 50–55 µm wide laterally, algal layers continuous to the base or solitarily remaining in amphithecium, algal cells 5–25 µm diam., cortical layer hyaline with gold to yellow-brown pigment concolorous to epihymenium at periphery, 15–20 µm thick. Parathecium inconspicuous, hyaline but gold to yellow-brown at periphery, ca. 10 µm wide laterally and ca. 20 µm wide at periphery. Epihymenium gold to yellow-brown, granular, pigment K+ wine red and dissolved, 10–20 µm high. Hymenium hyaline, 45–55 µm high. Hypothecium hyaline, 35–45 µm high. Oil droplets present, small, along paraphyses and more in the base of hymenium and hypothecium. Paraphyses septate, anastomosing, 2–3 µm wide, simple or branched at tips, tips swollen or slightly swollen, not pigmented, 3.5–5.5 µm wide. Asci clavate, 8-spored, 35–48 × 14–17 µm (n = 5). Ascospores generally ellipsoid, occasionally globose, 1-septate, polarilocular or narrow septum remaining, hyaline permanently, 7.5–12 × 4.5–7.5 µm (mean = 9.9 × 5.7 µm; SD = 0.9(L), 0.6(W); L/W ratio 1.2–2.3, ratio mean = 1.8, ratio SD = 0.2; n = 104), globose spores 7.5–9 × 7.0–9.2 µm (mean = 8.0 × 7.7 µm; SD = 0.8(L), 0.9(W); L/W ratio 1.0–1.1, ratio mean = 1.0, ratio SD = 0.1; n = 11). Pycnidia not detected.

Chemistry. Thallus K–, KC–, C–, Pd–. Apothecia K+ wine red. Epihymenium K+ wine red. Epihymenium and hymenium I+ blue. UV–. No lichen substance was detected by TLC.

Distribution and ecology. The species occurs on the calcareous rock. The species is currently known from the type collection.

Etymology. The species epithet indicates the lichen's thallus colour, dark green, which is the key characteristic distinguished from all the species in the genus *Huriella*.

Notes. The morphological classification of the new species is not clear between *Huriella* and *Squamulea* because the new species has some characteristics for the former genus and others for the latter, i.e. the new species represents mainly areolate thallus without lobed margin and smaller apothecia for the former, whilst showing some squamulose thallus and wider ascospores for the latter (Table 2). The molecular results concluded the new species classification into the former genus, *Huriella*.

The new species is unique with the key characteristics of green pigmented thallus (with a distinct green layer in a section) and the substrate preference to calcareous rocks amongst all *Huriella* species.

Table 2. Comparison of the new species with two type species in *Huriella* and *Squamulea*.

Species	<i>Huriella aeruginosa</i>	<i>Huriella loekoესiana</i>	<i>Squamulea subsoluta</i>
Thallus	mainly areolate, rimose or placodioid around edge, but without lobes	areolate (not squamulose)	squamulose, areolate or subsquamulose, margin slightly lobed
Apothecia (mm in diam.)	0.2–0.4	0.2–0.4(–0.5)	0.1–0.6
Ascospores (μm)	7.5–12 \times 4.5–7.5	(8.5–)9–11(–12) \times (4.5)5–6	9.5–12.5 \times 5.5–7
Molecular phylogeny	Huriella	Huriella	Squamulea
Reference	–	Kondratyuk et al. 2017b	Nash III et al. 2007; Arup et al. 2013

The new species is similar to '*Squamulea chelonina*, *Squamulea galactophylla*, '*Squamulea humboldtiana*, *S. parviloba* and *S. subsoluta* in the substrate preference to calcareous rocks. However, the new species is different from '*Squamulea chelonina* by dark greenish-grey to grey thallus without pruina (vs. yellow orange to deep orange thallus with white pruina), gold to yellow-brown epihymenium (vs. orange epihymenium), larger ascospores (7.5–12 \times 4.5–7.5 μm vs. 8–10.4 \times 4.7–6.0 μm) and the chemistry (thallus K–, KC– and no substance vs. thallus K+ purple, KC \pm purplish and the presence of parietin, teloschistin, fallacinal, parietinic acid and emodin) (Bungartz et al. 2020).

The new species differs from *S. galactophylla* by thallus colour (dark greenish-grey to grey vs. dirty white to yellowish-brown), flat to convex disc (vs. flat disc only), yellowish-orange apothecia (vs. cinnamon-brown apothecia), smaller ascospores (7.5–12 \times 4.5–7.5 μm vs. 10–15 \times 5–7 μm) (Fink 1935; Arup 2013).

The new species is distinguished from '*Squamulea humboldtiana* by dark greenish-grey to grey thallus without pruina (vs. yellow-orange to deep orange thallus with pruina), absence of prothallus (vs. presence of prothallus), larger ascospores (7.5–12 \times 4.5–7.5 μm vs. 8.1–9.9 \times 4.8–5.9 μm) and the chemistry (thallus K–, KC– and no substance vs. thallus K+ purple, KC \pm purplish and the presence of parietin, teloschistin, fallacinal, parietinic acid and emodin) (Bungartz et al. 2020).

The new species differs from *S. parviloba* by dark greenish-grey to grey thallus (vs. yellow-orange to orange thallus), absence of lobes (vs. short narrow elongated lobes around edge), convex and yellow-orange disc (vs. flat and deep orange disc), smaller ascospores (7.5–12 \times 4.5–7.5 μm vs. 11–14 \times 5.5–7 μm) and the chemistry (thallus K– vs. thallus K+ red) (Wetmore 2003; Nash III et al. 2007).

The new species is different from *S. subsoluta* by dark greenish-grey to grey thallus (vs. yellow-orange, orange to reddish-orange thallus), absence of prothallus (vs. black prothallus), flat to convex, yellow-orange apothecia (vs. flat to concave, deep orange apothecia) and the chemistry (thallus K– and no substance vs. thallus K+ red, the presence of parietin, fallacinal, emodin and teloschistin) (Wetmore 2003; Nash III et al. 2007).

The most distinctive characteristic of the new species is the thallus colour, i.e. dark greenish-grey to grey, which is different from all comparable calcicolous species in the genus *Squamulea*.

Key to the species of *Huriella* and *Squamulea* (20 taxa)

Although some species of *Huriella* have distinct characteristics, different from *Squamulea*, such as mainly areolate and non-squamulose thallus without lobes at margin, smaller apothecia and narrower ascospores (Kondratyuk et al. 2017b), those morphological taxonomic keys do not clearly separate the two genera concerning all known species in the genera. The morphological characteristics are assumingly based on the comparison between type species of the comparable genera, but several species do not correspond to the characteristics (e.g. *Huriella aeruginosa*, *H. flakusii* Wilk and *H. salyangiana* S.Y. Kondr. & Hur with squamulose thalli), although those species are classified in the genus *Huriella* in molecular phylogeny. Such a discrepancy between morphology and molecular phylogeny occur in *Squamulea squamosa* (B. de Lesd.) Arup, Søchting & Frödén and *S. subsoluta* as well. Both species are considered conspecific in morphology. Both species are very similar in morphology and ecology occurring together on the same rock. Whereas the only difference between them is that the former has a thalline margin and it is lacking in the latter (Nash III et al. 2007), the latter representing a permanent thalline margin from the Galapagos Islands as well (Bungartz et al. 2020). However, the two species are separated and located distant from each other in molecular results of this study (Fig. 5). Nevertheless, those are still considered conspecific in the key below as a taxonomic key is based mainly on ecology, morphology and chemistry. The genera *Huriella* and *Squamulea* should be more studied in the future and here a preliminary key is updated from previous taxonomic keys of Wetmore (2003) and Bungartz et al. (2020).

- | | | |
|---|--|---------------------------------|
| 1 | Not directly on rock, but on lichen or bone..... | 2 |
| – | On rock..... | 4 |
| 2 | On lichen (<i>Aspicilia</i>) living on rock..... | <i>Squamulea nesodes</i> |
| – | On bone..... | 3 |
| 3 | Thallus generally areolate, without blastidia, not pruinose..... | |
| | | <i>'Squamulea' osseophila</i> |
| – | Thallus generally (sub)squamulose, blastidia abundant, not pruinose or faintly orange pruinose on thallus..... | <i>'Squamulea' phyllidizans</i> |
| 4 | On calcareous rocks..... | 5 |
| – | On siliceous rocks..... | 10 |
| 5 | Thallus pruinose..... | 6 |
| – | Thallus not pruinose..... | 7 |
| 6 | Thallus angular, areolate to subsquamulose, prothallus absent..... | |
| | | <i>'Squamulea' chelonia</i> |
| – | Thallus areolate or bullate, prothallus black when present..... | |
| | | <i>'Squamulea' humboldtiana</i> |
| 7 | Thallus whitish, greyish or greenish..... | 8 |
| – | Thallus yellow-orange to orange..... | 9 |
| 8 | Thallus dirty whitish, disc cinnamon-brown..... | <i>Squamulea galactophylla</i> |
| – | Thallus dark greenish-grey to grey, disc orange..... | <i>Huriella aeruginosa</i> |

9	Areole margins with small lobules	<i>Squamulea parviloba</i>
–	Areole margins without lobules.....	<i>Squamulea squamosa (S. subsoluta)</i>
10	With blastidia or soredia	11
–	Without blastidia or soredia.....	13
11	Thallus brownish-orange, apothecia rare, disc reddish to reddish-brown, ascospores 11–16 × 6–8 µm, isthmus 1–3 µm	<i>Squamulea kiamae</i>
–	Thallus yellowish-orange to deep orange, apothecia common, disc concolorous to thallus or slightly deeper, ascospores 8.4–13.3 × 5–7.1 µm, isthmus 2.5–4.6 µm.....	12
12	Blastidia abundant, sometimes faintly orange pruinose on thallus, but not pruinose on disc.....	<i>'Squamulea' phyllidizans</i>
–	Soredia rarely present, rarely white pruinose on disc, but not pruinose on thallus.....	<i>Squamulea squamosa (S. subsoluta)</i>
13	Thallus areolate to (sub)squamulose.....	14
–	Thallus areolate or bullate, but not squamulose.....	21
14	Prothallus distinctly blackened.....	<i>'Squamulea' oceanica</i>
–	Prothallus absent.....	15
15	Disc brownish to reddish or blackish	16
–	Disc orangish.....	19
16	Thallus orange, disc reddish, ascospores 11–14.2 × 5.9–7.5 µm	<i>Huriella flakusii</i>
–	Thallus brownish, disc pale brown, brownish-orange to blackish-brown ...	17
17	Disc dark brown-orange to black-brown, hypothecium 20–30 µm high, ascospores 7–9 × 4.5–6.5 µm.....	<i>Huriella salyangiana</i>
–	Disc pale brown to brownish-orange, hypothecium 50–150 µm high, ascospores 9–13 × 4.5–6 µm.....	18
18	Disc 0.4–0.9 mm diam., hypothecium 50–100 µm high, ascospores 9–13 × 5–6 µm.....	<i>Squamulea coreana</i>
–	Disc 0.2–0.4 mm diam., hypothecium 100–150 µm high, ascospores 10–10.5 × 4.5–6 µm.....	<i>Squamulea uttarkashiana</i>
19	Areole margins with small lobules	<i>Squamulea parviloba</i>
–	Areole margins without lobules.....	20
20	Ascospores 8–10.4 × 4.7–6 µm, isthmus 2.1–3.3, not pruinose on disc	<i>'Squamulea' chelonia</i>
–	Ascospores 8.4–13.3 × 5.2–7 µm, isthmus 2.5–4 µm, rarely pruinose on disc	<i>Squamulea squamosa (S. subsoluta)</i>
21	Thallus yellow-orange to deep orange, prothallus black when present, ascospores 8.1–9.9 × 4.8–5.9 µm, isthmus 2.7–3.2 µm	<i>'Squamulea' humboldtiana</i>
–	Thallus yellow-brownish or yellow-greenish, prothallus absent, ascospores 9–15 × 5–8 µm, isthmus 2–5 µm	22
22	Apothecia 0.2–0.3 mm diam., disc dull brown, dull yellow to bright yellow... ..	23
–	Apothecia 0.3–1 mm diam., disc orange, brownish-yellow to reddish-orange	24

- 23 Disc dull yellow to bright yellow, hymenium 50–60 μm high, hypothecium 20–30 μm high, ascospores 9–11 \times 5–6 μm , isthmus 4–5 μm *Huriella loekoesiana*
- Disc dull brown, hymenium 80–100 μm high, hypothecium 80–110 μm high, ascospores 13–14.5 \times 7–8 μm , isthmus 3–4 μm *Huriella upretiana*
- 24 On mountain, thallus yellow-brown, disc orange, isthmus 3–4 μm *Squmulea micromera*
- On coast, thallus dull green-yellow to yellow-brown, disc orange to red-orange, isthmus 2–3 μm *Huriella pohangensis*

Acknowledgements

This work was supported by a grant from the Korean National Research Resource Center Program (NRF-2017M3A9B8069471).

References

- Aptroot A, Moon KH (2014) 114 new reports of microlichens from Korea, including the description of five new species, show that the microlichen flora is predominantly Eurasian. *Herzogia* 27(2): 347–365. <https://doi.org/10.13158/heia.27.2.2014.347>
- Aptroot A, Moon KH (2015) New lichen records from Korea, with the description of the lichenicolous *Halecania parasitica*. *Herzogia* 28(1): 193–203. <https://doi.org/10.13158/heia.28.1.2015.193>
- Arup U, Søchting U, Frödén P (2013) A new taxonomy of the family Teloschistaceae. *Nordic Journal of Botany* 31(1): 016–083. <https://doi.org/10.1111/j.1756-1051.2013.00062.x>
- Bouckaert RR, Drummond AJ (2017) bModelTest: Bayesian phylogenetic site model averaging and model comparison. *BMC Evolutionary Biology* 17(1): e42. <https://doi.org/10.1186/s12862-017-0890-6>
- Bouckaert R, Vaughan TG, Barido-Sottani J, Duchêne S, Fourment M, Gavryushkina A, Heled J, Jones G, Kühnert D, De Maio N, Matschiner M, Mendes FK, Müller NF, Ogilvie HA, du Plessis L, Popinga A, Rambaut A, Rasmussen D, Siveroni I, Suchard MA, Wu CH, Xie D, Zhang C, Stadler T, Drummond AJ (2019) BEAST 2.5: An advanced software platform for Bayesian evolutionary analysis. *PLoS Computational Biology* 15(4): e1006650. <https://doi.org/10.1371/journal.pcbi.1006650>
- Bungartz F, Søchting U, Arup U (2020) Teloschistaceae (lichenized Ascomycota) from the Galapagos Islands: a phylogenetic revision based on morphological, anatomical, chemical, and molecular data. *Plant and Fungal Systematics* 65(2): 515–576. <https://doi.org/10.35535/pfsyst-2020-0030>
- Edler D, Klein J, Antonelli A, Silvestro D (2019) raxmlGUI 2.0 beta: a graphical interface and toolkit for phylogenetic analyses using RAxML. *bioRxiv*. <https://doi.org/10.1101/800912>
- Ekman S (2001) Molecular phylogeny of the Bacidiaceae (Lecanorales, lichenized Ascomycota). *Mycological Research* 105: 783–797. <https://doi.org/10.1017/S0953756201004269>

- Fink B (1935) The Lichen Flora of the United States. University of Michigan Press, MI, USA
<https://doi.org/10.3998/mpub.9690813>
- Frolov I, Vondrák J, Fernández-Mendoza F, Wilk K, Khodosovtsev A, Halıcı MG (2016) Three new, seemingly-cryptic species in the lichen genus *Caloplaca* (Teloschistaceae) distinguished in two-phase phenotype evaluation. *Annales Botanici Fennici* 53(3–4): 243–262.
<https://doi.org/10.5735/085.053.0413>
- Hall TA (1999) BioEdit: A User-Friendly Biological Sequence Alignment Editor and Analysis Program for Windows 95/98/NT. *Nucleic Acids Symposium Series* 41: 95–98.
- Joshi Y, Wang XY, Koh YJ, Hur JS (2009) *Thelotrema subtile* and *Verrucaria muralis* New to Korea. *Mycobiology* 37(4): 302–304. <https://doi.org/10.4489/MYCO.2009.37.4.302>
- Khodosovtsev A, Kondratyuk S, Kärnefelt I (2002) *Caloplaca albopustulata*, a new saxicolous lichen from Crimea Peninsula, Ukraine. *Graphis Scripta* 13: 5–8.
- Kondratyuk SY, Lőkös L, Halda JP, Haji Moniri M, Farkas E, Park JS, Lee BG, Oh SO, Hur JS (2016a) New and noteworthy lichen-forming and lichenicolous fungi 4. *Acta Botanica Hungarica* 58(1–2): 75–136. <https://doi.org/10.1556/034.58.2016.1-2.4>
- Kondratyuk SY, Lőkös L, Halda JP, Upreti DK, Mishra GK, Haji Moniri M, Farkas E, Park JS, Lee BG, Liu D, Woo JJ, Jayalal RGU, Oh SO, Hur JS (2016b) New and noteworthy lichen-forming and lichenicolous fungi 5. *Acta Botanica Hungarica* 58(3–4): 319–396. <https://doi.org/10.1556/ABot.58.2016.3-4.7>
- Kondratyuk SY, Lőkös L, Halda JP, Roux C, Upreti DK, Schumm F, Mishra GK, Nayaka S, Farkas E, Park JS, Lee BG, Liu D, Woo JJ, Hur JS (2017a) New and noteworthy lichen-forming and lichenicolous fungi 6. *Acta Botanica Hungarica* 59(1–2): 137–260. <https://doi.org/10.1556/034.59.2017.1-2.7>
- Kondratyuk SY, Lőkös L, Upreti DK, Nayaka S, Mishra GK, Ravera S, Jeong MH, Jang SH, Park JS, Hur JS (2017b) New monophyletic branches of the Teloschistaceae (lichen-forming Ascomycota) proved by three gene phylogeny. *Acta Botanica Hungarica* 59(1–2): 71–136. <https://doi.org/10.1556/034.59.2017.1-2.6>
- Kondratyuk SY, Lőkös L, Oh SO, Kondratiuk TO, Parnikoza IY, Hur JS (2020) New and Noteworthy Lichen-Forming and Lichenicolous Fungi, 11. *Acta Botanica Hungarica* 62(3–4): 225–291. <https://doi.org/10.1556/034.62.2020.3-4.3>
- Kossowska M (2008) Lichens growing on calcareous rocks in the Polish part of the Sudety Mountains. *Zakład Bioróżnorodności i Ochrony Szaty Roślinnej, Instytut Biologii Roślin Uniwersytetu Wrocławskiego, Wrocław*.
- Nash III TH, Ryan BD, Diederich P, Gries C, Bungartz F (2007) Lichen Flora of the Greater Sonoran Desert Region, Vol III. Lichens Unlimited/Arizona State University, Tempe.
- Orange A, James PW, White FJ (2001) *Microchemical Methods for the Identification of Lichens*. The British Lichen Society, London.
- Pykälä J, Launis A, Myllys L (2017) Four new species of *Verrucaria* from calcareous rocks in Finland. *The Lichenologist* 49(1): 27–37. <https://doi.org/10.1017/S0024282916000542>
- Rehner SA, Samuels GJ (1994) Taxonomy and phylogeny of *Gliocladium* analysed from nuclear large subunit ribosomal DNA sequences. *Mycological Research* 98: 625–634. [https://doi.org/10.1016/S0953-7562\(09\)80409-7](https://doi.org/10.1016/S0953-7562(09)80409-7)

- Rambaut A (2014) FigTree v1.4.2. University of Edinburgh, Edinburgh. <http://tree.bio.ed.ac.uk/software/figtree>
- Schultz M, Moon KH (2011) Notes on taxonomy and distribution of some critical cyanobacterial lichens from South Korea. *Nova Hedwigia* 92(3): 479–486. <https://doi.org/10.1127/0029-5035/2011/0092-0479>
- Schwarz G (1978) Estimating the dimension of a model. *Annals of Statistics* 6: 461–464. <https://doi.org/10.1214/aos/1176344136>
- Stecher G, Tamura K, Kumar S (2020) Molecular Evolutionary Genetics Analysis (MEGA) for macOS. *Molecular Biology and Evolution* 37(4): 1237–1239. <https://doi.org/10.1093/molbev/msz312>
- Tretiach M, Pinna D, Grube M (2003) *Caloplaca erodens* [sect. *Pyrenodesmia*], a new lichen species from Italy with an unusual thallus type. *Mycological Progress* 2(2): 127–136. <https://doi.org/10.1007/s11557-006-0050-7>
- Tretiach M, Muggia L (2006) *Caloplaca badioreagens*, a new calcicolous, endolithic lichen from Italy. *The Lichenologist* 38(3): 223–229. <https://doi.org/10.1017/S0024282906005305>
- van den Boom PP, Elix JA (2005) Notes on *Halecania* species, with descriptions of two new species from Asia. *The Lichenologist* 37(3): 237–246. <https://doi.org/10.1017/S0024282905014787>
- Vondrák J, Khodosovtsev A, Pavel Ř (2008) *Caloplaca concreticola* (Teloschistaceae), a new species from anthropogenic substrata in Eastern Europe. *The Lichenologist* 40(2): 97–104. <https://doi.org/10.1017/S002428290800755X>
- Watson W (1918) The bryophytes and lichens of calcareous soil. *Journal of Ecology* 6(3): 189–198. <https://doi.org/10.2307/2255303>
- Wetmore CM (2003) The *Caloplaca squamosa* group in North and Central America. *The Bryologist* 106(1): 147–156. [https://doi.org/10.1639/0007-2745\(2003\)106\[0147:TCSGIN\]2.0.CO;2](https://doi.org/10.1639/0007-2745(2003)106[0147:TCSGIN]2.0.CO;2)
- White TJ, Bruns T, Lee S, Taylor JW (1990) Amplification and direct sequencing of fungal ribosomal RNA genes for phylogenetics. *PCR protocols: a guide to methods and applications* 18(1): 315–322. <https://doi.org/10.1016/B978-0-12-372180-8.50042-1>
- Zoller S, Scheidegger C, Sperisen C (1999) PCR primers for the amplification of mitochondrial small subunit ribosomal DNA of lichen-forming ascomycetes. *The Lichenologist* 31(5): 511–516. <https://doi.org/10.1006/lich.1999.0220>

Novel *Mucor* species (Mucoromycetes, Mucoraceae) from northern Thailand

Vedprakash G. Hurdeal^{1,2,3}, Eleni Gentekaki^{1,2}, Kevin D. Hyde²,
Thuong T.T. Nguyen³, Hyang Burm Lee³

1 School of Science, Mae Fah Luang University, Chiang Rai, 57100, Thailand **2** Center of Excellence in Fungal Research, Mae Fah Luang University, Chiang Rai, 57100, Thailand **3** Environmental Microbiology Lab, Dept. of Agricultural Biological Chemistry, College of Agriculture and Life Sciences, Chonnam National University, Gwangju 61186, South Korea

Corresponding author: Hyang Burm Lee (hblee@jnu.ac.kr), Eleni Gentekaki (gentekaki.ele@mfu.ac.th)

Academic editor: Kerstin Voigt | Received 13 July 2021 | Accepted 27 September 2021 | Published 01 November 2021

Citation: Hurdeal VG, Gentekaki E, Hyde KD, Nguyen TTT, Lee HB (2021) Novel *Mucor* species (Mucoromycetes, Mucoraceae) from northern Thailand. MycoKeys 84: 57–78. <https://doi.org/10.3897/mycokeys.84.71530>

Abstract

Mucor species are common fast-growing fungi found in soil. Two new species of *Mucor* and one new geographical record of *M. nederlandicus* were collected from northern Thailand and are described in this study. Evidence from morphophysiological data and phylogenetic analysis supports the introduction of the new taxa. Phylogenetic analysis based on the internal transcribed spacer (ITS) and large subunit of the nuclear ribosomal RNA (LSU) data showed that the new isolates cluster distinctly from other *Mucor* species with high or maximum bootstrap support. *Mucor aseptatophorus* is characterized by aseptate sporangiophores, globose columella, resistant and deliquescent sporangia, has sympodial, and monopodial branches and shows growth at 37 °C. It also differs from *M. irregularis* in having smaller sporangiospores, and larger sporangia. *Mucor chiangraiensis* has subglobose or slightly elongated globose columella, produces hyaline sporangiospores, and resistant and deliquescent sporangia. Furthermore, this species has wider sporangiophore, smaller sporangia and lower growth than *M. nederlandicus*. A detailed description of the species and illustrations are provided for the novel species.

Keywords

Molecular phylogeny, Mucorales, 1 geographical record, soil fungi, 2 new species

Introduction

Soil fungi play key roles in nutrient cycling and the functioning of terrestrial ecosystems (Torsvik and Øvreås 2002; Fraç et al. 2018; Peng et al. 2020; Zhou et al. 2020). To date, only a few fungal taxonomic studies are available from tropical forest soil (Sato et al. 2015; Amma et al. 2018; Cordeiro et al. 2020; Lima et al. 2020). Taxonomic studies on these groups are even scarcer in Southeast Asia despite the region harboring extraordinary genetic diversity (Amma et al. 2018). Up to 96% of fungi isolated from the northern part of Thailand are projected to be novel taxa and new species are regularly being discovered (Hyde et al. 2018; 2020). However, the diversity of non-Dikarya soil fungi in the country remains to be fully explored (Khuna et al. 2019; Hurdeal et al. 2021; Suwannarach et al. 2021).

Mucorales are cosmopolitan fungi commonly found in soil (Pawłowska et al. 2019; Muszewska et al. 2021). It is an early-diverging fungal group in a basal position with respect to Ascomycota and Basidiomycota in the fungal tree of life (Spatafora et al. 2016; Nicolás et al. 2020). The order comprises 55 genera with over 260 species (Walther et al. 2019; Cordeiro et al. 2020; Lima et al. 2020; Nicolás et al. 2020; Wijayawardene et al. 2020; Hurdeal et al. 2021). However, for the majority of these species, their ecological roles and geographical distributions are unknown. Mucoralean fungi are usually fast-growing and produce coenocytic or irregularly septate hyphae. Septae are usually formed to delimit reproductive structures but are not dispersed in regular intervals as in Dikarya fungi (Walther et al. 2019; Wagner et al. 2020). Characters including homothallism, formation of sporangiola, and the shape of the suspensors have been previously employed to describe mucoralean taxa (Walther et al. 2019). However, the application of molecular phylogenetics has transformed the taxonomy of Mucorales as it has revealed that some of the above-mentioned morphological characters are not taxonomically informative.

Mucor is the most species-rich genus within Mucorales commonly found in soil and dung. Its species comprise mainly saprobes, but also endophytes, parasites of plants and human pathogens causing mucormycosis (e.g. *M. irregularis*) (Mendoza et al. 2014; Lunge et al. 2015; Mishra et al. 2019; Wagner et al. 2020). *Mucor* was first described by Fresenius (1850) and has over 300 species cited in previous literature (Kirk 1986; Jacobs and Botha 2008; Nguyen et al. 2016; Lima et al. 2020). The suggested number of valid taxa varies from 50 to 91 species (Walther et al. 2019; Lima et al. 2020; Wijayawardene et al. 2020). *Mucor* species form fast-growing colonies characterized by simple or branched sporangiophores, non-apophysate and globose sporangia, deliquescent, and incrustated sporangial wall, and zygospores on opposed or tong-like suspensors. However, morphology-based classification of *Mucor* is highly debated. For example, previous literature used rhizoids to demarcate *Rhizomucor* from *Mucor* (Lima et al. 2020; Nguyen et al. 2020). Contrary to this, recent studies have revealed that some species of *Mucor* produce rhizoids (Lima et al. 2018; Nguyen and Lee 2020). *Mucor* comprises mesophilic species with some growing at high temperatures, but never at temperatures above 42 °C (Walther et al. 2019).

While studying the diversity of soil fungi in northern Thailand, two *Mucor* isolates differed morphologically and genetically from other known species. Using molecular phylogeny of ITS and LSU genetic markers along with morphological characterization, two new species of *Mucor* are proposed. Full description, taxonomic notes, photoplates, and phylogenetic trees are provided.

Materials and methods

Collections and field sites

Soil samples were collected from the provinces of Chiang Mai, and Chiang Rai, Thailand. Superficial organic matter (1–3 cm deep) was manually removed and a clean shovel was used to dig the soil. Samples were placed in a zip lock bag and stored at 4 °C until further use. The collecting site in Chiang Rai comprised a maple tree plantation and the sample was collected during the winter season in December 2019. The temperature in the province during this month is usually around 13.5 °C, while the annual rainfall is 2172 mm. The samples collected, consisted of peat and grainy soil. In Chiang Mai, moist peat soil was collected from a deciduous forest during the monsoon season in October 2019. During this season, the temperature is around 31 °C with an annual rainfall of 1108 mm.

Isolation, culture and morphological studies

The dilution plating method was used for the isolation of fungal species (Senanayake et al. 2020). Soil samples were diluted to a ratio of 1:5 and 1:10 with sterilized distilled water. The mixture was shaken at 25 °C and 200 rpm for two hours using an incubator shaker. 100 µL of the suspension was then plated on agar plates. All Petri plates used herein were 90 mm. To maximize the number of fungi isolated, four different media were used: yeast malt extract (YMA) (yeast extract: 3g; malt extract: 3g; peptone: 5g; glucose: 10g; agar: 15g; distilled water: 1L), plate count agar (PCA) (enzymatic digest of casein: 5g; yeast extract: 2.5g; glucose: 1g; ; agar: 15g; distilled water: 1L), nutrient agar (NA) and modified choanephora agar (CH) (glucose: 3 g; pancreatic digest of casein: 2 g; KH_2PO_4 : 1 g; $\text{MgSO}_4 \cdot 7\text{H}_2\text{O}$: 0.5 g; thiamine HCl: 25 mg; agar: 20 g; distilled water: 1L) with or without benomyl. Benomyl (2 mg/L) was used to limit the growth of other fungi. Suspension of each soil sample was spread on four media using a flame sterilized rod spreader in triplicate. Plates were sealed and incubated at 20, 30, and 37 °C.

All plates were checked daily. Once fungal colonies were seen, the plates were screened using a microscope (400X) (Zeiss Primostar). Recovered strains were divided into morphotypes based on colony appearance and the presence of specific sporulation structures, when possible. A sterile straw was used to cut the fungal tips, which were transferred to a new agar plate. This process was done 2 or 3 days post-inoculation,

before different fungal colonies overlapped on the plate. Growth experiments were performed using MEA media incubated at 8, 20, 25, 30, and 37 °C.

Once grown, the cultures were examined using a compound microscope (Nikon Eclipse Ni) and pictures were taken with a Nikon DS-RI2 digital camera. The cultures were maintained in 15% glycerol at 4 °C. Herbarium and type specimens were deposited in Mae Fah Luang University (MFLU) Herbarium, Chiang Rai, Thailand as inactive dried cultures. Ex-type living cultures were deposited in the Mae Fah Luang culture collection (MFLUCC), Chiang Rai, Thailand.

DNA extraction and PCR amplification

Total genomic DNA was extracted from fungal mycelia using the SolgTM Genomic DNA Prep Kit following the manufacturer's instructions. Polymerase chain reaction (PCR) was used to amplify the partial fragments of internal transcribed spacer (ITS), and large subunit ribosomal RNA (LSU) using fungal-specific primers (Vilgalys and Hester 1990; White et al. 1990; De Hoog and Van Den Ende 1998). The PCR reaction mixture consisted of the fungal DNA, 14 µL dH₂O, 1 µL AccuPower PCR PreMix (BioneerCorp., Daejeon, Korea) and 1.5 µL (5 pmol/µL) each of forward and reverse primers resulting in a final volume of 20 µL.

Amplification of the ITS and LSU fragments was performed using the following conditions: initial heat treatment of 5 min at 94 °C, 30 cycles with a denaturation step at 94 °C for 30 sec, annealing at 52 °C for 45 sec and an elongation step of 1 minute and 30 sec at 72 °C and a final elongation period of 7 minutes at 72 °C.

The PCR products were then purified using an Accuprep PCR Purification Kit (Bioneer). Sequencing was performed by Macrogen (South Korea) using an Applied Biosystems 3130XL DNA analyzer.

Sequence and phylogenetic analysis

Raw reads were edited by removing ambiguous bases in the ends using BioEdit. The forward and reverse trimmed reads were assembled into contigs using SeqMan Version 7.1.0. Newly generated sequences were used as queries to perform blast searches against the nucleotide database in GenBank (Altschul et al. 1990). This was done to check for possible contamination and to find the closest taxa. The taxon sampling spans the diversity of the genus with the exception of some phylogenetically closely related species in the *M. circinelloides* complex. Information on each species was extracted from GenBank taxonomy and correlated with Species Fungorum (<http://www.speciesfungorum.org/>), Index Fungorum (<http://www.indexfungorum.org/>) and MycoBank (<https://www.mycobank.org/>) to determine the validity and current name of each taxon. Datasets of the ITS and LSU genetic markers were built. The software MAFFT Version 7 available on the online server <https://mafft.cbrc.jp/alignment/server/> (Katoh and Toh 2008) was used to align the sequences and each matrix was trimmed using TrimAl

Table I. Data used for phylogenetic analysis in this study and their corresponding GenBank accession numbers. Type, ex-neotype, ex-isotype, and ex-type strains are denoted by T, NT, IT, and ET, respectively. Sequences derived in this study are shown in bold letters.

Strain name	Voucher No.	ITS	LSU
<i>M. abundans</i> ^{NT}	CBS 388.35	JN206111	NG_063979
<i>M. abundans</i>	CBS 521.66	JN206110	JN206457
<i>M. aligarensis</i> ^T	CBS 993.70	NR_103634	NG_057920
<i>M. aligarensis</i>	NNIBRFG6255	MN267431	-
<i>M. amethystinus</i>	CBS 526.68	JN206015	JN206426.1
<i>M. amethystinus</i> ^T	CBS 846.73	JN206014	-
<i>M. amphibiorum</i> ^T	CBS 763.74	NR_103615	NG_057877
<i>M. ardhlaengiktus</i>	ATCC-MYA-4767	NR_111683	NG_042602
<i>M. ardhlaengiktus</i> ^{ET}	CBS 210.80	NR_152960	NG_069778
<i>M. atramentarius</i> ^T	CBS 202.28	MH854979.1	JN206418.1
<i>M. azygosporus</i> ^T	CBS 292.63	NR_103639	NG_057928
<i>M. bacilliformis</i> ^T	CBS 251.53	NR_145285	NG_057916
<i>M. baimieri</i> ^{IT}	CBS 293.63	NR_103628	JN206424
<i>M. caatinguensis</i> ^T	URM 7223	KT960377	KT960371
<i>M. chiangraiensis</i>^T	MFLU 21-0079	MZ433253	MZ433250
<i>M. chuxiongensis</i> ^T	CBS 14370	MG255732	MG255711
<i>M. circinatus</i>	URM 90063	KY008576	KY008571
<i>M. circinelloides</i>	B5-2	KT876701	-
<i>M. circinelloides</i>	CBS 108.16	JN205954	MH866163
<i>M. corticola</i>	CBS 362.68	JN206132	JN206449
<i>M. ctenidius</i> ^{IT}	CBS 293.66	MH858796	JN206417
<i>M. durus</i>	CBS 156.51	NR_145295	NG_057918
<i>M. endophyticus</i>	CBS 385.95	NR_111661	NG_057970
<i>M. exponens</i>	CBS 141.20	MH854686	JN206441
<i>M. falcatus</i>	CBS 251.35	NR_103647	NG_057931
<i>M. fluvii</i>	CNUFC-MSW21-1	MF667992	MF667995
<i>M. fluvii</i>	CNUFC-MSW21-2	MF667991	MF667996
<i>M. flavus</i> ^T	CBS 230.35	JN206061	JN206464
<i>M. fuscus</i>	CBS 132.22	JF723619	MH866227
<i>M. fuscus</i>	CBS 230.29	JN206204	FN650659
<i>M. fusiformis</i>	CBS 336.68	NR_111660	NG_057915
<i>M. genevensis</i> ^T	CBS 114.08	NR_103632	NG_057971
<i>M. genevensis</i>	CBS 535.78	-	-
<i>M. gigasporus</i>	CBS 566.91	NR_103646	NG_057926
<i>M. griseocyanus</i> ^T	CBS 116.08	NR_126136	NG_056283
<i>M. guiliermondii</i>	CBS 174.27	NR_103636	NG_057923
<i>M. guiliermondii</i>	ABTSJ72	KP790014	-
<i>M. heterogamus</i>	CBS 338.74	JN206169	JN206488
<i>M. hiemalis</i>	CBS 115.18	JN206127	-
<i>M. inaequisporus</i>	CBS 255.36	JN206177	NG_057929
<i>M. inaequisporus</i>	CBS 351.50	JN206178	MH868169
<i>M. indicus</i>	CBS 226.29	NR_077173	NG_057878
<i>M. irregularis</i> ^T	CBS 103.93	JN206150	NG_056285
<i>M. irregularis</i>	CBS 977.68	JX976259	JX976214
<i>M. irregularis</i>	CBS 700.71	JX976247	JN206450
<i>M. irregularis</i>	CBS 100164	JX976258	JX976213
<i>M. irregularis</i>	CBS 609.78	JX976260	JX976215
<i>M. irregularis</i>	TWS48Abf-e	MN629208	-
<i>M. japonicus</i> ^{NT}	CBS 154.69	JN206158	JN206446
<i>M. koreanus</i>	EML-QT1	KT936259	NG_068529
<i>M. koreanus</i>	EML-QT2	KT936260	KT936254
<i>M. laxorrbizus</i>	CBS 143.85	NR_103642	NG_057914

Strain name	Voucher No.	ITS	LSU
<i>M. lusitanicus</i> ^{ET}	CBS 108.17	JN205980	NG_056279
<i>M. luteus</i>	CBS 243.35	JX976254	NG_057969
<i>M. megalocarpus</i>	CBS 215.27	NR_145286	NG_057925
<i>M. merdicola</i> ^T	URM 7222	KT960374	KT960372
<i>M. merdophylus</i> ^T	URM 7908	MK775467	MK775466
<i>M. minutus</i> ^T	CBS 586.67	NR_152958	JN206463
<i>M. moelleri</i> ^T	CBS 406.58	NR_111659	MH869359
<i>M. mousanensis</i>	CBS 999.70	NR_103629	NG_057912
<i>M. mucedo</i>	CBS 542.66	JN206086	-
<i>M. mucedo</i>	CBS 987.68	JN206089	JN206480
<i>M. multiplex</i>	CBS 110662	NR_111662	NG_057924
<i>M. nederlandicus</i>	CBS 735.70	MH859923	MH871720
<i>M. nederlandicus</i>	MFLU 21–0078	MZ433254	MZ433251
<i>M. nidicola</i>	Isolate H13	KX375786	KX375769
<i>M. odoratus</i>	CBS 130.41	NR_145287	NG_057927
<i>M. orantomantidis</i> ^T	CNUFC-MID1–1	MH594737	MH591457
<i>M. parviseptatus</i>	CBS 417.77	JN206108	JN206453
<i>M. pernambucoensis</i> ^T	URM 7640	MH155323	MH155322
<i>M. piriformis</i>	CBS 169.25	NR_103630	NG_057874
<i>M. plasmaticus</i>	CBS 275.49	JN206078	JN206483
<i>M. plumbeus</i>	CBS 634.74	HM999955	HM849677
<i>M. prayagensis</i>	CBS 652.78	JN206189	JN206498
<i>M. pseudocircinelloides</i> ^T	CBS 541.78	JN206013.1	JN206431.1
<i>M. pseudolusitanicus</i> ^T	CBS 540.78	MF495059	NG_073591
<i>M. pseudolusitanicus</i>	CBS 543.80	MF495060.1	-
<i>M. racemosus</i>	CBS 115.08	JN206433	JN939201
<i>M. racemosus</i>	CBS 260.68	NR_126135	HM849676
<i>M. namosissimus</i> ^{NT}	CBS 135.65	NR_103627	NG_056280
<i>M. rudolphii</i>	WU 35867	KT736104	-
<i>M. rudolphii</i>	WU 35869	NR_152977	-
<i>M. saturninus</i> ^T	CBS 974.68	NR_103635	JN206458
<i>M. septatum</i>	URM 7364	KY849814	KY849816
<i>M. silvaticus</i>	CBS 249.35	JN206122	JN206455
<i>M. aseptatophorus</i> ^T	MFLU 21–0040	MZ433252	MZ433249
<i>M. souzae</i>	URM 91186	KY992878	KY992879
<i>Mucor</i> sp.	MFLU 21–0082	MZ379497	MZ379500
<i>Mucor</i> sp.	P1	EU551186	
<i>Mucor</i> sp.	P2	FJ613116	FJ613117
<i>M. stercorarius</i>	CNUFC-UK2–1	KX839689	KX839685
<i>M. stercorarius</i>	CNUFC-UK2–2	KX839680	KX839682
<i>M. strictus</i>	CBS 100.66	JN206035	JN206477
<i>M. ucrainicus</i>	CBS 674.88	JN206192	JN206507
<i>M. ucrainicus</i>	CBS 221.71	MH860077	MT523853
<i>M. variicolumellatus</i> ^T	CBS 236.35	JN205979	JN206422.1
<i>M. variicolumellatus</i>	JMRC SF012536	MF495054.1	-
<i>M. variisporus</i>	CBS 837.70	NR_152951	NG_057972
<i>M. zonatus</i>	CBS 148.69	NR_103638	NG_057917
<i>M. zychae</i>	CBS 416.67	NR_103641	NG_057930
<i>B. dispersa</i>	CBS 195.28	JN206271	JN206530
<i>B. grandis</i> ^T	CBS 186.87	NR_103648	JN206527

Isolates and accession numbers determined in the current study are indicated in bold. ATCC: American Type Culture Collection, Virginia, United States; CBS: Centraalbureau voor Schimmelcultures, Utrecht, The Netherlands; CNUFC: Chonnam National University Fungal Collection, Gwangju, South Korea; JMRC: Jena Microbial Resource Collection, Jena Germany; MFLU: Mae Fah Luang University Herbarium, Chiang Rai, Thailand; URM: Departamento de Micrologia of the Universidade Federal de Pernambuco, Recife, Brazil.

(Capella-Gutiérrez et al. 2009). Genetic distances were calculated using the kimura2 parameter in MEGAX with the pairwise deletion gap option.

The nucleotide substitution models were evaluated for each genetic marker on the online CIPRES Portal (<https://www.phylo.org/portal2>) using the jModelTest2 on XSEDE and GTR + I + G was deemed as the best suited.

Maximum likelihood (ML) analysis was performed on the online CIPRES Portal using RAxML-HPC2 on XSEDE Version 8.2.12 with bootstrap support obtained from 1000 pseudoreplicates (Miller et al. 2010; Stamatakis 2014). The ML analysis was performed by partitioning the dataset according to the specific genetic marker. Bayesian inference (BI) analysis (Huelsenbeck and Ronquist 2001) was also performed on the online CIPRES Portal using MrBayes on XSEDE Version 3.2.7a. The analysis was conducted by running four simultaneous chains for 5,000,000 generations in two independent runs with a sampling frequency of 100 and temp parameter was adjusted to 0.05. At the end of the analysis the standard deviation of split frequency was less than 0.01 at which point convergence of the runs was declared.

Results

Phylogenetic analyses

The blast search against the NCBI database indicated that the strains belonged to *Mucor* as the majority of results were of the same genus with some being type species. The phylogenetic tree comprised 102 taxa including the strains isolated in this study. *Backusella dispersa* (CBS 195.28), and *B. grandis* (CBS 186.87) were used as outgroup taxa. After the removal of ambiguous positions, the ITS alignment contained 553 sites for ITS and that of LSU 1464 sites. The concatenated ITS-LSU alignment consisted of 2017 characters. The final concatenated matrix comprised 813 distinct alignment patterns and 39.49% of undermined characters or gaps. The tree topologies from ML and BI were mostly congruent. Phylogenetic analysis showed that the new strains formed distinct clades with maximum bootstrap support (BS). The isolate MFLU 21–0145 was sister to the clade formed by *Mucor* sp. MFLU 21–0082 and *Mucor* sp. TWS48Abf-e (BS:82/PP:0.97) and the three to *M. irregularis* (BS:100/PP:1.00). The MFLU 21–0079 strain was sister to the clade formed by *Mucor* sp. P1 and *Mucor* sp. P2 (BS:100/PP:1.00). The MFLU 21–0078 strain grouped with *M. nederlandicus* (BS:100/PP:1.00). The MFLU 21–0082 and MFLU 21–0078 clades grouped together (BS:100/PP:1.00) and as sister to *M. inaequisporus*, however this latter relationship is not strongly supported (CBS 255.36, CBS 351.50; PP: 0.95). The genetic distance between the novel taxa and their closely related taxa in the trimmed ITS gene region (578 bp for MFLU 21–0145 and *M. irregularis* group; 563 bp for MFLU 21–0079, MFLU 21–0078, and *M. inaequisporus* group) is shown in Table 2.

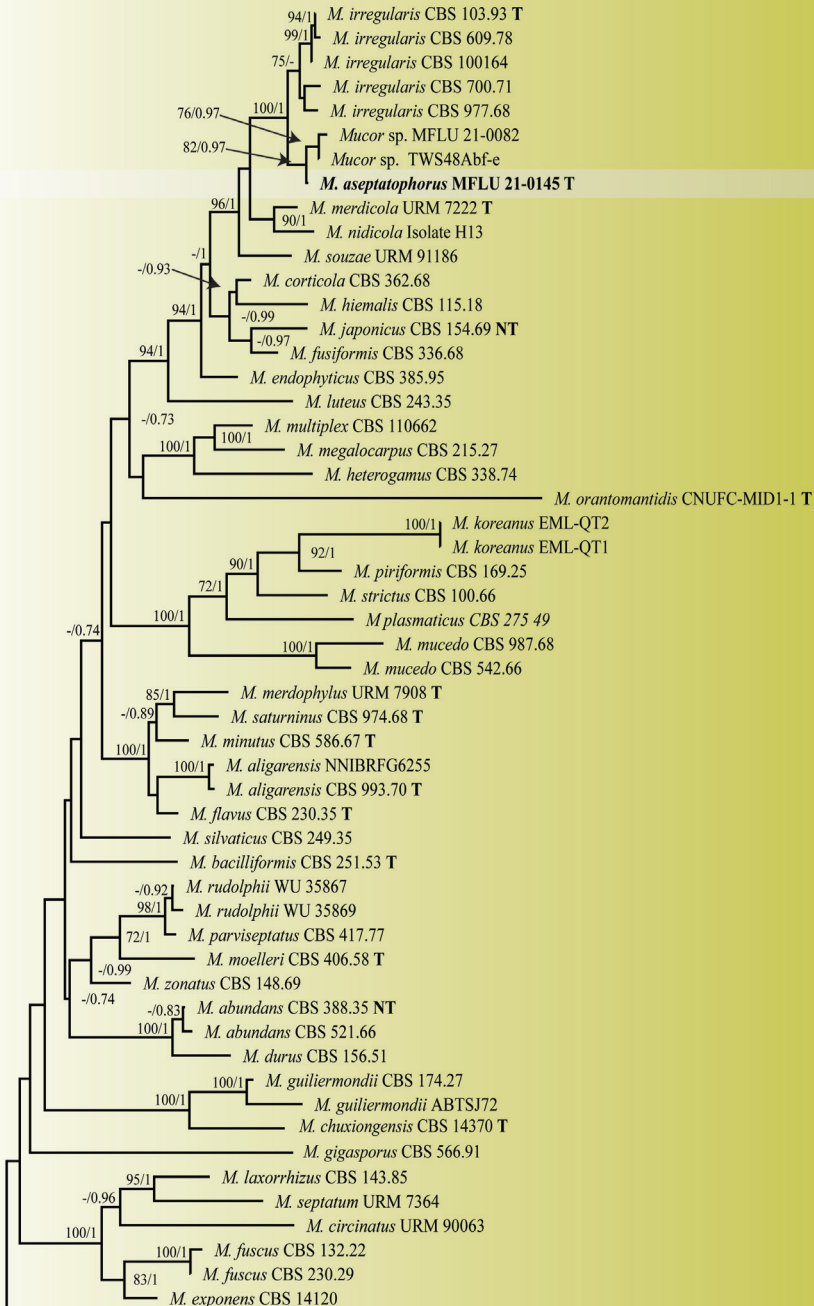


Figure 1. Maximum likelihood phylogram inferred from 102 taxa and 2017 characters based on ITS, and LSU matrix using GTR+G+I model and partition analysis. Maximum likelihood bootstrap support ($\geq 70\%$) and Bayesian posterior probability (≥ 0.70) are indicated above the branches or near the nodes in this order. The tree is artificially rooted using *Backusella dispersa* (CBS 195.28), and *B. grandis* (CBS 186.87). The new species are in bold and the type species in the dataset are indicated using T. (-) represent bootstrap support lower than 70% or posterior probability lower than 0.70.

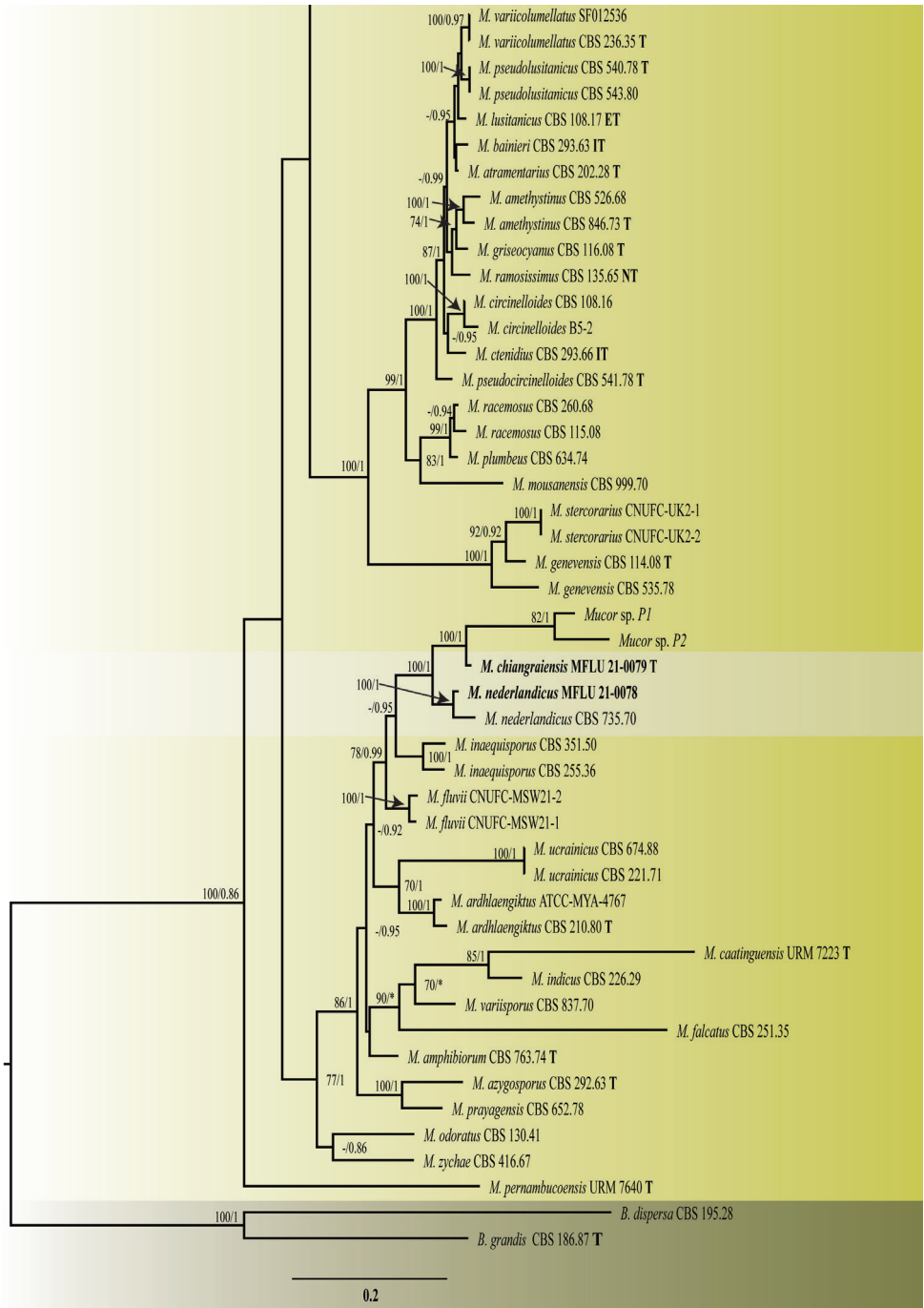


Figure 1. — continued.

Table 2. Genetic distance (%) of the trimmed ITS region between the newly described *Mucor* species and their respective sister taxa. Distances were calculated using the Kimura2 parameter and gaps were considered as pairwise deletion.

Strains	% Genetic distance	
	<i>M. aseptatophorus</i> MFLU 21–0145	
<i>Mucor</i> sp. MFLU 21–0082	2.5	
<i>Mucor</i> sp. TWS48Abf-c	1	
<i>M. irregularis</i> CBS 977.68	3.5	
<i>M. irregularis</i> CBS 103.93	4.5	
<i>M. irregularis</i> CBS 609.78	4.5	
<i>M. irregularis</i> CBS 100164	4	
<i>M. irregularis</i> CBS 700.71	3	
	<i>M. chiangraiensis</i> MFLU 21–0079	
<i>Mucor</i> sp. P1	1.5	
<i>Mucor</i> sp. P2	1	
<i>M. nederlandicus</i> MFLU 21–0078	7.5	
<i>M. nederlandicus</i> CBS 735.70	5.5	
<i>M. nederlandicus</i> CBS 255.36	12.5	
<i>M. inaequisporus</i> CBS 351.50	13.5	

Taxonomy

***Mucor aseptatophorus* V.G. Hurdeal, E. Gentekaki, K.D. Hyde & H.B. Lee, sp. nov.**

MycoBank No: 840562

Facesoffungi Number: FoF09923

Figs 1, 2

Etymology. Named after the aseptate sporangiophores produced by this species.

Holotype. MFLU 21–0145

Gene sequences. (ITS) MZ433252; (LSU) MZ433249

Diagnosis. *Mucor aseptatophorus* is phylogenetically distinct from *M. irregularis*. In the phylogenetic analysis, *M. aseptatophorus* groups as sister to two *Mucor* sp. and all of them cluster as sister to the clade formed by *M. irregularis* strains with high bootstrap support. In contrast to *M. irregularis*, the ellipsoidal, cylindrical, or pyriform columella are not observed in *M. aseptatophorus*. Columella formed in the latter are globose. *Mucor aseptatophorus* has smaller sporangiospores ($3.5\text{--}5 \times 2\text{--}2.5 \mu\text{m}$), slightly bigger sporangia, forms sympodial, and monopodial branching of sporangiospores and has a lower growth rate than *M. irregularis*. The species differs from *M. merdicola* and *M. nidicola*, by having smaller columella, sporangia and sporangiospore. Compared to *M. souzae*, sporangiophores in *M. aseptatophorus* are aseptate (below sporangia). Septation, when observed, is usually present at the branching point. Septae below the sporangia rarely observed.

Material examined. THAILAND. Chiang Mai Province, Omkoi District, Sop Khong, $17^{\circ}45'25''\text{N}$; $98^{\circ}20'21''\text{E}$, from soil, 24th October 2019, collected by Oundhyalah Devi Padaruth, and isolated by Vedprakash Godadhar Hurdeal, ex-type living culture, MFLUCC 21–0040.

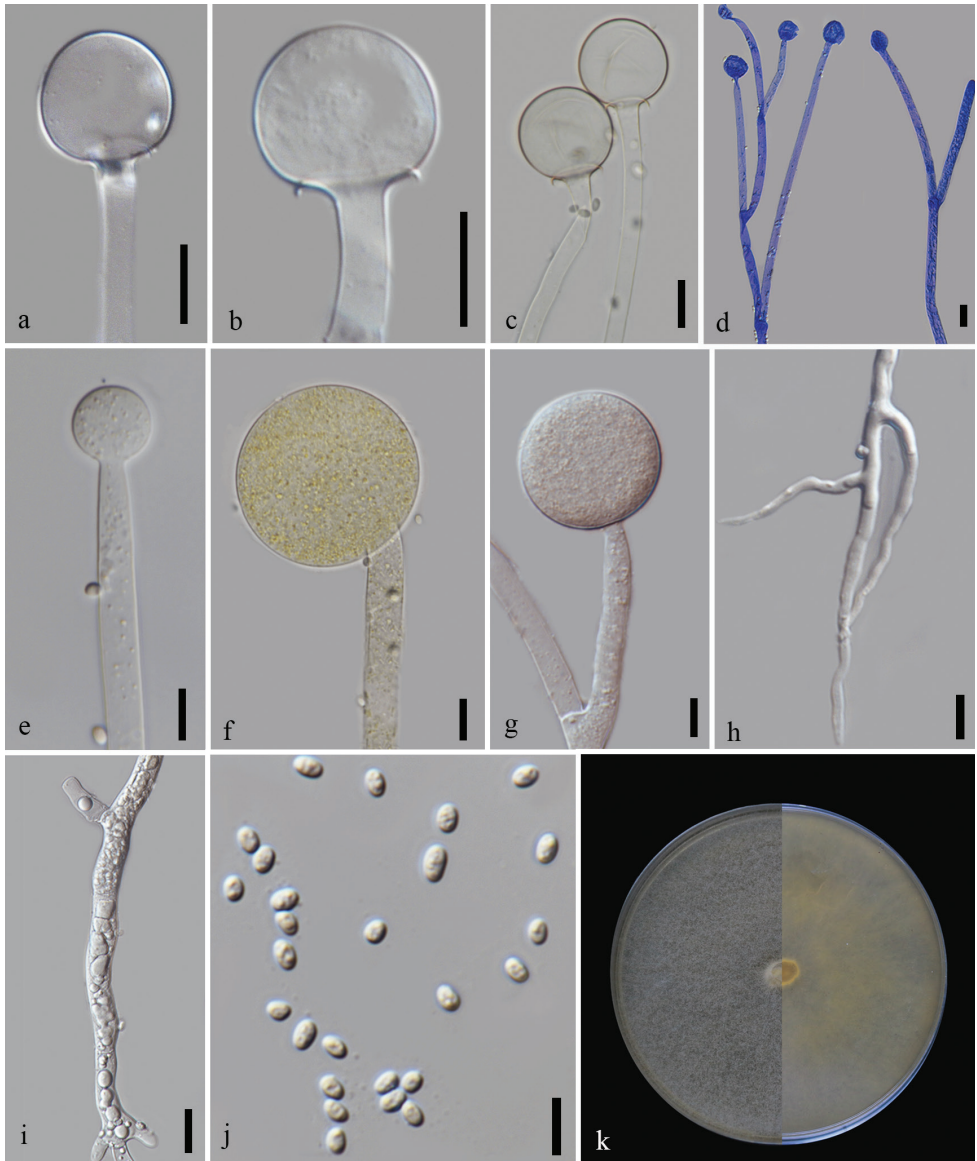


Figure 2. *Mucor aseptatophorus* (MFLU 21–0145) **a–c** columnella with collar **d** branching of sporangiophores **e, f** developing sporangium **g** short sporangiophore with sporangium **h** rhizoids **i** granular content in mycelium **j** sporangiospores **k** front and reverse of the colony in MEA. Scale bars: 10 μm (**a–c, e–h, j**); 20 μm (**d, i**).

Description. Asexual morph (based on cultures grown in MEA at 25 °C): Sporangiophores hyaline to pale brown, variable in length, erect, arising directly from the substrate, up to 17 μm in width ($\bar{x} = 8.5 \mu\text{m}$, $n = 30$), sympodial, and monopodial, with occasional circinate branches (mostly sympodial branches), and no septae ob-

served. Sporangia $18\text{--}56.5 \times 19\text{--}54 \mu\text{m}$ ($\bar{x} = 41.5 \times 41.5 \mu\text{m}$, $n = 40$), globose to subglobose, smooth-walled, thick-walled and persistent, yellow to pale brown. Columellae $13\text{--}35 \times 14\text{--}37.5 \mu\text{m}$ ($\bar{x} = 19 \times 20 \mu\text{m}$, $n = 40$), globose, with very short collar, hyaline to pale brown, non-collapsing, smooth-walled. Sporangiospores $3.5\text{--}6 \times 2\text{--}4 \mu\text{m}$ ($\bar{x} = 4 \times 3 \mu\text{m}$, $n = 70$), mostly ellipsoidal, occasionally oval to globose, some irregular, hyaline. Chlamydospores and rhizoids present. Sexual morph not observed.

Culture characteristics. Colonies on MEA reaching 62 mm diameter after 2 days of incubation at 25 °C. Colony white at first, becoming pale yellow with age; reverse pale yellow. Colony fully covers the Petri plate (90 mm) by the third day at 25 and 30 °C but does not reach the lid of the plate. At 20 °C, colony reaches a diameter of 70.5 mm after 3 days. Vertical growth is lower at 25 and 30 °C than at 20 °C. The colony does not reach the lid after 3 days. At 30 °C, sporulation is excellent, with branching of sporangiophore more frequent than in others. Monopodial branching more prominent but sympodial and dichotomous branches also observed. On PDA, cultures are white and pale brown in the middle with grey to pale brown sporangia. Colony reaching 64 mm diameter after 3 days of incubation at 25 °C. Optimal growth and excellent sporulation were observed on both MEA and PDA media at 30 °C. At 37 and 8 °C in MEA, growth is observed but with no sporulation. The colony reaches a diameter of 31 mm at 37 °C after 3 days. At 8 °C, the colony reaches a diameter of 14 mm after 9 days. Growth is observed at temperatures ranging from 8 to 37 °C.

Distribution. Thailand.

***Mucor chiangraiensis* V.G. Hurdeal, E. Gentekaki, K.D. Hyde & H.B. Lee, sp. nov.**

MycoBank No: 840564

Facesoffungi Number: FoF09924

Figs 1, 3

Etymology. The epithet refers to the province of Chiang Rai where the species was isolated.

Holotype. MFLU 21–0079

Gene sequences. (ITS) MZ433253; (LSU) MZ433250

Diagnosis. In contrast to *M. nederlandicus*, this species produces smaller sporangia and has wider sporangiophores. The sporangia formed by *M. nederlandicus* are echinulate at maturity, while in *M. chiangraiensis* they are smooth-walled. This species mostly has subglobose or slightly elongated globose columellae while in *M. nederlandicus* they are mostly globose. Physiological data indicate that *M. nederlandicus* has a faster growth than *M. chiangraiensis* in MEA at 25 °C. Molecular phylogeny indicates that the newly isolated strain groups separately from *M. nederlandicus* and *M. inaequisporus*. Comparison with the protologue of *M. inaequisporus* indicates that *M. chiangraiensis* has smaller sporangia, columella and sporangiospores. The columellae in the latter are

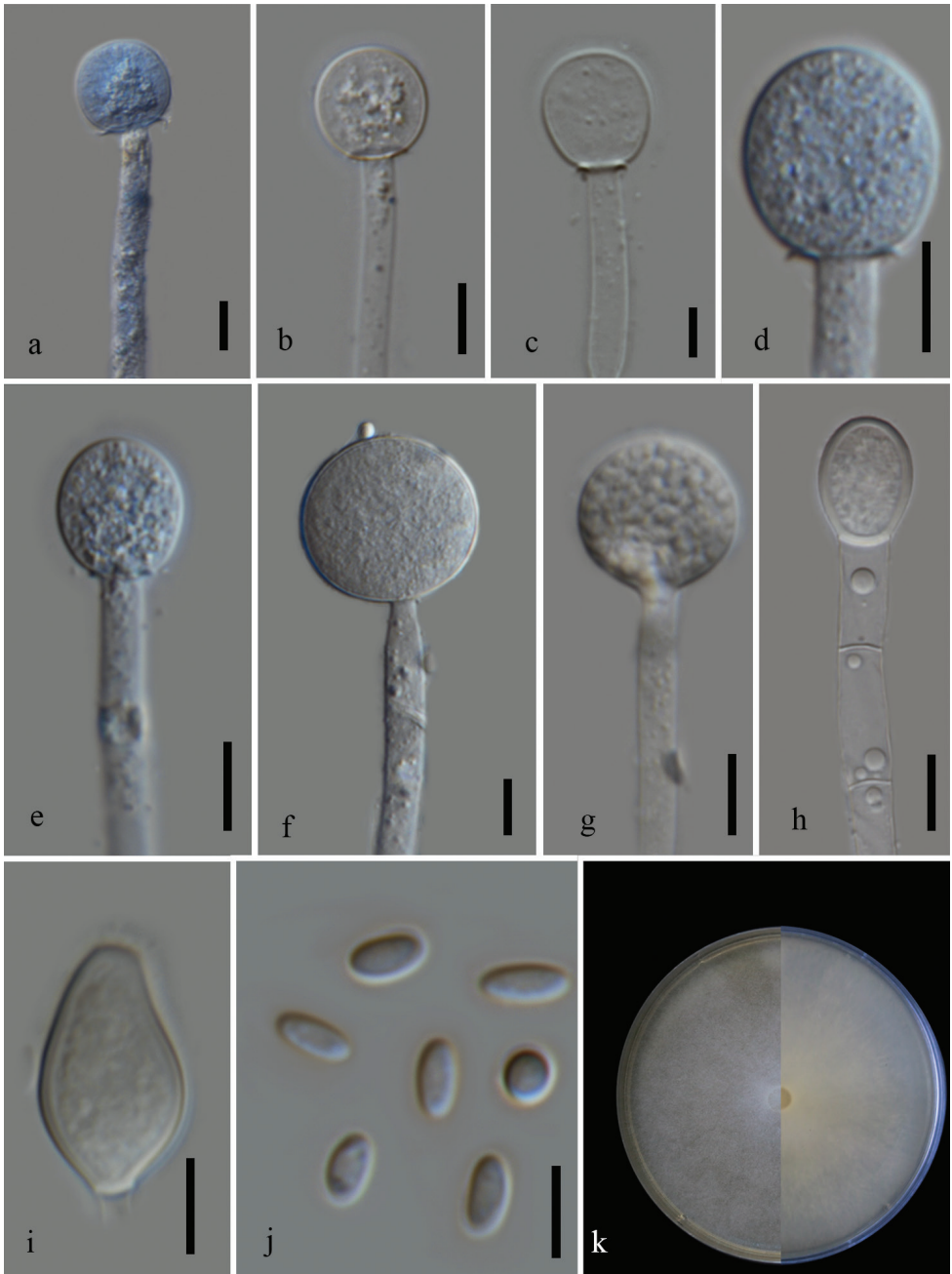


Figure 3. *Mucor chiangraiensis* (MFLU 21-0079) **a-e** columella with and without collars **f, g** sporangia **h-i** chlamydospores **j** sporangiospores **k** front and reverse of the colony grown in MEA. Scale bars: 10 µm (**a-j**).

subglobose or slightly elongated globose columellae rather than commonly obovoid-pyriform or subspherical as in *M. inaequisporus*. Although the shape and size of sporangiospores are often variable in both species, the majority of spores of *M. chiangraiensis* are ellipsoidal. Sporangiospores are usually colorless and hyaline as compared to pale or greenish-yellow in *M. inaequisporus*.

Material examined. THAILAND. Chiang Rai Province, Doi Chang District, 19°49'9.984"N; 99°34'36.768"E, from soil, 7th December 2019, collected and isolated by Vedprakash Godadhar Hurdeal, ex-type living culture, MFLUCC 21–0042.

Description. Asexual morph (based on cultures grown in MEA at 25 °C): Sporangioophores hyaline, up to 12 µm (\bar{x} = 6, n = 30) in diameter, erect, unbranched or sympodial branches. Hyphae irregular septate, with occasional hyphal bulges. Sporangia 18–40.5 × 18.5–40.5 µm (\bar{x} = 28.5 × 27.5 µm, n = 30), globose, wall resistant, deliquescent, hyaline to pale brown. Columellae 12.5–23.5 × 11.5–23 µm (\bar{x} = 19 × 17 µm, n = 30), subglobose or slightly elongated globose columellae, obovoid, ellipsoid and sometimes round to subglobose without or with short collar, hyaline to pale brown, smooth-walled. Sporangiospores 4–6.5 × 2–3.5 µm (\bar{x} = 5 × 2.5 µm, n = 50) µm, mostly ellipsoidal, oval, smooth-walled, hyaline. Chlamydospores abundant, intercalary, terminal, variable in shape and size. Rhizoids absent. Sexual morph not observed.

Culture characteristics. Day-old cultures are white, cottony, floccose, have erect sporangioophores with hyphae reaching the lid of the Petri plate in MEA. The white color of the colony persists even after 6 days. At maturity, the colony reverse is white or pale yellow. On MEA at 25 °C, the colony reaches a diameter of 51 mm after 3 days of incubation. At 20 and 30 °C, the colony reaches a diameter of 47 mm and 44.5 mm respectively after 3 days. Sporulation is excellent at 20 to 30 °C. At 30 °C, mostly unbranched sporangioophores are observed with few sympodial branches. On PDA at 25 °C, colony reaches a diameter of 48 mm after 3 days of incubation. The front and reverse of the colony are white in both MEA and PDA. Growth is observed at temperatures ranging from 8 to 30 °C. Optimal growth and excellent sporulation were observed at 25 °C on both MEA and PDA media. No growth was observed at 37 °C. At 8 °C in MEA, the colony reached a diameter of 34 mm after 9 days but with no sporulation.

Distribution. Thailand.

Mucor nederlandicus Váňová, *Česká Mykol.* 45(3): 128 (1991)

MycoBank No: 354494

Figs 1, 4

Gene sequences. (ITS) MZ433254; (LSU) MZ433251

Material examined. Thailand, Chiang Rai Province, Muang District, Mae Salong Nai, 20°12'38.0"N; 99°37'55.6"E, from soil, 10th June 2020, collected by Bhavesh Raghonundon, and isolated by Vedprakash Godadhar Hurdeal, living culture, MFLUCC 21–0045.

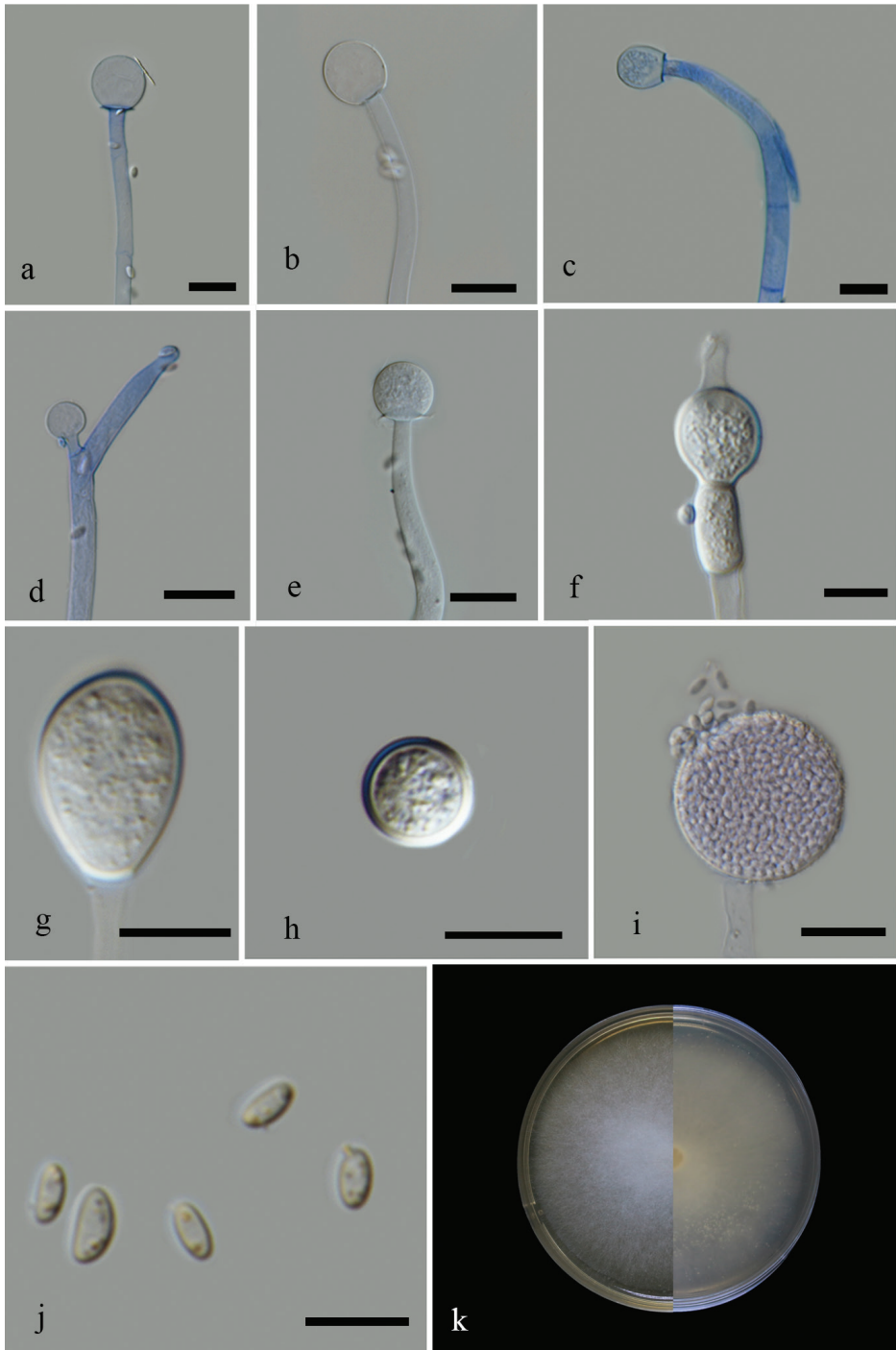


Figure 4. *Mucor nederlandicus* (MFLU 21–007) **a–c** columella with highly reduced collar **d** sterile sporangium **e** columella with visible collar **f–h** chlamydospores **i** mature sporangia **j** sporangiospores **k** front and reverse of the colony in MEA. Scale bars: 20 μm (**a–e, i**); 10 μm (**f–h**).

Description. Asexual morph (based on cultures grown in MEA at 25 °C): Sporangioophores hyaline, up to 7.5 μm ($\bar{x} = 5$, $n = 30$) in diameter, undulate, occasionally curved, irregular septate near the base (1–2), unbranched, sympodial branches formed. Sporangia 20–47.5 \times 20–45.5 μm ($\bar{x} = 34 \times 35.5 \mu\text{m}$, $n = 28$), globose, smooth-walled, thick-walled, wall echinulate, deliquescent in mature sporangia, hyaline to pale brown. Columellae 12.5–23.5 \times 12–22.5 μm ($\bar{x} = 16 \times 15.5 \mu\text{m}$, $n = 30$), mostly globose to subglobose, and sometimes oblong, obovoid, and rarely ellipsoid, without or with short collar, hyaline to pale brown, smooth-walled. Sporangiospores 3.5–6.5 \times 2–4 μm ($\bar{x} = 5 \times 2.5 \mu\text{m}$, $n = 30$) μm , mostly ellipsoidal, sometimes flattened on one side, oval or cylindrical, smooth-walled, hyaline with one or more granules. Chlamydospores abundant, intercalary, terminal, variable in shape and size. Rhizoids absent. Sexual morph not observed.

Culture characteristics. Colonies on MEA reaching a diameter of 60 mm after 3 days of incubation at 25 °C. At temperatures 20 and 30 °C, the colony diameter is 46 mm and 45.5 mm respectively after 3 days. Colony growth is observed at 8 to 30 °C with optimal growth at 25 °C. Unbranched or sympodial branching of sporangiophore are prominent at 30 °C. Colonies on PDA, reaching 51 mm after 3 days of incubation at 25 °C. In both culture media, colony from above and reverse: white or very pale yellow, and cottony. No growth was observed at 37 °C. At 8 °C, the colony reached a diameter of 21 mm after 9 days but with no sporulation in MEA.

Distribution. Thailand, United Kingdom.

Discussion

Thailand has extraordinary fungal diversity with many fungal species having been described from the northern provinces of the country (Hyde et al. 2018). The present study introduces two new species of *Mucor* and one new geographical record of *M. nederlandicus* from soil habitats in northern Thailand based on molecular and morphophysiological data. Many *Mucor* species have been isolated from soil and other substrates including postharvest crops, dung, and leaf litter (Lima et al. 2020; Nguyen et al. 2020). The newly-described *Mucor* species exhibit overall characteristic morphology observed in the genus, including branched sporangiophores and globose sporangia (Hoffmann et al. 2013; Walther et al. 2019). Commonly used morphological characters for species-level delimitation are the size and shape of structures, such as sporangiospores and columella (Chai et al. 2019; Lima et al. 2020). Morphological examination revealed that the newly isolated strains differ from their known sister taxa. This includes differences in the sporangia and columellae sizes. For example, *M. aseptatophorus* differs from its sister taxon *M. irregularis* in having smaller sporangiospores, but larger sporangia. Phenotypic characters comprise a pivotal aspect of modern fungal taxonomy. Nonetheless, some Mucorales groups display morphological plasticity, hence their taxonomy cannot be solely based on morphological features as these might not always be taxonomically informative.

In our phylogenetic analyses, placement of the new species was stable with high statistical support using both ML and BI methods of inference. Genetic distance analysis of the ITS region contributed further evidence to the introduction of the two novel *Mucor* species. The percentage nucleotide difference in the ITS genetic marker to the sister taxa is 2.5–4.5% for *M. aseptatophorus* and 1–13.3% for *M. chiangraiensis* (Table 2), exceeding the threshold for establishing new species (Walther et al. 2013; Jeewon and Hyde 2016).

Most studies focusing on *Mucor* species delimitation use ITS and LSU as these are the most widely available genetic markers (Madden et al. 2012; Lima et al. 2018; Chai et al. 2019; Lima et al. 2020). In the *Mucor circinelloides* complex, protein-coding genes, such as the largest subunit of RNA polymerase II (*rpb1*) are also available for most species (Walther et al. 2019; Wagner et al. 2020). Several genetic markers, which have been traditionally used in the taxonomy of Dikarya fungi, cannot be applied in Mucorales due to the presence of paralogous and multiple-copy genes in the latter (Walther et al. 2019; Wagner et al. 2020). In general, the number of genetic markers necessary for species delimitation varies depending on the approach (Luo et al. 2018; Bhunjun et al. 2020). For instance, automatic barcode gap discovery can be used or best suited with single locus, while at least a couple of unlinked markers from independent loci are necessary for the genealogical concordance phylogenetic species recognition (GCPSR) concept (Laurence et al. 2014). Thus, only comparatively few studies use the latter (Taylor et al. 2000; Walther et al. 2019; Wagner et al. 2020). In the case of *Mucor*, the availability of only ITS and LSU for most taxa precludes the use of the GCPSR concept, as both markers belong to the same locus. Recently, phylogenomics approaches using hundreds of genes have started to emerge in an effort to delineate problematic fungal taxa (Vandepol et al. 2020). Nonetheless, in the case of *Mucor*, using ITS and LSU to delineate species has been adequate.

Herein, *M. aseptatophorus* showed growth at 37 °C. *Mucor irregularis*, which has close phylogenetic affinity to the new species also has the ability to grow at this temperature. *Mucor irregularis* is an opportunistic pathogen causing cutaneous mucoromycosis mostly in immunocompromised individuals (Lu et al. 2013; Xu et al. 2018; Soare et al. 2020). Thermotolerance in *Mucor* usually hints at pathogenic potential, however not all thermotolerant species are pathogens. Thus, the thermotolerant ability of *M. aseptatophorus* warrants further investigation in order to determine whether or not it is pathogenic.

In the last decade, at least 20 new *Mucor* species have been introduced and described from soil, freshwater, leaf litter, and dung habitats, indicating that we are nowhere near to discovering all taxa in the genus (Hyde et al. 2020). Information on the geographic distribution of *Mucor* has started to emerge. Its species have been isolated in Brazil, Great Britain, the USA, China, South Korea, Finland, Germany, and France, suggesting that *Mucor* has worldwide distribution occupying diverse habitats. Here-with, this study contributes to the study of *Mucor* in Thailand. As more species are being discovered, and the diversity of these organisms is being explored, the ecological roles of *Mucor* remain largely unknown and many habitats are yet to be explored. This

highlights the need for more studies that explore the ecological importance, diversity, and accurate taxonomic classification of Mucorales.

Acknowledgments

Vedprakash G. Hurdeal would like to thank Miss Oundhyalah D. Padaruth and Mr. Bhavesh Raghoonundon for the collection of the soil samples in the provinces of Chiang Mai, and Chiang Rai, Thailand. He also thanks Mae Fah Luang University and the Mushroom Research Foundation for Ph.D. scholarship and supporting research on basal fungi. He acknowledges the Chonnam National University, South Korea, for the exchange student program. Kevin D. Hyde thanks the Thailand Research Fund for the grant on the Impact of climate change on fungal diversity and biogeography in the Greater Mekong Subregion (RDG6130001MS). Hyang Burm Lee is supported by the Graduate Program for the Undiscovered Taxa of Korea, and the Project on Survey and Discovery of Indigenous Fungal Species of Korea funded by National Institute of Biological Resources of the Ministry of Environment (MOE), Korea. The authors thank the reviewers for their valuable input and constructive criticism.

References

- Altschul SF, Gish W, Miller W, Myers EW, Lipman DJ (1990) Basic local alignment search tool. *Journal of Molecular Biology* 215: 403–410. [https://doi.org/10.1016/S0022-2836\(05\)80360-2](https://doi.org/10.1016/S0022-2836(05)80360-2)
- Amma S, Toju H, Wachrinrat C, Sato H, Tanabe AS, Artchawakom T, Kanzaki M (2018) Composition and diversity of soil fungi in Dipterocarpaceae-dominated seasonal tropical forests in Thailand. *Microbes and Environments* 33: 135–143. <https://doi.org/10.1264/jsme2.ME17168>
- Bhunjun CS, Dong Y, Jayawardena RS, Jeewon R, Phukhamsakda C, Bundhun D, Hyde KD, Sheng J (2020) A polyphasic approach to delineate species in *Bipolaris*. *Fungal Diversity* 102: 225–256. <https://doi.org/10.1007/s13225-020-00446-6>
- Capella-Gutiérrez S, Silla-Martínez JM, Gabaldón T (2009) TrimAl: a tool for automated alignment trimming in large-scale phylogenetic analyses. *Bioinformatics* 25: 1972–1973. <https://doi.org/10.1093/bioinformatics/btp348>
- Chai C, Liu W, Cheng H, Hui F (2019) *Mucor chuxiongensis* sp. nov., a novel fungal species isolated from rotten wood. *International Journal of Systematic and Evolutionary Microbiology* 69: 1881–1889. <https://doi.org/10.1099/ijsem.0.003166>
- Cordeiro TRL, Nguyen TTT, Lima DX, Da Silva SBG, De Lima CF, Leitão JDAA, Gurgel LMS, Lee HB, Santiago ALCMDA (2020) Two new species of the industrially relevant genus *Absidia* (Mucorales) from soil of the Brazilian Atlantic Forest. *Acta Botanica Brasílica* 34: 549–558. <https://doi.org/10.1590/0102-33062020abb0040>

- De Hoog G, Van Den Ende AHGG (1998) Molecular diagnostics of clinical strains of filamentous Basidiomycetes. *Mycoses* 41: 183–189. <https://doi.org/10.1111/j.1439-0507.1998.tb00321.x>
- Frąc M, Hannula SE, Bełka M, Jędrzycka M (2018) Fungal biodiversity and their role in soil health. *Frontiers in Microbiology* 9. <https://doi.org/10.3389/fmicb.2018.00707>
- Fresenius G (1850) *Mucor mucedo*. *Beiträge zur Mykologie* 1: 1–38. <https://doi.org/10.5962/bhl.title.51534>
- Hoffmann K, Pawłowska J, Walther G, Wrzosek M, De Hoog GS, Benny GL, Kirk PM, Voigt K (2013) The family structure of the Mucorales: a synoptic revision based on comprehensive multigene-genealogies. *Persoonia* 30: 57–76. <https://doi.org/10.3767/003158513X666259>
- Huelsenbeck JP, Ronquist F (2001) MrBayes: Bayesian inference of phylogenetic trees. *Bioinformatics* 17: 754–755. <https://doi.org/10.1093/bioinformatics/17.8.754>
- Hurdeal VG, Gentekaki E, Lee HB, Jeewon R, Hyde KD, Tibpromma S, Mortimer PE, Xu J (2021) Mucoralean fungi in Thailand: novel species of *Absidia* from tropical forest soil. *Cryptogamie, Mycologie* 42: 39–61. <https://doi.org/10.5252/cryptogamie-mycologie2021v42a4>
- Hyde KD, Norphanphoun C, Chen J, Dissanayake AJ, Doilom M, Hongsanan S, Jayawardena RS, Jeewon R, Perera RH, Thongbai B, Wanasinghe DN, Wisitrasameewong K, Tibpromma S, Stadler M (2018) Thailand's amazing diversity: up to 96% of fungi in northern Thailand may be novel. *Fungal Diversity* 93: 215–239. <https://doi.org/10.1007/s13225-018-0415-7>
- Hyde KD, Jeewon R, Chen Y-J, Bhunjun CS, Calabon MS, Jiang H-B, Lin C-G, Norphanphoun C, Sysouphanthong P, Pem D, Tibpromma S, Zhang Q, Doilom M, Jayawardena RS, Liu J-K, Maharachchikumbura SSN, Phukhamsakda C, Phookamsak R, Al-Sadi AM, Thongklang N, Wang Y, Gafforov Y, Gareth Jones EB, Lumyong S (2020) The numbers of fungi: is the descriptive curve flattening? *Fungal Diversity* 103: 219–271. <https://doi.org/10.1007/s13225-020-00458-2>
- Jacobs K, Botha A (2008) *Mucor renisporus* sp. nov., a new coprophilous species from southern Africa. *Fungal Diversity* 29: 27–35.
- Jeewon R, Hyde KD (2016) Establishing species boundaries and new taxa among fungi: recommendations to resolve taxonomic ambiguities. *Mycosphere* 7: 1669–1677. <https://doi.org/10.5943/mycosphere/7/11/4>
- Katoh K, Toh H (2008) Recent developments in the MAFFT multiple sequence alignment program. *Briefings in Bioinformatics* 9: 286–298. <https://doi.org/10.1093/bib/bbn013>
- Khuna S, Suwannarach N, Kumla J, Meerak J, Nuangmek W, Kiatsiriroat T, Lumyong S (2019) *Apophysomyces thailandensis* (Mucorales, Mucoromycota), a new species isolated from soil in northern Thailand and its solubilization of non-soluble minerals. *Myckeys* 45: 75–92. <https://doi.org/10.3897/myckeys.45.30813>
- Kirk PM (1986) (815) Proposal to conserve *Mucor* Fresenius over *Mucor* Micheli ex L. and (816) proposal to conserve *Rhizopus* Ehrenberg over *Ascophora* Tode (fungi) with notes on the nomenclature and taxonomy of *Mucor*, *Ascophora*, *Hydrophora* and *Rhizopus*. *Taxon* 35: 371–377. <https://doi.org/10.2307/1221300>
- Laurence MH, Summerell BA, Burgess LW, Liew ECY (2014) Genealogical concordance phylogenetic species recognition in the *Fusarium oxysporum* species complex. *Fungal Biology* 118: 374–384. <https://doi.org/10.1016/j.funbio.2014.02.002>

- Lima C, Lima D, Souza C, Oliveira R, Cavalcanti I, Gurgel L, Santiago A (2018) Description of *Mucor pernambucoensis* (Mucorales, Mucoromycota), a new species isolated from the Brazilian upland rainforest. *Phytotaxa* 350: e274. <https://doi.org/10.11646/phytotaxa.350.3.6>
- Lima DX, Barreto RW, Lee HB, Cordeiro TRL, De Souza CAF, De Oliveira RJV, Santiago AL-CMDA (2020) Novel mucoralean fungus from a repugnant substrate: *Mucor merdophylus* sp. nov., isolated from dog excrement. *Current Microbiology* 77: 2642–2649. <https://doi.org/10.1007/s00284-020-02038-8>
- Lu XL, Najafzadeh MJ, Dolatabadi S, Ran YP, Gerrits van den Ende AHG, Shen Y-N, Li C-Y, Xi L-Y, Hao F, Zhang Q-Q, Li R-Y, Hu Z-M, Lu G-X, Wang J-J, Drogari-Apiranthitou M, Klaassen C, Meis JF, Hagen F, Liu W-D, de Hoog GS (2013) Taxonomy and epidemiology of *Mucor irregularis*, agent of chronic cutaneous mucormycosis. *Persoonia* 30: 48–56. <https://doi.org/10.3767/003158513X665539>
- Lunge SB, Sajjan V, Pandit AM, Patil VB (2015) Rhinocerebrocutaneous mucormycosis caused by *Mucor* species: A rare causation. *Indian dermatology online journal* 6: 189–192. <https://doi.org/10.4103/2229-5178.156393>
- Luo A, Ling C, Ho SYW, Zhu C-D (2018) Comparison of Methods for Molecular Species Delimitation Across a Range of Speciation Scenarios. *Systematic Biology* 67: 830–846. <https://doi.org/10.1093/sysbio/syy011>
- Madden AA, Stchigel AM, Guarro J, Sutton D, Starks PT (2012) *Mucor nidicola* sp. nov., a fungal species isolated from an invasive paper wasp nest. *International Journal of Systematic and Evolutionary Microbiology* 62: 1710–1714. <https://doi.org/10.1099/ij.s.0.033050-0>
- Mendoza L, Vilela R, Voelz K, Ibrahim A, Voigt K, Lee SC (2014) Human Fungal Pathogens of Mucorales and Entomophthorales. In: *Cold Spring Harbor perspectives in medicine*. 1–33. <https://doi.org/10.1101/cshperspect.a019562>
- Miller MA, Pfeiffer W, Schwartz T (2010) Creating the CIPRES Science Gateway for inference of large phylogenetic trees. *Gateway Computing Environments Workshop (GCE)*, 2010. 1–8. <https://doi.org/10.1109/GCE.2010.5676129>
- Mishra R, Kushveer JS, Sarma VV (2019) A worldwide list of endophytic fungi with notes on ecology and diversity. *Mycosphere* 10. <https://doi.org/10.5943/mycosphere/10/1/19>
- Muszevska A, Okrańska A, Steczkiewicz K, Drgas O, Orłowska M, Perlińska-Lenart U, Aleksandrak-Piekarczyk T, Sztraj K, Zielenkiewicz U, Piłsyk S, Malc E, Mieczkowski P, Kruszevska JS, Bernat P, Pawłowska J (2021) Metabolic potential, ecology and presence of associated bacteria is reflected in genomic diversity of Mucoromycotina. *Frontiers in Microbiology* 12: e239. <https://doi.org/10.3389/fmicb.2021.636986>
- Nguyen TTT, Lee H (2020) *Mucor cheongyangensis*, a new species isolated from the surface of *Lycorma delicatula* in Korea. *Phytotaxa* 446: 33–42. <https://doi.org/10.11646/phytotaxa.446.1.4>
- Nguyen TTT, Lee SH, Bae S, Jeon SJ, Mun HY, Lee HB (2016) Characterization of two new records of zygomycete species belonging to undiscovered taxa in Korea. *Mycobiology* 44: 29–37. <https://doi.org/10.5941/MYCO.2016.44.1.29>
- Nguyen TTT, Jeon YJ, Mun HY, Goh J, Chung N, Lee HB (2020) Isolation and characterization of four unrecorded *Mucor* species in Korea. *Mycobiology* 48: 29–36. <https://doi.org/10.1080/12298093.2019.1703373>

- Nicolás FE, Murcia L, Navarro E, Navarro-Mendoza MI, Pérez-Arques C, Garre V (2020) Mucorales species and macrophages. *Journal of Fungi* 6: e94. <https://doi.org/10.3390/jof6020094>
- Pawłowska J, Okraśińska A, Kisło K, Aleksandrak-Piekarczyk T, Szatraj K, Dolatabadi S, Muszewska A (2019) Carbon assimilation profiles of mucoralean fungi show their metabolic versatility. *Scientific Reports* 9: e11864. <https://doi.org/10.1038/s41598-019-48296-w>
- Peng W, Song T, Du H, Chen H, Zeng F, Liu Y, Luo Y, Tan W (2020) Inconsistent diversity patterns of soil fungi and woody plants among habitat types in a karst broadleaf forest. *Forest Ecology and Management* 474: e118367. <https://doi.org/10.1016/j.foreco.2020.118367>
- Sato H, Tanabe AS, Toju H (2015) Contrasting Diversity and Host Association of Ectomycorrhizal Basidiomycetes versus Root-Associated Ascomycetes in a Dipterocarp Rainforest. *PLOS ONE* 10: e0125550. <https://doi.org/10.1371/journal.pone.0125550>
- Senanayake IC, Rathnayaka AR, Marasinghe DS, Calabon MS, Gentekaki E, Lee HB, Hurdeal VG, Pem D, Dissanayake LS, Wijesinghe SN, Bundhun D, Nguyen TT, Goonasekara ID, Abeywickrama PD, Bhunjun CS, Jayawardena RS, Wanasinghe DN, Jeewon R, Bhat DJ, Xiang MM (2020) Morphological approaches in studying fungi: collection, examination, isolation, sporulation and preservation. *Mycosphere* 11(1): 2678–2754. <https://doi.org/10.5943/mycosphere/11/1/20>
- Soare AY, Watkins TN, Bruno VM (2020) Understanding Mucormycoses in the Age of “omics.” *Frontiers in Genetics* 11: e699. <https://doi.org/10.3389/fgene.2020.00699>
- Spatafora JW, Chang Y, Benny GL, Lazarus K, Smith ME, Berbee ML, Bonito G, Corradi N, Grigoriev I, Gryganskyi A, James TY, O'Donnell K, Roberson RW, Taylor TN, Uehling J, Vilgalys R, White MM, Stajich JE (2016) A phylum-level phylogenetic classification of zygomycete fungi based on genome-scale data. *Mycologia* 108: 1028–1046. <https://doi.org/10.3852/16-042>
- Stamatakis A (2014) RAxML version 8: a tool for phylogenetic analysis and post-analysis of large phylogenies. *Bioinformatics* 30: 1312–1313. <https://doi.org/10.1093/bioinformatics/btu033>
- Suwanarach N, Kumla J, Supo C, Honda Y, Nakazawa T, KHANONGNUCH C, Wongputtisin P (2021) *Cunninghamella saisamornae* (Cunninghamellaceae, Mucorales), a new soil fungus from northern Thailand. *Phytotaxa* 509: 291–300. <https://doi.org/10.11646/phytotaxa.509.3.4>
- Taylor JW, Jacobson DJ, Kroken S, Kasuga T, Geiser DM, Hibbett DS, Fisher MC (2000) Phylogenetic species recognition and species concepts in fungi. *Fungal Genetics and Biology* 31: 21–32. <https://doi.org/10.1006/fgbi.2000.1228>
- Torsvik V, Øvreås L (2002) Microbial diversity and function in soil: from genes to ecosystems. *Current Opinion in Microbiology* 5: 240–245. [https://doi.org/10.1016/S1369-5274\(02\)00324-7](https://doi.org/10.1016/S1369-5274(02)00324-7)
- Vandepol N, Liber J, Desirò A, Na H, Kennedy M, Barry K, Grigoriev IV, Miller AN, O'Donnell K, Stajich JE, Bonito G (2020) Resolving the Mortierellaceae phylogeny through synthesis of multi-gene phylogenetics and phylogenomics. *Fungal Diversity* 104: 267–289. <https://doi.org/10.1007/s13225-020-00455-5>
- Vilgalys R, Hester M (1990) Rapid genetic identification and mapping of enzymatically amplified ribosomal DNA from several *Cryptococcus* species. *Journal of Bacteriology* 172: 4238. <https://doi.org/10.1128/jb.172.8.4238-4246.1990>

- Wagner L, Stielow JB, de Hoog GS, Bensch K, Schwartz VU, Voigt K, Alastruey-Izquierdo A, Kurzai O, Walther G (2020) A new species concept for the clinically relevant *Mucor circinelloides* complex. *Persoonia* 44: 67–97. <https://doi.org/10.3767/persoonia.2020.44.03>
- Walther G, Wagner L, Kurzai O (2019) Updates on the taxonomy of Mucorales with an emphasis on clinically important taxa. *Journal of Fungi* 5. <https://doi.org/10.3390/jof5040106>
- Walther G, Pawłowska J, Alastruey-Izquierdo A, Wrzosek M, Rodriguez-Tudela JL, Dolatabadi S, Chakrabarti A, de Hoog GS (2013) DNA barcoding in Mucorales: an inventory of biodiversity. *Persoonia* 30: 11–47. <https://doi.org/10.3767/003158513X665070>
- White TJ, Bruns TD, Lee SB, Taylor JW (1990) Amplification and direct sequencing of fungal ribosomal RNA genes for phylogenetics. In: Michael AI, David HG, John JS, Thomas JW (Eds) *PCR Protocols, A Guide to Methods and Applications*, 315–322.
- Wijayawardene NN, Hyde KD, Al-Ani LKT, Tedersoo L, Haelewaters D, Rajeshkumar KC, Zhao RL, Aptroot A, Leontyev DV, Saxena RK, Tokarev YS, Dai DQ, Letcher PM, Stephenson SL, Ertz D, Lumbsch HT, Kukwa M, Issi IV, Madrid H, Phillips AJL, Selbmann L, Pfliegler WP, Horváth E, Bensch K, Kirk PM, Kolaříková K, Raja HA, Radek R, Papp V, Dima B, Ma J, Malosso E, Takamatsu S, Rambold G, Gannibal PB, Triebel D, Gautam AK, Avasthi S, Suetrong S, Timdal E, Fryar SC, Delgado G, Réblová M, Doilom M, Dolatabadi S, Pawłowska J, Humber RA, Kodsueb R, Sánchez-Castro I, Goto BT, Silva DKA, de Souza FA, Oehl F, da Silva GA, Silva IR, Błaszczowski J, Jobim K, Maia LC, Barbosa FR, Fiuza PO, Divakar PK, Shenoy BD, Castañeda-Ruiz RF, Somrithipol S, Lateef AA, Karunarathna SC, Tibpromma S, Mortimer PE, Wanasinghe DN, Phookamsak R, Xu J, Wang Y, Tian F, Alvarado P, Li DW, Kušan I, Matočec N, Maharachchikumbura SSN, Papizadeh M, Heredia G, Wartchow F, Bakhshi M, Boehm E, Youssef N, Hustad VP, Lawrey JD, Santiago ALCMA, Bezerra JDP, Souza-Motta CM, Firmino AL, Tian Q, Houbraken J, Hongsanan S, Tanaka K, Dissanayake AJ, Monteiro JS, Grossart HP, Suija A, Weerakoon G, Etayo J, Tsurukau A, Vázquez V, Mungai P, Damm U, Li QR, Zhang H, Boonmee S, Lu YZ, Becerra AG, Kendrick B, Brearley FQ, Motiejūnaitė J, Sharma B, Khare R, Gaikwad S, Wijesundara DSA, Tang LZ, He MQ, Flakus A, Rodriguez-Flakus P, Zhurbenko MP, McKenzie EHC, Stadler M, Bhat DJ, Liu JK, Raza M, Jeewon R, Nasonova ES, Prieto M, Jayalal RGU, Erdoğan M, Yurkov A, Schnittler M, Shchepin ON, Novozhilov YK, Silva-Filho AGS, Liu P, Cavender JC, Kang Y, Mohammad S, Zhang LF, Xu RF, Li YM, Dayarathne MC, Ekanayaka AH, Wen TC, Deng CY, Pereira OL, Navathe S, Hawksworth DL, Fan XL, Dissanayake LS, Kuhnert E, Grossart HP, Thines M (2020) Outline of fungi and fungus-like taxa. *Mycosphere* 11: 1160–1456. <https://doi.org/10.5943/mycosphere/11/1/8>
- Xu W, Peng J, Li D, Tsui CKM, Long Z, Wang Q, Mei H, Liu W (2018) Transcriptional profile of the human skin pathogenic fungus *Mucor irregularis* in response to low oxygen. *Medical Mycology* 56: 631–644. <https://doi.org/10.1093/mmy/myx081>
- Zhou Z, Wang C, Luo Y (2020) Meta-analysis of the impacts of global change factors on soil microbial diversity and functionality. *Nature Communications* 11: e3072. <https://doi.org/10.1038/s41467-020-16881-7>

Two novel species and two new records of *Distoseptispora* from freshwater habitats in China and Thailand

Hong-Wei Shen^{1,2,3}, Dan-Feng Bao^{1,2,4}, Kevin D. Hyde^{2,3,5},
Hong-Yan Su¹, Darbhe J. Bhat⁶, Zong-Long Luo¹

1 College of Agriculture and Biological Sciences, Dali University, Dali 671003, Yunnan, China **2** Center of Excellence in Fungal Research, Mae Fah Luang University, Chiang Rai 57100, Thailand **3** School of Science, Mae Fah Luang University, Chiang Rai 57100, Thailand **4** Department of Entomology and Plant Pathology, Faculty of Agriculture, Chiang Mai University, Chiang Mai 50200, Thailand **5** Innovative Institute of Plant Health, Zhongkai University of Agriculture and Engineering, Guangzhou 510225, China **6** No. 128/1-J, Azad Housing Society, Curca, Goa Velha, 403108, India

Corresponding author: Zong-Long Luo (luozonglongfungi@163.com)

Academic editor: Jennifer Luangsa-ard | Received 22 July 2021 | Accepted 12 October 2021 | Published 8 November 2021

Citation: Shen H-W, Bao D-F, Hyde KD, Su H-Y, Bhat DJ, Luo Z-L (2021) Two novel species and two new records of *Distoseptispora* from freshwater habitats in China and Thailand. MycoKeys 84: 79–101. <https://doi.org/10.3897/mycokeys.84.71905>

Abstract

During investigations into freshwater fungi from the Great Mekong Subregion, four *Distoseptispora* taxa were collected from China and Thailand. Based on morphological characteristics, and phylogenetic analyses of combined LSU, ITS, SSU, TEF1- α , and RPB2 sequence data, two new species *Distoseptispora bangkokensis* and *D. lancangjiangensis* are introduced, and two known species *D. clematidis* and *D. thysanolaenae* were first reported in freshwater habitat. Illustrations and descriptions of these taxa are provided, along with comparisons with extant taxa in the genus.

Keywords

2 new taxa, Distoseptisporales, freshwater fungi, morphology, phylogeny, taxonomy

Introduction

Distoseptisporaceae was introduced by Su et al. (2016) based on morphological and phylogenetic analyses, with *Distoseptispora* as type genus. Distoseptisporaceae is placed in Distoseptisporales, which was introduced by Luo et al. (2019), and currently comprises two families, Aquapteridosporaceae and Distoseptisporaceae (Luo et al. 2019; Wijayawardene et al. 2020; Hyde et al. 2021). Species of both families are commonly reported from freshwater habitats (Yang et al. 2015, 2018; u et al. 2016; Li et al. 2021; Hyde et al. 2016a, 2019, 2020; Luo et al. 2018, 2019; Song et al. 2020; Dong et al. 2021).

Distoseptispora as a single genus in Distoseptisporaceae was introduced by Su et al. (2016) with *D. fluminicola* as the type species. The genus is characterized by monoblastic, cylindrical, conidiogenous cells, with percurrent proliferation, acrogenous, solitary, brown or yellowish/reddish brown, olivaceous, distoseptate or euseptate, cylindrical, obclavate, rostrate conidia, truncate base, with rounded apices, basal cell with a cross wall and basal scar. This genus is not known for its sexual morph (Su et al. 2016; Yang et al. 2018; Hyde et al. 2019, 2020; Luo et al. 2019; Sun et al. 2020). Currently, 32 species are accepted in the genus of which 13 from terrestrial habitats and 19 were reported from freshwater environments (Su et al. 2016; Hyde et al. 2016a, 2019, 2020; Xia et al. 2017; Yang et al. 2018; Luo et al. 2018, 2019; Monkai et al. 2020; Song et al. 2020; Sun et al. 2020; Li et al. 2021; Index Fungorum 2021 <http://www.indexfungorum.org>).

During our ongoing study of freshwater fungi along the north-south gradient in the Asian/Australian region (Hyde et al. 2016b), we collected four species in the genus. Two new species, *Distoseptispora bangkokensis* and *D. lancangjiangensis*, are introduced in this study, *D. clematidis* and *D. thysanolaenae* are newly recorded from freshwater habitats for the first time in China. Morphological descriptions and illustrations of the species and an updated multi-gene phylogenetic tree are provided to reveal their taxonomic position among the species in the Distoseptisporales, and also provided the comparison of morphological characteristics, habitats and hosts information of species newly added to *Distoseptispora* after Monkai et al. (2020) (Table 2).

Materials and methods

Isolation and morphology

Specimens of submerged decaying wood were collected from Dulongjiang, Nanpanjiang, Lancangjiang and Chao Phraya River in China and Thailand respectively. Multiple samples will be collected at each collection site at different times, allowing more strains to be obtained for each species. Methods of morphological observation and isolation follow Luo et al. (2018) and Senanayake et al. (2020). IFW (Tarosoft(R) Image Frame Work) was used for measurement of photomicrograph, and Adobe Photoshop CS5 software was used to process images for making photo-plates (Adobe Systems

Inc., USA). Single spore isolation was performed according to the following steps: The conidia suspension from specimens, absorbed with a sterilized pipette, was placed on potato dextrose agar (PDA) and incubated at room temperature overnight. Germinated conidia were transferred to new PDA/MEA (Beijing land bridge technology CO., LTD., China) plates and incubated in an incubator at room temperature (25 °C). Specimens were deposited in the Kunming Institute of Botany, Academia Sinica herbarium (KUN-HKAS), and Mae Fah Luang University herbarium (MFLU). Cultures were deposited in the Dali University Culture Collection (DLUCC), China General Microbiological Culture Collection Center (CGMCC), and Mae Fah Luang University Culture Collection (MFLUCC). Facesoffungi number was obtained as described in Jayasiri et al. (2015) and Index Fungorum number was also registered (<http://www.indexfungorum.org/Names/Names.asp>). In this study, multiple samples were collected for each sample site and related environment, but unfortunately, there were still no more strains for the two new species in the paper.

DNA extraction, PCR amplification, and sequencing

DNA extraction, PCR amplification, sequencing and phylogenetic analysis follow Disayanake et al. (2020) with the following modifications. Fungal mycelia (200–500 mg) were scraped from grown on PDA/MEA plates using sterile scalpel, transferred to microcentrifuge tube with sterilized needles, and then grind with liquid nitrogen or quartz sand to break the cells. DNA was extracted using the Trelief™ Plant Genomic DNA Kit (TSP101) according to the manufacturer's instructions.

Five gene regions, LSU, ITS, SSU, TEF1- α , and RPB2 were amplified using LR0R/LR5, ITS5/ITS4, NS1/NS4, 983F/EF1-2218R, and RPB2-5F/RPB2-7cR (Vilgalys and Hester 1990; White et al. 1990; Liu et al. 1999) primer pairs respectively. Primer sequences are available at the WASABI database at the AFTOL website (aftol.org). The PCR mixture contained 12.5 μ L of 2 \times Power Taq PCR Master Mix (a premix and ready to use solution, including 0.1 Units/ μ L Taq DNA Polymerase, 500 μ m dNTP Mixture each (dATP, dCTP, dGTP, dTTP), 20 mm Tris-HCl pH 8.3, 100 Mm KCl, 3 mM MgCl₂, stabilizer and enhancer), 1 μ L of each primer including forwarding primer and reverse primer (10 μ m), 1 μ L template DNA extract and 9.5 μ L deionized water (Luo et al. 2018). The PCR cycling conditions of LSU, ITS, SSU and TEF1- α were as follows: 94 °C for 3 min, followed by 35 cycles of denaturation at 94 °C for 30s, annealing at 55 °C for 50s, elongation at 72 °C for 1 min, and a final extension at 72 °C for 10 min. The PCR thermal cycle of RPB2 has a total of 40 cycles, and the conditions are as follows: initially denature at 95 °C for 5 min, and then enter 40 cycles: denaturation at 95 °C for 1 min, annealing at 52 °C for 2 min, extension at 72 °C for 90s, and finally at 72 °C for 10 min. PCR products were then purified using minicolumns, purification resin, and buffer according to the manufacturer's protocols (Amersham product code: 27–9602–01). The sequences were carried out at Beijing Tsingke Biotechnology Co., Ltd. (Beijing, P.R. China).

Table 1. Strains used for phylogenetic analysis and their corresponding GenBank numbers. The type strain are in bold font.

Species	Source	GenBank accession number					Reference
		LSU	ITS	TEF1- α	RPB2	SSU	
<i>Aquapteridospora fusiformis</i>	MFLUCC 18-1606	MK849798	MK828652	MN194056	–	–	Luo et al. (2019)
<i>A. lignicola</i>	MFLUCC 15-0377	KU221018	–	–	–	–	Yang et al. (2015)
<i>Distoseptispora adscendens</i>	HKUCC 10820	DQ408561	–	–	DQ435092	–	Shenoy et al. (2006)
<i>D. appendiculata</i>	MFLUCC 18-0259	MN163023	MN163009	MN174866	–	–	Luo et al. (2019)
<i>D. aquatica</i>	MFLUCC 15-0374	KU376268	MF077552	–	–	–	Su et al. (2016)
<i>D. bambusae</i>	MFLUCC 20-0091	MT232718	MT232713	MT232880	MT232881	MT232716	Sun et al. (2020)
<i>D. bambusae</i>	MFLUCC 14-0583	MT232717	MT232712	–	MT232882	–	Sun et al. (2020)
<i>D. bangkokensis</i>	MFLUCC 18-0262	MZ518206	MZ518205	–	–	MZ518208	This study
<i>D. cangshanensis</i>	MFLUCC 16-0970	MG979761	MG979754	MG988419	–	–	Luo et al. (2018)
<i>D. caricis</i>	CBS 146041	MN567632	MN562124	–	MN556805	–	Crous et al. (2019)
<i>D. clematidis</i>	MFLUCC 17-2145	MT214617	MT310661	–	MT394721	MT226728	Phukhamsakda et al. (2020)
<i>D. clematidis</i>	KUN-HKAS 112708	MW879523	MW723056	MW729784	–	MW774580	This study
<i>D. debongensis</i>	KUMCC 18-0090	MK079662	MK085061	MK087659	–	–	Hyde et al. (2019)
<i>D. euseptata</i>	MFUCC 20-0154	MW081544	MW081539	–	MW151860	–	Li et al. (2021)
<i>D. euseptata</i>	DLUCC S2024	MW081545	MW081540	MW084994	MW084996	–	Li et al. (2021)
<i>D. fasciculata</i>	KUMCC 19-0081	MW287775	MW286501	MW396656	–	–	Dong et al. (2021)
<i>D. fluminicola</i>	MFLUCC 15-0417	KU376270	MF077553	–	–	–	Su et al. (2016)
<i>D. guttulata</i>	MFLUCC 16-0183	MF077554	MF077543	MF135651	–	MF077532	Yang et al. (2018)
<i>D. hydei</i>	MFLUCC 20-0115	MT742830	MT734661	–	MT767128	–	Monkai et al. (2020)
<i>D. lancangjiangensis</i>	KUN-HKAS 112712	MW879522	MW723055	–	MW882260	–	This study
<i>D. leonensis</i>	HKUCC 10822	DQ408566	–	–	DQ435089	–	Shenoy et al. (2006)
<i>D. lignicola</i>	MFLUCC 18-0198	MK849797	MK828651	–	–	MK828318	Luo et al. (2019)
<i>D. longispora</i>	HFJAU 0705	MH555357	MH555359	–	–	MH555431	Song et al. (2020)
<i>D. martinii</i>	CGMCC 3.18651	KX033566	KU999975	–	–	KX033537	Xia et al. (2017)
<i>D. multiseptata</i>	MFLUCC 16-1044	MF077555	MF077544	MF135652	MF135644	MF077533	Yang et al. (2018)
<i>D. multiseptata</i>	MFLUCC 15-0609	KX710140	KX710145	MF135659	–	NG_065693	Hyde et al. (2016)
<i>D. neostrata</i>	MFLUCC 18-0376	MN163017	MN163008	–	–	–	Luo et al. (2019)
<i>D. obclavata</i>	MFLUCC 18-0329	MN163010	MN163012	–	–	–	Luo et al. (2019)

Species	Source	GenBank accession number					Reference
		LSU	ITS	TEF1- α	RPB2	SSU	
<i>D. obpyriformis</i>	MFLUCC 17-01694	MG979764	–	MG988422	MG988415	–	Luo et al. (2018)
<i>D. obpyriformis</i>	DLUCC 0867	MG979765	MG979757	MG988423	MG988416	–	Luo et al. (2018)
<i>D. palmarum</i>	MFLUCC 18-1446	MK079663	MK085062	MK087660	MK087670	MK079661	Hyde et al. (2019)
<i>D. phangngaensis</i>	MFLUCC 16-0857	MF077556	MF077545	MF135653	–	MF077534	Yang et al. (2018)
<i>D. rayongensis</i>	MFLUCC 18-0415	MH457137	MH457172	MH463253	MH463255	MH457169	Hyde et al. (2012)
<i>D. rostrata</i>	MFLUCC 16-0969	MG979766	MG979758	MG988424	MG988417	–	Luo et al. (2018)
<i>D. saprophytica</i>	MFLUCC 18-1238	MW287780	MW286506	MW396651	MW504069	–	Dong et al. (2021)
<i>D. songblhaensis</i>	MFLUCC 18-1234	MW287755	MW286482	MW396642	–	–	Dong et al. (2021)
<i>D. suoluensis</i>	MFLUCC 17-0224	MF077557	MF077546	MF135654	–	MF077535	Yang et al. (2018)
<i>D. suoluensis</i>	MFLUCC 17-1305	MF077558	MF077547	–	–	MF077536	Yang et al. (2018)
<i>D. tectonae</i>	MFLUCC 12-0291	KX751713	KX751711	KX751710	KX751708	–	Hyde et al. (2016)
<i>D. tectonae</i> ^{*1}	MFLUCC 16-0946	MG979768	MG979760	MG988426	MG988418	–	Luo et al. (2018)
<i>D. tectonigena</i>	MFLUCC 12-0292	KX751714	KX751712	–	KX751709	–	Hyde et al. (2016)
<i>D. thailandica</i>	MFLUCC 16-0270	MH260292	MH275060	MH412767	–	MH260334	Tibpromma et al. (2018)
<i>D. thysanolaenae</i>	KUN-HKAS 102247	MK064091	MK045851	MK086031	–	–	Phookamsak et al. (2019)
<i>D. thysanolaenae</i>	KUN-HKAS 112710	MW879524	MW723057	MW729783	–	–	This study
<i>D. xishuangbannaensis</i>	KUMCC 17-0290	MH260293	MH275061	MH412768	MH412754	MH260335	Tibpromma et al. (2018)
<i>D. yunnanensis</i>	MFLUCC 20-0153	MW081546	MW081541	MW084995	MW151861	–	Li et al. (2021)
<i>Myrmecridium aquaticum</i>	MFLUCC 15-0366	MK849804	–	–	–	MK828323	Luo et al. (2019)
<i>M. aquaticum</i>	S-1158	MK849803	MK828656	MN194061	MN124540	MK828322	Luo et al. (2019)
<i>M. banksiae</i>	CBS 132536	JX069855	JX069871	–	–	–	Crous et al. (2012)
<i>Pseudostanjehughesia aquitropica</i>	MFLUCC 16-0569	MF077559	MF077548	MF135655	–	MF077537	Yang et al. (2018)
<i>P. lignicola</i>	MFLUCC 15-0352	MK849787	MK828643	MN194047	MN124534	–	Luo et al. (2019)
<i>Sporidesmium dulongense</i>	MFLUCC 17-0116	MH795817	MH795812	MH801191	MH801190	–	Luo et al. (2019)
<i>S. lageniforme</i>	DLUCC 0880	MK849782	MK828640	MN194044	MN124533	–	Luo et al. (2019)
<i>S. pyriformatum</i>	MFLUCC 15-0620	KX710141	KX710146	MF135662	MF135649	–	Hyde et al. (2016)
<i>S. thailandense</i>	MFLUCC 15-0617	MF077561	MF077550	MF135657	–	–	Yang et al. (2018)
<i>S. thailandense</i>	MFLUCC 15-0964	MF374370	MF374361	MF370957	MF370955	–	Zhang et al. (2017)

*1 Ex-type strain of *Distoseptispora submersa*.

Phylogenetic analysis

Preliminary identification of genes obtained from fresh strains by GenBank database. The LSU, ITS, SSU, TEF1- α , and RPB2 used for phylogenetic analysis are selected based on the preliminary identification results and the related publications (Yang et al. 2018; Monkai et al. 2020). The sequences were aligned using MAFFT online service: Multiple alignment program for amino acid or nucleotide sequences MAFFT version 7 (Kato and Standley 2013: <http://mafft.cbrc.jp/alignment/server/index.html>), and edited manually in BioEdit v. 7.0 (Hall 1999). The sequence dataset was combined using SquenceMatrix v.1.7.8 (Vaidya et al. 2011). The alignment formats were change to PHYLIP and NEXUS formats by ALignment Transformation EnviRonment (ALTER) website (<http://sing.ei.uvigo.es/ALTER/>).

Maximum likelihood (ML) analysis was carried out using the RAxML-HPC2 on XSEDE (8.2.12) (Stamatakis 2006; Stamatakis et al. 2008) of CIPRES Science Gateway website (Miller et al. 2010: <http://www.phylo.org/portal2>) and the estimated proportion of invariant sites is (GTRGAMMA+I) model.

Bayesian analyses were performed in MrBayes 3.2.6 (Ronquist et al. 2012) and the best-fit model (LSU, ITS, SSU, TEF1- α , and RPB2 are all GTR+I+G) of sequences evolution was estimated via MrModeltest 2.2 (Guindon and Gascuel 2003; Nylander 2004; Darriba et al. 2012). The Markov Chain Monte Carlo (MCMC) sampling approach was used to calculate posterior probabilities (PP) (Rannala and Yang 1996). Bayesian analyses of six simultaneous Markov chains were run for 10000000 generations with trees sampled every 1000 generations.

Phylogenetic trees were visualized using FigTree v1.4.0 (Rambaut 2012: <http://tree.bio.ed.ac.uk/software/figtree/>), editing and typesetting using Adobe Illustrator (AI) (Adobe Systems Inc., the United States). The new sequences were submitted in GenBank and the strain information used in this paper is provided in Table 1. The alignments and phylogenetic trees were deposited in TreeBASE (<http://www.treebase.org/>, accession number: 28758).

Results

Phylogenetic analysis

The dataset composed of LSU (1–744 bp), ITS (745–1310 bp), TEF1- α (1311–2161 bp), RPB2 (2162–3178 bp), and SSU (3179–4199 bp) gene, comprising a total of 4199 characters (including gaps), including 56 taxa with *Pseudostanzehughesia aquitropica* (MFLUCC 16-0569) and *P. lignicla* (MFLUCC 15-0352) as the outgroup taxa (Figure 1). The ML and BI phylogenetic analyses produced similar topology. The combined dataset analysis of RAxML generates a best-scoring tree (Figure 1), with the final ML optimization likelihood value of -30393.557997. The aligned matrix had 1624 distinct alignment patterns, with 36.44% completely undetermined characters or gaps. The

Table 2. Comparison of morphological characteristic, habitats and hosts' information of species added to *Distoseptispora* after Monkai et al. (2020) (for other species see Monkai et al. 2020).

Species	Conidiophore (µm)	Conidia (µm)	Conidia septation	Conidia characteristic	Habitat	Host	Reference
<i>Distoseptispora bangkokensis</i>	37–55 × 3–4	400–568 × 13–16	Multi-distoseptate	Elongate, obclavate, rostrate, dark olivaceous to dark brown	Freshwater	Unidentified submerged wood	This study
<i>D. lancangjiangensis</i>	30–41 × 5–6	83–220 × 12–14	16–41-distoseptate	Obclavate, cylindrical, elongated, straight or curved, brown to greenish-brown	Freshwater	Unidentified submerged wood	This study
<i>D. euseptata</i>	19–28 × 4–5	37–54 × 8–9	4–7-euseptate	Obpyriform to obclavate, straight or curved, olivaceous	Freshwater	Unidentified submerged wood	Li et al. 2021
<i>D. fasciculata</i>	12–16 × 5–6	46–200 × 10–16.5	10–40-distoseptate	Subcylindrical to obclavate, mostly curved, olivaceous when young, dark brown when mature	Freshwater	Unidentified submerged wood	Dong et al. 2021
<i>D. longispora</i>	17–37 × 6–10	189–297 × 16–23	31–56-distoseptate	Obclavate, elongated, straight or slightly curved, to yellowish brown	Freshwater	Unidentified submerged wood	Song et al. 2020
<i>D. saprophytica</i>	50–140 × 3.2–4.2	14.5–30 × 4.5–7.5	2–6-distoseptate	Subcylindrical to obclavate, straight or curved, olivaceous to brown	Freshwater	Unidentified submerged wood	Dong et al. 2021
<i>D. songkhaensis</i>	70–90 × 4–5.5	44–125 × 9–14.5	9–16-distoseptate	Obclavate, straight or curved, olivaceous to brown	Freshwater	Unidentified submerged wood	Dong et al. 2021
<i>D. yunnanensis</i>	131–175 × 6–7	58–108 × 8–10	6–10-euseptate	Obclavate, rostrate, straight or slightly curved, mid olivaceous to brown	Freshwater	Unidentified submerged wood	Li et al. 2021

base frequency and rate are as follows: A = 0.243915, C = 0.259360, G = 0.279029, T = 0.217696; rate AC = 1.166355, AG = 2.813539, AT = 1.110401, CG = 0.796371, CT = 5.621229, GT = 1.000000; gamma distribution shape: $\alpha = 0.221933$. Bootstrap support values with a maximum likelihood (ML) greater than 70%, and Bayesian posterior probabilities (PP) greater than 0.97 are given above the nodes.

The phylogenetic tree shows that the new species *Distoseptispora bangkokensis* (MFLUCC 18-0262) was placed as a sister taxon to *D. bambusae* (MFLUCC 14-0583 and MFLUCC 20-0091), *D. dehongensis* (KUMCC 18-0090), *D. euseptata* (MFUCC 20-0154 and DLUCC S2024), *D. lancangjiangensis* (KUN-HKAS 112712), *D. suoluoensis* (MFLUCC 17-0224 and MFLUCC 17-1305), *D. thysanolaenae* (KUN-HKAS 102247 and KUN-HKAS 112710), and *D. yunnanensis* (MFLUCC 20-0153) with low bootstrap support with low bootstrap support (Figure 1), whereas *D. lancangjiangensis* clustered with *D. suoluoensis* with 97%ML/0.98PP support. *Distoseptispora thysanolaenae* (KUN-HKAS 112710) and *D. clematidis* (KUN-HKAS 112708) clustered with the ex-type strain of *D. thysanolaenae* (KUN-HKAS 102247) and *D. clematidis* (MFLUCC 17-2145), respectively, with 100%ML/1.00PP and 97%ML/0.99PP bootstrap support.

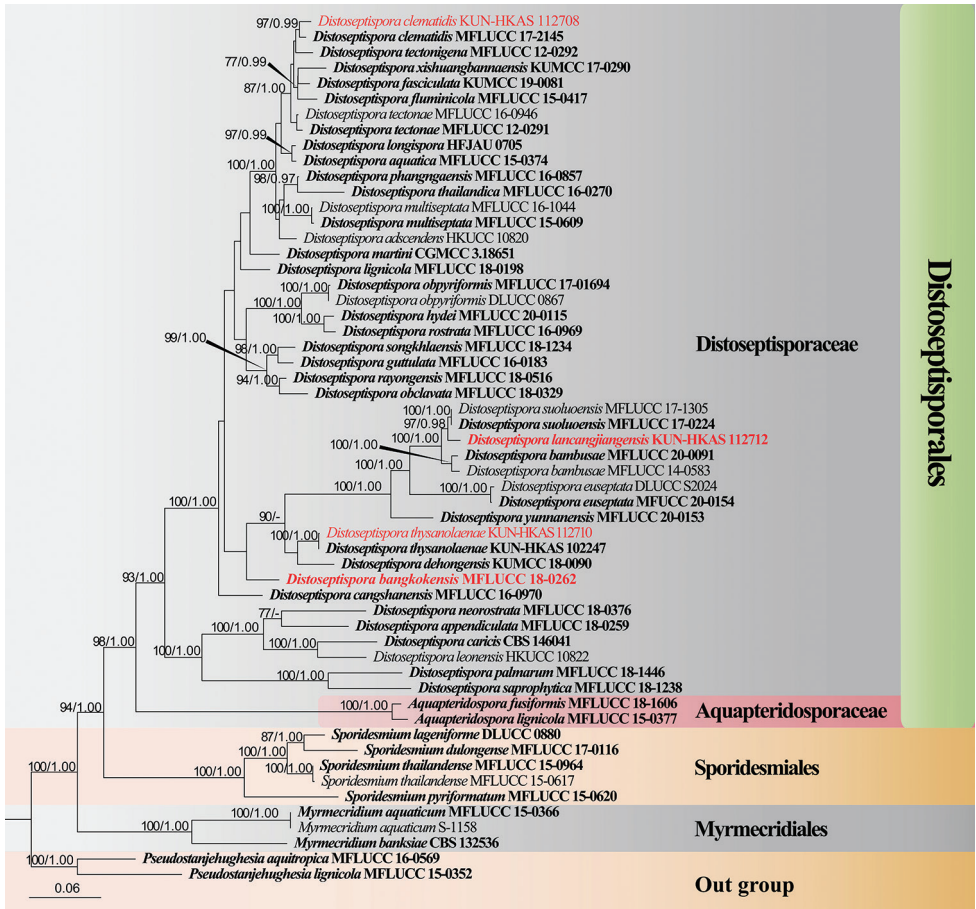


Figure 1. Maximum likelihood (ML) tree is based on combined of LSU, ITS, SSU, TEF1- α , and RPB2 sequence data. Bootstrap support values with an ML greater than 70% and Bayesian posterior probabilities (PP) greater than 0.97 given above the nodes, shown as “ML/PP”. The tree is rooted with *Pseudostanjehughesia aquitropica* (MFLUCC 16-0569) and *P. lignicola* (MFLUCC 15-0352). New species are indicated in red and type strains are in bold.

Taxonomy

Distoseptispora bangkokensis H.W. Shen, D.F. Bao, K.D. Hyde & Z.L. Luo, sp. nov.

Index Fungorum Number No: IF558556

Facesoffungi Number No: FoF09993

Figure 2

Etymology. Referring to the collecting location, Bangkok, Thailand.

Holotype. MFLU 21-0110

Description. *Saprobic* on submerged wood in freshwater stream. **Sexual morph:** Undetermined. **Asexual morph:** Colonies effuse, glistening, hairy, brown to dark brown. *Mycelium* partly superficial in the substratum, composed of hyaline to pale brown, sep-

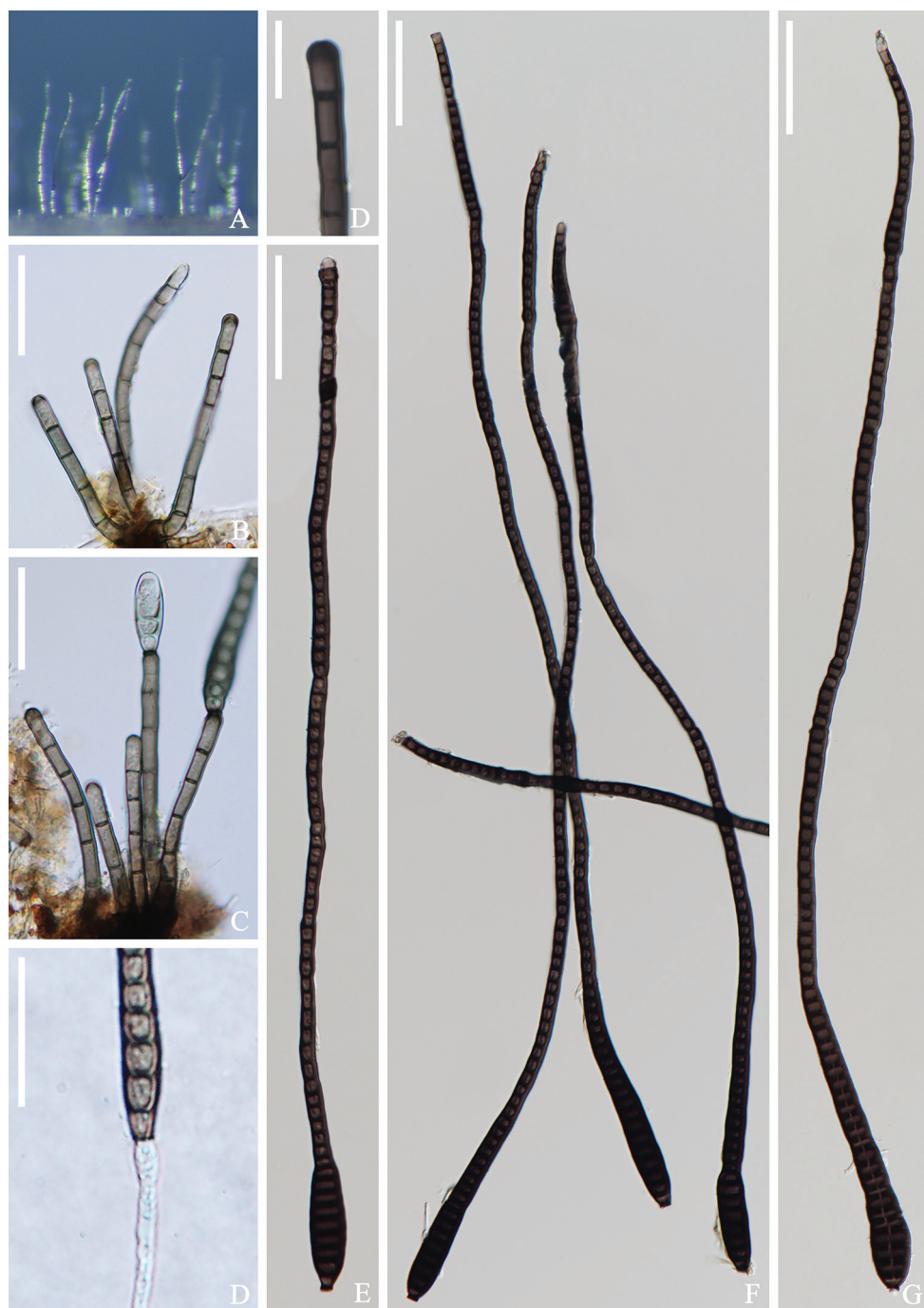


Figure 2. *Distoseptispora bangkokensis* (MFLU 21-0110, holotype) **A** colonies on the substratum **B** conidiophores **C** conidiophores with conidia **D** conidiogenous cell **E-G** conidia **H** germinating conidium. Scale bars: 20 μm (**B, C, H**); 10 μm (**D**); 50 μm (**E-G**).

tate, branched hyphae. *Conidiophores* $37\text{--}55 \times 3\text{--}4 \mu\text{m}$ ($\bar{x} = 46 \times 3 \mu\text{m}$, $n = 15$) macronematous, mononematous, solitary or in a small group of 2–4, cylindrical, straight or slightly flexuous, 3–8-septate, dark brown, paler at the apical part, rounded at the apex. *Conidiogenous cells* $6\text{--}8 \times 3\text{--}4 \mu\text{m}$ ($\bar{x} = 7 \times 3 \mu\text{m}$, $n = 15$), integrated, terminal, monoblastic, cylindrical, brown. *Conidia* $400\text{--}568 \times 13\text{--}16 \mu\text{m}$ ($\bar{x} = 484 \times 15 \mu\text{m}$, $n = 20$), 6–7 μm at the narrowest apical region, acrogenous, solitary, elongate, obclavate, rostrate, multi-distoseptate, tapering towards the apex, truncate at the base, rounded at apex, dark olivaceous to dark brown, straight or slightly curved, guttulate, thick-walled, smooth, conidia percurrent proliferation which forms another conidium at the apex.

Culture characteristics. Conidia cultivated on PDA within 12h and germ tubes produced at the ends. Colonies on PDA, reaching 6 cm in 1 month at room temperature (25 °C). Mycelium loose, flocculent, smooth edge, brown to dark brown, dark brown on the reverse.

Material examined. THAILAND, Bangkok Province, Khwaeng Phra Khanong Nuea, 13°42'41"N; 100°36'03"E, on submerged decaying wood, 1 October 2017, Zonglong Luo, S-3083 (MFLU 21-0110, **holotype**), ex-type living culture (MFLUCC 18-0262).

Notes. *Distoseptispora bangkokensis* is comparable to *D. cangshanensis* and *D. multiseptata* in having elongate, obclavate, or rostrate conidia (Su et al. 2016; Hyde et al. 2016a; Yang et al. 2018). However, *D. bangkokensis* has shorter and narrower conidiophores than those of *D. cangshanensis* ($37\text{--}55 \times 3\text{--}4 \mu\text{m}$ vs. $44\text{--}68 \times 4\text{--}8 \mu\text{m}$), but has longer conidia ($400\text{--}568 \mu\text{m}$ vs. $58\text{--}166 \mu\text{m}$); *D. multiseptata* (MFLU 17-0856) is similar to *D. bangkokensis* in conidial morphology, with conidia mostly 300–600 μm long (up to 700 μm) and significantly longer than those of the holotype (up to 380 μm long). However, Yang et al. (2018) did not give a detailed description of *D. multiseptata* (MFLU 17-0856). Phylogenetic analyses showed that *D. bangkokensis* clustered with *D. bambusae*, *D. dehongensis*, *D. euseptata*, *D. lancangjiangensis*, *D. suoluensis*, *D. thysanolaenae*, and *D. yunnanensis* with low bootstrap support (26%ML/0.53PP; Figure 1). *Distoseptispora bangkokensis* is distoseptate conidia, and it is easily distinguished from *D. bambusae*, *D. euseptata*, *D. lancangjiangensis*, *D. suoluensis*, and *D. yunnanensis*, which are euseptate. *Distoseptispora bangkokensis* is resemble to *D. dehongensis* and *D. thysanolaenae* in having obclavate, distoseptate conidia, but are distinguished by conidia characteristics, *D. bangkokensis* has elongate, obclavate, rostrate, multi-distoseptate, and longer conidia than *D. dehongensis* ($400\text{--}568 \times 13\text{--}16 \mu\text{m}$ vs. $17\text{--}30 \times 7.5\text{--}10 \mu\text{m}$) and *D. thysanolaenae* ($400\text{--}568 \times 13\text{--}16 \mu\text{m}$ vs. $30\text{--}70 \times 5\text{--}8 \mu\text{m}$), respectively.

***Distoseptispora lancangjiangensis* H.W. Shen, H.Y. Su, K.D. Hyde & Z.L. Luo, sp. nov.**

Index Fungorum Number No: IF558555

Facesoffungi Number No: FoF09994

Figure 3

Etymology. Referring to the collecting location, Lancangjiang River in China.



Figure 3. *Distoseptispora lancangjiangensis* (KUN-HKAS 112712, holotype) **A** colonies on the substratum **B** conidiophore and conidium **C-E** conidiophores **F, G** conidiogenous cells **H** conidiogenous cell with conidium **I-Q** conidia **R** germinating conidium **S, T** culture on PDA. Scale bars: 50 μ m (**B-E**); 20 μ m (**F-R**).

Holotype. KUN-HKAS 112712

Description. *Saprobic* on submerged wood in freshwater River. **Sexual morph:** Undetermined. **Asexual morph:** *Colonies* effuse, hairy, glistening, brown to dark. *Mycelium* partly immersed in the substratum, composed of hyaline to pale brown, septate, branched hyphae. *Conidiophores* 144–204 × 5–6 μm (\bar{x} = 175 × 6 μm, n = 20) macronematous, mononematous, solitary, inflate at the base, cylindrical, straight or slightly flexuous, 6–11-septate, dark brown, hyaline and rounded at apex. *Conidiogenous cells* 12–24 × 4–5 μm (\bar{x} = 18 × 5 μm, n = 20) integrated, terminal, monoblastic, cylindrical, brown. *Conidia* 64–84 × 9–10 μm (\bar{x} = 74 × 10 μm, n = 20), acrogenous, solitary, narrowly obclavate or obspathulate, truncated at base, tapering towards apex, 3–10-euseptate, brown to dark brown, thin-walled, becoming paler or hyaline towards apex, guttulate, with a darkened scar at base, smooth-walled.

Culture characteristics. Conidia cultivated on PDA within 12h and germ tubes produced at the apex. Colonies on PDA, reaching 4.5 cm in 1 month at room temperature (25 °C). Mycelium loose, flocculent, smooth edges, convex middle, pale brown to dark brown on the surface of PDA. Smooth, black on the reverse.

Material examined. CHINA, Yunnan Province, Dali City, Lancangjiang River, 22°36'36"N; 100°37'59"E, on submerged decaying wood, 20 July 2017, Qishan Zhou and Qingxiong Ruan S–1864 (KUN-HKAS 112712, **holotype**; MFLU 21-0111, **isotype**), ex-type living culture (DLUCC 1864 = CGMCC 3.20265).

Notes. Phylogenetic analysis showed that *Distoseptispora lancangjiangensis* clustered as a sister taxon to *D. suoluoensis* with 97%ML/0.98PP support. *Distoseptispora lancangjiangensis* is similar to *D. suoluoensis* in having long conidiophores, monoblastic conidiogenous cells, and obclavate to rostrate, euseptate conidia. However, *D. suoluoensis* has yellowish-brown or dark olivaceous, verrucose conidia, while in *D. lancangjiangensis* conidia are brown to dark brown and smooth-walled. Moreover, *D. lancangjiangensis* has smaller conidia than those of *D. suoluoensis* (64–84 × 9–10 μm vs. 80–125 × 8–13 μm) (Yang et al. 2018). *Distoseptispora lancangjiangensis* and *D. bambusae* have similar conidial shapes, but *D. lancangjiangensis* is having longer conidia (64–84 × 9–10 μm vs. 45–74 × 5.5–10 μm) and longer conidiophores (144–204 × 5–6 μm vs. 40–96 × 4–5.5 μm). Furthermore, *D. bambusae* has polyblastic or monoblastic conidiogenous cells and olivaceous or brown conidia, while *D. lancangjiangensis* only has monoblastic conidiogenous cells and brown to dark brown conidia (Sun et al. 2020).

***Distoseptispora clematidis* Phukhams., M.V. de Bult & K.D. Hyde, in Phukham-sakda et al., Fungal Diversity 102: 168 (2020)**

Index Fungorum Number No: IF557301

Facesofungi Number No: FoF07261

Figure 4

Description. *Saprobic* on submerged wood in freshwater River. **Sexual morph:** Undetermined. **Asexual morph:** *Colonies* on the substratum superficial, effuse, scattered, hairy, dark brown. *Mycelium* partly immersed in substrate, composed of branched, smooth,



Figure 4. *Distoseptispora clematidis* (KUN-HKAS 112708) **A** colonies on the substratum **B-C** conidiophores with conidia **D** conidiogenous cells **E-H** conidia **I** germinating conidium **J** culture on PDA Scale bars: 30 μ m (**B, C, E-I**); 20 μ m (**D**).

septate, brown to dark brown hyphae. *Conidiophores* 30–41 × 5–6 μm (\bar{x} = 36 × 6 μm, n = 15), macronematous, mononematous, single or in a small group, straight or slightly flexuous, unbranched, septate, erect, 2–4-septate, cylindrical, smooth, dark brown to brown. *Conidiogenous cells* 7–9 × 5–6 μm (\bar{x} = 8 × 5 μm, n = 15), monoblastic, integrated, determinate, terminal, cylindrical, pale brown to brown. *Conidia* 83–220 × 12–14 μm (\bar{x} = 151 × 13 μm, n = 20), acrogenous, solitary, obclavate, cylindrical, elongated, straight or curved, truncate at base, rounded at apex, 16–41-distoseptate, slightly constricted at some septa, smooth, brown to greenish-brown, thick-walled.

Culture characters. Conidia cultivated on PDA within 12h and germ tubes produced at the ends. Colonies on PDA, attaining 4 cm after 1 month at room temperature (25 °C), gray at first, later becoming dark gray, loose, flocculent, smooth edge, dark brown on the reverse.

Material examined. CHINA, Yunnan Province, Kunming City, Yiliang County, Nanpanjiang River, 24°38'28"N; 103°09'38"E, on submerged decaying wood, 12 June 2018; Hongwei Shen and Xiu He, S-1797 (KUN-HKAS 112708), living culture (DLUCC 1797).

Notes. Our new isolate clustered with the ex-type strain of *Distoseptispora clematidis* (MFLU 17-1501) (Phukhamsakda et al. 2020) with 97%ML/0.99PP bootstrap support (Figure 1). *Distoseptispora clematidis* (MFLU 17-1501) was collected on dead culms of *Thysanolaena maxima* (Roxb. ex Hornem.) Honda in Yunnan Province, China. Based on morphological analysis, the size and shape of the conidia and conidiophores of our new isolate are similar to *D. clematidis*. Therefore, we identified our new isolate as *D. clematidis* and it is a new record from freshwater habitats in China.

***Distoseptispora thysanolaenae* Goonas., Dayarathne, Phookamsak & K.D.Hyde, in Phookamsak et al., Fungal Diversity 95: 126 (2019)**

Index Fungorum Number No: IF555408

Facesoffungi Number No: FoF05011

Figure 5

Description. *Saprobic* on submerged wood in freshwater River. **Sexual morph:** Undetermined. **Asexual morph:** *Colonies* on the substratum superficial, effuse, scattered, hairy, dark brown. *Mycelium* partly immersed, composed of branched, septate, smooth, brown to dark brown hyphae. *Conidiophores* 41–59 × 4–5 μm (\bar{x} = 50 × 5 μm, n = 20) macronematous, mononematous, unbranched, single, erect, straight or slightly curved, smooth, 3–6-septate, pale brown to brown. *Conidiogenous cells* monoblastic, integrated, determinate, terminal, dark brown, cylindrical. *Conidia* 46–87 × 9–12 μm (\bar{x} = 67 × 10 μm, n = 25) acrogenous, solitary, dry, smooth, obclavate, elongated, straight or slightly curved, truncate at base, tapering towards apex, 6–19-septate, dark grayish-brown to light yellow-green, thick-walled.



Figure 5. *Distoseptispora thysanolaenae* (KUN-HKAS 112710) **A** colonies on the substratum **B-D** conidiophores with conidia **E, F** conidiogenous cells **G-N** conidia **O** germinating conidium **P, Q** culture on PDA Scale bars: 30 μm (**B-D**); 10 μm (**E, F**); 20 μm (**G-O**).

Culture characteristics. Conidia cultivated on PDA within 12 h and germ tubes produced at the apex. Colonies on PDA, reaching 6 cm after 6 weeks at room temperature (25 °C). Mycelium loose, flocculent, neat edges, convex in middle, pale brown to dark brown. Black, smooth on the back.

Material examined. CHINA, Yunnan Province, Lushui City, Nujiang River, 26°23'12"N; 98°53'94"E, on submerged decaying wood, 3 May 2016, Zonglong Luo and Songming Tang, S-876 (KUN-HKAS 112710), living culture (DLUCC 876 = KUNCC 21-10710)

Notes. Our new collection is identical to *Distoseptispora thysanolaenae* in characters of the conidiophores, conidiogenous cell, and conidia (Phookamsak et al. 2019). Furthermore, our new isolate phylogenetically clusters with the ex-type strain of *D. thysanolaenae* (KUN-HKAS 102247) with 100%ML/1.00PP support (Figure 1). *Distoseptispora thysanolaenae* was collected from terrestrial habitats in China, while, our new isolate was collected from freshwater habitat in China. Therefore, we identified our new collection as *D. thysanolaenae*, and it is new to freshwater habitats in China.

Discussion

Distoseptispora has been reported from both freshwater and terrestrial habitats. Of these, species have been collected from freshwater environments (Su et al. 2016; Hyde et al. 2016a, 2019, 2020; Luo et al. 2018; Xia et al. 2017, 2019; Yang et al. 2018; Tibpromma et al. 2018; Crous et al. 2019; Phookamsak et al. 2019; Monkai et al. 2020; Phukhamsakda et al. 2020; Song et al. 2020; Sun et al. 2020; Li et al. 2021). To date, 18 species of *Distoseptispora* have been reported from Thailand, 14 species from China. In this study, we collected four *distoseptispora*-like taxa from rivers and streams in China and Thailand. Phylogenetic analysis showed that all four species were well-placed in *Distoseptispora* (Figure 1). Two new species and records are introduced based on morphological and phylogenetic analysis.

Species of *Distoseptispora* are highly diverse in morphology, especially the conidial shape. Conidia of most species are obclavate to cylindrical or rostrate (e.g. *D. aquatica*, *D. tectonae*, and *D. suoluoensis*), but a few are ellipsoid to subglobose (e.g. *D. martinii*), lanceolate (e.g. *D. guttulata* and *D. multiseptata*), and some species have conidia with a sheath at the apex (e.g. *D. appendiculata*) (Hyde et al. 2016a; Su et al. 2016; Xia et al. 2017; Yang et al. 2018; Luo et al. 2018, 2019). Some species also differ in the conidiogenous cells (*D. palmarum*, *D. dehongensis*, and *D. bambusae* are monoblastic or polyblastic, while the others are monoblastic) and conidial septate (*D. bambusae*, *D. euseptatisensis*, *D. guttulata*, *D. lignicola*, *D. rayongensis*, *D. suoluoensis*, and *D. yunnanensis* are euseptate, while other species are distoseptate) (Yang et al. 2018; Hyde et al. 2019; Luo et al. 2019; Sun et al. 2020; Dong et al. 2021; Li et al. 2021).

Based on the key morphological characteristics, viz. conidiophores, conidiogenous cells, and conidia, Subramanian (1992) redispersed seven genera, viz., *Sporidesmium*, *Polydesmus*, *Sporidesmiella*, *Stanjehughesia*, *Repetophragma*, *Penzigomyces*, and *Ellisem-*

bia to accommodate several *Sporidesmium*-like taxa. Based on multi-gene phylogenetic analysis and morphology, Su et al. (2016) introduced a new *Sporidesmium*-like genus *Distoseptispora*. Some *Sporidesmium*-like taxa were introduced in different lineages and synonymized *Ellisembia* under *Sporidesmium*. Although *Distoseptispora* was only introduced from submerged wood in freshwater habitat in 2016 (Su et al. 2016), the genus has previously been reported from both freshwater and terrestrial habitats as species in other genera. For example, Cai et al. (2002), Ho et al. (2001, 2002) and Luo et al. (2004) reported *Distoseptispora* as other species (*Ellisembia*, *Sporidesmiella*, and *Sporidesmium*) from submerged wood in freshwater habitats, and Kodsueb et al. (2016), Mena-Portales et al. (2016) and Zhou et al (2001) reported from terrestrial habitats. However, none of these records had molecular data and it is impossible to consider the placement of these isolates. In these species *distoseptisporalsporidesmium*-like genera, it is therefore better to describe taxa based on molecular data.

Based on phylogenetic analysis, Xia et al. (2017) transferred *Acrodictys martinii* to *Distoseptispora* as *Distoseptispora martinii*. The species is characterized by solitary erect, unbranched conidiophores, monoblastic conidiogenous cells with percurrent extensions and subhyaline to pale brown and solitary, transversal ellipsoid, oblate or subglobose, muriform conidia, separated by septa, sometimes with pores in the septa and pale brown to brown. However, the current understanding of Distoseptisporaceae, *D. martinii* is significantly different from other *Distoseptispora* taxa; thus, needs to be verified in the future (Luo et al. 2018; Sun et al. 2020).

Acknowledgment

We would like to thank the National Natural Science Foundation of China (Project ID: 32060005 and 31970021), and Fungal Diversity Conservation and Utilization Innovation Team of Dali University (ZKLX2019213) for financial support. Kevin D Hyde thanks the Thailand Research Fund for the grant (RDG6130001MS), Impact of climate change on fungal diversity and biogeography in the Greater Mekong Sub-region. Hongwei Shen thanks Saranyaphat Boonmee for her help in sample collection and herbarium deposit. Qishan Zhou, Qingxiong Ruan, Songming Tang, and Xiu He are thanked for their help on sample collection. We are grateful to Yanmei Zhang, Longli Li, and Wenli Li for their help on DNA extraction and PCR amplification.

References

- Cai L, Tsui CKM, Zhang KQ, Hyde KD (2002) Aquatic fungi from Lake Fuxian, Yunnan, China. *Fungal Diversity* 9: 57–70.
- Capella-Gutiérrez S, Silla-Martínez JM, Gabaldón T (2009) trimAl: a tool for automated alignment trimming in large-scale phylogenetic analyses. *Bioinformatics* 25: 1972–1973. <https://doi.org/10.1093/bioinformatics/btp348>

- Crous PW, Summerell BA, Shivas RG, Burgess TI, Decock CA, Dreyer LL, Granke LL, Guest DI, Hardy GESTJ, Hausbeck MK, Hüberli D, Jung T, Koukol O, Lennox CL, Liew ECY, Lombard L, McTaggart AR, Pryke JS, Roets F, Saude C, Shuttleworth LA, Stukely MJC, Vánky K, Webster BJ, Windstam ST, Groenewald JZ (2012) Fungal Planet description sheets: 107–127. *Persoonia* 28: 138–182. <https://doi.org/10.3767/003158512X652633>
- Darriba D, Taboada GL, Doallo R, Posada D (2012) jModelTest 2: more models, new heuristics and parallel computing. *Nature Methods* 9: 772–772. <https://doi.org/10.1038/nmeth.2109>
- Dong W, Hyde KD, Jeewon R, Doilom M, Yu XD, Wang GN, Liu NG, Hu DM, Nalumpang S (2021) Towards a natural classification of Annulatascaceae-like taxa II: introducing five new genera and eighteen new species from freshwater. *Mycosphere* 12: 1–88. <https://doi.org/10.5943/mycosphere/12/1/1>
- Guindon S, Gascuel O (2003) A simple, fast, and accurate algorithm to estimate large phylogenies by maximum likelihood. *Systematic Biology* 52: 696–704. <https://doi.org/10.1080/10635150390235520>
- Hall TA (1999) BioEdit: a user-friendly biological sequence alignment editor and analysis program for Windows 95/98/NT. *Nucleic Acids Symposium Series* 41: 95–98. <http://wwwmbio-ncsuedu/bioedit/bioedithtml>
- Ho WH, Hyde KD, Hodgkiss IJ, Yanna (2001) Fungal communities on submerged wood from streams in Brunei, Hong Kong, and Malaysia. *Mycological* 105: 1492–1501. <https://doi.org/10.1017/S095375620100507X>
- Ho WH, Yanna, Hyde KD, Hodgkiss IJ (2002) Seasonality and sequential occurrence of fungi on wood submerged in Tai Po Kau Forest Stream, Hong Kong. *Fungal Diversity* 10: 21–43.
- Hyde KD, Bao DF, Hongsanan S, Chethana KWT, Yang J, Suwanarach N (2021) Evolution of freshwater Diaporthomycetidae (Sordariomycetes) provides evidence for five new orders and six new families. *Fungal Diversity* 107: 71–105. <https://doi.org/10.1007/s13225-021-00469-7>
- Hyde KD, Fryar S, Tian Q, Bahkali AH, Xu JC (2016b) Lignicolous freshwater fungi along a north-south latitudinal gradient in the Asian/Australian region; can we predict the impact of global warming on biodiversity and function? *Fungal Ecology* 19: 190–200. <https://doi.org/10.1016/j.funeco.2015.07.002>
- Hyde KD, Hongsanan S, Jeewon R, Bhat DJ, McKenzie EHC, Jones EBG, Phookamsak R, Ariyawansa HA, Boonmee S, Zhao Q, Abdel-Aziz FA, Abdel-Wahab MA, Banmai S, Chomnunti P, Cui BK, Daranagama DA, Das K, Dayarathne MC, de Silva NI, Dissanayake AJ, Doilom M, Ekanayaka AH, Gibertoni TB, Góes-Neto A, Huang SK, Jayasiri SC, Jayawardena RS, Konta S, Lee HB, Li WJ, Lin CG, Liu JK, Lu YZ, Luo ZL, Manawasinghe IS, Manimohan P, Mapook A, Niskanen T, Norphanphoun C, Papizadeh M, Perera RH, Phukhamsakda C, Richter C, de A. Santiago ALCM, Drechsler-Santos ER, Senanayake IC, Tanaka K, Tennakoon TMDS, Thambugala KM, Tian Q, Tibpromma S, Thongbai B, Vizzini A, Wanasinghe DN, Wijayawardene NN, Wu HX, Yang J, Zeng XY, Zhang H, Zhang JF, Bulgakov TS, Camporesi E, Bahkali AH, Amoozegar MA, Araujo-Neta LS, Ammirati JF, Baghela A, Bhatt RP, Bojantchev D, Buyck B, da Silva GA, de Lima CLF, de Oliveira RJV, de Souza CAF, Dai YC, Dima B, Duong TT, Ercole E, Mafalda-Freire F,

- Ghosh A, Hashimoto A, Kamolhan S, Kang JC, Karunarathna SC, Kirk PM, Kytövuori I, Lantieri A, Liimatainen K, Liu ZY, Liu XZ, Lücking R, Medardi G, Mortimer PE, Nguyen TTT, Promputtha I, Raj KNA, Reck MA, Lumyong S, Shahzadeh-Fazeli SA, Stadler M, Soudi MR, Su HY, Takahashi T, Tangthirasunun N, Uniyal P, Wang Y, Wen TC, Xu JC, Zhang ZK, Zhao YC, Zhou JL, Zhu L (2016a) Fungal diversity notes 367–490: taxonomic and phylogenetic contributions to fungal taxa. *Fungal Diversity* 80: 1–270. <https://doi.org/10.1007/s13225-016-0373-x>
- Hyde KD, Norphanphoun C, Maharachchikumbura SSN, Bhat DJ, Jones EBG1, Bundhun D, Chen YJ, Bao DF, Boonmee S, Calabon MS, Chaiwan N, Chethana KWT, Dai DQ, Dayarathne MC, Devadatha B, Dissanayake AJ, Dissanayake LS, Doilom M, Dong W, Fan XL, Goonasekara ID, Hongsanan S, Huang SK, Jayawardena RS, Jeewon R, Karunarathna A, Konta S, Kumar V, Lin CG, Liu JK, Liu NG, Luangsa-ard J, Lumyong S, Luo ZL, Marasinghe DS, McKenzie EHC, Niego AGT, Niranjana M, Perera RH, Phukhamsakda C, Rathnayaka AR, Samarakoon MC, Samarakoon SMBC, Sarma VV, Senanayake IC, Shang QJ, Stadler M, Tibpromma S, Wanasinghe DN, Wei DP, Wijayawardene NN, Xiao YP, Yang J, Zeng XY, Zhang SN, Xiang MM (2020) Refined families of Sordariomycetes. *Mycosphere* 11: 305–1059. <https://doi.org/10.5943/mycosphere/11/1/7>
- Hyde KD, Tennakoon DS, Jeewon R, Bhat DJ, Maharachchikumbura SSN, Rossi W, Leonardi M, Lee HB, Mun HY, Houbraken J, Nguyen TTT, Jeon SJ, Frisvad JC, Wanasinghe DN, Lücking R, Aptroot A, Cáceres MES, Karunarathna SC, Hongsanan S, Phookamsak R, de Silva NI, Thambugala KM, Jayawardena RS, Senanayake IC, Boonmee S, Chen J, Luo ZL, Phukhamsakda C, Pereira OL, Abreu VP, Rosado AWC, Bart B, Randrianjohany E, Hofstetter V, Gibertoni TB, Soares AMdS, Plautz HL, Sorão HMP, Xavier WKS, Bezerra JDP, de Oliveira TGL, de Souza-Motta CM, Magalhães OMC, Bundhun D, Harishchandra D, Manawasinghe IS, Dong W, Zhang SN, Bao DF, Samarakoon MC, Pem D, Karunarathna A, Lin CG, Yang J, Perera RH, Kumar V, Huang SK, Dayarathne MC, Ekanayaka AH, Jayasiri SC, Xiao Y, Konta S, Niskanen T, Liimatainen K, Dai YC, Ji XH, Tian XM, Mešić A, Singh SK, Phutthacharoen K, Cai L, Sorvongxay T, Thiyagaraja V, Norphanphoun C, Chaiwan N, Lu YZ, Jiang HB, Zhang JF, Abeywickrama PD, Aluthmuhandiram JVS, Brahmanage RS, Zeng M, Chethana T, Wei D, Réblová M, Fournier J, Nekvindová J, do Nascimento Barbosa R, dos Santos JEF, de Oliveira NT, Li GJ, Ertz D, Shang QJ, Phillips AJL, Kuo CH, Camporesi E, Bulgakov TS, Lumyong S, Jones EBG, Chomnunti P, Gentekaki E, Bungartz F, Zeng XY, Fryar S, Tkalčec Z, Liang J, Li G, Wen TC, Singh PN, Gafforov Y, Promputtha I, Yasanthika E, Goonasekara ID, Zhao RL, Zhao Q, Kirk PM, Liu JK, Yan J, Mortimer PE, Xu J, Doilom M (2019) Fungal diversity notes 1036–1150: taxonomic and phylogenetic contributions on genera and species of fungal taxa. *Fungal Diversity* 96: 1–242. <https://doi.org/10.1007/s13225-019-00429-2>
- Index Fungorum (2021) Index Fungorum. www.indexfungorum.org [accessed 4 September 2021]
- Jayasiri SC, Hyde KD, Abd-Elsalam KA, Abdel-Wahab MA, Ariyawansa HA, Bhat J, Buyck B, Dai YC, Ertz D, Hidayat I, Jeewon R, Jones EBG, Karunarathna SC, Kirk P, Lei C, Liu JK, Maharachchikumbura SSN, McKenzie E, Ghobad-Nejhad M, Nilsson H, Pang KL, Phookamsak R, Rollins AW, Romero AI, Stephenson S, Suetrong S, Tsui CKM, Vizzini A,

- Wen TC, De Silva NI, Promputtha I, Kang JC (2015) The Facesoffungi database: fungal names linked with morphology, molecular and human attributes. *Fungal Diversity* 74: 3–18. <https://doi.org/10.1007/s13225-015-0351-8>
- Katoh K, Standley DM (2013) MAFFT multiple sequence alignment software version 7: improvements in performance and usability. *Molecular Biology and Evolution* 30: 772–780. <https://doi.org/10.1093/molbev/mst010>
- Kodsueb R, Lumyong S, McKenzie EHC, Bahkali AH, Hyde KD (2016) Relationships between terrestrial and freshwater lignicolous fungi. *Fungal Ecology* 19: 155–168. <https://doi.org/10.1016/j.funeco.2015.09.005>
- Li WL, Dissanayake AJ, Luo ZL, Su HY, Liu JK (2021) Additions to *Distoseptispora* (Distoseptisporaceae) associated with submerged decaying wood in China. *Phytotaxa* 520: 75–86. <https://doi.org/10.11646/PHYTOTAXA.520.1.5>
- Liu YJ, Whelen S, Hall BD (1999) Phylogenetic relationships among ascomycetes: evidence from an RNA polymerase II subunit. *Molecular Biology and Evolution* 16: 1799–1808. <https://doi.org/10.1093/oxfordjournals.molbev.a026092>
- Luo J, Yin JF, Cai L, Zhang KQ, Hyde KD (2004) Freshwater fungi in Lake Dianchi, a heavily polluted lake in Yunnan, China. *Fungal diversity* 16: 93–112.
- Luo ZL, Hyde KD, Liu JK, Bhat DJ, Bao DF, Li WL, Su HY (2018) Lignicolous freshwater fungi from China II: Novel *Distoseptispora* (Distoseptisporaceae) species from northwestern Yunnan Province and a suggested unified method for studying lignicolous freshwater fungi. *Mycosphere* 9: 444–461. <https://doi.org/10.5943/mycosphere/9/3/2>
- Luo ZL, Hyde KD, Liu JK, Maharachchikumbura SSN, Jeewon R, Bao DF, Bhat DJ, Lin CG, Li WL, Yang J, Liu NG, Lu YZ, Jayawardena RS, Li JF, Su HY (2019) Freshwater Sordariomycetes. *Fungal Diversity* 99: 451–660. <https://doi.org/10.1007/s13225-019-00438-1>
- Mckenzie EHC (1995) Dematiaceous Hyphomycetes on Pandanaceae. 5. *Sporidesmium* sensu lato. *Mycotaxon* 56: 9–29.
- Mena-Portales J, Hernandez-Restrepo M, Guarro J, Minters DW, Gené J (2016) New species of *Penzigomyces*, *Sporidesmium* and *Stanjehughesia* from plant debris in Spain. *Nova Hedwigia* 103: 359–371. https://doi.org/10.1127/nova_hedwigia/2016/0355
- Miller MA, Pfeiffer W, Schwartz T (2010) Creating the CIPRES Science Gateway for inference of large phylogenetic trees. Gateway Computing Environments Workshop (GCE 2010), 14: 1–8. <https://doi.org/10.1109/GCE.2010.5676129>
- Monkai J, Boonmee S, Ren GC, Wei DP, Phookamsak R, Mortimer PE (2020) *Distoseptispora hydei* sp. nov. (Distoseptisporaceae), a novel lignicolous fungus on decaying bamboo in Thailand. *Phytotaxa* 459: 93–107. <https://doi.org/10.11646/phytotaxa.459.2.1>
- Nylander J (2004) MrModeltest v2. Program distributed by the author: Evolutionary Biology Centre. Uppsala University, Sweden: <http://www.ebc.uu.se/systzoo/staff/nylander.html>
- Phookamsak R, Hyde KD, Jeewon R, Bhat DJ, Jones EBG, Maharachchikumbura SSN, Rasapé O, Karunaratna SC, Wanasinghe DN, Hongsanan S, Doilom M, Tennakoon DS, Machado AR, Firmino AL, Ghosh A, Karunaratna A, Mešić A, Dutta, AK, Thongbai, B, Devadatha, B, Norphanphoun, C, Senwanna, C, Wei, D, Pem, D, Ackah, FK, Wang GN, Jiang HB, Madrid H, Lee HB, Goonasekara ID, Manawasinghe IS, Kušan Cano J, Gené J, Li J, Das K, Acharya K, Raj KNA, Latha KPD, Chethana KWT, He MQ, Dueñas

- M, Jadan M, Martín MP, Samarakoon MC, Dayarathne MC, Raza M, Park MS, Telleria MT, Chaiwan N, Matočec N, de Silva NI, Pereira OL, Singh PN, Manimohan P, Uniyal P, Shang QJ, Bhatt RP, Perera RH, Alvarenga RLM, Nogal-Prata S, Singh SK, Vadthanarat S, Oh SY, Huang SK, Rana S, Konta S, Paloi S, Jayasiri SC, Jeon SJ, Mehmood T, Gibertoni TB, Nguyen TTT, Singh U, Thiyagaraja V, Sarma VV, Dong W, Yu XD, Lu YZ, Lim YW, Chen Y, Tkalčec Z, Zhang ZF, Luo ZL, Daranagama DA, Thambugala KM, Tibpromma S, Camporesi E, Bulgakov T, Dissanayake AJ, Senanayake IC, Dai DQ, Tang LZ, Khan S, Zhang H, Promputtha I, Cai L, Chomnunti P, Zhao RL, Lumyong S, Boonmee S, Wen TC, Mortimer PE, Xu J (2019) Fungal diversity notes 929–1035: taxonomic and phylogenetic contributions on genera and species of fungal taxa. *Fungal Diversity* 95: 1–273. <https://doi.org/10.1007/s13225-019-00421-w>
- Phukhamsakda C, McKenzie E, Phillips AJL, Jones EBG, Bhat DJ, Marc S, Bhunjun CS, Wanasinghe DN, Thongbai B, Camporesi E, Ertz D, Jayawardena RS, Perera RH, Ekanayake AH, Tibpromma S, Doilom M, Xu J, Hyde KD (2020) Microfungi associated with *Clematis* (Ranunculaceae) with an integrated approach to delimiting species boundaries. *Fungal Diversity* 102: 1–203. <https://doi.org/10.1007/s13225-020-00448-4>
- Rambaut A (2012) FigTree v1. 4. <http://tree.bio.ed.ac.uk/> [accessed January 14, 2019].
- Rannala B, Yang Z (1996) Probability distribution of molecular evolutionary trees: a new method of phylogenetic inference. *Journal of Molecular Evolution* 43: 304–311. <https://doi.org/10.1007/BF02338839>
- Ronquist F, Teslenko M, Van Der Mark P, Ayres DL, Darling A, Höhna S, Larget B, Liu L, Suchard MA, Huelsenbeck JP (2012) MrBayes 3.2: efficient Bayesian phylogenetic inference and model choice across a large model space. *Systems Biology* 61: 539–542. <https://doi.org/10.1093/sysbio/sys029>
- Senanayake IC, Rathnayaka AR, Marasinghe DS, Calabon MS, Gentekaki E, Wanasinghe DN, Lee HB, Hurdeal VG, Pem D, Dissanayake LS, Wijesinghe SN, Bundhun D, Nguyen TT, Goonasekara ID, Abeywickrama PD, Bhunjun CS, Chomnunti P, Boonmee S, Jayawardena RS, Wijayawardene NN, Doilom M, Jeewon R, Bhat JD, Zhang HX, Xie N (2020) Morphological approaches in studying fungi: collection, examination, isolation, sporulation and preservation. *Mycosphere* 11: 2678–2754. <https://doi.org/10.5943/mycosphere/11/1/20>
- Shenoy BD, Jeewon R, Wu WP, Bhat DJ, Hyde KD (2006) Ribosomal and RPB2 DNA sequence analyses suggest that *Sporidesmium* and morphologically similar genera are polyphyletic. *Mycological* 110: 916–928. <https://doi.org/10.1016/j.mycres.2006.06.004>
- Shoemaker RA, White GP (1985) *Lasiosphaeria caesariata* with *Sporidesmium hormiscioides* and *L. triseptata* with *S. ascendens*. *Sydowia* 38: 278–283
- Song HY, El Sheikh AF, Zhai ZJ, Zhou JP, Chen MH, Huo GH, Huang XG, Hu DM (2020) *Distoseptispora longispora* sp. nov. from freshwater habitats in China. *Mycotaxon* 135: 513–523. <https://doi.org/10.5248/135.513>
- Stamatakis A (2006) RAxML-VI-HPC: maximum likelihood-based phylogenetic analyses with thousands of taxa and mixed models. *Bioinformatics* 22: 2688–2690. <https://doi.org/10.1093/bioinformatics/btl446>
- Stamatakis A, Hoover P, Rougemont J (2008) A rapid bootstrap algorithm for the RAxML web servers. *Systems Biology* 57: 758–771. <https://doi.org/10.1080/10635150802429642>

- Su HY, Hyde KD, Maharachchikumbura SSN, Ariyawansa HA, Luo Z, Promputtha I, Tian Q, Lin C, Shang Q, Zhao Y, Chai H, Liu X, Bahkali AH, Bhat JD, McKenzie EHC, Zhou D (2016) The families Distoseptisporaceae fam. nov., Kirschsteiniotheliaceae, Sporormiaceae and Torulaceae, with new species from freshwater in Yunnan Province, China. *Fungal Diversity* 80: 375–409. <https://doi.org/10.1007/s13225-016-0362-0>
- Subramanian CV (1992) A reassessment of *Sporidesmium* (Hyphomycetes) and some related taxa. *Proceedings of the Indian National Science Academy Part B Biological sciences* 58: 179–190.
- Sun YR, Goonasekara ID, Thambugala KM, Jayawardena RS, Wang Y, Hyde KD (2020) *Distoseptispora bambusae* sp. nov. (Distoseptisporaceae) on bamboo from China and Thailand. *Biodiversity Data Journal* 8: e53678. <https://doi.org/10.3897/BDJ.8.e53678.figure4>
- Tibpromma S, Hyde KD, McKenzie EHC, Bhat DJ, Phillips AJL, Wanasinghe DN, Samarakoon MC, Jayawardena RS, Dissanayake AJ, Tennakoon DS, Doilom M, Phookamsak R, Tang AMC, Xu J, Mortimer PE, Promputtha I, Maharachchikumbura SSN, Khan S, Karunarathna SC (2018) Fungal diversity notes 840–928: micro-fungi associated with Pandanaceae. *Fungal Diversity* 93: 1–160. <https://doi.org/10.1007/s13225-018-0408-6>
- Vaidya G, Lohman DJ, Meier R (2011) SequenceMatrix: concatenation software for the fast assembly of multi-gene datasets with character set and codon information. *Cladistics* 27: 171–180. <https://doi.org/10.1111/j.1096-0031.2010.00329.x>
- Vilgalys R, Hester M (1990) Rapid genetic identification and mapping of enzymatically amplified ribosomal DNA from several *Cryptococcus* species. *Journal of Bacteriology* 172: 4238–4246. <https://doi.org/10.1128/jb.172.8.4238-4246.1990>
- White TJ, Bruns TD, Lee SB, Taylor JW (1990) Amplification and direct sequencing of fungal ribosomal RNA genes for phylogenetics. *PCR Protocols: A Guide to Methods and Applications*: 315–322. <https://doi.org/10.1016/B978-0-12-372180-8.50042-1>
- Wijayawardene NN, Hyde KD, Al-Ani LKT, Tedersoo L, Haelewaters D, Rajeshkumar KC, Zhao RL, Aptroot A, Leontyev DV, Saxena RK, Tokarev YS, Dai DQ, Letcher PM, Stephenson SL, Ertz D, Lumbsch HT, Kukwa M, Issi IV, Madrid H, Phillips AJL, Selbmann L, Pfliegler WP, Horváth E, Bensch K, Kirk P, Kolaříková Z, Raja HA, Radek R, Papp V, Dima B, Ma J, Malosso E, Takamatsu S, Rambold G, Gannibal PB, Triebel D, Gautam AK, Avasthi S, Suetrong S, Timdal E, Fryar SC, Delgado G, Réblová M, Doilom M, Dolatabadi S, Pawłowska J, Humber RA, Kodsueb R, Sánchez-Castrov I, Goto BT, Silva DKA, de Souza FA, Oehl F, da Silva GA, Silva IR, Błaszowski J, Jobim K, Maia LC, Barbosa FR, Fiuza PO, Divakar PK, Shenoy BD, Castañeda-Ruiz RF, Somrithipol S, Karunarathna SC, Tibpromma S, Mortimer PE, Wanasinghe DN, Phookamsak R, Xu J, Wang Y, Fenghua T, Alvarado P, Li DW, Kušan I, Matočec N, Maharachchikumbura SSN, Papizadeh M, Heredia G, Wartchow F, Bakhshi M, Boehm E, Youssef N, Hustad VP, Lawrey JD, Santiago ALCM, Bezerra JDP, Souza-Motta CM, Firmino AL, Tian Q, Houbroken J, Hongsanan S, Tanaka K, Dissanayake AJ, Monteiro JS, Grossart HP, Suija A, Weerakoon G, Etayo J, Tsurukau A, Kuhnert E, Vázquez V, Mungai P, Damm U, Li QR, Zhang H, Boonmee S, Lu YZ, Becerra AG, Kendrick B, Brearley FQ, Motiejūnaitė J, Sharma B, Khare R, Gaikwad S, Wijesundara DSA, Tang LZ, He MQ, Flakus A, Rodriguez-Flakus P, Zhurbenko MP, McKenzie EHC, Stadler M, Bhat DJ, Liu JK, Raza M, Jeewon R., Nassonova ES,

- Prieto M, Jayalal RGU, Yurkov A, Schnittler M, Shchepin ON, Novozhilov YK, Liu Pu, Cavender JC, Kang Y, Mohammad S, Zhang LF, Xu RF, Li YM, Dayarathne MC, Ekanayaka AH, Wen TC, Deng CY, Lateef AA, Pereira OL, Navathe S, Hawksworth DL, Fan XL, Dissanayake LS, Erdoğan M (2020) Outline of fungi and fungus-like taxa. *Mycosphere* 11: 1060–1456. <https://doi.org/10.5943/mycosphere/11/1/8>
- Xia JW, Ma YR, Li Z, Zhang XG (2017) *Acrodictys*-like wood decay fungi from southern China, with two new families Acrodictyceae and Junewangiaceae. *Scientific Reports* 7: 78–88. <https://doi.org/10.1038/s41598-017-08318-x>
- Yang J, Maharachchikumbura SSN, Hyde KD, Bhat DJ, McKenzie EH, Bahkali AH, Gareth Jones EB, Liu ZY (2015) *Aquapteridospora lignicola* gen. et sp. nov., a new hyphomycetous taxon (Sordariomycetes) from wood submerged in a freshwater stream. *Cryptogamie Mycologie* 36: 469–478. <https://doi.org/10.7872/crym/v36.iss4.2015.469>
- Yang J, Maharachchikumbura SSN, Liu JK, Hyde KD, Gareth Jones EB, Al-Sadi AM, Liu ZY (2018) *Pseudostanjehughesia aquitropica* gen. et sp. nov. and *Sporidesmium sensu lato* species from freshwater habitats. *Mycological Progress* 17: 591–616. <https://doi.org/10.1007/s11557-017-1339-4>
- Zhang H, Dong W, Hyde KD, Maharachchikumbura SS, Hongsanan S, Bhat DJ, Al-Sadi AM, Zhang D (2017) Towards a natural classification of *Annulatascaceae*-like taxa: introducing Atractosporales ord. nov. and six new families. *Fungal Diversity* 85: 75–110. <https://doi.org/10.1007/s13225-017-0387-z>
- Zhaxybayeva O, Gogarten JP (2002) Bootstrap, Bayesian probability and maximum likelihood mapping: exploring new tools for comparative genome analyses. *BMC Genomics* 3: 1–15. <https://doi.org/10.1186/1471-2164-3-4>
- Zhou DQ, Hyde KD, Wu XL (2001) New records of *Ellisembia*, *Penzigomyces*, *Sporidesmium* and *Repetophragma* species on bamboo from China. *Acta Botanica Yunnanica*. 1: 45–w51.

Three new *Russula* species in sect. *Ingratae* (Russulales, Basidiomycota) from southern China

Guo-Jie Li^{1*}, Shou-Mian Li^{1*}, Bart Buyck², Shi-Yi Zhao¹, Xue-Jiao Xie¹,
Lu-Yao Shi¹, Chun-Ying Deng³, Qing-Feng Meng⁴, Qi-Biao Sun⁵,
Jun-Qing Yan⁶, Jing Wang³, Ming Li¹

1 Key Laboratory of Vegetable Germplasm Innovation and Utilization of Hebei, Collaborative Innovation Center of Vegetable, College of Horticulture, Hebei Agricultural University, No 2596 South Lekai Rd, Lianchi District, Baoding 071001, Hebei Province, China **2** Institut de Systématique, Ecologie et Biodiversité (ISYEB), Muséum national d'Histoire naturelle, CNRS, Sorbonne Université, EPHE, 57 rue Cuvier, CP 39, 75005 Paris, France **3** Institute of Biology, Guizhou Academy of Sciences, No 1 Shanxi Rd, Yunyan District, Guiyang 550001, Guizhou Province, China **4** School of Public Health, Zunyi Medical University, No.201 Dalian Road, Huichuan District, Zunyi 563003, Guizhou Province, China **5** College of Pharmacy and Life Science, Jiujiang University, No 320 East Xunyang Rd, Xunyang District, Jiujiang 332000, Jiangxi Province, China **6** Jiangxi Fungal Resources Laboratory of Protection and Utilization, College of Bioscience and Bioengineering, Jiangxi Agricultural University, No1101 Zhimin Rd, Qingshanhu District, Nanchang 330045, Jiangxi Province, China

Corresponding authors: Chun-Ying Deng (171934233@qq.com), Ming Li (346399877@qq.com)

Academic editor: Alfredo Vizzini | Received May 2021 | Accepted 4 October 2021 | Published 8 November 2021

Citation: Li G-J, Li S-M, Buyck B, Zhao S-Y, Xie X-J, Shi L-Y, Deng C-Y, Meng Q-F, Sun Q-B, Yan J-Q, Wang J, Li M (2021) Three new *Russula* species in sect. *Ingratae* (Russulales, Basidiomycota) from southern China. MycoKeys 84: 103–139. <https://doi.org/10.3897/mycokeys.84.68750>

Abstract

Three new species of *Russula* section *Ingratae*, found in Guizhou and Jiangsu Provinces, southern China, are proposed: *R. straminella*, *R. subpectinatoides* and *R. succinea*. Photographs, line drawings and detailed morphological descriptions for these species are provided with comparisons against closely-related taxa. Phylogenetic analysis of the internal transcribed spacer (ITS) region supported the recognition of these specimens as new species. Additionally, *R. indocatillus* is reported for the first time from China and morphological and phylogenetic data are provided for the Chinese specimens.

Keywords

Agaricomycetes, ITS, morphology, phylogeny, Russulaceae, taxonomy

* These two authors contributed equally.

Introduction

Russula Pers. is a widespread genus that contains at least 2000, but possibly as many as 3000 species worldwide (Li et al. 2018; Adamčík et al. 2019; He et al. 2019). Members of this genus form symbiotic relationships with a diversity of plant species in broad-leaved and coniferous forests, scrubland and meadows. The brightly tinged pileus, abundant sphaerocytes responsible for the fragile gills and stipe, amyloid spore ornamentation, gleocystidia staining in sulpho-aldehydes, lack of clamp connections and absence of a ramifying lactifer system ending in pseudocystidia are the main morphological features of this genus (Li et al. 2015a; Buyck et al. 2018; Looney et al. 2018). Due to frequent convergence or extreme plasticity of morphological features, precise identification of *Russula* species is difficult and establishing accurate taxonomy is challenging (Miller and Buyck 2002; Bazzicalupo et al. 2017).

Russula sect. *Ingratae* Quél. is characterised by tawny, ochraceous or ashy-grey to dark brown pileus with tuberculate striate margin, acute to subacute equal lamellae, flesh with a distinct fetid, spermatic or waxy odour, or like bitter almonds, cream-coloured spore print, spores partly showing inamyloid reaction in the suprahilar area, small- to medium-sized unicellular pileocystidia and articulated and branched hyphal ends in the pileipellis (Shaffer 1972; Romagnesi 1985; Sarnari 1998). The combination of these characters makes this section one of the more easily distinguishable groups in the *Russula* subgenus *Heterophyllidiae* Romagn. Recent multi-locus phylogenetic studies indicated that this morphologically well-defined group corresponded to the earlier subsections, *Foetentinae*, *Pectinatinae* and *Subvelatae*, representing a natural, well-supported monophyletic clade in phylogenetic topology of the northern temperate region (Looney et al. 2016; Buyck et al. 2018). The other easily distinguishable groups of subgenus *Heterophyllidiae* include subsections *Amoeninae*, *Virescentinae* and *Substriatinae*. Phylogenetic analyses also indicated it is more difficult to match a field aspect with a single monophyletic lineage (Wang et al. 2019; Deng et al. 2020; Wisitrassameewong et al. 2020).

Compared with Europe (Romagnesi 1985; Sarnari 1998), detailed analyses of *Russula* sect. *Ingratae* in Asia began relatively late. In southern China, several species were previously misidentified, based on morphological characters, with European or North American names, such as *R. foetens* Pers., *R. grata* Britzelm. (= *R. laurocerasi* Melzer) and *R. pectinatoides* Peck (Song et al. 2007; Li 2014). Rapid progress has been made in the past two decades, resulting in 15 new *Russula* species in Asian *Ingratae*, based on modern phylogenetic methods: *R. abbotensis* K. Das & J.R. Sharma, *R. abmadii* Jabeen et al., *R. arunii* S. Paloi et al., *R. catillus* H. Lee et al., *R. dubdiana* K. Das et al., *R. foetentoides* Razaq et al., *R. gelatinosa* Y. Song & L.H. Qiu, *R. indocatillus* Ghosh et al., *R. natarajanii* K. Das et al., *R. obscuricolor* K. Das et al., *R. pseudocatillus* F. Yuan & Y. Song, *R. pseudopectinatoides* G.J. Li & H.A. Wen, *R. rufobasalis* Y. Song & L.H. Qiu, *R. subpunctipes* J. Song and *R. tsokae* K. Das et al. These new species were originally described from East Asia and the adjacent Himalayan area (Das et al. 2006, 2010, 2013, 2017; Razaq et al. 2014; Li et al. 2015b; Jabeen et al. 2017; Lee et al. 2017; Song et al. 2018, 2020; Ghosh et al. 2020). The initial sequence data have supported the valid

recognition of *R. punctipes* Singer and *R. senecis* Imai, but are still lacking for *R. guangdongensis* Z.S. Bi & T.H. Li and *R. periglypta* Berk & Broome (Lee et al. 2017; Song et al. 2018). Recent rDNA ITS phylogenetic analyses of *R. sect. Ingratae* in the Northern Hemisphere showed numerous unknown taxa and constant misidentifications of species in this group (Avis 2012; Melera et al. 2017; Park et al. 2017).

The importance of precise identification of *Russula* spp. in sect. *Ingratae* also comes from their economic value as several species are commonly sold as edible fungi in markets of southern China under the local name “You-la-gu (oily, acrid mushroom)”. Several species of *R. sect. Ingratae* may cause gastrointestinal problems if not properly pre-cooked (Dai et al. 2010; Bau et al. 2014; Chen et al. 2016). During recent years, several field investigations have been carried out on campuses and, in parks, natural reserves and wild mushroom markets of south-western China to unveil the species diversity of sect. *Ingratae* in this region. A number of *Russula* taxa have been discovered as new to science, based on morphological and molecular phylogenetic evidence, of which three members of *R. sect. Ingratae* are described and illustrated herein. Additionally, we report *R. indocatillus* as a new record for China.

Materials and methods

Morphological analyses

Specimens were collected in Guizhou, Jiangxi and Jiangsu Provinces from July to September in 2017 and 2018. The majority of the samplings are from Guizhou Province of south-western China. This mountainous Province lies in the eastern end of the Yungui Plateau. This region has a humid subtropical monsoon climate and is mostly covered by subtropical evergreen forests (Editorial Board of Vegetation in China 1980; Chen et al. 2020). Each of the specimens was collected from different patches of forest to avoid duplications from a single mycelium. Photographs of fresh basidiocarps were taken using a Canon Powershot G1 X Mark II digital camera in the field. Macroscopic characters were recorded at the same time under daylight. The colour codes and names from Ridgway (1912) were employed in descriptions. Specimen desiccation was accomplished in a Fruit FD-770C food dryer at a constant temperature of 65 °C over 12 h. Small tissue pieces of lamellae and pileipellis for microscopic observations were taken from dried specimens, sectioned by hand with a Dorco razor blade and rehydrated in 5% potassium hydroxide (KOH). Microscopical characters were observed using a Nikon Eclipse Ci-L photon microscope and Olympus BH2 with a drawing tube. Staining of basidiospores, mycelia and cystidia were performed by chemical reaction with Melzer’s Reagent and sulphovanillin (SV). Measurements and line drawings of basidiospores (exclusive of apiculus and spore ornamentation) and elements in hymenium, pileipellis and stipitipellis were executed from microphotographs taken at 1600× magnification with a Cossim U3CMOS14000 camera. A JSM-IT300 cold-field scanning electron microscope was used for examination of basidiospore ornamentation. At least 20 observation data were employed for each morphological character of every analysed collection. The format, $\alpha/\beta/\gamma$, represented the numbers of basidiospores,

basidiocarps and specimens that were measured microscopically. For those basidiospore dimensions, these were indicated as $(a-)$ $b-c$ $(-d)$, the extremes of the measured values (a and d) are displayed in brackets. The values of b and c are 5th and 95th percentiles when observed readings were arranged from small to large. Q is the ratio of basidiospore length to width. The Q in bold is the mean value of Q plus or minus standard deviation. The pileipellis was vertically sectioned at the edge and centre of the pileus. Shapes and sizes of basidia, cystidia and hypha were observed, measured and illustrated. For other details on microscopic observation and measurement, see Li (2014) and Adamčík et al. (2019). Exsiccatae of these new species are preserved in the Macrofungus Section, Mycological Herbarium of Guizhou Academy of Sciences (HGAS-MF), Herbarium of Hebei Agricultural University (HBAU) and Herbarium of Fungi, Jiangxi Agricultural University (HFJAU).

DNA extraction, polymerase chain reaction (PCR) and sequencing

Tissue samples from dried specimens were ground in centrifuge tubes using abrasive rods attached to an electric drill. DNA extractions were performed using a modified CTAB method as in Li (2014). PCR reactions were carried out in a Dragonlab TC1000-G 96-well thermocycler. Sequences in the ITS region were amplified with primers ITS5 and ITS4 (White et al. 1990) using the reaction conditions of Li et al. (2019). PCR products were separated by electrophoresis on 1.2% agarose gels and stained with Biotium GelRed. The concentrations of extracted DNA and PCR products were determined by a ThermoFisher Scientific NanoDrop One spectrophotometer. Nucleotide concentration > 50 ng/μl was used as the criterion of a qualified PCR product for Sanger sequencing by GENEWIZ Inc. An ABI 3730XL DNA analyser and an Applied Biosystems Sanger sequencing kit were used following manufacturer's procedures by Biomed Gene Technology Company (Beijing, China).

Phylogenetic analyses

Bidirectional sequencing results were assembled with MegAlign in DNASTar LaserGene 7.1 (<https://www.dnastar.com>). Low quality nucleotide sites at both ends of the sequences were trimmed. All new sequences from this study were deposited in GenBank (<http://www.ncbi.nlm.nih.gov/nucleotide/>). The BLAST algorithm was used to search the similar sequences and for the new species. Table 1 contains closely matched ITS sequences of the new species (percent identities over 97%) retrieved from GenBank and UNITE (<https://unite.ut.ee/>) databases. Sampling for the phylogenetic backbone of *Russula* section *Ingratae* referred to Melera et al. (2017), Park et al. (2017) and Song et al. (2018). These sequences were combined with those of the new species and aligned in Mafft 7.428 with L-INS-I strategy applied (Nakamura et al. 2018). Five sequences from species of the other sections of *Russula* subgenus *Heterophyllidiae*, *R. cyanoxantha* (Schaeff.) Fr., *R. grisea* Fr., *R. heterophylla* (Fr.) Fr., *R. ilicis* Romagn. and *R. substriata* J. Wang et al., were chosen as out-group. The matrix file was manually optimised using BioEdit 7.0.5 (Hall 1999) and deposited in TreeBASE repository with study ID S28207 (<http://purl.org/phylo/treebase/phyloWS/>

study/TB2:S28207?x-access-code=cda6b439c0eada24d5199bc264971fb5&format=html). Phylogenetic analyses were executed using Bayesian Inference (BI), Maximum Likelihood (ML) and Maximum Parsimony (MP) methods. Bayesian analysis was performed in MrBayes 3.2.7a (Ronquist et al. 2012). Best evolutionary model selection was carried out with MrModeltest 2.4 operated on PAUP* 4.0a165 through Akaike's Information Criteria (AIC) calculation (Nylander 2004). The calculation of posterior probabilities (PP) parameters was performed through the Markov chain Monte Carlo (MCMC) algorithm. The sampling frequency of the trees was set as every 100th generation. One cold and three hot Markov chains were run for 2×10^6 generations. The analysis ceased when the average standard deviation was maintained below 0.01. A percentage of 25% trees were discarded as burn-in before the construction of the 50% majority rule consensus tree. MP analysis was conducted in PAUP* 4.0a167 (Swofford 2004). The tree bisection-reconstruction (TBR) was carried out with a heuristic search. A total of 1000 replicates were set for bootstrap support (Felsenstein 1985). The setting of maxtrees was 5000. Branches collapsed when minimum length was zero. A Kishino-Hasegawa (KH) test (Kishino and Hasegawa 1989) was executed to determine whether trees were significantly different. The consistency index (CI), homoplasy index (HI), retention index (RI), rescaled consistency index (RC) and tree length (TL) were performed in MP analysis. ML analysis was performed in raxmlGUI 1.5b3 with 1000 replicates (Silvestro and Michalak 2012). Trees were displayed and exported in FigTree 1.4.4 (<http://tree.bio.ed.ac.uk/software/figtree/>). Names of species in Fig. 1 and Table 1 were cited from source databanks. Definitions for clades and complexes were also presented in Fig. 1.

Results

Phylogenetic analyses

A total of 112 ITS sequences (107 of sect. *Ingratae* and 5 of out-groups), including 13 newly-generated ones, were analysed in this study. The alignment for ITS phylogenetic analyses was composed of 543 characters including gaps. Of these characters in the matrix, 266 were variable, 201 were parsimony-informative, 65 variable characters were parsimony-uninformative. The parameters of MP analysis were CI 0.444, HI 0.784, RI 0.784, RC 0.348 and TL 869. The most suitable model for BI and MP analyses is GTR+I+G.

The resulting MP, ML and BI phylograms are consistent in topology of highly supported basal ranks (Clades A, B, C, D, E, F, H and I); thus, only the MP tree is presented in Fig. 1. A total of nine complexes and 24 species rank clades can be recognised with high support values. The 11 Chinese sequences were grouped in three clades that were further described as new species of *R. straminella*, *R. subpectinatoides* and *R. succinea*. High bootstraps and posterior probabilities supporting these clades are distinctly independent from those of other known taxa. Clades H, F and C in Fig. 1 generally corresponded with clades 1, 4 and 3 of Lee et al. (2017), in which species in Clade 2 are represented by Clades E and I in this study. The Indian and Chinese specimens of

Table 1. The species, specimens and GenBank accession numbers of ITS sequences analysed in this study.

Species	Specimen No.	Origin	GenBank accession	Reference
<i>Russula</i> aff. <i>pilosella</i>	MEL H4784	Australia: Tasmania	EU019932	Lebel and Tonkin (2007)
<i>R. abmadii</i>	LAH 35004	Pakistan: Khyber Pakhtunkhwa	KT834638	Jabeen et al. (2017)
	LAH 18081013	Pakistan: Khyber Pakhtunkhwa	KU535609	Jabeen et al. (2017)
	SB138	Pakistan	HG796943	Jabeen (2016)
<i>R. amerorecondita</i>	F PGA17-017	USA: Indiana	MN130066	Adamčík et al. (2019)
<i>R. ammophila</i>	MA-Fungi 51165	Spain: Huelva	AJ438038	Vidal et al. (2002)
<i>R. amoenolens</i>	TUB nl27.9.95.6	Germany	AF418615	Eberhardt (2002)
	MICH 12838	France	KF245510	–
<i>R. cf. amoenolens</i>	HMJAU37317	China: Heilongjiang	KY357332	Liu et al. (2017)
<i>R. aromatica</i>	PNW 5607	USA: Oregon	AY239331	–
<i>R. arunii</i>	CUH AM261	India: West Bengal	KY450661	Crous et al. (2017)
<i>R. brunneonigra</i>	DAR H5813	Australia: New South Wales	EU019945	Lebel and Tonkin (2007)
<i>R. catillus</i>	SFC 20120827-01	Korea: Daehak-dong	KK574686	Lee et al. (2017)
	SFC 20120919-35	Korea: Daehak-dong	KX574688	Lee et al. (2017)
	LHJ150915-19	China: Guangdong	MK860690	–
<i>R. cerolens</i>	OSC 76727	USA: Oregon	KF245505	–
	F 36	USA: California	JN681168	–
<i>R. cf. amoenolens</i>	MICH12838	France	KF245510	–
<i>R. cf. pulverulenta</i>	NYBG 4-1144IS79	USA	AY061736	Miller and Buyck (2002)
<i>R. cyanoxantha</i>	PC SM/BB 5	Europe	AY061669	Miller and Buyck (2002)
<i>R. echidna</i>	HO 593336	Australia: Tasmania	MN130079	Adamčík et al. (2019)
	HO 593337	Australia: Tasmania	MN130080	Adamčík et al. (2019)
<i>R. fluvialis</i>	KUO JR8666	Finland: Savonia Borealis	MN130084	Adamčík et al. (2019)
	KUO JR8313	Finland: Northern Savonia	MN130085	Adamčík et al. (2019)
	HMJAU 32234	China: Heilongjiang	KX095018	–
<i>R. foetens</i>	TUB hue124	Germany	AF418613	Eberhardt (2002)
	GENT FH-12-277	Germany: Keula	KT934016	Looney et al. (2016)
	HMJAU38004	China: Heilongjiang	KY681438	Liu et al. (2017)
<i>R. foetentoides</i>	LAH 04081023	Pakistan: Khyber Pakhtunkhwa	HE647707	Razaq et al. (2014)
	LAH 13081034	Pakistan: Khyber Pakhtunkhwa	HE647708	Razaq et al. (2014)
<i>R. foetentula</i>	156	USA: Tennessee	KJ834623	Melera et al. (2017)
	128	Switzerland	KJ834574	Melera et al. (2017)
<i>R. fragrantissima</i>	98	Italy	KJ530751	Melera et al. (2017)
	108	Italy	KJ834596	Melera et al. (2017)
<i>R. galbana</i>	BRIT13425	Australia: Queensland	EU019936	Lebel and Tonkin (2007)
<i>R. garyensis</i>	F PGA17-008	USA: Indiana	MN130088	Adamčík et al. (2019)
<i>R. gelatinosa</i>	K 16053119	China: Guangdong	MH168574	Song et al. (2018)
	K 15052626	China: Guangdong	MH168575	Song et al. (2018)
<i>R. granulata</i>	PC BB2004-226	USA: Tennessee	EU598192	–
	PC BB2004-225	USA: Tennessee	EU598190	–
	HMAS252604	China: Jilin	KF850414	Li (2014)
<i>R. grata</i>	E 00290534	UK: Scotland	KF245532	–
	TUB nl1348	Germany	AF418614	Eberhardt (2002)
	HMJAU38008	China: Heilongjiang	KY681444	Liu et al. (2017)
<i>R. grisea</i>	PC 2-1129IS75	Europe	AY061679	Miller and Buyck (2002)
<i>R. heterophylla</i>	PC 209RUF24	Europe	AY061681	Miller and Buyck (2002)
<i>R. hortensis</i>	IB 1997/0787	Italy	HG798528	–
<i>R. ilicis</i>	PC 563IC52	Europe	AY061682	Miller and Buyck (2002)
<i>R. illota</i>	MICH 73719	France	KF245509	–
	UE 26.07.2002-3	Sweden	DQ422024	Eberhardt (2002)
<i>R. inamoena</i>	107	Italy: Punta Chiappa	KJ834597	Melera et al. (2016)
	109	Italy: Punta Chiappa	KJ834595	Melera et al. (2016)
<i>R. indocatillus</i>	HGAS-MF 009917	China: Guizhou	MN649191	This study
	HGAS-MF 009903	China: Guizhou	MN649192	This study
<i>R. indocatillus</i>	AG 18-1653	India: Uttarakhand	MN581165	Ghosh et al. (2020)
<i>R. insignis</i>	HMAS 267740	China: Heilongjiang	KF850404	Li (2014)
	PC Buyck 00.2149	Europe	AY061700	Miller and Buyck (2002)
<i>R. mistiformis</i>	JC170305	Spain: Castilla-Leon	MK105677	Vidal et al. (2019)
	AMC H-69	Spain: Castilla-Leon	MK105680	Vidal et al. (2019)

Species	Specimen No.	Origin	GenBank accession	Reference
<i>R. mutabilis</i>	BHI-F384a	USA: Massachusetts	MF161239	Haelwaters et al. (2018)
	DPL 10654	USA: Texas	KF810137	–
<i>R. neerimea</i>	MEL2101871	Australia: Victoria	EU019915	Lebel and Tonkin (2007)
<i>R. nondistincta</i>	OSC 62139	USA: Oregon	KP859276	–
<i>R. obscuricolor</i>	KD 16-30	India: Sikkim	MF805816	Das et al. (2017)
	KD 16-22	India: Sikkim	MF805817	Das et al. (2017)
<i>R. oleifera</i>	TU 116011	Benin	UDB016936	–
	TU 102082	Zambia	UDB013811	–
<i>R. ombrophila</i>	86	Spain	KF971694	Melera et al. (2016)
<i>R. parksii</i>	Trappe 14997	USA	AY239335	–
<i>R. pectinata</i>	PC Buyck 2304	Europe	AY061706	Miller and Buyck (2002)
	2010BT02	Germany	KF318081	Melera et al. (2016)
	2010BT48	Germany	KF318082	Melera et al. (2016)
<i>R. pectinatoides</i>	MICH 52692	USA: Tennessee	KF245518	–
	HMAS251202	China: Yunnan	JX425405	Li (2014)
	NYS2303.1	USA: New York	KU640189	Melera et al. (2016)
<i>R. pila</i>	MA-Fungi 30667	Spain	AF230893	Calonge and Martín (2000)
<i>R. pilosella</i>	BRI-H5974	Australia: Queensland	EU019941	Lebel and Tonkin (2007)
<i>R. praetervisa</i>	UE 2006-11-12-01	Italy	UDB019333	–
	IB 1997-0812	Italy	UDB019331	–
<i>R. pseudocatillus</i>	GDGM 75338	China: Guangdong	MK049974	Yuan et al. (2019)
	K 15060706	China: Guangdong	MK049975	Yuan et al. (2019)
<i>R.</i>	HMAS 265020	China: Xizang	KM269079	Li et al. (2015b)
<i>pseudopectinatoides</i>	HMAS 251523	China: Xizang	KM269077	Li et al. (2015b)
<i>R. pulverulenta</i>	PC BB2004-245	USA: Tennessee	EU598186	–
<i>R. punctipes</i>	K 17052318	China: Guangdong	MH168576	Yuan et al. (2019)
	K 16051001	China: Guangdong	MH168577	Yuan et al. (2019)
<i>R. putida</i>	IB 1997/0791	Italy	HG798527	–
<i>R. recondita</i>	UPS AT2001049	Sweden	DQ422026	Eberhardt (2002)
	WGS 84	Switzerland	KJ530750	Melera et al. (2016)
	TU106223	Estonia: Saare maakond	UDB011156	–
<i>R. rufobasalis</i>	H15060622	China: Guangdong	MH168567	Song et al. (2018)
	H17052204	China: Guangdong	MH168570	Song et al. (2018)
<i>R. senecis</i>	SFC 20110921-18	Korea: Socho-myeon	KX574698	Lee et al. (2017)
<i>R. shafferi</i>	CUH AM102	India: West Bengal	KP142981	Khatua et al. (2015)
<i>R. similaris</i>	OSC 51046	USA: Washington	AY239327	–
<i>R. similis</i>	OSC 44426	USA: California	AY239329	–
	Trappe 7753	USA: Oregon	AY239349	–
<i>Russula</i> sp.	LHJ170913-01	China: Guangdong	MK860691	Song et al. (2020)
<i>R. straminella</i>	HGAS-MF 009920	China: Guizhou	MN649194	This study
	HGAS-MF 009922	China: Guizhou	MN649195	This study
	HGAS-MF 009925	China: Guizhou	MN649189	This study
<i>R. subfoetens</i>	HMJAU38006	China: Heilongjiang	KY681430	Liu et al. (2017)
	TU101908	Finland: Nilsia	UDB016206	–
<i>R. subfulva</i>	Trappe 14998	USA: Oregon	AY239321	–
<i>R.</i>	HBAU15023	China: Jiangsu	MW041163	This study
<i>subpectinatoides</i>	HBAU15024	China: Jiangsu	MW041164	This study
	HBAU15025	China: Jiangsu	MW041165	This study
	HBAU15026	China: Jiangsu	MW041166	This study
<i>R. subpunctipes</i>	RITF 2616	China: Guangdong	MK860692	Song et al. (2020)
	RITF 2617	China: Guangdong	MK860693	Song et al. (2020)
<i>R. substriata</i>	HKAS 102278	China: Yunnan	MH724921	Wang et al. (2019)
<i>R. succinea</i>	HGAS-MF 009909	China: Guizhou	MN649196	This study
	HGAS-MF 009904	China: Guizhou	MN649188	This study
	HGAS-MF 009906	China: Guizhou	MN649198	This study
	HGAS-MF 009915	China: Guizhou	MN649190	This study
<i>R. succinea</i>	HFJAU0301	China: Jiangxi	MN258682	–
<i>R. ventricosipes</i>	PC 0142480	USA	KY800364	Buyck et al. (2017)
<i>R.</i>	PDD 64246	New Zealand	GU222258	–
<i>vinaceocuticulata</i>				

Note: Species, specimens and GenBank accession numbers in bold are newly collected and sequenced in this study.

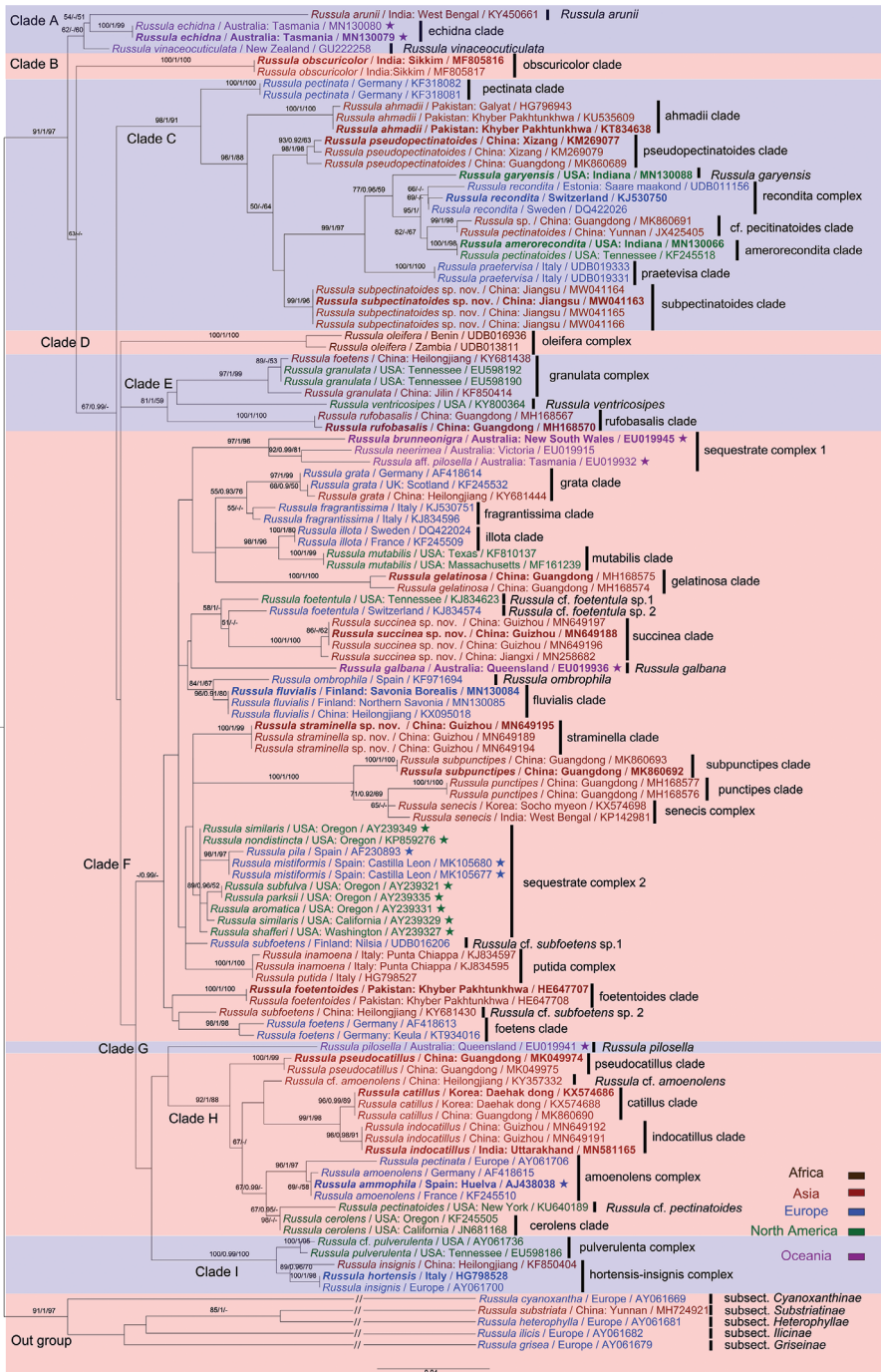


Figure 1. Phylogenetic tree generated from Bayesian analysis of ITS sequences. Main clades corresponding to subsections of sect. *Ingratae* are indicated in colour blocks. Holotypes of the new species are shown in bold. Values of posterior probabilities (PP) of MrBayes (≥ 0.9) and bootstraps of ML and MP analyses (≥ 50) are presented above the nodes as (MLBS/PP/MPBS).

R. indocatillus clustered together and formed a strongly supported, distinct clade (MLBS 96, PP 0.99, MPBS 89). The new species, *R. straminella*, formed an independent lineage in Clade F. The concrete phylogenetic status of *R. straminella* still remains unsolved in ITS sequence analyses. The new species *R. succinea* and two North American specimens were identified as *R. foetentula* with passable support (MPBS 58, PP 1). The new species, *R. subpectinatoides*, clustered with a majority of members from clade C and formed a highly supported clade (MLBS 96, PP 1, MPBS 88). The close relationship with *R. pseudopectinatoides* indicated in similarity searching was not supported in phylogenetic topologies.

The DNA sequence similarity search results for the ITS1–5.8S–ITS2 region of the new species are as follows: two North American specimens of gasteroid *R. similis* Trappe & T.F. Elliott (AY239349 and KC152107) had the highest sequence identity (98.2%) to the new species *R. straminella*, then *R. nondistincta* Trappe & Castellano (KP859276) (98.1%); *R. pseudopectinatoides* (KM269079) had the highest sequence similarity (98%) to the new species *R. subpectinatoides*, then *R. praetervisa* Sarnari (95%); *R. foetentula* Peck (KJ834623) had the highest sequence identity (96.9%) to the new species *R. succinea*, then *R. subfoetens* W.G. Sm. (UDB016206) (94%). The Chinese collections of *R. indocatillus* had sequence identities of 99% to its type specimens (MN581483 and MN581165) from India.

Taxonomy

***Russula indocatillus* A. Ghosh, K. Das & R.P. Bhatt, Nova Hedwigia 111(1–2): 124. 2020.**

Figs 2a, 3a, 4 and 5.

Basidiomata small to medium sized. Pileus 35–46 mm in diam., hemispherical when young, then plano-convex to applanate, depressed at centre when mature, rarely infundibuliform, viscid when wet, brownish tinged, intermixed with greyish-yellow fringe, Verona Brown (XXIX13"k), Chocolate (XXVIII7"m), to Cinnamon Brown (XV15"l) at centre, sometimes with a tinge of Argus Brown (III13m) or Brussels Brown (III15m), Pecan Brown (XXVIII13"i) or Hazel (XIV11"l) when old and dry; margin acute, slightly incurved first, straight when mature, slightly undulate, often cracked, tuberculate-striate 10–15 mm from the edge inwards, peeling 1/5–1/4 towards the centre, Ochraceous Tawny (XV15'i), Mikado Brown (XXIX13"i) or Tawny Olive (XXIX17"i) when young, often Avellaneous (XL17"b), Cinnamon (XXXI15") to Clay Colour (XXIX17") when mature. *Lamellae* adnate, rarely sub-free, 2–5 mm in height at mid-radius of pileus, fragile, rarely forked near the stipe, interveined, pale cream tinged, White (LIII) when young, Cream Colour (XVI19'f) in age, often stained yellowish to brownish with Buckthorn Brown (XV17'i) to Yellow Ochre (XV17); edge even, narrowing towards the pileus margin, 9–16 per cm near the pileus margin; lamellulae rare. *Stipe* subcentral to central, 2.5–4.7 × 1–1.4 cm, cylindrical to subclavate, rarely tapered towards the base, annulus absent, first smooth, then often longitudinally rugulose in age, White (LIII), rarely stained with brownish tinge of

Aniline Yellow (IV19i) to Honey Yellow (XXX19"), first stuffed, hollow when mature. *Context* 2–4 mm thick at the centre of pileus, initially White (LIII), Light Ochraceous-Salmon (XV13'd) to Primuline Yellow (XVI19') when mature, unchanging or slowly turning Ochraceous-Tawny (XV15') to Buckthorn Brown (XV17'i) when injured or touched, brittle; taste mild, rarely slightly acrid when young; odour indistinct. *Spore print* cream-coloured (Romagnesi IIc–IIId).

Basidiospores [200/8/4] (4.9–) 5.3–6.8 (–7.3) × (4.7–) 5.0–5.9 (–6.3) μm, $Q = (1.01–) 1.05–1.28 (–1.33)$ ($Q = 1.18 \pm 0.08$), 6.1 × 5.5 μm in average, subglobose to broad ellipsoid, ornamentation composed of conical to verrucous amyloid warts of very different sizes, mostly isolated, rarely linked as short ridges or with occasional line connections, not reticulate, warts 0.7–1 μm in height; suprahilar spot inamyloid and indistinct. Basidia 27–39 × 8–9 μm, hyaline in KOH, clavate to subclavate, four-spored, projecting 15–20 μm beyond the hymenium; sterigmata 3–6 μm, pointed, often straight, slightly tortuous towards the tip. Hymenial cystidia rare, less than 200/mm², 56–70 × 6–9 μm, fusiform to subclavate, rarely subcylindrical, thin-walled, projecting 20–40 μm beyond the hymenium, apex often mucronate, contents sparse, unevenly distributed, granular, greyish in SV. Pileipellis two layered, composed of suprapellis (80–150 μm thick) and subpellis (100–150 μm thick). Suprapellis an ixotrichoderm at pileus centre, composed of oblique to erect, septate, hyaline hyphae; acid-resistant encrustations absent, terminal cells cylindrical to subcylindrical, apex obtuse, rarely mucronate, mostly 40–70 μm in length; pileus margin a trichoderm composed of repent to tilted elements, terminal cells mostly 7–20 (–25) μm in length, ampullaceous, ellipsoid or cylindrical, obtuse to mucronate at apex, longer terminal cells similar to those in pileus centre also present; subapical cells contain islands of more or less inflated, 2–4 septate cells. Pileocystidia present in suprapellis and subpellis, abundant at pileus centre, dispersed at margin, one-celled, subulate, lageniform, fusiform, cylindrical, rarely appendiculate, 4–6 μm in width, many in suprapellis 15–25 μm in length, others up to 60 μm, even reaching a length of 100 μm in subpellis, apex mucronate, acicular to lanceolate in suprapellis, obtuse in subpellis, contents granulate, sparse, greyish in SV. Subpellis composed of repent to irregularly interlaced, inflated, septate hyphae 3–5 μm wide. Clamp connections absent in all tissues.

Specimens examined. China, Guizhou Province, Weining Yi, Hui, and Miao Autonomous County, Caohai National Nature Reserve, 26°53'N, 104°12'E, alt. 2171 m, on the ground in coniferous forest, 9 September 2017, C.Y. Deng A (HGAS-MF 009903); *ibid.*, alt. 1987 m, C.Y. Deng dcy2306 (HGAS-MF 009918); *ibid.*, alt. 2053 m, C.Y. Deng dcy2303 (HGAS-MF 009911); *ibid.*, alt. 2106 m, C.Y. Deng CH2017090971 (HGAS-MF 009917).

Habit and habitat. Single to scattered on yellow brown soil in coniferous forest dominated by *Pinus armandii* and *P. yunnanensis* at 1900–2200 m altitude.

Distribution. China (Guizhou) and India (Uttarakhand).

Notes. The Chinese collections fit well with the original description of Ghosh et al. (2020), except for a few differences. The Indian specimens have longer basidia, 35–60 × 9–11 μm. The original description of *R. indocatilus* also noted that the type

specimen was collected in a temperate mixed forest with *Myrica*, *Quercus* and *Rhododendron*. The coniferous tree species in this habitat were not mentioned. The Chinese collection is from a subalpine coniferous forest of subtropical region dominated by *Pinus* spp. with the main undergrowth species of *Berberis cavaleriei*, *Corylus yunnanensis*, *Elaeagnus umbellata* and *Rosa sweginzowii* (He et al. 2019).

Amongst the closely-related species in Clade H, *R. amoenolens* Romagn. and *R. cerolens* Shaffer have a strongly acrid taste, disagreeable sub-spermatocystidial odour, basidiospore length up to 9 μm and longer hymenial cystidia up to 100 μm (Shaffer 1972; Romagnesi 1985; Sarnari 1998); *R. catillus* lacks lamellulae, has longer basidia 42–49 \times 9.3–11.7 μm , shorter pileipellis terminal cells 41–72 \times 3–7 μm and lacks pileocystidia (Lee et al. 2017); *R. pseudocatillus* has larger basidiospores 7–9.2 \times 5.1–6.7 μm with higher ornamentation (up to 1.2 μm) which is never reticulate (Yuan et al. 2019).

Some members of *R. sect. Ingratae*, which were originally described from Himalayan Mountains and adjacent south-western China, may be confused with *R. indocatillus* in the field. Their main morphological differences are as follows: *R. abbotensis* has a crustose to areolate pileus with purplish-red to reddish-brown tinges, an ixotrichoderm pileipellis with pileocystidia 5 μm in width and an occurring in ectomycorrhizal association with *Quercus* spp. (Das and Sharma 2005); *R. arunii* can be distinguished by its fishy odour, amyloid suprahilar spot, 3–4 μm wide pileocystidia, mostly with a capitate apex and habitat in a tropical rain forest of *Pterygota alata* (Crous et al. 2017); *R. ahmadii* has larger basidiospores (5.6–) 6.1–9.2 (–9.4) \times (5–) 5.1–6 (–6.5) μm with low (up to 0.3 μm high), partly reticulated ornamentation and cutis type of pileipellis (Jabeen et al. 2017); *R. foetentoides* can be distinguished from *R. indocatillus* by its smooth pileus margin, absence of lamellulae and its basidiospore ornamentation of 1.7–2 μm in height (Razaq et al. 2014); *R. natarajanii* differs in having larger basidiospores, 6.8–8.8 \times 5.8–7.1 μm and longer hymenial cystidia, 60–90 \times 6–10.5 μm (Das et al. 2006); *R. pseudopectinatoides* has larger basidiospores (6–) 6.5–9 (–9.5) \times (5–) 5.1–6 (–6.5) μm with partly reticulate ornamentation, longer hymenial cystidia up to 90 μm and terminal cells of suprapellis hyphae often with obtuse to ventricose apex (Li et al. 2015b); *R. succinea* differs in larger basidiospores with incompletely reticulated ornamentations, longer basidia and pileocystidia up to 10 μm in width (Figs 10 and 11); *R. tsokae* can be distinguished from *R. indocatillus* by its larger basidiomata 8–13 cm in diam., yellowish-orange tinged stipe and larger basidiospores 6.8–8.8 \times 5.8–7.1 μm with reticulated ornamentation up to 2 μm high (Das et al. 2010).

***Russula straminella* G.J. Li & C.Y. Deng, sp. nov.**

Figs 2b, 3b, 6 and 7.

Fungal Names: FN 570758

Etymology. referring to the yellowish tinged pileus

Holotype. China, Guizhou Province, Guiyang City, Yunyan District, Guizhou Botany Garden, 26°37'N, 106°43'E, alt. 1107 m, on the ground in coniferous forest,



Figure 2. Basidiomata **A** *Russula indocattillus* **B** *R. straminella* **C–D** *R. subpectinatoides* **E–F** *R. succinea*. Bars: 10 mm.

8 July 2017, C.Y. Deng 2017–209 (HGAS-MF 009922, **Holotype**). GenBank accession: MN649195 (ITS).

Diagnosis. This species is characterized by the yellow, brownish-yellow to brown pileus, tuberculate-striate margin, adnate lamellae tinged ochraceous when bruised, rare lamellulae, white stipe turning brownish-yellow when injured, mild to rarely acrid context, cream spore print, globose, subglobose to broad ellipsoid basidiospores (5.4–) 5.8–7.1 (–7.6) × (4.7–) 5.1–6.5 μm, 6.4 × 5.6 μm on average, with verrucous to conical, partly reticulate ornamentations 0.7–1 μm in height, subclavate to clavate basidia 33–40 × 9–11 μm, clavate to subclavate hymenial cystidia 56–70 × 8–10 μm, a suprapellis composed of two layers, a trichoepithelium at pileus centre and an ixotrichoderm towards the margin, pileocystidia abundant at pileus centre, but sparse in margin, a cutis type of subpellis and habitat on the ground in coniferous forests.

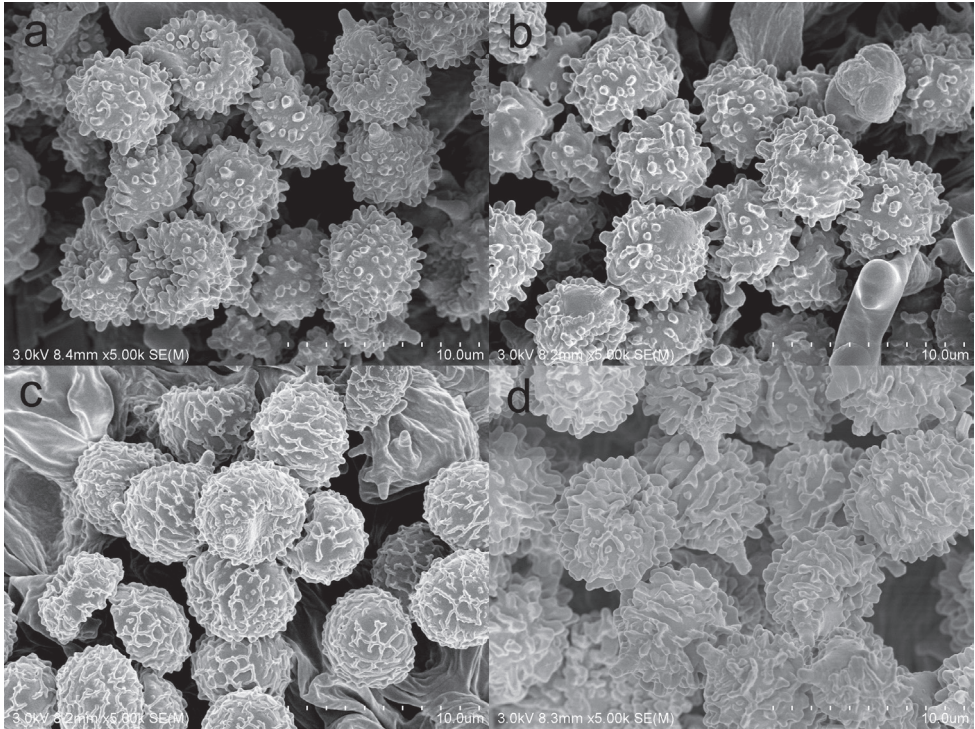


Figure 3. SEM photo of basidiospores **A** *Russula indocatillus* **B** *R. straminella* **C** *R. subpectinatoides* **D** *R. succinea*.

Description. *Basidiomata* small to medium sized. Pileus 33–57 mm in diam., initially flat to hemispherical, then plano-convex to applanate, finally often concave at centre, gelatinised, yellowish to brownish-yellow tinged, intermixed with brownish fringe, Argus Brown (III13m), Warm Sepia (XXIX13"m), to Verona Brown (XXIX13"k) at centre, rarely with a paler tinge of Mikado Brown (XXIX13"i), Rood's Brown (XXVIII11"k) to Cacao Brown (XXVIII9"i); margin acute to subacute, enrolled when young, often undulate, sometimes cracked when mature, tuberculate-striate 8–15 mm from the edge inwards, peeling 1/5–1/4 towards the centre, first Aniline Yellow (IV19i), Sayal Brown (XXIX15") to Cinnamon Buff (XXIX15"d), finally Mikado Brown (XXIX13"i), Snuff Brown (XXIX15"k) to Clay Colour (XXIX17"). *Lamel-lae* adnate, fragile, occasionally forked near the stipe and pileus margin, interveined, first White (LIII), then of Cream Colour (XVI19'f) when mature, often having an ochraceous tinge of Olive Ochre (XXX21"), Isabella Colour (XXX19"i) to Honey Yellow (XXX19") when bruised, taste mild to slightly acrid; edge even, narrowing towards the pileus edge, 8–16 pieces per cm in the edge; lamellulae rare. *Stipe* central, 3.5–6.5 × 1–1.5 cm, cylindrical, slightly tapering towards the base, annulus absent, first smooth, slightly longitudinally rugulose when mature, White (LIII) when young, turning a pale brownish-yellow tinge of Kaiser Brown (XIV9'k), Aniline Yellow (IV19i)

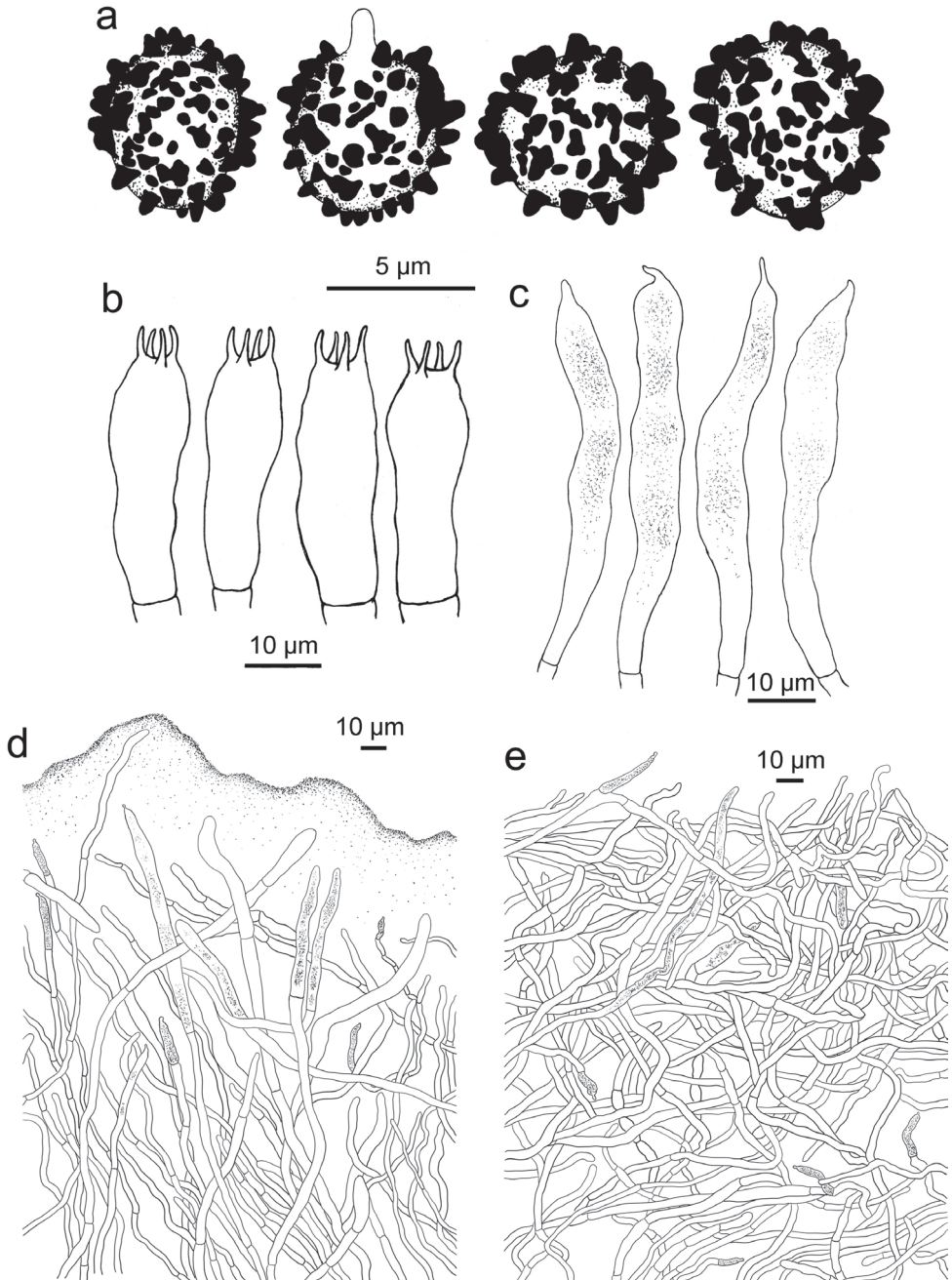


Figure 4. *Russula indocatillus*, holotype **A** basidiospores **B** basidia **C** hymenial cystidia **D** suprapellis in pileus centre **E** suprapellis in pileus margin.

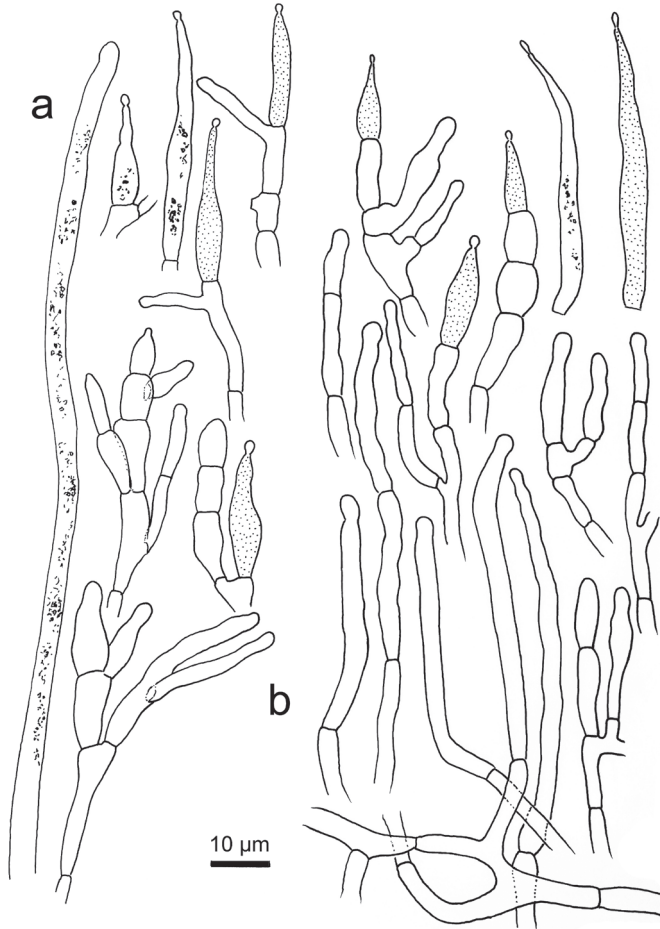


Figure 5. *Russula indocatillus*, holotype **A** hyphal extremities in pileipellis margin **B** hyphal extremities in pileus centre.

to Buckthorn Brown (XV17'i) after bruising, initially stuffed, fistulous to hollow when mature. *Context* White first, slowly turning a pale ochraceous tinged of Yellow Ochre (XV17') to Ochraceous-Buff (XV15'b) when injured, 2–4 mm thick at the centre of pileus, compact; taste mild, rarely slightly acrid, with no distinct odour. *Spore print* cream coloured (Romagnesi IIc–II d).

Basidiospores [150/6/3] (5.4–) 5.8–7.1 (–7.6) × (4.7–) 5.1–6.5 µm, $Q = (1.00–) 1.03–1.28 (–1.31)$ ($Q = 1.15 \pm 0.07$), 6.4 × 5.6 µm in average, globose, subglobose to broadly ellipsoid, rarely ellipsoid, ornamentation amyloid, composed of verrucous to conical warts 0.7–1 µm in height, often linked by fine lines as short ridges, partly reticulate, rarely isolated; suprahilar area inamyloid, but distinct. *Basidia* 33–40 ×

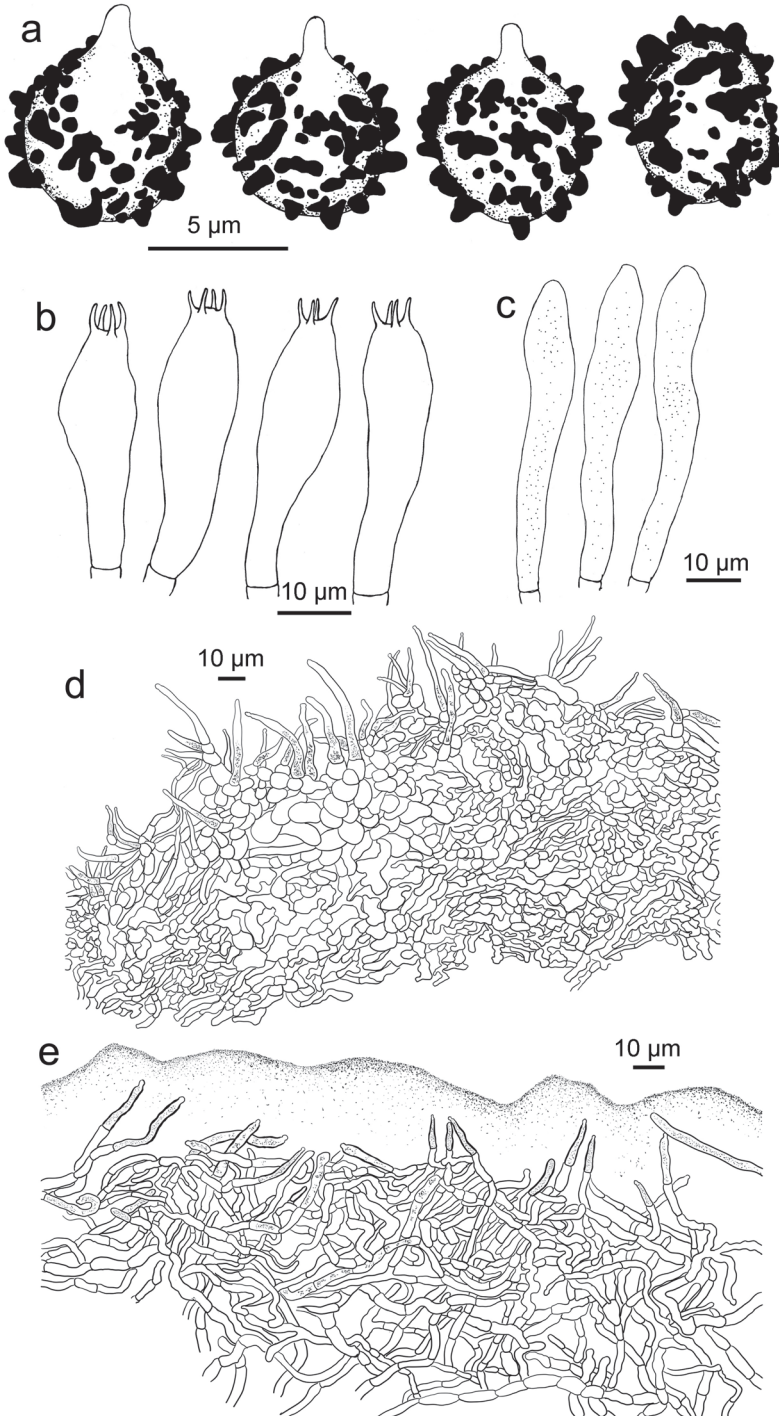


Figure 6. *Russula straminella*, holotype **A** basidiospores **B** basidia **C** hymental cystidia **D** suprapellis and partial subpellis in pileus centre **E** suprapellis in pileus margin.

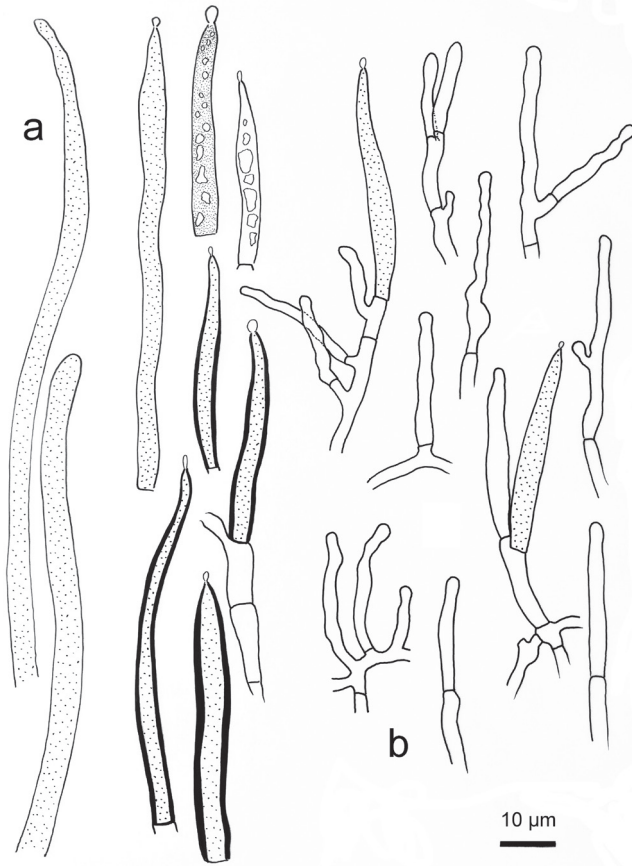


Figure 7. *Russula straminella*, holotype **A** hyphal ends in pileipellis margin **B** hyphal ends in pileus centre.

9–11 μm , hyaline, often yellowish in KOH, subclavate to clavate, sometimes cylindrical, mostly with four sterigmata 4–7 μm long. *Hymenial cystidia* rare, less than 500/mm², 56–70 \times 8–10 μm , clavate to subclavate, rarely subfusiform, projecting 20–40 μm beyond hymenium, apex rounded, contents sparse, granular, evenly distributed, pale greyish in SV. *Pileipellis* two-layered, clearly distinguished from the subjacent sphaerocytes. *Suprapellis* 70–130 μm thick, acid-resistant encrustations absent, a trichoepithelium at pileus centre, partly an ixo-trichoepithelium, composed of erect to suberect hyphae, terminal cells cylindrical, 20–40 \times 3–5 μm , obtuse at apex, partly ventricose, subapical cells sometimes inflated, rarely branched, 15–25 \times 8–12 μm , an ixotrichoderm at pileus margin, composed of erect to ascending, rarely repent hyphae, terminal cells 30–55 \times 3–5 μm , cylindrical, often thick-walled, tapered to mucronate at apex. *Pileocystidia* abundant, often fasciculate at pileus centre, narrowly lanceolate to bayonet-shaped, 30–60 \times 5–8 μm , one-celled, contents granular, blackish-grey in SV. *Pileocystidia* sparse at the pileus margin, cylindrical, 4–8 μm in width, slightly tapered at apex, contents grey in SV. *Subpellis* composed of

loosely interwoven, mostly repent, septate hyphae often inflated, 3–8 μm in width. *Clamp connections* absent in all tissues.

Additional specimens examined. China, Guizhou Province, Guiyang City, Yunyan District, Guizhou Botany Garden, 26°37'N, 106°43'E, alt. 1074 m, on the ground in coniferous forest, 8 July 2017, C.Y. Deng dcy2305 (HGAS-MF 009920, paratype); *ibid.*, alt. 1385 m, C.Y. Deng dcy2302 (HGAS-MF 009925, paratype).

Habit and habitat. Single to scattered on yellow brown soil in coniferous forest dominated by *Pinus armandii* and *P. massoniana* at 1100–1400 m altitude.

Distribution. China (Guizhou).

Notes. This new species can be distinguished from members of *R.* sect. *Ingratae* described from China and the Himalayan region as follows: *Russula gelatinosa*, *R. guangdongensis* Z.S. Bi & T.H. Li, *R. punctipes*, *R. senecis*, *R. subpunctipes* and *R. tsokae* have basidiospore ornamentation composed of high wings (often above 2 μm), ranging over long distances or even encircling (Bi and Li 1986; Song et al. 2018, 2020). The Asian species of *R.* sect. *Ingratae*, *R. ahmadii*, *R. natarajanii* and *R. pseudopectinatoides* have basidiospore ornamentation lower than 0.7 μm (Das et al. 2006; Li et al. 2015b; Jabeen et al. 2017). For species that have similar basidiospore ornamentation, *R. abbotensis* has reddish-brown to purplish-red tinges on pileus surface, pruinose to scurfy stipe at base, larger basidiospores, 8–10 \times 7.3–8.5 μm and hymenial cystidia with mucronate apices (Das and Sharma 2005); *R. arunii* has pileus turning light orange to greyish-orange when old, context having a fishy odour and narrow pileocystidia 3–4 μm in width (Crous et al. 2017); *R. indocatillus* has hymenial cystidia with mucronate, capitate, moniliform, rostrate or appendiculate apex with cylindrical or slightly inflated subapical cells (Ghosh et al. 2020); *R. obscuricolor* has a pale yellowish-white tinge in pileus margin, pungent and bitterish context, narrow pileocystidia 3–5 μm in width (Das et al. 2017); *R. pseudoocatillus* has greyish-brown pileus centre, towards the margin very pale yellow, larger basidiospores, 7–9 μm in diam. and narrower pileocystidia (3–6 μm in width) unchanging in SV (Yuan et al. 2019); *R. rufobasalis* has reddish stipe base, mucronate or appendiculate apex of hymenial cystidia and thick-walled terminal cells (Song et al. 2018).

***Russula subpectinatoides* G.J. Li & Q.B. Sun, sp. nov.**

Figs 2c, 2d, 3c, 8 and 9.

Fungal Names: FN 570759

Etymology. named for its morphological resemblance to *R. pectinatoides* Peck.

Holotype. China, Jiangsu Province, Nanjing City, Qixia District, Nanjing Normal University, 32°06'N, 118°54'E, alt. 84 m, on the ground in coniferous forest, 28 August 2018, Q.B. Sun 2018001 (HBAU15030, **Holotype**). GenBank accession: MW1041163 (ITS).

Diagnosis. This species is characterised by the greyish-brown to brownish-yellow pileus, striate margin, adnate to subadnate lamellae rarely staining reddish-brown when bruised, infrequent lamellulae, context slowly turning pale ochre after injury and

slightly to moderately acrid taste, cream spore print, subglobose to broadly ellipsoid basidiospores (5.3–) 5.6–6.3–7 (–7.3) × (4.1–) 4.6–5.2–6 (–6.3) μm, ornamentation 0.3–0.5 μm in height, composed of long ridges forming an incomplete to complete reticulum, fusiform to subclavate, basidia 27–50 × 8–12 μm, fusiform to subclavate hymenial cystidia 56–73 × 6–12 μm, pileipellis with one-celled, slender, mucronate, conical, needle-shaped to cylindrical pileocystidia, 5–7 μm in width; and habitat in coniferous forest.

Description. *Basidiomata* small to medium-sized. *Pileus* 18–95 mm in diam., initially hemispherical, concave at centre, turning appanate with age, often depressed at stipe, slightly viscous when young or humid, greyish-brown to brownish-yellow tinged, intermixed with dark brown fringe, Buffy Citrine (XVI19'k) to Light Brownish Olive (XXX19'k) at centre, Citrine-Drab (XL19''i), Drab (XLVI17''m) to Benzo Brown (XLVI13''i) when mature, often turning Buffy Olive (XXX21'k) to Saccardo's Olive (XVI19'm) when old and dry; margin acute to subacute, involute when young, straight with maturity, sometimes dehiscent, undulate to curled-up when old, striate 1/4–1/3 towards the centre, not or rarely weakly tuberculate, peeling 1/5–1/3 towards the centre, rarely flaking in small patches, with an ochre tinge of Old Gold (XVI19'i), Olive Ochre (XXX21'') to Tawny-Olive (XXIX17''i). *Lamellae* adnate to subadnate, 3–6 mm in height at the midpoint, sometimes forked near the stipe and the pileus edge, interveined, white to pale cream, White (LIII) when young, Light Buff (XV17'f) to Cream Colour (XVI19'f) with age, rarely stained reddish-brown tinge of Buckthorn Brown (XV17'i) when bruised, taste slightly to moderately acrid; edge even, constricted towards the margin, 9–19 pieces per cm at the edge; lamellulae infrequent. *Stipe* central to subcentral, 2.4–9.3 × 1.3–2.7 cm, slightly narrowing towards the base and apex, smooth at first, longitudinally slightly rugulose when mature, White (LIII) first, sometimes faintly stained with Honey Yellow (XXX19'') to Olive Ochre (XXX21'') when bruised, stuffed first, fistulous to hollow when old. Context 2–5 mm thick above the stipe, initially White (LIII), unchanging or slowly turning pale ochre tinge of Cinnamon Buff (XXIX15'd) when bruised, pale greyish-yellow tinge of Cartridge Buff (XXX19'f) at base when old, taste slightly to moderately acrid, with no distinct odour. Spore print cream coloured (Romagnesi IIc–IIId).

Basidiospores [250/10/5] (5.3–) 5.6–7 (–7.3) × (4.1–) 4.6–6 (–6.3) μm, $Q = (1.02–) 1.05–1.31 (–1.37)$ ($Q = 1.19 \pm 0.09$), 6.3 × 5.2 μm in average, mostly subglobose to broadly ellipsoid, rarely globose and ellipsoid, ornamentation amyloid, composed of long ridges forming an incomplete to complete reticulum, rarely intermixed with an isolated conical to verrucous warts and short crests, 0.3–0.5 μm in height; suprahilar spot inamyloid and indistinct. *Basidia* 27–50 × 8–12 μm, hyaline in KOH, subcylindrical to subclavate, rarely clavate or subfusiform, inflated towards the upper end or mid-piece, 4-spored, projecting 15–30 μm beyond hymenium; sterigmata 3–6 μm, slightly tortuous, sometimes straight. *Hymenial cystidia* sparsely distributed, fewer than 200/mm², 56–73 × 6–12 μm, fusiform to subclavate, projecting 20–40 μm beyond the hymenium, contents granular, sparsely distributed, slightly greyish in SV; apex subacute, rarely obtuse; lamellar edge sterile. *Pileipellis* two layered, composed of suprapellis (80–140 μm thick) and subpellis (100–150 μm thick). Suprapellis an ixotrichoderm,

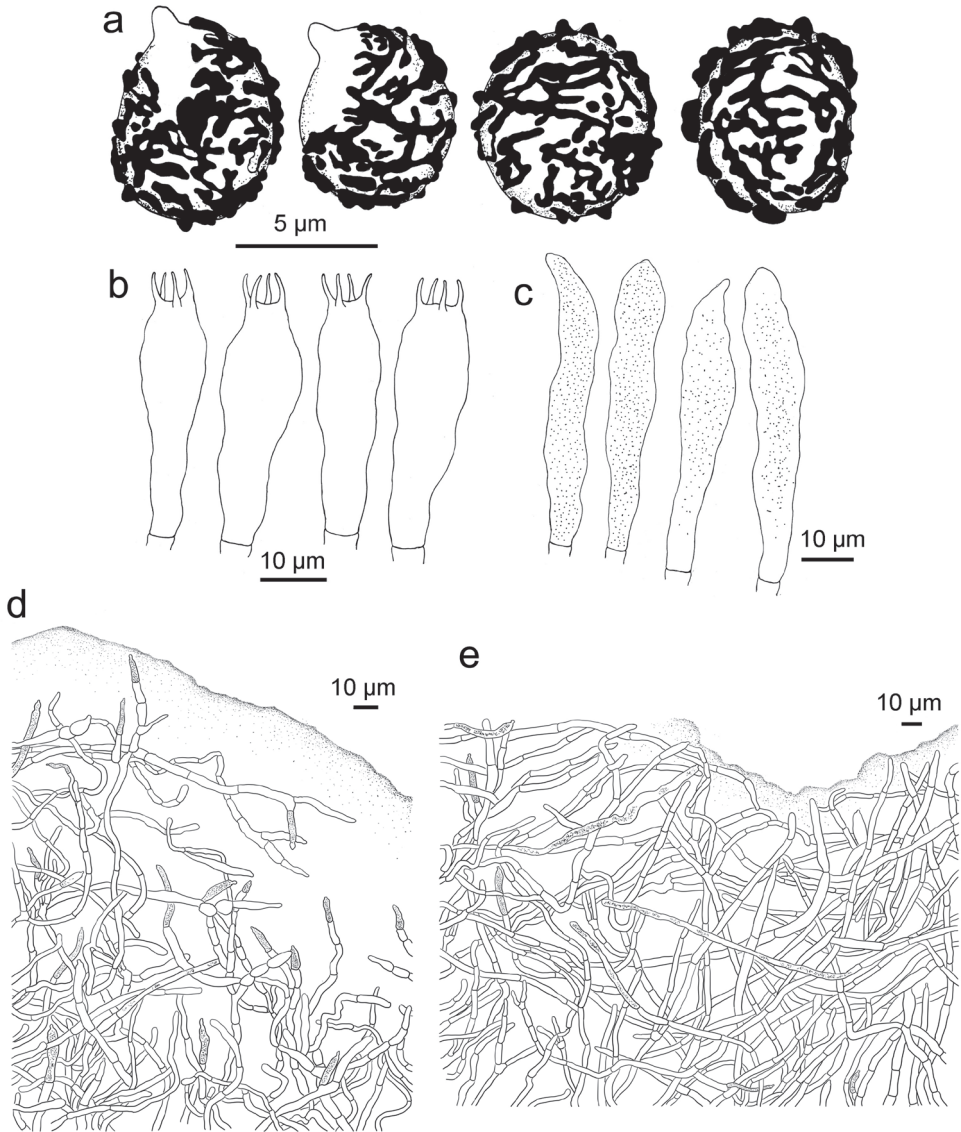


Figure 8. *Russula subpectinatoides*, holotype **A** basidiospores **B** basidia **C** hymenial cystidia **D** suprapellis in pileus centre **E** suprapellis in pileus margin.

composed of gelatinised, ascending to vertical, septate hyphae, acid-resistant encrustations absent, terminal cells mostly lanceolate to bayonet-shaped at pileus centre, mostly tapered at apex, rarely cylindrical, $20\text{--}30 \times 4\text{--}7 \mu\text{m}$, subapical cells sometimes inflated, barrel-shaped, ellipsoid or almost subglobose to globose; when compared with suprapellis at pileus centre, its margin is also an ixotrichoderm, but contains more repeat elements, $3\text{--}5 \mu\text{m}$ in width, inflated hyphal cells not observed, lateral short ramifications frequent; pileocystidia long, cylindrical, non-septate, $3\text{--}5 \mu\text{m}$ in width,

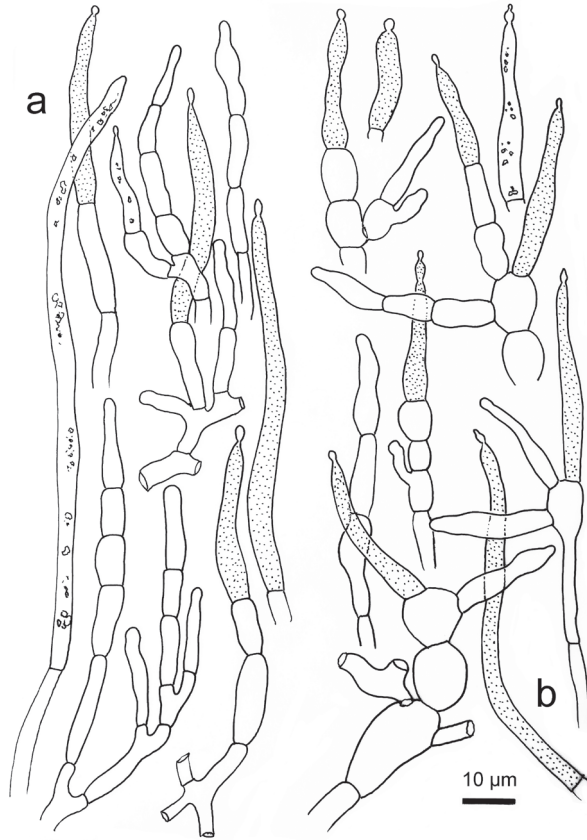


Figure 9. *Russula subpectinatoides*, holotype **A** hyphal extremities in pileipellis margin **B** hyphal extremities in pileus centre.

apex mucronate, contents granulate, sparse, pale grey in SV. Subpellis *a* composed of cylindrical, sometimes inflated, septate, loosely intricate, gelatinous, hyaline hyphae 3–6 µm in width. *Clamp connections* absent in all parts.

Additional specimens examined. China, Jiangsu Province, Nanjing City, Qixia District, Nanjing Normal University, 32°06'N, 118°54'E, alt. 84 m, on the ground in coniferous forest, 28 August 2018, Q.B. Sun 2018002 (HBAU15031, paratype); *ibid*, 2018003 (HBAU15032, paratype); *ibid*, 2018004 (HBAU15033, paratype).

Habit and habitat. Single to scattered on yellow brown soil in coniferous forest of subtropical monsoon climate zone dominated by *Cedrus deodara*, *Pinus parviflora* and *P. thunbergii*.

Distribution. China (Jiangsu).

Notes. This new species is similar to *R. pseudopectinatoides* in its brownish-yellow pileus, slightly acrid taste, cream spore print, spores with low, subreticulate ornamentation and gelatinous pileipellis. It is notable that basidiomata of *R. subpectinatoides* were collected from a forest of introduced coniferous tree species. *Cedrus deodara* is native in the western Himalayas, while *Pinus parviflora* and *P. thunbergii* are naturally distrib-

uted in the Japanese archipelago and Korean peninsula. Therefore, this new taxon may also occur in these introduced areas with its accompanying trees.

The Asian species of sect. *Ingratae* already recognizable by their long slender stipe, such as *R. gelatinosa*, *R. guangdongensis*, *R. punctipes*, *R. senecis*, *R. subpunctipes* and *R. tsokae* and cannot be confused with our new species, even more so because they have basidiospores composed of long wings, 2 µm high or more (Song et al. 2018, 2020). A similarly-winged spore ornamentation also differentiates species of the *R. grata* lineage which, moreover, usually have a distinct bitter almond smell. The more golden yellow pileus of species in the *R. foetens* or *R. subfoetens* lineages also avoids confusion with our new species and because many of these are distinctly very acrid. The strong yellowish stipe base that turns immediately red with KOH easily allows one to distinguish the few species of the *R. insignis* lineage. In the *R. granulata* lineage, the Asian species *R. rufobasalis* has reddish tinged stipe base, pleurocystidia with mucronate or appendiculate apices and longer terminal cells, up to 60 µm (Song et al. 2018). Finally, the typically very acrid taste allows us to eliminate most species of the *R. amoenolens* lineage, notwithstanding their sometimes quite similar colouration. The same very acrid taste also differentiates *R. obscuricolor*, which was described from the Indian Himalayas (Das et al. 2017) and showed close affinity to some Southern Hemisphere *Ingratae* in our phylogeny.

After application of these criteria, we are principally left with the phylogenetically closer species of the *R. praetervisa* lineage as potential sources of confusion, most of which are mild to merely slightly acrid. From Asia, this concerns essentially *R. pseudopectinatoides*, a species that can be distinguished by its larger basidiospores (6–) 6.5–9 (–9.5) × 5–7.5 (–8) µm, hymenial cystidia sometimes with moniliform or capitate appendages and terminal cells of pileipellis with obtuse to ventricose apices (Li et al. 2015b); *R. ahmadii* differs in small basidiomata with pileus 1–4.5 cm in diam. and pileipellis a cutis with bifurcated terminal cells (Jabeen et al. 2017). The European species *R. recondita* Melera & Ostellari has a fruity-acidic, but overall unpleasant context smell, larger basidiospores 7–8.5 × 5.5–7 µm, with ornamentation composed of mostly isolated obtuse conical warts up to 1 µm high (Melera et al. 2017). From North America, *R. amerorecondita* Avis & Barajas has a strongly tuberculate-striate pileus margin, white to pale cream spore print, larger basidiospores (6.5–) 7.1–7.6–8.1 (–9.5) × (5–) 5.6–6.3–6.9 (–8) µm with more isolated ornamentation and a habitat in hardwood forest dominated by *Quercus*; *R. garyensis* Avis & Barajas has context with unpleasant, bleachy, fishy to parmesan smell, higher basidiospore ornamentation (0.6–) 0.8–1 (–1.4) µm, longer hymenial cystidia (62–) 71.5–81.4–91 (–103) × 7–8.1–9 (–10) µm and apex sometimes with two, long, usually narrow appendages (Adamčík et al. 2019).

***Russula succinea* G.J. Li & C.Y. Deng, sp. nov.**

Figs 2e, 2f, 3d, 10 and 11.

Fungal Names: FN 570760

Etymology. referring to the pale brownish tinged pileus.

Holotype. China, Guizhou Province, Weining Yi, Hui, and Miao Autonomous County, Caohai National Nature Reserve, 26°53'N, 104°12'E, alt. 2183 m, on the ground in coniferous forest, 15 July 2017, C.Y. Deng CH2017071509 (HGAS-MF 009904, **Holotype**). GenBank accession: MN649188 (ITS).

Diagnosis. This species is characterised by the yellowish-brown to pale brown pileus, with tuberculate-striate margin, adnate and pale cream-coloured lamellae, subclavate to subcylindrical stipe turning cream to pale ochre when bruised, white context unchanging after injury, slightly acrid to mild taste, pale cream spore print, globose, subglobose to broadly ellipsoid basidiospores (5.8–) 6.1–7.8 (–8.3) × (4.9–) 5.2–6.8 (–7.3) μm, 7.0 × 6.0 μm on average, ornamentation 0.8–1.2 μm in height, forming incomplete reticulum, rarely intermixed with isolated warts, clavate to subcylindrical basidia, 44–66 × 10–12 μm, fusiform hymenial cystidia 71–88 × 9–15 μm, two-layered pileipellis, ixotrichodermal suprapellis in pileus centre, a trichoderm at the margin, subpellis a cutis and habitat in coniferous forests.

Description. *Basidiomata* small to medium sized. *Pileus* 32–54 mm in diam., initially hemispherical, then plano-convex, flat when mature, often slightly depressed at centre, strongly viscid when wet, yellowish-brown tinged, pale brownish tinged, often intermixed with greyish-yellow fringe, Hazal (XIV11'k), Russet (XV13'k), Cinnamon Brown (XV15'k) to Tawny (XV15') at centre, rarely with Liver Brown (XIV17'm), Pecan Brown (XXVIII13'i) or Rood's Brown (XXVIII11'k) when old and dry; margin subacute to acute, straight, rarely split or inward-turned, tuberculate-striate 14–25 mm from the edge inwards, peeling 1/3–1/2 towards the centre, pale yellowish tinged, first Deep Colonial Buff (XXX21'b), Honey Yellow (XXX19") to Light Ochraceous Salmon (XV13'd), then Light Cadmium (IV19), Maize Yellow (III19f) when mature. *Lamellae* adnate, 3–6 mm in height at the halfway point of pileus radius, brittle, often forked near the stipe and pileus edge, interveined, pale cream-coloured, first White (LIII), Cream Colour (XVI19'f) when mature, sometimes stained with Martius Yellow (III23f) to Baryta Yellow (IV21f); edge entire, narrowing towards the pileus margin, 13–22 pieces per cm in the edge; lamellulae absent. *Stipe* slightly subcentral, rarely central, 4.2–8.3 × 1.5–2.2 cm, subclavate to subcylindrical, often narrowing towards the base, rarely slightly curved, smooth when young, rugulose longitudinally in age, dry, Cream Colour (XVI19'f), staining Sudan Brown (III15k) to Orange-Citrine (IV19k) when bruised, Tawny Olive (XXIX17'i), Sayal Brown (XXIX15") to Isabella Colour (XXX19'i) at base, initially solid, turning hollow in age. Context White (LIII), unchanging when bruised or touched, 3–5 mm thick at the centre of pileus, fragile, taste first slightly acrid, mild when mature, odour indistinct. *Spore print* pale cream (Romagnesi IIc–IIId).

Basidiospores [350/14/7] (5.8–) 6.1–7.8 (–8.3) × (4.9–) 5.2–6.8 (–7.3) μm, $Q = (1.00\text{--}) 1.03\text{--}1.30$ (–1.33) ($Q = 1.17 \pm 0.08$), 7.0 × 6.0 μm on average, globose, subglobose to broadly ellipsoid, rarely ellipsoid, composed of verrucous to subcylindrical amyloid warts 0.8–1.2 μm in height, often linked as short to long crests and ridges, forming an incomplete reticulum, rarely intermixed with isolated warts; suprahilar spot distinct, but not amyloid. *Basidia* 44–66 × 10–12 μm, mostly 4-spored, clavate to subcylindrical; sterigmata 4–6 μm in length, straight to tortuous. *Hymenial cys-*

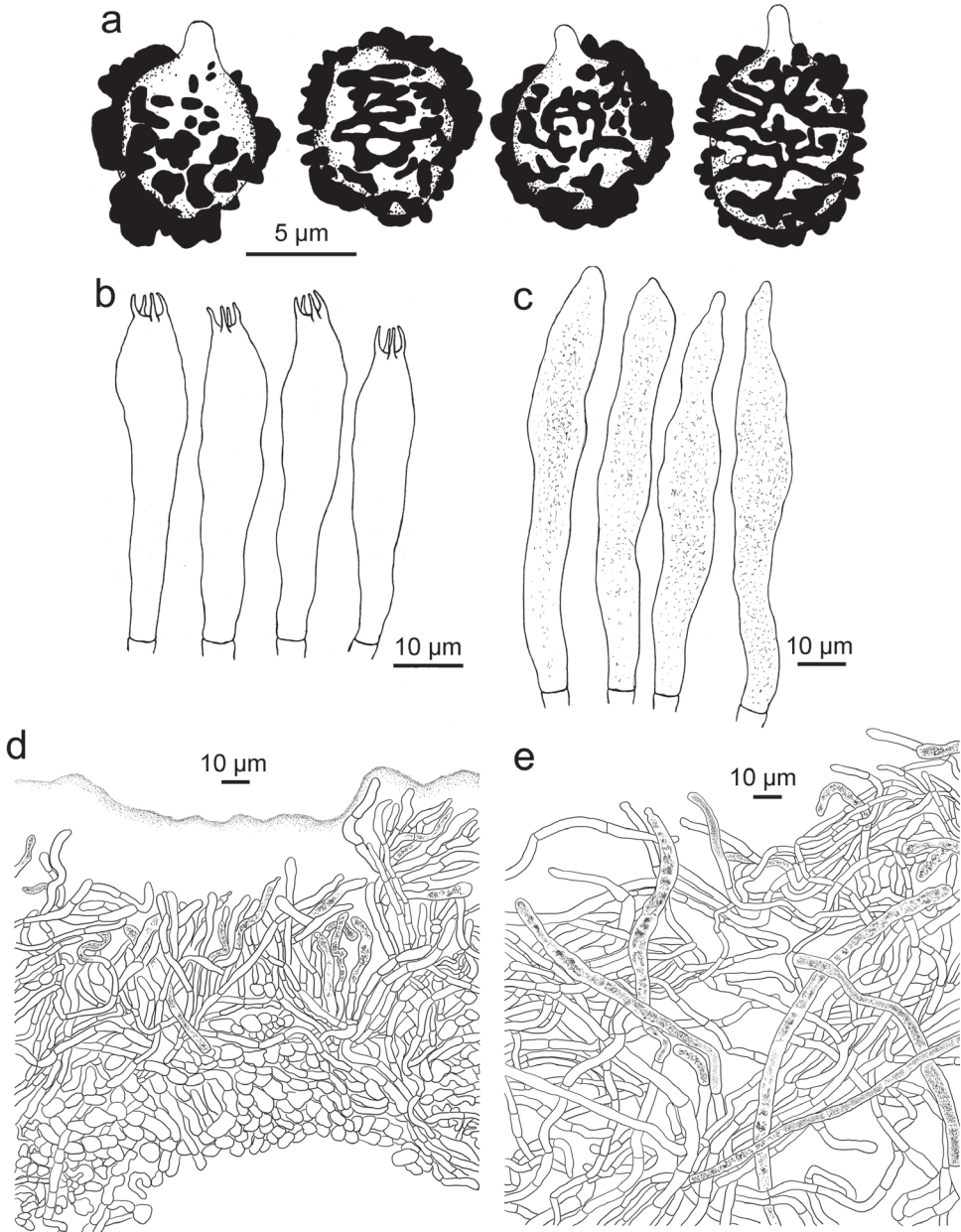


Figure 10. *Russula succinea*, holotype **A** basidiospores **B** basidia **C** hymenial cystidia **D** suprapellis partial subpellis in pileus centre **E** suprapellis in pileus margin.

tidia moderately numerous, ca. 700–1300/mm², 71–88 × 9–15 µm, fusiform, sometimes cylindrical, thin-walled, apex obtuse, rarely mucronate, projecting 20–40 µm beyond the hymenium, contents granular to crystalline, partly dense, blackish-grey

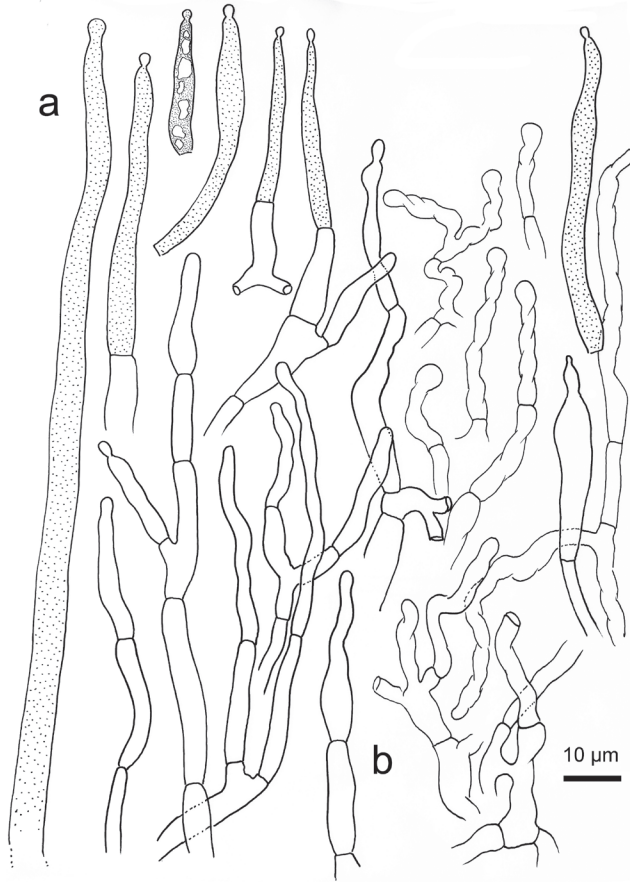


Figure 11. *Russula succinea*, holotype **A** hyphal ends in pileipellis margin **B** hyphal ends in pileus centre.

in SV. *Pileipellis* two-layered, distinctly delimited from the underlying context. The upper suprapellis (70–130 µm thick) in pileus centre an ixotrichoderm, composed of ascending to erect hyphae 4–7 µm in width, septate, cylindrical, often slightly inflated, acid-resistant encrustations absent, terminal cells sometimes narrowing towards the apex, subapical cells cylindrical, not branched; suprapellis a trichoderm in pileus margin, composed of repent, slender, cylindrical, hyaline hyphae 3–5 µm in width, acid-resistant encrustations absent. *Pileocystidia* abundant, long, cylindrical, often septate, 4–10 µm in width, apex obtuse, contents granulate, dense, blackish-grey in SV. The lower layer subpellis (50–90 µm thick) composed of loosely interwoven, mostly repent, cylindrical, septate hyaline hyphae often inflated, 2–7 µm in width. *Clamp connections* not observed in all parts.

Additional specimens examined. China, Guizhou Province, Weining Yi, Hui and Miao Autonomous County, Caohai National Nature Reserve, 26°53'N, 104°12'E, alt. 2215 m, on the ground in coniferous forest, 16 July 2017, C.Y. Deng CH2017071602 (HGAS-MF 009915, paratype); *ibid.*, alt. 2136 m, 15 July 2017, C.Y. Deng dcy2307

(HGAS-MF 009909, paratype); *ibid.*, alt. 2005 m, C.Y. Deng dcy2309 (HGAS-MF 009906, paratype); alt. 2057 m, C.Y. Deng dcy2308 (HGAS-MF 009902, paratype); alt. 2103 m, C.Y. Deng dcy2304 (HGAS-MF 009914, paratype); Jiangxi Province, Jiujiang City, Lushan City, Lushan Mountains, alt. 1257 m, on the ground in coniferous forest, 19 October 2016, J.B. Zhang (HFJAU 0301).

Habit and habitat. Single to scattered on yellow brown soil in coniferous forest dominated by *Pinus armandii*, *P. massoniana* and *P. yunnanensis* at 1200–2200 m altitude.

Distribution. China (Guizhou and Jiangxi).

Notes. This new species is reminiscent of *R. foetentula*, *R. obscuricolor* and *R. rufobasalis* because of the reddish-brown or burnt sienna colour at the stipe base (Peck 1907; Song et al. 2018). The following characters are helpful for differentiating these two species from *R. succinea*: *R. foetentula* has lower basidiospore ornamentations 0.5–0.9 μm connected by occasional to rare line connections, hymenial cystidia with mucronate-appendiculate apices 2–7 μm long, pileocystidium apex often constricted to 1–2.5 μm in width; North American distribution (Peck 1907; Adamčík et al. 2013); *R. obscuricolor* has darker brown to chocolate brown tinges at pileus centre, bitter to pungent taste of context and shorter hymenial cystidia (pleurocystidia 30–65 \times 6–9 μm , cheilocystidia 23–33 \times 5–7 μm) (Das et al. 2017); *R. rufobasalis* has bright reddish tinge at stipe base, basidiospore ornamentations 0.3–0.8 μm in height and frequently thick-walled, narrower terminal cells 2–5 μm in width (Song et al. 2018).

For those Asian sect. *Ingratae* members that have similar pileus tinges, *R. ahmadii* can be distinguished from *R. succinea* by lower basidiospore ornamentations up to 0.3 μm , shorter basidia (29–) 29.7–38.9 (–40.1) \times (9.2–) 9.4–11.3 (–11.8) μm and pileipellis a cutis (Jabeen et al. 2017); *R. arunii* differs from the new species in the orange tinge intermixed on pileus surfaces, white spore print, narrow pileocystidia 3–4 μm in width and a habit of broad-leaved *Pterigota alata* forest (Crous et al. 2017); *R. catillus* differs in that basidiospore ornamentation is composed of mostly isolated, verrucous to conical warts, absence of pileocystidia in pileipellis and a habitat of oak hardwood forest (Lee et al. 2017); *R. indocatillus* can be differentiated from the new species for white spore print, shorter basidia 34–40 \times 9–11 μm and capitate hymenial cystidium apex (Ghosh et al. 2020); *R. natarajanii* differs in having light to medium brown spots at the pileus periphery, shorter basidia 28–35 \times 7.5–9 μm and a habitat of *Quercus* forest (Das et al. 2006); *R. pseudocatillus* differs in the presence of lamellula, basidiospores ornamented with isolated warts never forming a reticulum and a habitat of broad-leaved evergreen forest (Yuan et al. 2019); *R. pseudoplectinatoides* can be distinguished from the new species in having hymenial cystidia with moniliform or capitate apex, larger basidiospores up to 9 μm in diam. and absence of pileocystidia (Li et al. 2015b); *R. straminella* differs in its shorter basidia and hymenial cystidia, often thick-walled terminal cells in pileipellis of pileus margin (Figs 6 and 7); *R. gelatinosa*, *R. punctipes*, *R. seneicis*, *R. subpunctipes* and *R. tsokae* differ from *R. succinea* in their larger basidiospores (9 μm in diam.) with high ornamentation up to 2 μm in height (Khatua et al. 2015; Lee et al. 2017; Song et al. 2018; 2020).

Discussion

The modern taxonomy of *Russula* calls for a combination of detailed microscopic observations with universal and specific standard, multi-gene phylogenetic analyses and accurate symbiotic plant species information (Buyck et al. 2018; Adamčík et al. 2019). The ITS phylogenetic analyses are the most common for practical identification of *Russula* species, because ITS is regarded as an adequate single gene DNA barcode for this genus (Li et al. 2019) and it has the largest number of available referential sequences in open databases (Schoch et al. 2012). A combination of morphological and ITS phylogenetic analyses supported the three new species amongst Asian *Ingratae*: *R. straminella*, *R. subpectinatoides* and *R. succinea*. The results of this study also indicate that *R. indocatillus* may have a wider distribution, from the Himalayan region to south-western China. The four species discussed here have distinct morphologies that allow each one to be differentiated from the others:

- *R. subpectinatoides* and *R. indocatillus* possess the more or less inflated, short-celled chains of hyphal ends, typical for most species in the subgenus *Heterophyllidiae* (Figs 4, 5, 8 and 9). These are abundant in *R. subpectinatoides*, but less so in *R. indocatillus* and absent in both other species which possess very dense, intricate and strongly branching, narrow ends in the pileipellis, more or less cemented in mucus that make microscopic examination of these hyphal ends very difficult. Compared to *R. straminella*, hyphal ends in the pileus centre of *R. succinea* have a more wavy-undulate form (Figs 6, 7, 10 and 11).

All four species have similar pileocystidia, but in *R. indocatillus*, they are smaller overall at the pileus surface compared to the other three species (Figs 4 and 5), while in *R. straminella*, they are often more or less thick-walled (Figs 6 and 7).

When comparing basidiospores, *R. subpectinatoides* stands out because of the low subreticulate ornamentation (Figs 3 and 8), whereas the other species have more developed, higher warts or ridges that are much less interconnected, while *R. indocatillus* has almost completely isolated warts (Figs 3 and 4).

Some European members of section *Ingratae*, viz. *R. amoenolens* Romagn., *R. pectinata* Fr., *R. pectinatoides* Peck and *R. sororia* (Fr.) Romell may have been confused morphologically with some of these new species (Wu 1989; Ying and Zang 1994), but more recent diversity analyses indicated that some Chinese specimens, identified as *R. amoenolens* and *R. insignis* Quél., have broad morphological similarities, but also considerable difference (ca. 2%) in the ITS sequence compared to European samples of these species (Li 2014; Liu et al. 2017; Cao et al. 2019). Whether these Chinese specimens represent unknown taxa or intraspecific geographically-separated populations is still debatable (Wang 2020). The factual presence of these species of European and North American origin in China have been analysed in recent years (Li 2014; Zhang 2014; Wang 2019; Liu 2019) and symbiotic host plants were found to be very similar between north-eastern China, Europe and North America (Wu 1979).

The topology of the ITS phylogram (Fig. 1) in this study largely corresponds to that of Park et al. (2017). Of the three subsections in sect. *Ingratae*, the majority of subsect. *Pectinatinae* Bon (type species *R. pectinata*) with species that are typically more greyish-brown to greyish-cream is distributed over clades C and H (Bon 1988), while *Subvelatae* (Singer) Singer (type species *R. subvelata* Singer) with members that have velar rudiments consisting of loosely, arachnoid-pulverulent floccons on pileus surface (Singer 1986), forms the highly-supported clade I. The species *R. indocatillus*, newly-recorded from China in this study, is located in Clade H. This well-supported clade also contains the *R. amoenolens* complex from Europe and *R. cerolens* and allies from North America. The African species complex of *R. oleifera* Buyck in subsect. *Oleiferinae* Buyck (type species *R. oleifera* Buyck) with species that sometimes present an annulus, corresponds to Clade D (Sanon et al. 2014). This clade was a sister clade to the remainder of sect. *Ingratae* in the multilocus phylogenetic analysis of Buyck et al. (2018). The large majority of European species that cluster around *R. foetens* compose clade F, a clade highly supported by Bayesian analysis only. The latter clade is typically composed of yellowish-brown to orange brown species and roughly corresponds to species traditionally placed in subsect. *Foetentinae* (Melzer & Zvara) Singer (type species *R. foetens*), of which it is characterised by dull, ochraceous or pallid coloured pileus, often with pectinate-sulcate to tuberculate-sulcate and distinctly subacute to acute margin, context odour of nitrobenzene, oily, fish, iodoform, or of other unpleasant smells (Singer 1986). Clade F also contains two of our new species, *R. straminella* and *R. succinea*, which share a similar pileipellis structure. Clade E received higher support in ML and MP analyses and shared with Clade F that two of the three species were also yellowish- to orange brown. This clade harbours three species: *R. rufobasalis* from Asia and the North American *R. granulata* Peck and *R. ventricosipes*. The results of our phylogenetic analyses, based on ITS sequences, indicate that more unknown subsections may exist in sect. *Ingratae*. More complex multi-gene analyses are urgently needed to clarify the phylogenetic relationships amongst species in this section.

Compared with previous analyses (Melera et al. 2016; Lee et al. 2017), more gasteroid species of sect. *Ingratae* were included in our study. The majority of gasteroid taxa clustered as two branches in Clade F. The other gasteroid species were mainly scattered in clades of agaricoid taxa. The phylogenetic topologies and low supported branches within sequestered complex 2 may indicate an urgent need to study the type material of these gasteroid species for clarification of synonyms.

Lee et al. (2017) summarised the general patterns observed for spores in the four clades of sect. *Ingratae* by showing a trend for basidiospore size to increase, while the shape changes from ellipsoid to spherical and for species that have smaller spores to have more ellipsoid spores and vice versa. However, these patterns were less clear when gasteroid species of this section were taken into account (Table 2). These gasteroid species suggest that the patterns, proposed in Lee et al. (2017), do not fit well with all members of the sect. *Ingratae*. Gasteroid taxa are known to have typically more globose and larger spores, because there are no evolutionary pressures of asymmetrical spores with hilar appendages for ballistospory in agaricoid species (Wilson et al. 2011). According to statistics, exceptions that do not follow these general patterns are common in sect. *Ingratae*. Over 40% (5/11) of counted gasteroid species of this section have sub-

Table 2. Spore sizes and shapes of gasteroid sect. *Ingratae* species.

Species	Spore size (μm)	Spore shape (Q value)	Reference
<i>R. ammophila</i> (J.M. Vidal & Calonge) Trappe & T.F. Elliott	7–9 × 5.5–7.5	subglobose to broadly ellipsoid	Vidal et al. (2002)
<i>Russula aromatica</i> Trappe & T.F. Elliott	8–11 × 7.5–10	globose to subglobose	Smith (1963)
<i>R. brunneonigra</i> T.Label	11–14(–15) × 11–13(–15)	globose (Q = 1.00–1.03)	Label and Tonkin (2007)
<i>R. galbana</i> T.Label	8–10 × 8–10	globose (Q = 1.01–1.06)	Label and Tonkin (2007)
<i>R. mistiformis</i> (Mattir.) Trappe & T.F. Elliott	(8.5–) 9.5–11 (–12.5) × (8–) 8.5–10 (–10.5)	subglobose to broadly ellipsoid (Q = 1.1–1.2)	Vidal et al. (2019)
<i>R. nondistincta</i> (Trappe & Castellano) Trappe & T.F. Elliott	7–11 in diam.	globose	Trappe and Castellano (2000)
<i>R. parksii</i> (Singer & A.H. Sm.) Trappe & T.F. Elliott	8–11 × 7–9/10–14(–18) × 9–12(–14)	subglobose to ellipsoid	Singer and Smith (1960)
<i>R. pilosella</i> (Cribb) T.Label	8.5–10 × 8–9.5	subglobose to broadly ellipsoid (Q = 1.07–1.2)	Label and Tonkin (2007)
<i>R. similis</i> Trappe & T.F. Elliott	9–12 × 8–10	globose to subglobose	Singer and Smith (1960)
<i>Russula shafferi</i> Trappe & T.F. Elliott	8–11 × 8–9	subglobose to broadly ellipsoid	Singer and Smith (1960)
<i>Russula subfulva</i> (Singer & A.H. Sm.) Trappe & T.F. Elliott	9–12 × 8–11	globose to subglobose	Singer and Smith (1960)

globose to broadly ellipsoid, even ellipsoid spores. In simple terms, a significant portion of gasteroid species have larger, but still more ellipsoidal spores. The authors suggested that these exceptions may be ascribed to the multiple and irreversible evolutions of gasteromycetation (Miller et al. 2001; Hibbett 2007). Ancestor genotype, divergence time and environmental factors all may exert different influences on this phenotype.

Spore ornamentations consisting of winged ridges are regarded as one of the most distinctive morphological characters for some members of sect. *Ingratae*. These species include *R. grata*, *R. fragrantissima* and *R. illota* from Europe and northern China, *R. mutabilis* from North America, *R. gelatinosa*, *R. punctipes*, *R. subpunctipes* and *R. senecis* from eastern and southern Asia. A majority of these species and *R. foetens* formed a not highly supported clade in phylogenetic analyses of Lee et al. (2017). As more samplings and species of sect. *Ingratae* were involved, the monophyly of winged-spore species was not supported in this analysis. Close phylogenetic relationships were detected in strongly-supported clades of *R. grata*–*R. fragrantissima*, *R. mutabilis*–*R. illota* and *R. punctipes*–*R. subpunctipes*–*R. senecis*. This phylogenetic inconsistency called for a further multi-gene analysis.

The habitats of the four species of this study show a common feature of coniferous forests dominated by *Pinus* spp. The current altitudes of distributions of *R. indocatillus* and *R. succinea* indicate a habitat of subalpine climate. These two species may have wider distributions than current records because the corresponding ectomycorrhizal symbiotic trees are representative and widespread species in Sino-Japanese and Sino-Himalayan floral subregions (Wu 1980; Chen et al. 2020). For *R. straminella* and *R. subpectinatoides* which were collected from reforested plantations and transplanted botanic gardens, intensive samplings on initial areas of symbiotic trees are needed for clarifying the types of habitats.

Specimens of the four species in this analysis were all collected on yellow brown soil. Local analyses showed high nitrogen conditions in soil environments of these species (Cai et al. 2010; Wang et al. 2010; Zhang et al. 2014). This result supported the conclusions in Avis (2012) that nitrophilic tendencies appear throughout fetid Russulas.

Acknowledgements

This work was financially supported by the Science and Technology Support Project of Guizhou Province [(2019) 2451–2, (2018) 4002], Talent Introduction Scientific Research Special Project of Hebei Agricultural University (YJ201849), National Natural Science Foundation of China (Nos. 31500013, 30770013, 31960008), the Biodiversity Survey and Assessment Project of the Ministry of Ecology and Environment of China (No. 2019HJ2096001006), the Provincial Key Technologies R&D Program of Guizhou [(2017) 2513], the Earmarked Fund for Hebei Edible Fungi Innovation Team of Modern Agro-industry Technology Research System (No. HBCT2018050205), Key Research and Development Planning Project in Science and Technology of Hebei Province (No. 21326315D), Jiangxi Province Department of Education Science and Technology Research Project, (No. GJJ190925), Construction and Application of the main Edible and Medicinal Fungal Resource Information-based Intelligent Platform of Guizhou Province [(2019) 4007] and the Science and Technology Foundation Project of Guizhou Province [(2016) 1153].

References

- Adamčík S, Carteret X, Buyck B (2013) Type studies on some *Russula* species described by C.H. Peck. *Cryptogamie Mycologie* 34(4): 367–391. <https://doi.org/10.7872/crym.v34.iss2.2013.367>
- Adamčík S, Jančovičová S, Buyck B (2018) The *Russulas* described by Charles Horton Peck. *Cryptogamie Mycologie* 39(1): 3–108. <https://doi.org/10.7872/crym/v39.iss1.2018.3>
- Adamčík S, Looney B, Caboň M, Jančovičová S, Adamčíková K, Avis PG, Barajas M, Bhatt RP, Corrales A, Das K, Hampe F, Ghosh A, Gates G, Kälviäinen V, Khalid AN, Kiran M, Lange RD, Lee H, Lim YW, Kong A, Manz C, Ovrebo C, Saba C, Taipale T, Verbeken A, Wisitrassameewong K, Buyck B (2019) The quest for a globally comprehensible *Russula* language. *Fungal Diversity* 99(1): 369–449. <https://doi.org/10.1007/s13225-019-00437-2>
- Avis PG (2012) Ectomycorrhizal iconoclasts: the ITS rDNA diversity and nitrophilic tendencies of fetid *Russula*. *Mycologia* 104: 998–1007. <https://doi.org/10.3852/11-399>
- Bau T, Bao HY, Li Y (2014) A revised checklist of poisonous mushrooms in China. *Mycosystema* 33(3): 517–548. <https://doi.org/10.13346/j.mycosystema.130256>
- Bazzicalupo AL, Buyck B, Saar I, Vauras J, Carmean D, Berbee ML (2017) Troubles with mycorrhizal mushroom identification where morphological differentiation lags behind barcode sequence divergence. *Taxon* 66(4): 791–810. <https://doi.org/10.12705/664.1>
- Bi ZS, Li TH (1986) A preliminary report note on *Russula* species from Guangdong, with a new species and a new variety. *Guihaia* 6(3): 193–199
- Bon M (1988) Clé monographique des russules d'Europe. *Documents Mycologiques* 18 (70–71): 1–120
- Buyck B, Duhem B, Das K, Jayawardena RS, Niveiro N, Pereira OL, Prasher IB, Adhikari S, Albertó EO, Bulgakov TS, Castañeda-Ruiz RF, Hembrom ME, Hyde KD, Lewis DP,

- Michlig A, Nuytinck J, Parihar A, Popoff OF, Ramirez NA, da Silva M, Verma RK, Hofstetter V (2017) Fungal biodiversity profiles 21–30. *Cryptogamie Mycologie* 38(1): 101–146. <https://doi.org/10.7872/crym/v38.iss1.2017.101>
- Buyck B, Zoller S, Hofstetter V (2018) Walking the thin line... ten years later: the dilemma of above- versus below-ground features to support phylogenies in the Russulaceae (Basidiomycota). *Fungal Diversity* 89(1): 267–292. <https://doi.org/10.1007/s13225-018-0397-5>
- Cai XL, Huang XZ, Liao DP (2010) Analysis of chemical properties of farmland soil in Caohai National Nature Reserve. *Inner Mongolia Agricultural Science and Technology* 3: 60–61
- Calonge FD, Martín MP (2000) Morphological and molecular data on the taxonomy of *Gymnomyces*, *Martellia* and *Zelleromyces* (Elasmomycetaceae, Russulales). *Mycotaxon* 76: 9–15
- Cao B, Li GJ, Zhao RL (2019) Species diversity and geographic components of *Russula* from the Greater and Lesser Khinggan Mountains. *Biodiversity Science* 27(8): 854–866. <https://doi.org/10.17520/biods.2019040>
- Chen YF, Zang RG, Yue TX, Zhang YX, Wang XH, Li YD, Li FR, Chen Q (2020) Forest vegetation in China. China Forestry Publishing House, Beijing, 1–799.
- Chen ZH, Yang ZL, Bau T, Li TH (2016) Poisonous mushrooms: recognition and poisoning treatment. Science Press, Beijing, 1–308.
- Crous PW, Wingfield MJ, Burgess TI, Hardy GE, Barber PA, Alvarado P, Barnes CW, Buchanan PK, Heykoop M, Moreno G, Thangavel R, van der Spuy S, Barili A, Barrett S, Cacciola SO, Cano-Lira JF, Crane C, Decock C, Gibertoni TB, Guarro J, Guevara-Suarez M, Hubka V, Kolařík M, Lira CRS, Ordoñez ME, Padamsee M, Ryvarden L, Soares AM, Stchigel AM, Sutton DA, Vizzini A, Weir BS, Acharya K, Aloï F, Baseia IG, Blanchette RA, Bordallo JJ, Bratek Z, Butler T, Cano-Canals J, Carlavilla JR, Chander J, Cheewangkoon R, Cruz RHSE, da Silva M, Dutta AK, Ercole E, Escobio V, Esteve-Raventós F, Flores JA, Gené J, Góis JS, Haines L, Held BW, Jung MH, Hosaka K, Jung T, Jurjević Ž, Kautman V, Kautmanova I, Kiyashko AA, Kozanek M, Kubátová A, Lafourcade M, LaSpada F, Latha KPD, Madrid H, Malysheva EF, Manimohan P, Manjón JL, Martín MP, Mata M, Merényi Z, Morte A, Nagy I, Normand AC, Paloi S, Pattison N, Pawłowska J, Pereira OL, Petterson ME, Picillo B, Raj KNA, Roberts A, Rodríguez A, Rodríguez-Campo FJ, Romański M, Ruszkiewicz-Michalska M, Scanu B, Schena L, Semelbauer M, Sharma R, Shouche YS, Silva V, Staniaszek-Kik M, Stielow JB, Tapia C, Taylor PWJ, Toome-Heller M, Vabeik-hokhei JMC, van Diepeningen AD, Van Hoa N, Van Tri M, Wiederhold NP, Wrzosek M, Zothanzama J, Groenewald JZ (2017) Fungal planet description sheets: 558–624. *Persoonia* 38:240–384. <https://doi.org/10.3767/003158517X698941>
- Dai YC, Zhou LW, Yang ZL, Wen HA, Bau T, Li TH (2010) A revised checklist of edible fungi in China. *Mycosystema* 29(1): 1–21. <https://doi.org/10.13346/j.mycosystema.2010.01.022>
- Darriba D, Taboada GL, Doallo R, Posada D (2012) jModelTest 2: more models, new heuristics and parallel computing. *Nature Methods* 9(8): e772. <https://doi.org/10.1038/nmeth.2109>
- Das K, Sharma JR (2005) Russulaceae of Kumaon Himalaya. Botanical Survey of India, Ministry of Environment and Forests, Government of India, Kolkata. 167–168
- Das K, Sharma JR, Atri NS (2006) *Russula* in Himalaya 3: a new species of subgenus *Ingratula*. *Mycotaxon* 95: 271–275

- Das K, Putte VDP, Buyck B (2010) New or interesting *Russula* from Sikkim Himalaya (India). *Cryptogamie Mycologie* 31: 373–387. <https://doi.org/10.7872/crym.v32.iss4.2011.365>
- Das K, Atri NS, Buyck B (2013) Three new *Russula* (Russulales) from India. *Mycosphere* 4:722–732. <http://dx.doi.org/10.5943/mycosphere/4/4/9>
- Das K, Ghosh A, Chakraborty D, Li JW, Qiu LH, Baghela A, Halama M, Hembrom ME, Mehmood T, Parihar A, Pencakowski B, Bielecka M, Reczynska K, Sasiela D, Singh U, Song Y, Swierkosz K, Szczesniak K, Uniyal P, Zhang JB, Buyck B (2017) Fungal biodiversity profiles 31–40. *Cryptogamie Mycologie* 38(3): 353–406. <https://doi.org/10.7872/crym/v38.iss3.2017.353>
- Deng CY, Shi LY, Wang J, Xiang Z, Li SM, Li GJ, Yang H (2020) Species diversity of the *Russula virescens* complex “qingtoujun” in southern China. *Mycosystema* 39(9): 1661–1683. <https://doi.org/10.13346/j.mycosystema.200145>
- Eberhardt U (2002) Molecular kinship analyses of the agaricoid Russulaceae: correspondence with mycorrhizal anatomy and sporocarp features in the genus *Russula*. *Mycological Progress* 1: 201–223. <http://dx.doi.org/10.1007/s11557-006-0019-6>
- Felsenstein J (1985) Confidence intervals on phylogenetics: an approach using bootstrap. *Evolution* 39: 783–791. <https://doi.org/10.1111/j.1558-5646.1985.tb00420.x>
- Ghosh A, Das K, Bhatt RP, Hembrom ME (2020) Two new species of the genus *Russula* from western Himalaya with morphological details and phylogenetic estimations. *Nova Hedwigia*: https://doi.org/10.1127/nova_hedwigia/2020/0588
- Haelewaters D, Dirks AC, Kappler LA, Mitchell JK, Quijada L, Vandegrift R, Buyck B, Pfister DH (2018) A preliminary checklist of fungi at the Boston Harbor Islands. *Northeastern Naturalist* 25(sp9): 45–76. <https://doi.org/10.1656/045.025.s904>
- Hall TA (1999) BioEdit: a user-friendly biological sequence alignment editor and analysis program for Windows 95/98/NT. *Nucleic Acids Symposium Series* 41: 95–98
- He B, Li Q, Feng T, Liu Y (2019) Research on community characteristics of the forest in Cao-hai National Nature Reserve. *Journal of Henan Agricultural University* 53(5): 783–790.
- He MQ, Zhao RL, Hyde KD, Begerow D, Kemler M, Yurkov A, McKenzie EHC, Raspé O, Kakishima M, Sánchez-Ramírez S, Vellinga EC, Halling R, Papp V, Zmitrovich IV, Buyck B, Ertz D, Wijayawardene NN, Cui BK, Schoutteten N, Liu XZ, Li TH, Yao YJ, Zhu XY, Liu AQ, Li GJ, Zhang MZ, Ling ZL, Cao B, Antonín V, Boekhout T, da Silva BDB, De Crop E, Decock C, Dima B, Dutta AK, Fell JW, Geml J, Ghobad-Nejhad M, Giachini AJ, Gibertoni TB, Gorjón SP, Haelewaters D, He SH, Hodkinson BP, Horak E, Hoshino T, Justo A, Lim YW, Menolli Jr. N, Mešić A, Moncalvo J, Mueller GM, Nagy LG, Nilsson RH, Noordeloos M, Nuytinck J, Orihara T, Ratchadawan C, Rajchenberg M, Silva-Filho AGS, Sulzbacher MA, Tkalčec Z, Valenzuela R, Verbeken A, Vizzini A, Wartchow F, Wei TZ, Weiß M, Zhao CL, Kirk PM (2019) Notes, outline and divergence times of Basidiomycota. *Fungal Diversity* 99: 105–367. <https://doi.org/10.1007/s13225-019-00435-4>
- Imai S (1938) Studies on the Agaricaceae of Hokkaido. II. *Journal of the Faculty of Agriculture of the Hokkaido Imperial University* 43: 179–378
- Jabeen S (2016) Ectomycorrhizal fungal communities associated with Himalayan cedar from Pakistan. PhD dissertation. University of the Punjab, Lahore. 1–269

- Jabeen S, Razaq A, Niazi ARK, Ahmad I, Grebenc T, Khalid AN (2017) *Russula ahmadii* (Basidiomycota, Russulales), a new species in section *Ingratae* and its ectomycorrhiza from coniferous forests of Pakistan. *Phytotaxa* 321(3): 241–253. <https://doi.org/10.11646/phytotaxa.321.3.2>
- Katoh K, Standly DM (2013) MAFFT Multiple sequence alignment software version 7: Improvements in performance and usability. *Molecular Biology and Evolution* 30(4): 772–780. <https://doi.org/10.1093/molbev/mst010>
- Khatua S, Dutta AK, Acharya K (2015) Prospecting *Russula senecis*: a delicacy among the tribes of West Bengal. *PeerJ* 3: e810. <https://doi.org/10.7717/peerj.810>
- Kishino H, Hasegawa M (1989) Evaluation of the maximum likelihood estimate of the evolutionary tree topologies from DNA sequence data, and the branching order in Hominoidea. *Journal of Molecular Evolution* 29: 170–179. <https://doi.org/10.1007/BF02100115>
- Lebel T, Tonkin JE (2007) Australasian species of *Macowanites* are sequestrate species of *Russula* (Russulaceae, Basidiomycota). *Australian Systematic Botany* 20: 355–381. <https://doi.org/10.1071/SB07007>
- Lee H, Park MS, Jung PE, Eimes JA, Seok SJ, Lim YW (2017) Re-evaluation of the taxonomy and diversity of *Russula* section *Foetentinae* (Russulales, Basidiomycota) in Korea. *Mycoscience* 58(5): 351–360. <https://doi.org/10.1016/j.myc.2017.04.006>
- Li GJ (2014) Taxonomy of *Russula* from China. PhD dissertation. Institute of Microbiology, Chinese Academy of Sciences & University of Chinese Academy of Sciences, Beijing. 1–554. <https://doi.org/10.13140/RG.2.2.20380.59522>
- Li GJ, Li SF, Zhao D, Wen HA (2015a) Recent research progress of *Russula* (Russulales, Agaricomycetes): a review. *Mycosystema* 34(5): 821–848. <https://doi.org/10.13346/j.mycosystema.150085>
- Li GJ, Zhao D, Li SF, Wen HA (2015b) *Russula chiui* and *R. pseudopectinatoides*, two new species from southwestern China supported by morphological and molecular evidence. *Mycological Progress* 14(6): 33. <https://doi.org/10.1007/s11557-015-1054-y>
- Li GJ, Zhao RL, Zhang CL, Lin FC (2019) A preliminary DNA barcode selection for the genus *Russula* (Russulales, Basidiomycota). *Mycology* 10(2): 61–74. <https://doi.org/10.1080/21501203.2018.1500400>
- Liu HY (2019) The study on *Russula* species on Taishan. Shandong Agricultural University, Tai'an. 1–111. <https://doi.org/10.27277/d.cnki.gsdnu.2019.000008>
- Liu XL, Bau T, Wang XH (2017) Species diversity of *Russula* from the Greater and Lesser Hinggan Mountains in Northeast China. *Mycosystema* 36(10): 1355–1368. <https://doi.org/10.13346/j.mycosystema.170015>
- Looney BP, Ryberg M, Hampe F, Sánchez-García M, Matheny PB (2016) Into and out of the tropics: global diversification patterns in a hyperdiverse clade of ectomycorrhizal fungi. *Molecular Ecology* 25(2): 630–647. <https://doi.org/10.1111/mec.13506>
- Looney BP, Meidl P, Piatek MJ, Miettinen O, Martin FM, Matheny PB, Labbé JL (2018) Russulaceae: a new genomic dataset to study ecosystem function and evolutionary diversification of ectomycorrhizal fungi with their tree associates. *New Phytologist* 218(1): 54–65. <https://doi.org/10.1111/nph.15001>
- Melera S, Ostellari C, Roemer N, Avis, PG, Tonolla M, Barja F, Narduzzi-Wicht, B (2017) Analysis of morphological, ecological and molecular characters of *Russula pectinatoides*

- Peck and *Russula praetervisa* Sarnari, with a description of the new taxon *Russula recondite* Melera & Ostellari. *Mycological Progress* 16 (2): 117–134. <https://doi.org/10.1007/s11557-016-1256-y>
- Miller SL, Buyck B (2002) Molecular phylogeny of the genus *Russula* in Europe with a comparison of modern infrageneric classifications. *Mycological Research* 106(3): 259–276. <https://doi.org/10.1017/S0953756202005610>
- Nakamura T, Yamada KD, Tomii K, Katoh K (2018) Parallelization of MAFFT for large-scale multiple sequence alignments. *Bioinformatics* 34(14): 2490–2492. <https://doi.org/10.1093/bioinformatics/bty121>
- Nylander JAA (2004) MrModelTest v2. Program distributed by the author. Evolutionary Biology Centre, Uppsala University. 1–2
- Peck CH (1907) New York species of *Russula*. *Bulletin of the New York State Museum of Natural History* 116: 67–98
- Razaq A, Ilyas S, Khalid AN, Niazi AR (2014) *Russula foetentoides* (Russulales, Russulaceae)—a new species from Pakistan. *Sydowia* 66(2): 289–298. [https://doi.org/10.12905/0380.sydowia66\(2\)2014-0289](https://doi.org/10.12905/0380.sydowia66(2)2014-0289)
- Ridgway R (1912) Color standards and color nomenclature. Robert Ridgway, Washington, 1–270. <https://doi.org/10.5962/bhl.title.144788>
- Romagnesi H, 1985. Les Russules d'Europe et d'Afrique du Nord. Reprint with supplement. J.Cramer, Lehre, 1–1030.
- Ronquist F, Teslenko M, van der Mark P, Ayres D, Darling A, Höhna S, Larget B, Liu L, Suchard MA, Huelsenbeck JP, (2012) MrBayes 3.2: Efficient Bayesian phylogenetic inference and model choice across a large model space. *Systematic Biology* 61(3): 539–542. <https://doi.org/10.1093/sysbio/sys029>
- Sanon E, Guissou KML, Yorou NS, Buyck B (2014) Le genre *Russula* au Burkina Faso (Afrique de l'Ouest): quelques espèces nouvelles de couleur brunâtre. *Cryptogamie Mycologie* 35(4): 377–397. <https://doi.org/10.7872/crym.v35.iss4.2014.377>
- Sarnari M (1998) Monografia illustrate de genere *Russula* in Europa. Tomo Primo. AMB, Centro Studi Micologici. Trento, 1–800.
- Schoch CL, Seifert KA, Huhndorf S, Robert V, Spouge JL, Levesque CA, Chen W (2012) Nuclear ribosomal internal transcribed spacer (ITS) region as a universal DNA barcode marker for fungi. *Proceedings of the National Academy of Sciences of the United States of America* 109: 6241–6246. <https://doi.org/10.1073/pnas.1117018109>
- Shaffer RL (1972) North American russulas of the subsection *Foetentinae*. *Mycologia* 64(5): 1008–1053. <https://doi.org/10.2307/3758072>
- Singer R (1935) Supplemente zu meiner monographie der gutting *Russula*. *Annales Mycologici* 33: 297–352.
- Singer R, Smith AH (1960) Studies on secotiaceous fungi IX the astrogastraceous series. *Memoirs of the Torrey Botanical Club* 21(3): 1–112. <https://doi.org/10.2307/43392224>
- Singer R (1986) The Agaricales in modern taxonomy. 4th Ed. Koeltz Scientific Books, Königstein, 1–981.
- Silvestro D, Michalak I (2012) raxmlGUI: a graphical front-end for RAxML. *Organisms Diversity and Evolution* 12: 335–337. <https://doi.org/10.1007/s13127-011-0056-0>

- Smith AH (1963) New astrogastraceous fungi from the Pacific Northwest. *Mycologia* 55(4): 421–441. <https://doi.org/10.2307/3756337>
- Song B, Li TH, Wu XL, Li JJ, Shen YH, Lin QY (2007) Known species of *Russula* from China and their distribution. *Journal of Fungal Research* 5(1): 20–42. <https://doi.org/10.13341/j.jfr.2007.01.007>
- Song J, Chen B, Liang JF, Li HJ, Wang SK, Lu JK (2020) Morphology and phylogeny reveal *Russula subpunctipes* sp. nov., from southern China. *Phytotaxa* 459(1): 16–24. <https://doi.org/10.11646/phytotaxa.459.1.2>
- Song Y, Buyck B, Li JW, Yuan F, Zhang ZW, Qiu LH (2018) Two novel and a forgotten *Russula* species in sect. *Ingratae* (Russulales) from Dinghushan Biosphere Reserve in southern China. *Cryptogamie Mycologie* 39(3): 341–357. <https://doi.org/10.7872/crym/v39.iss3.2018.341>
- Swofford DL (2004) PAUP*: phylogenetic analysis using parsimony and other methods. Version 4.0b10. Sinauer, Sunderland.
- Trappe JM, Castellano MA (2000) New sequestrate Ascomycota and Basidiomycota covered by the Northwest Forest Plan. *Mycotaxon* 75: 153–179.
- Vidal JM, Calonge FD, Martin MP (2002) *Macowanites ammophilus* (Russulales) a new combination based on new evidence. *Revista Catalana De Micologia* 24: 69–74.
- Vidal JM, Alvarado P, Loizides M, Konstantinidis G, Chachuła P, Mleczko P, Moreno G, Vizzini A, Krakhmalnyi M, Paz A, Cabero J, Kaounas V, Slavova M, Moreno-Arroyo B, Llistosella J (2019) A phylogenetic and taxonomic revision of sequestrate Russulaceae in Mediterranean and temperate Europe. *Persoonia* 42: 127–185. <https://doi.org/10.3767/persoonia.2019.42.06>
- Wang J, Buyck B, Wang XH, Tolgor B (2019) Visiting *Russula* (Russulaceae, Russulales) with samples from southwestern China finds one new subsection of *R.* subg. *Heterophyllidia* with two new species. *Mycological Progress* 18(6): 771–784. <https://doi.org/10.1007/s11557-019-01487-1>
- Wang JM, Lu ZH, Wu JF, Xiao QL, Zhu MY, Wang HH (2010) The characteristics and distribution patterns of soil types in Mt Lushan. *Acta Agriculturae Universitatis Jiangxiensis* 32(6): 1284–1290. <https://doi.org/10.13836/j.jjau.2010223>
- Wang XH (2020) Taxonomic comments on edible species of Russulaceae. *Mycosystema* 39(9): 1617–1639. <https://doi.org/10.13346/j.mycosystema.200209>
- White TJ, Bruns T, Lee S, Taylor J (1990) Amplification and direct sequencing of fungal ribosomal RNA genes for phylogenies. In: Innis MA, Gelfand DH, Sninsky JJ, White TJ (Eds) PCR protocols, a guide to methods and applications. Academic, San Diego, 315–322. <https://doi.org/10.1016/B978-0-12-372180-8.50042-1>
- Wilson AW, Binder M, Hibbett DS (2011) Effects of gasteroid fruiting body morphology on diversification rates in three independent clades of fungi estimated using binary state speciation and extinction analysis. *Evolution* 65(5): 1305–1322. <https://doi.org/10.1111/j.1558-5646.2010.01214.x>
- Wisitrassameewong K, Park MS, Lee H, Ghosh A, Das K, Buyck B, Looney BP, Caboň M, Adamčík S, Kim C, Kim CS, Lim YW (2020) Taxonomic revision of *Russula* subsection *Amoeninae* from South Korea. *MycKeys* 75: 1–29. <https://doi.org/10.3897/mycokeys.75.53673>
- Wu XL (1989) The macrofungi from Guizhou, China. Guizhou People's Publishing House, Guiyang, 1–198.

- Wu ZY (1979) The regionalization of Chinese flora. *Acta Botanica Yunnanica* 1(1): 1–22.
- Wu ZY (1980) *The Vegetation of China*. Beijing: Science Press, Beijing, 1–1375.
- YingJZ, ZangM (1994) *Economic macrofungi from southwestern China*. Science Press, Beijing, 1–400.
- Yuan F, Song Y, Buyck B, Li JW, Qiu LH (2019) *Russula viridicinnamomea* F. Yuan & Y. Song, sp. nov. and *R. pseudocatillus* F. Yuan & Y. Song, sp. nov., two new species from southern China. *Cryptogamie Mycologie* 40(4): 45–56. <https://doi.org/10.5252/cryptogamie-mycologie2019v40a4>
- Zhang H, Wang XK, Xu JP, Zhang YC, Ai YC (2014) Distribution characteristics of soil carbon and nitrogen and its influencing factors in different farming regions of Jiangsu Province. *Jiangsu Journal of Agricultural Sciences* 30(5): 1028–1036. <https://doi.org/10.3969/j.issn.1000-4440.2014.05.017>
- Zhang X (2014) *Researches on taxonomy of some species in Russula from China and phylogeny of the genus*. Southwest Forestry University, Kunming, 1–72.

Supplementary material 1

Fasta file for phylogenetic analyses

Authors: Guo-Jie Li

Data type: phylogenetic data

Copyright notice: This dataset is made available under the Open Database License (<http://opendatacommons.org/licenses/odbl/1.0/>). The Open Database License (ODbL) is a license agreement intended to allow users to freely share, modify, and use this Dataset while maintaining this same freedom for others, provided that the original source and author(s) are credited.

Link: <https://doi.org/10.3897/mycokeys.84.68750.suppl1>

Supplementary material 2

Phylogeny file for ML analysis

Authors: Guo-Jie Li

Data type: phylogenetic

Copyright notice: This dataset is made available under the Open Database License (<http://opendatacommons.org/licenses/odbl/1.0/>). The Open Database License (ODbL) is a license agreement intended to allow users to freely share, modify, and use this Dataset while maintaining this same freedom for others, provided that the original source and author(s) are credited.

Link: <https://doi.org/10.3897/mycokeys.84.68750.suppl2>

Supplementary material 3

Nexus file for Bayesian analysis

Authors: Guo-Jie Li

Data type: phylogenetic

Copyright notice: This dataset is made available under the Open Database License (<http://opendatacommons.org/licenses/odbl/1.0/>). The Open Database License (ODbL) is a license agreement intended to allow users to freely share, modify, and use this Dataset while maintaining this same freedom for others, provided that the original source and author(s) are credited.

Link: <https://doi.org/10.3897/mycokeys.84.68750.suppl3>

Supplementary material 4

Nexus file for MP analysis

Authors: Guo-Jie Li

Data type: phylogenetic

Copyright notice: This dataset is made available under the Open Database License (<http://opendatacommons.org/licenses/odbl/1.0/>). The Open Database License (ODbL) is a license agreement intended to allow users to freely share, modify, and use this Dataset while maintaining this same freedom for others, provided that the original source and author(s) are credited.

Link: <https://doi.org/10.3897/mycokeys.84.68750.suppl4>

Phylogenetic analyses and morphological characters reveal two new species of *Ganoderma* from Yunnan province, China

Jun He^{1,2}, Zong-Long Luo¹, Song-Ming Tang^{2,3,4},
Yong-Jun Li², Shu-Hong Li², Hong-Yan Su¹

1 College of Agriculture and Biological Sciences, Dali University, Dali 671003, Yunnan, China **2** Institute of Biotechnology and Germplasm Resources, Yunnan Academy of Agricultural Sciences, Kunming 650223, China **3** Center of Excellence in Fungal Research, Mae Fah Luang University, Chiang Rai 57100, Thailand **4** School of science, Mae Fah Luang University, Chiang Rai 57100, Thailand

Corresponding authors: Shu-Hong Li (shuhongfungi@126.com), Hong-Yan Su (suhongyan16@163.com)

Academic editor: Bao-Kai Cui | Received 10 June 2021 | Accepted 17 October 2021 | Published 12 November 2021

Citation: He J, Luo Z-L, Tang S-M, Li Y-J, Li S-H, Su H-Y (2021) Phylogenetic analyses and morphological characters reveal two new species of *Ganoderma* from Yunnan province, China. MycoKeys 84: 141–162. <https://doi.org/10.3897/mycokeys.84.69449>

Abstract

Ganoderma dianzhongense **sp. nov.** and *G. esculentum* **sp. nov.** are proposed as two new species based on both phenotypic and genotypic evidences. *Ganoderma dianzhongense* is characterized by the stipitate basidiomata, laccate and oxblood red pileus, gray white pore surface, duplex context and broadly ellipsoid basidiospores (9.0–12.5 × 6.5–9.0 μm) with coarse interwall pillars. *Ganoderma esculentum* is characterized by its basidiomata with slender stipe, white pore surface, homogeneous pileus context, and slightly truncate, narrow basidiospores (8.0–12.5 × 5.0–8.0 μm). Phylogenetic analyses were carried out based on the internal transcribed spacer (ITS), translation elongation factor 1-α (TEF1-α) and the second subunit of RNA polymerase II (RPB2) sequence data. The illustrations and descriptions for the new taxa are provided.

Keywords

Ganodermataceae, novel species, phylogeny, taxonomy

Introduction

Ganodermataceae was introduced by Donk (1948) which belongs to Polyporales and the latest studies indicated that it is a monophyletic group (Costa-Rezende et al. 2020). Currently, eleven genera viz. *Amauroderma* Murril, *Amaurodermellus* Costa-Rezende, *Cristataspora* Costa-Rezende, *Foraminispora* Robledo, Costa-Rezende & Drechsler-Santos, *Furtadoa* Costa-Rezende, Robledo & Drechsler-Santos, *Ganoderma* P. Karst., *Haddowia* Steyaert, *Humphreyia* Steyaert, *Magoderma* (Murrill) Steyaert, *Sanguinoderma* Y.F. Sun, D.H. Costa & B.K. Cui and *Tomophagus* Murrill are accepted in Ganodermataceae and supported by morphology and phylogeny (Steyaert 1972; Furtado 1981; Corner 1983; Zhao et al. 2000; Ryvarden 2004; Thametal 2012; Costa-Rezende et al. 2017; Costa-Rezende et al. 2020; Sun et al. 2020).

Ganoderma P. Karst (Ganodermataceae, Polyporales) was introduced to accommodate a laccate and stipitate fungus, *Ganoderma lucidum* (Curtis) P. Karst (Karsten 1881). *Ganoderma* is characterized by double-walled basidiospores with inter-wall protuberances (Karsten 1881; Moncalvo and Ryvarden 1997). There are 462 records in the Index Fungorum (<http://www.Indexfungorum.org/>; accessed date: 7 October 2021) and 506 records in MycoBank (<http://www.mycobank.org/>; accessed date: 7 October 2021). *Ganoderma* is one of the most taxonomically scrutinized genera among the Ganodermataceae and even in Polyporales (Richter et al. 2015; Costa-Rezende et al. 2020). Most *Ganoderma* species are wood decomposers, found in all temperate and tropical regions (Pilotti et al. 2004; Cao et al. 2012; Zhou et al. 2015).

Ganoderma has long been regarded as one of the most important medicinal fungi in the world (Paterson 2006); they have been used as medicine for over two millennia in China (Dai et al. 2009). Several *Ganoderma* species are known to be prolific sources of highly active bioactive compounds, especially polysaccharides, protein, sterols, and triterpenoids (Ahmadi and Riazipour 2007; Chan et al. 2007). These compounds are known to possess extensive therapeutic properties, such as antioxidant, antitumor, and antiviral agents, and improve sleep function (De Silva et al. 2013).

Species diversity of *Ganoderma* is abundant in China and more than 30 species have been described (Zhao et al. 2000; Wang et al. 2009; Cao et al. 2012; Li et al. 2015; Xing et al. 2016; Hapuarachchi et al. 2018; Liu et al. 2019; He et al. 2019; Wu et al. 2020). Yunnan province is considered as one of the hot-spots for studying biodiversity of polypores, and some new *Ganoderma* species have been described (Zhao 1989; Wang et al. 2010; Cao and Yuan 2013).

During our investigation into the diversity of *Ganoderma* in Yunnan province, several specimens of *Ganoderma* were collected from central and southern Yunnan. Phylogenetic analysis showed that the seven collections formed two distinct lineages and can be recognized as new species, hence two new species, namely *G. dianzhongense* and *G. esculentum* are introduced based on morphology and phylogeny.

Materials and methods

Sample collection

Seven *Ganoderma* specimens were collected during the rainy season from July 2016 to August 2019 in Yunnan Province of China. The samples were then photographed and transported back to the laboratory where their fresh macroscopic details were described. The specimens were deposited in the herbarium of Kunming Institute of Botany Academia Sinica (KUN-HKAS).

Morphological studies

Macro-morphological characters were described based on fresh material field notes, and the photographs provided here. Color codes are from Kornerup and Wanscher (1978). Micro-morphological data were obtained from the dried specimens and observed by using a microscope following Li et al. (2015). Sections were studied at magnification of up to 1000× using a NiKon E400 microscope and phase contrast illumination. Microscopic features and measurements were made from slide preparations stained with 5% potassium hydroxide (KOH) and 2% Melzer's reagent. Basidiospore features, hyphal system, color, sizes and shapes were recorded and photographed. Measurements were made using the Image Frame work v.0.9.7 to represent variation in the size of basidiospores, 5% of measurements were excluded from each end of the range and extreme values are given in parentheses.

The following abbreviations are used: IKI = Melzer's reagent, IKI- = neither amyloid nor dextrinoid, KOH = 5% potassium hydroxide, CB = Cotton Blue, CB+ = Cyanophilous (Xing et al. 2018). The abbreviation for basidiospores measurements (n/m/p) denote "n" basidiospores measured from "m" basidiomata of "p" specimens. Basidiospore dimensions (and "Q" values) are given as (a) b-*av*-c (d), where "a" represents the minimum, "d" the biggest, "*av*" the average "b" and "c" covers a minimum of 90% of the values. "Q", the length/width ratio of a spore in side view, and "Q_m" for the average of all basidiospores ± standard deviation (Wang et al. 2015).

DNA extraction, PCR amplification, and sequencing

Total genomic DNA was extracted from dried pieces of pileus with tubes with modified CTAB protocol Doyle (1987). The genes ITS, TEF1- α and RPB2 were amplified by polymerase chain reaction (PCR) technique. The primers ITS1F / ITS4, TEF1-983 / TEF1-1567, and RPB2-6f / fRPB2-7cR were used to amplify the ITS, TEF1- α , RPB2 region, respectively (White et al. 1990; Liu et al. 1999; Matheny et al. 2007). PCR reactions (25 μ L) contained mixture: 2.5 μ L PCR reaction buffer, 2.5 μ L 0.2% BSA, 2 μ L dNTP (2.5 mM), 0.5 μ L each of primer, 0.2 μ L 5 U/ μ L Taq DNA polymerase, 1–1.5 μ L DNA solution and 16 μ L sterilized distilled H₂O. The PCR cycling for ITS was as follows: initial denaturation at 94 °C for 5 min, followed by 35 cycles at

94 °C for 30 sec, 53 °C for 30 sec and 72 °C for 50 sec and a final extension of 72 °C for 10 min. The PCR cycling for TEF1- α was as follows: initial denaturation at 94 °C for 5 min, followed by 35 cycles at 94 °C for 30 sec, 55 °C for 30 sec and 72 °C for 50 sec and a final extension of 72 °C for 10 min. The PCR cycling for RPB2 was as follows: initial denaturation at 94 °C for 5 min, followed by 35 cycles at 94 °C for 30 sec, 50 °C for 30 sec and 72 °C for 50 sec and a final extension of 72 °C for 10 min. The PCR products were visualized via UV light after electrophoresis on 1% agarose gels stained with ethidium bromide. Successful PCR products were sent to Sangon Biotech Limited Company (Shanghai, China), using forward PCR primers. When sequences have heterozygous INDELS or ambiguous sites, samples were sequenced bidirectionally to make contigs of the amplified regions or verify the ambiguous sites (Wang et al. 2015). Raw DNA sequences were assembled and edited in Sequencher 4.1.4 and the assembled DNA sequences were deposited in GenBank (Table 1).

Sequencing and sequence alignment

Sequence data of three partial loci Internal transcribed spacer region (ITS), RNA polymerase II subunit 2 (RPB2), and translation elongation factor 1-alpha (TEF1- α) were used in the phylogenetic analyses. Besides the sequences generated from this study, other reference sequences were selected from GenBank for phylogenetic analyses (Table 1). Sequences were aligned using the online version of MAFFT v.7 (<http://mafft.cbrc.jp/alignment/server/>) (Kato and Standley 2013) and adjusted using BioEdit v.7.0.9 by hand (Hall 1999) to allow maximum alignment and minimize gaps. Ambiguous regions were excluded from the analyses and gaps were treated as missing data. The phylogeny website tool “ALTER” (Glez-Peña et al. 2010) was used to convert the alignment fasta file to Phylip format for RAxML analysis and AliView and PAUP 4.0b 10 were used to convert the alignment fasta file to a Nexus file for Bayesian analysis (Swofford 2003). Phylogenetic analyses were obtained from Maximum Likelihood (ML) and Bayesian analysis (BI).

Molecular phylogenetic analyses

The maximum likelihood (ML) and Bayesian inference (BI) methods were used to analyze the combined dataset of ITS, TEF1- α and RPB2 sequences. Maximum likelihood analysis was conducted with RAxML-HPC2 on the CIPRES Science Gateway (Miller et al. 2010), involved 100 ML searches; all model parameters were estimated by the program. The ML bootstrap values (ML-BS) were obtained with 1000 rapid bootstrapping replicates. Maximum likelihood bootstrap values (ML) equal to or greater than 70% are given above each node (Figure 1).

Bayesian analysis was performed with MrBayes v3.2 (Ronquist et al. 2012), with the best-fit model of sequence evolution estimated with MrModeltest 2.3 (Nylander et al. 2008) to evaluate posterior probabilities (PP) (Rannala and Yang 1996; Zhaxybayeva and Gogarten 2002) by Markov Chain Monte Carlo (MCMC) sampling. Six simultaneous Markov chains were run for 10,000,000 generations, trees were sampled every 500th generation, and 2,000 trees were obtained. The first 5000 trees, represent-

Table 1. Species, specimens, geographic origin and GenBank accession numbers of sequences used in this study.

Species	Voucher/strain	Origin	GenBank accession numbers			Reference
			ITS	TEF1- α	RPB2	
<i>Ganoderma aridicola</i>	Dai 12588 (Type)	South Africa	KU572491	KU572502	–	Xing et al. 2016
<i>G. adpersum</i>	GACP15061220	Thailand	MK345425	MK371431	MK371437	Hapuarachchi et al. 2019
	MFLU 19-2178	Thailand	MN396653	MN423149	MN423114	Luangharn et al. 2021
<i>G. angustisporum</i>	Cui 13817 (Type)	Fujian, China	MG279170	MG367563	MG367507	Xing et al. 2018
	Cui 14578	Guangdong, China	MG279171	MG367564	–	Xing et al. 2018
<i>G. austral</i>	CMW 47785	South Africa	MH571686	MH567276	–	Tchoumi et al. 2018
	CMW 48146	South Africa	MH571685	MH567283	–	Tchoumi et al. 2018
<i>G. austroafricanum</i>	CBS138724 (Type)	South Africa	KM507324	–	–	Coetzee et al. 2015
<i>G. aff. austroafricanum</i>	CMW25884	South Africa	MH571693	MH567296	–	Tchoumi et al. 2019
<i>G. bambusicola</i>	Wu 1207-151 (Type)	Taiwan, China	MN957781	LC517941	LC517944	Wu et al. 2020
	Wu 1207-152	Taiwan, China	MN957782	LC517942	LC517945	Wu et al. 2020
	Wu 1207-153	Taiwan, China	MN957783	LC517943	LC517946	Wu et al. 2020
<i>G. boninense</i>	WD 2028	Japan	KJ143905	KJ143924	KJ143964	Zhou et al. 2015
	WD 2085	Japan	KJ143906	KJ143925	KJ143965	Zhou et al. 2015
<i>G. calidophilum</i>	MFLU 19-2174	Yunnan, China	MN398337	–	–	Luangharn et al. 2021
	H36	Yunnan, China	MW750241	MW838997	MW839003	this study
<i>G. carnosum</i>	MJ 21/08	Czech R, Europe	KU572492	–	–	Xing et al. 2016
	JV 8709/8	Czech R, Europe	KU572493	–	–	Xing et al. 2016
<i>G. carocalcareus</i>	DMC 322 (Type)	Cameroon	EU089969	–	–	Douanla and Langer 2009
	DMC 513	Cameroon	EU089970	–	–	Douanla and Langer 2009
<i>G. casuarinicola</i>	Dai 16336 (Type)	Guangdong, China	MG279173	MG367565	MG367508	Xing et al. 2018
	Dai 16339	Guangdong, China	MG279176	MG367568	MG367511	Xing et al. 2018
<i>G. curtisii</i>	CBS 100131	NC, USA	JQ781848	KJ143926	KJ143966	Zhou et al. 2015
	CBS 100132	NC, USA	JQ781849	KJ143927	KJ143967	Zhou et al. 2015
<i>G. destructans</i>	CBS 139793 (Type)	South Africa	NR132919	–	–	Coetzee et al. 2015
	Dai 16431	South Africa	MG279177	MG367569	MG367512	Xing et al. 2018
<i>G. dunense</i>	CMW42157 (Type)	South Africa	MG020255	MG020227	–	Tchoumi et al. 2019
	CMW42150	South Africa	MG020249	MG020228	–	Tchoumi et al. 2019
<i>G. ecuadoriense</i>	ASL799 (Type)	Ecuador	KU128524	–	–	Crous et al. 2016
	PMC126	Ecuador	KU128525	–	–	Crous et al. 2016
<i>G. eickeri</i>	CMW 49692 (Type)	South Africa	MH571690	MH567287	–	Tchoumi et al. 2019
	CMW 50325	South Africa	MH571689	MH567290	–	Tchoumi et al. 2019
<i>G. ellipsoideum</i>	GACP1408966 (Type)	Hainan, China	MH106867	–	–	Hapuarachchi et al. 2018
	GACP14081215	Hainan, China	MH106886	–	–	Hapuarachchi et al. 2018
<i>G. enigmaticum</i>	Dai 15970	Africa	KU572486	KU572496	MG367513	Xing et al. 2016
	Dai 15971	Africa	KU572487	KU572497	MG367514	Xing et al. 2016
<i>G. esculentum</i>	L4935 (Type)	Yunnan, China	MW750242	MW838998	MW839004	this study
	L4946	Yunnan, China	MW750243	MW838999	–	this study
<i>G. flexipes</i>	Wei 5494	Hainan, China	JN383979	–	–	Cao and Yuan 2013
	MFLU 19-2198	Yunnan, China	MN398340	–	–	Luangharn et al. 2021
<i>G. gibbosum</i>	MFLU 19-2176	Thailand	MN396311	–	MN423118	Luangharn et al. 2021
	MFLU 19-2190	Laos	MN396310	–	MN423117	Luangharn et al. 2021
<i>G. heohmelianum</i>	Dai 11995	Yunnan, China	KU219988	MG367550	MG367497	Song et al. 2016
	Cui 13982	Guangxi, China	MG279178	MG367570	MG367515	Xing et al. 2018
<i>G. hochiminhense</i>	MFLU 19-2224 (Type)	Vietnam	MN398324	MN423176	–	Luangharn et al. 2021
	MFLU 19-2225	Vietnam	MN396662	MN423177	–	Luangharn et al. 2021
<i>G. knysnamense</i>	CMW 47755 (Type)	South Africa	MH571681	MH567261	–	Tchoumi et al. 2019
	CMW 47756	South Africa	MH571684	MH567274	–	Tchoumi et al. 2019
<i>G. leucocontextum</i>	GDGM 44303	Xizang, China	KJ027607	–	–	Li et al. 2015
	GDGM 44305	Xizang, China	KJ027609	–	–	Li et al. 2015
<i>G. lingzhi</i>	Cui 9166	China	KJ143907	JX029974	JX029978	Cao et al. 2012
	Dai 12574	Liaoning, China	KJ143908	JX029977	JX029981	Cao et al. 2012
<i>G. lobatum</i>	JV 1008/31	USA	KF605671	MG367553	MG367499	Xing et al. 2018
	JV 1008/32	USA	KF605670	MG367554	MG367500	Xing et al. 2018

<i>G. lucidum</i>	K 175217	UK	KJ143911	KJ143929	KJ143971	Zhou et al. 2015
	MT 26/10	Czech Republic	KJ143912	KJ143930	–	Zhou et al. 2015
<i>G. martinicense</i>	231NC	NC, USA	MG654182	MG754736	–	Loyd et al.2018
	246TX	TX, USA	MG654185	MG754737	MG754858	Loyd et al.2018
<i>G. mbrekobenum</i>	UMN7-3 GHA (Type)	Ghana	KX000896	–	–	Crous et al. 2016
	UMN7-4 GHA	Ghana	KX000898	–	–	Crous et al. 2016
<i>G. mexicanum</i>	MUCL 49453 SW17	Martinique	MK531811	MK531825	MK531836	Cabarroi-Hernández et al. 2019
	MUCL 55832	Martinique	MK531815	MK531829	MK531839	Cabarroi-Hernández et al. 2019
<i>G. mizonamense</i>	UMN-MZ4 (Type)	India	KY643750	–	–	Crous et al. 2017
	UMN-MZ5	India	KY643751	–	–	Crous et al. 2017
<i>G. multipileum</i>	CWN 04670	Taiwan, China	KJ143913	KJ143931	KJ143972	Zhou et al. 2015
	Dai 9447	Hainan, China	KJ143914	–	KJ143973	Zhou et al. 2015
<i>G. multiplicatum</i>	SPC9	Brazil	KU569553	–	–	Bolaños et al. 2016
	URM 83346	Brazil	JX310823	–	–	Bolaños et al. 2016
<i>G. mutabile</i>	CLZhao 982	Yunnan, China	MG231527	–	–	GenBank
	Yuan 2289(Type)	Yunnan, China	JN383977	–	–	Cao and Yuan 2013
<i>G. myanmarensis</i>	MFLU 19-2167 (Type)	Myanmar	MN396329	–	–	Luangharn et al. 2021
	MFLU 19-2169	Myanmar	MN396330	–	–	Luangharn et al. 2021
<i>G. nasalanense</i>	GACP17060211 (Type)	Laos	MK345441	–	–	Hapuarachchi et al. 2019
	GACP17060212	Laos	MK345442	–	–	Hapuarachchi et al. 2019
<i>G. neojaponicum</i>	FFPRI WD-1285	Tokyo, Japan	MN957784	–	–	Wu et al. 2020
	FFPRI WD-1532	Chiba, Japan	MN957785	–	–	Wu et al. 2020
<i>G. orbiforme</i>	Cui 13918	Hainan, China	MG279186	MG367576	MG367522	Xing et al. 2018
	Cui 13880	Hainan, China	MG279187	MG367577	MG367523	Xing et al. 2018
<i>G. parvulum</i>	MUCL 47096	Cuba	MK554783	MK554721	MK554742	Cabarroi-Hernández et al. 2019
	MUCL 52655	French Guiana	MK554770	MK554717	MK554755	Cabarroi-Hernández et al. 2019
<i>G. philippii</i>	Cui 14443	Hainan, China	MG279188	MG367578	MG367524	Xing et al. 2018
	Cui 14444	Hainan, China	MG279189	MG367579	MG367525	Xing et al. 2018
<i>G. resinaceum</i>	Rivoire 4150	France, Europe	KJ143915	–	–	Zhou et al. 2015
	CBS 19476	Netherlands, Europe	KJ143916	KJ143934	–	Zhou et al. 2015
<i>G. rywardenii</i>	HKAS 58053 (Type)	South Africa	HM138670	–	–	Kinge et al. 2011
	HKAS 58054	South Africa	HM138671	–	–	Kinge et al. 2011
<i>G. sessile</i>	111TX	TX, USA	MG654306	MG754747	MG754866	Loyd et al.2018
	113FL	FL, USA	MG654307	MG754748	MG754867	Loyd et al.2018
<i>G. shanxiense</i>	BJTC FM423(Type)	Shanxi, China	MK764268	MK783937	MK783940	Liu et al. 2019
	HSA 539	Shanxi, China	MK764269	–	MK789681	Liu et al. 2019
<i>G. sichuanense</i>	HMAS42798 (Type)	Sichuan, China	JQ781877	–	–	Cao et al. 2012
	Cui 7691	Guangdong, China	JQ781878	–	–	Cao et al. 2012
<i>G. sinense</i>	Wei 5327	Hainan, China	KF494998	KF494976	MG367529	Xing et al. 2018
	Cui 13835	Hainan, China	MG279193	MG367583	MG367530	Xing et al. 2018
<i>G. steyaertanum</i>	MEL:2382783	Australia	KP012964	–	–	GenBank
	6 WN 20B	Indonesia	KJ654462	–	–	Glen et al. 2014
<i>G. thailandicum</i>	HKAS 104640 (Type)	Thailand	MK848681	MK875829	MK875831	Luangharn et al. 2019
	HKAS 104641	Thailand	MK848682	MK875830	MK875832	Luangharn et al. 2019
<i>G. tropicum</i>	He 1232	Guangxi, China	KF495000	KF494975	MG367531	Xing et al. 2016
	HKAS 97486	Thailand	MH823539	–	MH883621	Luangharn et al. 2021
<i>G. tsugae</i>	UMNMI20	MI, USA	MG654324	MG754764	–	Loyd et al.2018
	UMNMI30	MI, USA	MG654326	MH025362	MG754871	Loyd et al.2018
<i>G. tuberculosum</i>	GVL-21	Veracruz, Mexico	MT232639	–	–	Espinosa-García et al. 2021
	GVL-40	Veracruz, Mexico	MT232634	–	–	Espinosa-García et al. 2021
<i>G. weberianum</i>	CBS 128581	Taiwan, China	MK603805	MK636693	MK611971	Cabarroi-Hernández et al. 2019
	CBS 219.36	Philippines	MK603804	MK611974	MK611972	Cabarroi-Hernández et al. 2019

<i>G. wiiroense</i>	UMN-21-GHA (Type)	Ghana	KT952363	–	–	Crous et al. 2015
	UMN-20-GHA	Ghana	KT952361	–	–	Crous et al. 2015
<i>G. dianzhongense</i>	L4331(Type)	Yunnan, China	MW750237*	MW838993*	MZ467043*	this study
	L4230	Yunnan, China	MW750236*	MW838992*	–	this study
	L4737	Yunnan, China	MW750238*	MW838994*	MW839000*	this study
	L4759	Yunnan, China	MW750239*	MW838995*	MW839001*	this study
	L4969	Yunnan, China	MW750240*	MW838996*	MZ467044*	this study
<i>G. zonatum</i>	FL-02	FL, USA	KJ143921	KJ143941	KJ143979	Zhou et al. 2015
	FL-03	FL, USA	KJ143922	KJ143942	KJ143980	Zhou et al. 2015
<i>Tomophagus colossus</i>	TC-02	Vietnam	KJ143923	KJ143943	–	Zhou et al. 2015

*Newly generated sequences for this study. Bold font = new species.

ing the burn-in phase of the analyses, were discarded, while the remaining 1500 trees were used for calculating posterior probabilities in the majority rule consensus tree (the critical value for the topological convergence diagnostic is 0.01).

The phylogenetic tree was visualized with FigTree version 1.4.0 (Rambaut 2012) and made in Adobe Illustrator CS5 (Adobe Systems Inc., USA). Sequences derived in this study were deposited in GenBank (<http://www.ncbi.nlm.nih.gov>). The final sequence alignments and the phylogenetic trees are available at TreeBase (<http://www.treebase.org>, accession number: 28875).

Results

Phylogenetic analyses

The dataset composed of ITS, TEF1- α and RPB2 genes, comprising a total of 2092 characters including gaps, ITS (1–656 bp), TEF1- α (657–1192 bp) and RPB2 (1193–2092 bp), including 57 taxa with *Tomophagus colossus* (Fr.) C.F. Baker as the out-group taxon (Wang et al. 2009; Cao et al. 2012). Best model for the combined 3-gene dataset estimated and applied in the Bayesian analysis was GTR+I+G, lset nst = 6, rates = invgamma; prset statefreqpr = dirichlet (1,1,1,1). The phylogenetic analysis of ML and BI produce similar topology. The combined dataset analysis of RAxML generates a best-scoring tree (Figure 1), with the final ML optimization likelihood value of -13861.891117. The aligned matrix had 993 distinct alignment patterns, with 38.83% completely undetermined characters or gaps. The base frequency and rate are as follows: A = 0.215319, C = 0.266028, G = 0.260220, T = 0.258433; rate AC = 0.885915, AG = 5.586021, AT = 0.936363, CG = 1.205084, CT = 6.595971, GT = 1.000000; gamma distribution shape: α = 0.246210. Bootstrap support values with a maximum likelihood (ML) greater than 70%, and Bayesian posterior probabilities (BPP) greater than 0.95 are given above the nodes (Figure 1).

Phylogenetic analysis showed that five collections clustered together with high bootstrap support, forming a clade sister to *G. shanxiense* with strong bootstrap support (ML-BS = 96%, BPP = 1.00, Figure 1). Two other collections clustered with *G. aridicola*, *G. bambusicola*, *G. casuarinicola*, *G. calidohilum*, *G. enigmaticum* and *G. thailandicum* (ML-BS = 100%, BPP = 1.00), but forming as a distinct lineage.

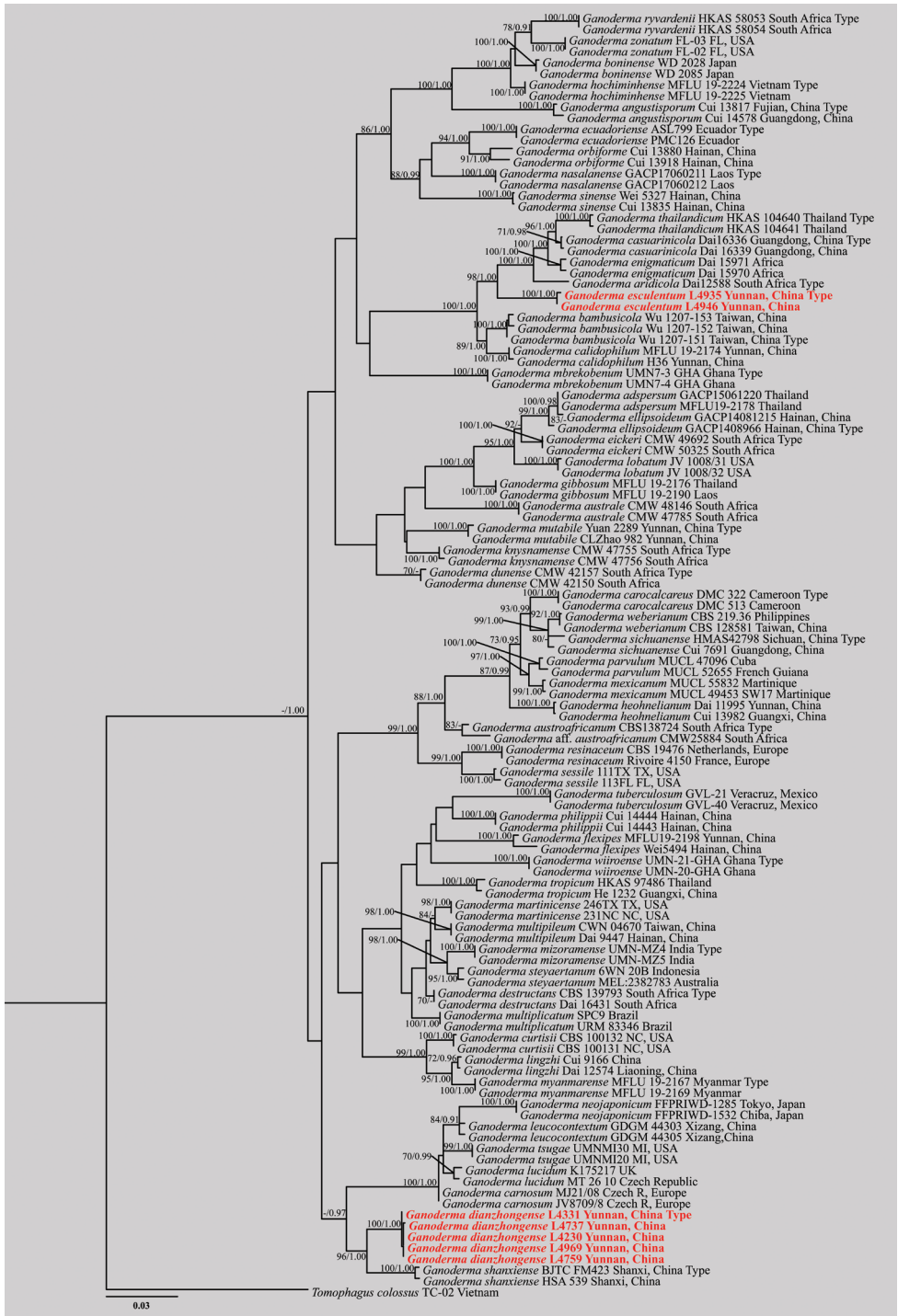


Figure 1. Phylogeny of the new *Ganoderma* species and related taxa based on ITS, TEF1- α and RPB2 sequence data. Branches are labeled with bootstrap values (ML) higher than 70%, and posterior probabilities (BPP) higher than 0.95. The new species are shown in bold red.

Taxonomy

Ganoderma dianzhongense J. He, H.Y. Su & S.H. Li, sp. nov.

Index Fungorum number: 558822

MycoBank No: 841408

Figure 2

Diagnosis. *Ganoderma dianzhongense* is characterized by its mesopodal basidiomata, oxblood red to violet brown pileus surface, melon seed kernel-shaped and broadly ellipsoid basidiospores.

Holotype. CHINA. Yunnan Province, Kunming City, Luquan County, on the rotten broad-leaved trees, alt. 2480 m, Shu-Hong Li, 8 Sept. 2016, L4331 (HKAS 110005).

Etymology. The epithet 'dianzhong' refers to central Yunnan province in Chinese, where the holotype was collected.

Description. **Basidiomata** annual, stipitate, sub-mesopodal to mesopodal or with the back sides fused, coriaceous to woody. **Pileus** single, suborbicular to reniform, up to 4.8–13.1 cm diam., 1.1 cm thick, weakly to strongly laccate, glossy and shiny, oxblood red (9E7) to violet brown (11F8), smooth, and covered by a thin hard crust, concentrically zonate or azonate. **Margin** distinct, slightly obtuse. **Stipe** 9.0–17.7 × 1.1–1.9 cm, central, cylindrical, strongly laccate, dark red brown (11C8) to purplish (14A8) or almost blackish red-brown (10F4), fibrous to woody. **Context** up to 0.4 cm thick, duplex; lower layer dark brown (8F8), fibrous, composed of coarse loose fibrils; upper layer putty (4B2); corky to woody, bearing distinct concentric growth zones, without black melanoid band. **Tubes** woody hard, grayish brown, up to 0.9 cm long, unstratified. **Pore** 4–6 per mm, round to angular, dissepiments slightly thick, entire; pore surface grey white to lead gray (2D2), turning light buff when dust (5D1).

Hyphal system trimitic. Generative hyphae 2.0–3.5 µm in diameter, colorless, thin-walled, clamp connections present; skeletal hyphae 3.0–6.0 µm in diameter, subthick-walled to solid, non-septate, arboriform with few branches, yellowish to golden-yellow; binding hyphae 1–2.5 µm in diameter, thick-walled, frequently branched, interwoven, hyaline to yellowish, scarce; all the hyphae IKI–, CB+; tissues darkening in KOH.

Pileipellis a crustohymeniderm, cells 20–45 × 5.5–7.5 µm, clavate to cylindrical, entire or rarely with one lateral protuberance, thick-walled, without granulations in the apex, golden-yellow to yellowish-brown, thick-walled, moderately amyloid at maturity.

Basidiospores (80/6/3) (9.0) 10–**11.0**–12.0 (12.5) × (6.5) 7.0–**7.9**–8.5 (9.0) µm, Q = (1.12) 1.25–1.55 (1.63), Q_m = 1.40±0.09 (including myxosporium); holotype: (40/2/1) 10.0–**10.9**–12 × 7.0–**7.9**–8.5 (9.0) µm, Q = (1.20) 1.25–1.52, Q_m = 1.39±0.08 (including myxosporium). mostly melon seed-shaped at maturity to broadly ellipsoid, usually with one end tapering and obtuse at maturity, with apical germ pore, yellowish to medium brown, IKI–, CB+, inamyloid; perisporium wrinkled, double-walled, with coarse interwall pillars. **Basidia** widely clavate to utriform, hyaline, with a clamp connection and four sterigmata, 11–19 × 10–13 µm; basidioles pear-shaped to fusiform, 10–15 × 8–12 µm.

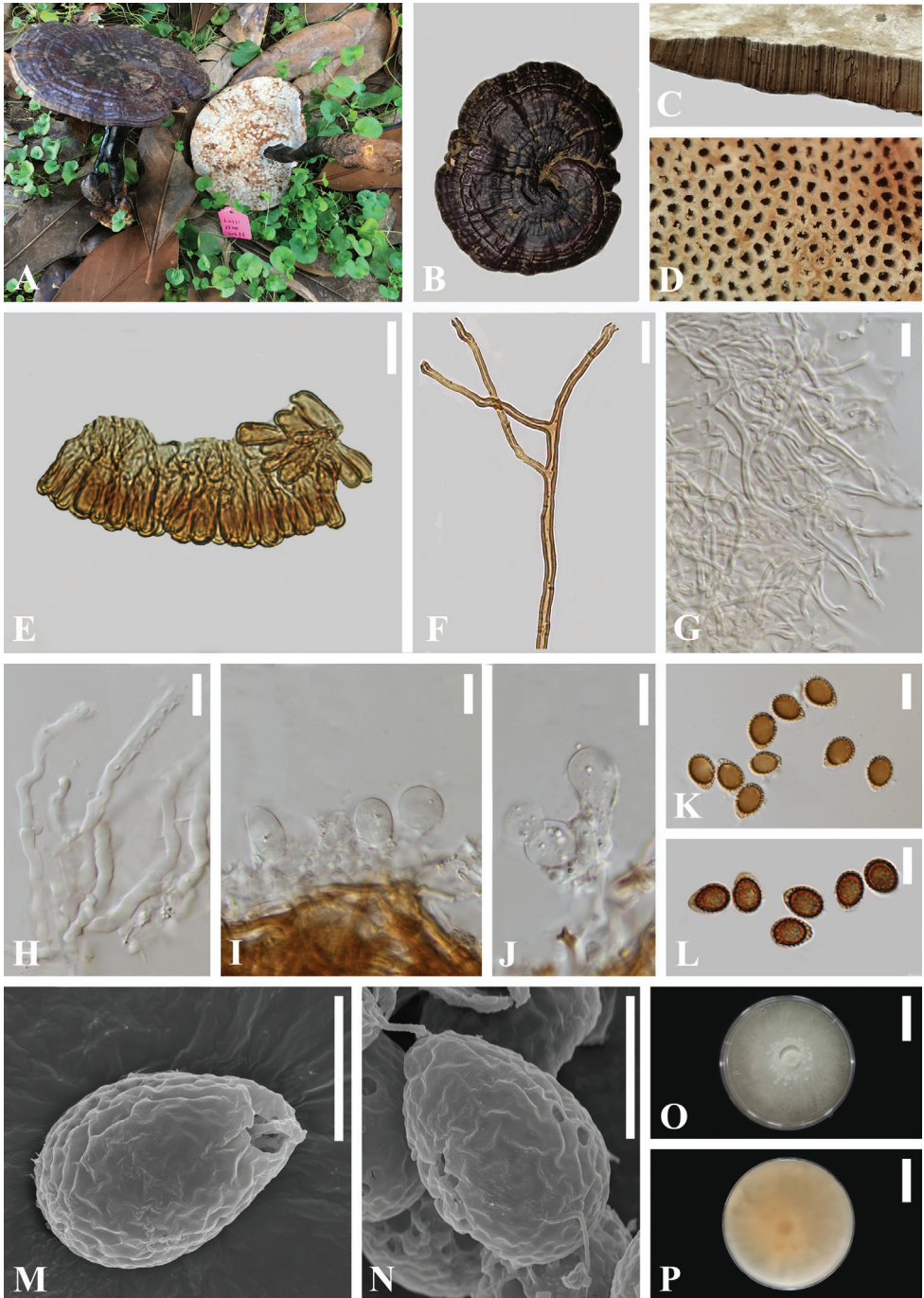


Figure 2. *Ganoderma dianzhongense* (HKAS 110005, holotype) **A** basidiomata **B** upper surface **C** cut side of pileus **D** pore surface **E** sections of pileipellis (LM) **F** skeletal hyphae from context (LM) **G** binding hyphae from tubes (LM) **H** generative hyphae from tubes (LM) **I–J** basidia and basidioles (LM) **K–L** basidiospores (LM) **M–N** basidiospores (SEM) **O–P** culture after incubation at 28 °C for 8 days. Scale bars: 20 mm (**O, P**); 10 μ m (**E–L**); 5 μ m (**M, N**). Photographs Jun He.

Habit. Scattered, during fall, decaying wood of broad-leaved trees including *Quercus* sp. Currently, only known from central Yunnan province, China.

Additional specimens examined. CHINA Yunnan province, Shilin County, alt. 2109m, Jun He, 28 Aug., 2019, L4969 (HKAS 112719); Songming County, alt. 2204m, Shu-Hong Li, 8 Jul., 2016, L4230 (HKAS 112716); Wuding County, alt. 2295m, Shu-Hong Li, 24 Jul., 2019, L4737 (HKAS 112717); *ibid.*, alt. 2432m, Jun He, 26 Jul., 2019, L4759 (HKAS 112718).

***Ganoderma esculentum* J. He & S.H. Li, sp. nov.**

Index Fungorum number: 558823

Mycobank No: 841409

Figure 3

Diagnosis. *Ganoderma esculentum* is characterized by its strongly laccate chocolate brown pileus surface, slender stipe and narrow ellipsoid basidiospores.

Holotype. CHINA. Yunnan Province, Honghe City, Mengzi County, on a decaying wood log, alt. 1370 m, Jun He, 26 Aug., 2019, L4935 (HKAS 110006).

Etymology. The epithet ‘*esculentum*’ refers to this species named after a food.

Description. **Basidiomata** annual, stipitate, pleuropodal, laccate, woody-corky. **Pileus** single, sub-orbicular to reniform to spathulate, up to 2.8–8.0 × 2.0–4.5 cm diam, 0.75 cm thick at the base, slightly convex to applanate; surface glabrous, rugose to radially rugose, strongly laccate, not cracking, with a hard crust, difficult to penetrate with the fingernail; surface brownish-black (6C8) to chocolate brown (6F4), almost homogeneous in the adult. **Margin** grayish orange(6B5) to concolorous, entire, acute to obtuse, smooth to sulcate. **Stipe** 10.0–17.5 × 0.5–1.0 cm, dorsally lateral to nearly dorsal, sub-cylindrical, solid, surface smooth, very shiny, dark brown (8F8) almost black, darker than pileus, fibrous to woody. **Context** up to 0.2 cm thick, composed of coarse loose fibrils, dark brown (8F8), with black melanoid band. **Tubes** 0.2–0.5 cm long, dark brown, woody hard, unstratified. **Pore** 5–8 per mm, circular or sub-circular, woody; pore surface white when fresh, darkening to soot brown(5F5) when aging and drying.

Hyphal system trimitic. Generative hyphae 1.5–3.0 μm in diameter, colorless, thin-walled, clamp connections present; skeletal hyphae 3.5–5.5 μm in diameter, thick-walled to solid, non-septate, arboriform or not, non-branched or with a few branches in the distal end, golden brown; binding hyphae 1.0–3.0 μm in diameter, thick-walled, much-branched, arboriform, hyaline to yellowish, scarce; all the hyphae IKI–, CB+; tissues darkening in KOH.

Pileipellis a crustohymeniderm, cells 20–55 × 10–15 μm, narrowly clavate to tubular, generally smooth, slightly thick-walled to thick-walled with a wide lumen, occasionally expanded at the apex, without granulations, entire, yellowish to leather brown, weakly to strongly amyloid.

Basidiospores (40/3/2) (8.0) 9.0–10.6–12.5 × (5.0) 5.5–6.6–7.5 (8.0) μm, $Q = (1.15) 1.34\text{--}1.62\text{--}2.01 (2.06)$, $Q_m = 1.62 \pm 0.19$ (including myxosporium); holo-

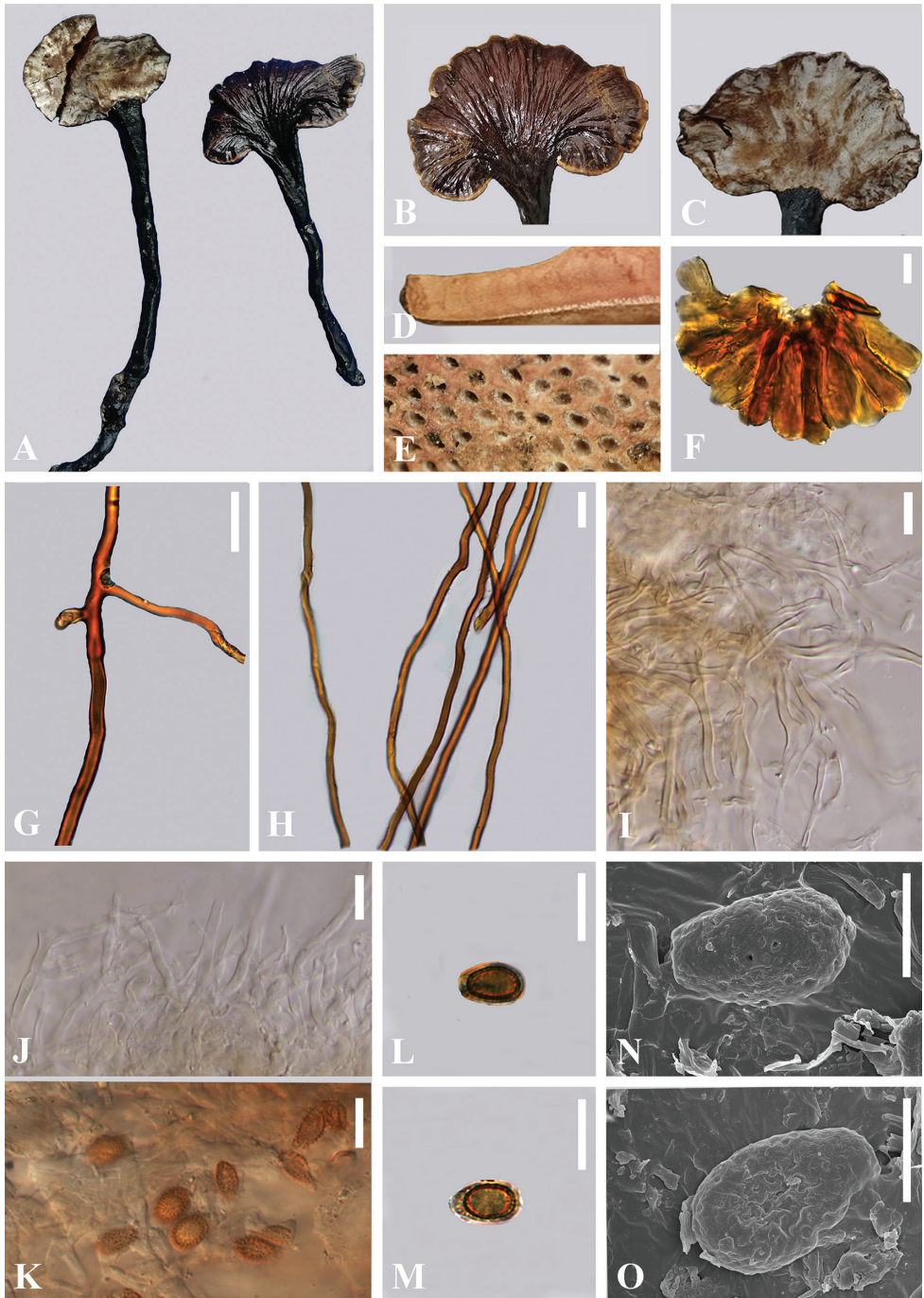


Figure 3. *Ganoderma esculentum* holotype (HKAS 110006) **A** basidiomata **B** upper surface **C** lower surface **D** cut side of pileus **E** pore surface **F** sections of pileipellis (LM) **G, H** skeletal hyphae from context (LM) **I** binding hyphae from tubes (LM) **J** generative hyphae from tubes (LM) **K–M** basidiospores (LM) **N, O** basidiospores (SEM). Scale bars: 20 μm (**H**); 10 μm (**F, G, I–M**); 5 μm (**N, O**). Photographs Jun He.

type: (20/2/1) 9.0–**10.6**–12.5 × (5.0) 5.5–**6.5**–7.0 (8.0) μm , $Q = (1.34) 1.45$ –**1.64**–1.83 (2.06), $Q_m = 1.64 \pm 0.15$ (including myxosporium). narrow ellipsoid to truncate, slightly visible apical germ pore, brownish orange to light brown, IKI–, CB+, inamyloid; with a brown eusporium bearing fine, overlaid by a hyaline myxosporium, with interwall pillars. **Basidia** not observed.

Habit. On decaying hardwood trees or bamboo roots, accompanied in humus rich soil with over heavily rotted litter on the ground.

Additional specimens examined. CHINA. Yunnan province, Mengzi City, Xinasuo Town, alt. 1328m, Jun He, 26 Aug., 2019, L4946 (HKAS 112720).

Discussion

Ganodermataceae is a large family of polypores, and has received great attention from mycologists for over many decades. However, species identification and circumscriptions have been unclear and taxonomic segregation of the genera has been controversial because of different viewpoints among mycologists (Moncalvo et al. 1995; Moncalvo and Ryvarden 1997; Costa-Rezende et al. 2020). Ganodermataceae was treated as a synonym of Polyporaceae and classify the genus *Ganoderma* into Polyporaceae by Justo et al. (2017). Later, Cui et al. (2019) excluded *Ganoderma* from Polyporaceae, due to *Ganoderma* having unique double-walled basidiospores. In addition, recent studies have clarified some uncertainties of generic delimitation and classification of polypores with ganodermatoid basidiospores, and proved that Ganodermataceae is a monophyletic group (Costa-Rezende et al. 2020). More collections of this family are needed in order to estimate the attributes of this taxon better.

In the phylogenetic inferences, *Ganoderma dianzhongense* is sister to *G. shanxiense*, which is known from the northern Shanxi province in China (Figure 1). Morphologically, both species share similar characters of the mesopodal basidiomata, suborbicular to reniform pileus, and broadly ellipsoid basidiospores (Table 2). However, *G. shanxiense* differs from *G. dianzhongense* in having a red to reddish-brown pileus surface, wider basidiospores (11.0–13.0 × 8.0–9.5 μm), and narrower skeletal hyphae (2.5–5.0 μm , Liu et al. 2019).

Ganoderma dianzhongense resembles *G. sinense* and *G. orbiforme* in having suborbicular pileus (Table 2). However, *G. sinense* is characterized by wider basidiospores (9.5–13.4 × 7.0–10.2 μm) and slightly longitudinally crested basidiospores (Wang and Wu 2007) and a uniformly brown to dark brown context. *Ganoderma orbiforme* has a purplish black to light brown pileus, a variably brown context, irregularly digitated pileipellis cells, and ellipsoid to ovoid basidiospores (6.9–10.6 × 3.6–5.7 μm) with fine and short echinulae, and a subtropical to tropical distribution (Wang et al. 2014). *Ganoderma orbiforme* is also phylogenetically unrelated (Figure 1).

In our multi-locus phylogeny analysis (Figure 1), *G. aridicola*, *G. bambusicola*, *G. casuarinicola*, *G. calidohilum*, *G. enigmaticum*, *G. mbrekobenum*, *G. thailandicum* and *G. esculentum* formed a distinct lineage, and was clearly separated from other *Ganoderma* species. It is easy to distinguish them from the morphological characteristics. *Gano-*

Table 2. Morphological comparison of *Ganoderma dianzhongense* sp. nov., and *G. esculentum* sp. nov., with their closest relatives in the combined phylogeny.

Species	Shape	Context	Pileipellis cells	Pores	Basidiospores (µm)	Reference
<i>Ganoderma aridicola</i>	sessile dimidiate	context corky, fuscous, black melanoid band absent	moderately amyloid at maturity, 30–55 × 5–8 µm	6–8 per mm	9.7–11.2 × 7.0–7.8	Xing et al. 2016
<i>G. bambusicola</i>	stipitate, reniform to semicircular	context fairly homogeneous, brownish, 1–2 mm thick	clavate or cylindrical, 35–65 × 8–16 µm	5–6 per mm	11.0–12.5 × 6.5–7.5	Wu et al. 2020
<i>G. carnosum</i>	laterally to rarely eccentrically stipitate, dimidiate, orbicular to reniform	whitish and soft-corky context	amyloid elements up to 75 µm from clamp to the apex	3–4 per mm	10.0–13 × 7.0–8.5	Patouillard 1889
<i>G. calidophilum</i>	stipitate, round or half-round	duplex context, 0.1–0.3 cm thick	–	4–6 per mm	10.0–13.0 × 6.2–8.7	Zhao et al. 1979
<i>G. casuarinicola</i>	stipitate, sectorial to shell-shaped	context corky, black melanoid band absent.	moderately amyloid at maturity, 40–70 × 5–13 µm	4–6 per mm	8.3–11.5 × 4.5–7.0	Xing et al. 2018
<i>G. dianzhongense</i>	stipitate, suborbicular to reniform	dark brown context, black melanoid band present	amyloid elements, 20–45 × 5.5–7.5 µm	5–8 per mm	9.0–12.5 × 6.5–9.0	this study
<i>G. enigmaticum</i>	stipitate globular pileus	context soft, dark brown	amyloid elements 20–46 × 5.5–9 µm	3–5 per mm	8.0–11.0 × 3.5–6.0	Coetzee et al. 2015
<i>G. esculentum</i>	stipitate, reniform to spatulate	dark brown context, without black melanoid bands	weakly to strongly amyloid, 20–55 × 10–15 µm	4–6 per mm	8.0–12.5 × 5.0–8.0	this study
<i>G. kunmingense</i>	stipitate, spatulate or half-round	context wood color	–	4 per mm	7.5–10.5 × 6.0–9.0	Zhao 1989
<i>G. lucidum</i>	stipitate to sessile	thinner context of white to slightly cream color context	amyloid hyphal end cells up to 7–11 µm diam	4–5 per mm	7.7–11.5 × 5.2–8.4	Ryvarden and Gilbertson 1993
<i>G. leucocontextum</i>	stipitate, reniform to flabelliform	thinner context of white to slightly cream color	amyloid elements 30–60 × 8–10 µm	4–6 per mm	9.5–12.5 × 7.0–9.0	Li et al. 2015
<i>G. mbrekobenum</i>	stipitate, maroon to liver brown	–	–	4–6 per mm	8.0–11.5 × 6.0–8.0	Crous et al. 2016
<i>G. neojaponicum</i>	stipitate, reniform to suborbicular	0.5 cm thick, duplex	brownish orange, clavate like cells	3–5 per mm	9.1–13.5 × 5.7–8.9	Imazeki et al. 1939
<i>G. orbiforme</i>	sessile, flabelliform or spatulate	context up to 0.4–1.0 cm thick, triplex	composed of apically acanthus like branched cells	4–6 per mm	7.1–11.8 × 5.2–7.7	Ryvarden 2000
<i>G. sinense</i>	stipitate, dimidiate, suborbicular	soft and fibrous, dark brown	clavate like cells, dextrinoid	5–6 per mm	9.5–13.8 × 6.9–8.7	Zhao 1979
<i>G. shanxiense</i>	stipitate, reniform to dimidiate	brown context	25–30 × 7.5–8.5 µm	4–5 per mm	11.0–13.0 × 8.0–9.5	Liu et al. 2019
<i>G. tsugae</i>	centrally to laterally stipitate, sub-dimidiate to dimidiate	whitish and soft corky context	60–75 × 7–10 µm	4–6 per mm	13.0–15.0 × 7.5–8.5	Murrill 1902
<i>G. thailandicum</i>	stipitate, greyish-red to brownish-red	context mostly brownish-red to reddish-brown	clavate to narrowly clavate, tuberculate	4–8 per mm	6.8–10.2 × 5.8–7.7	Luangharn et al. 2019

derma bambusicola has a longer pileipellis (35–65 × 8–16 µm) and wider basidiospores than those of *G. esculentum* (10.0–13.0 × 6.5–8.0 µm, Wu et al. 2020). *Ganoderma aridicola* can be easily distinguished from *G. esculentum* by the sessile basidiomata and a fuscous to black pileus surface (Xing et al. 2016). *Ganoderma casuarinicola* differs from

G. esculentum by the latter has smaller basidiospores ($8.3\text{--}11.5 \times 4.5\text{--}7.0 \mu\text{m}$, Xing et al. 2018), grayish brown longer pores and sectorial to shell-shaped pileus. *Ganoderma enigmaticum* mainly differs from *G. esculentum* by its golden yellow pileus surface, narrower basidiospores ($8.0\text{--}11.0 \times 3.5\text{--}6.0 \mu\text{m}$, Coetzee et al. 2015) and causes root and butt rot of living and dead trees. *Ganoderma thailandicum* can be distinguished from *G. esculentum*, by its brownish-red pileus surface without radially rugose, narrowly clavate pileipellis cells with tuberculate and smaller basidiospores ($6.8\text{--}10.2 \times 5.8\text{--}7.7 \mu\text{m}$, Luangharn et al. 2019). *Ganoderma mbrekobenum* can be differentiated from *G. esculentum* by its woody to corky texture when dried, with ovoid basidiospores ($25.0\text{--}57.0 \times 6.0\text{--}12.0 \mu\text{m}$, Crous et al. 2016). *Ganoderma calidophilum* has a larger diameter binding hypha ($2.4\text{--}5.2 \mu\text{m}$) than *G. esculentum* ($1.0\text{--}3.0 \mu\text{m}$) and *G. calidophilum* has larger basidiospores ($7.3\text{--}14.6 \times 5.3\text{--}9.6 \mu\text{m}$, Zhao et al. 1979; Luangharn et al. 2021) than *G. esculentum* (including myxosporium).

Morphologically, *G. esculentum* resemble *G. kunmingense* by radially rugose, the pileus and slender stipe (Table 2). However, *G. kunmingense* has narrower hyphae, tissues not darkening in KOH, and broadly ellipsoid to sub-globose basidiospores ($7.5\text{--}10.5 \times 6.0\text{--}9.0 \mu\text{m}$, Zhao et al. 1989). In addition, *G. esculentum* shares also similarities with *G. neojaponicum* but the latter has a double-layered context with the paler layer near the pileus surface and wider basidiospores than those of *G. esculentum* ($9.1\text{--}13.5 \times 5.7\text{--}8.9 \mu\text{m}$, Imazeki et al. 1939; Hapuarachchi et al. 2019).

Acknowledgements

The authors thank Kunming Institute of Botany for providing the experimental platform. Dr Xiang-Hua Wang helped to analyze the molecular data and molecular lab work. We also thank Dr. Dan-Feng Bao and Hong-Wei Shen for their valuable suggestions on this study.

The research was financed by the National Natural Science Foundation of China (Project No. 31970021, 32060006), Yunnan Financial Special Project [YCJ (2020)323, 202102AE090036–05], Yunnan Science Technology Department and Technology Talents and Platform Program “Yunnan Province Technology Innovation Talents Training Objects” (Project ID 2017HB084) and Science and technology innovation and R&D promotion project of Qamdo City.

References

- Ahmadi K, Riazipour M (2007) Effect of *Ganoderma lucidum* on Cytokine Release by Peritoneal Macrophages. *Iranian Journal of Immunology* 4: 220–226.
- Bolaños AC, Bononi VLR, de Mello Gugliotta A (2016) New records of *Ganoderma multiplicatum* (Mont.) Pat. (Polyporales, Basidiomycota) from Colombia and its geographic distribution in South America. *Check List* 12: 1–7. <https://doi.org/10.15560/12.4.1948>

- Cabarroi-Hernández M, Villalobos-Arámbula AR, Torres-Torres MG, Decock C, Guzmán-Dávalos L (2019) The *Ganoderma weberianum-resinaceum* lineage: multilocus phylogenetic analysis and morphology confirm *G. mexicanum* and *G. parvulum* in the Neotropics. MycoKeys 59: 95–131. <https://doi.org/10.3897/mycokeys.59.33182>
- Cao Y, Wu SH, Dai YC (2012) Species clarification of the prize medicinal *Ganoderma* mushroom “Lingzhi”. Fungal Diversity 56: 49–62. <https://doi.org/10.1007/s13225-012-0178-5>
- Cao Y, Yuan HS (2013) *Ganoderma mutabile* sp. nov. from southwestern China based on morphological and molecular data. Mycological Progress 12: 121–126. <https://doi.org/10.1007/s11557-012-0819-9>
- Chan WK, Law HK, Lin ZB, Lau YL, Chan GC (2007) Response of human dendritic cells to different immunomodulatory polysaccharides derived from mushroom and barley. International Immunopharmacology 19: 891–899. <https://doi.org/10.1093/intimm/dxm061>
- Coetzee MP, Marincowitz S, Muthelo VG, Wingfield MJ (2015) *Ganoderma* species, including new taxa associated with root rot of the iconic *Jacaranda mimosifolia* in Pretoria, South Africa. IMA Fungus 6: 249–256. <http://doi.org/10.5598/imafungus.2015.06.01.16>
- Corner EJJ (1983) Ad Polyporaceas I. *Amauroderma* and *Ganoderma*. Beihefte zur Nova Hedwigia, Weinheim.
- Costa-Rezende DH, Robledo GL, Goes-Neto A, Reck MA, Crespo E, Drechsler-Santos ER (2017) Morphological reassessment and molecular phylogenetic analyses of *Amauroderma* s.lat. r-aised new perspectives in the generic classification of the Ganodermataceae family. Persoonia 39: 254–269. <https://doi.org/10.3767/persoonia.2017.39.10>
- Costa-Rezende DH, Robledo GL, Drechsler-Santos ER, Glen M, Gates G, de Madriagnac BR, Popoff OF, Crespo E, Góes-Neto A (2020) Taxonomy and phylogeny of polypores with ganodermatoid basidiospores (Ganodermataceae). Mycological Progress 19: 725–741. <https://doi.org/10.1007/s11557-020-01589-1>
- Crous PW, Wingfield MJ, Le Roux JJ, Richardson DM, Strasberg D, Shivas RG, Alvarado P, Edwards J, Moreno G, Sharma R, Sonawane MS, Tan Y-P, Altés A, Barasubiye T, Barnes CW, Blanchette RA, Boertmann D, Bogo A, Carlavilla JR, Cheewangkoon R, Daniel R, de Beer ZW, de Jesús Yáñez-Morales M, Duong TA, Fernández-Vicente J, Geering ADW, Guest DI, Held BW, Heykoop M, Hubka V, Ismail AM, Kajale SC, Khemmuk W, Kolařík M, Kurli R, Lebeuf R, Lévesque CA, Lombard L, Magista D, Manjón JL, Marincowitz S, Mohedano JM, Nováková A, Oberlies NH, Otto EC, Paguigan ND, Pascoe IG, Pérez-Butrón JL, Perrone G, Rahi P, Raja HA, Rintoul T, Sanhueza RMV, Scarlett K, Shouche YS, Shuttleworth LA, Taylor PWJ, Thorn RG, Vawdrey LL, Vidal RS, Voitk A, Wong PTW, Wood AR, Zamora JC, Groenewald JZ (2015) Fungal Planet Description Sheets: 371–399. Persoonia 35: 264–327. <https://doi.org/10.3767/003158515X690269>
- Crous PW, Wingfield MJ, Richardson DM, Le Roux JJ, Strasberg D, Edwards J, Roets F, Hubka V, Taylor PWJ, Heykoop M, Martín MP, Moreno G, Sutton DA, Wiederhold NP, Barnes CW, Carlavilla JR, Gené J, Giraldo A, Guarnaccia V, Guarro J, Hernández-Restrepo M, Kolařík M, Manjón JL, Pascoe IG, Popov ES, Sandoval-Denis M, Woudenberg JHC, Acharya K, Alexandrova AV, Alvarado P, Barbosa RN, Baseia IG, Blanchette RA, Boekhout T, Burgess TI, Cano-Lira JF, Čmoková A, Dimitrov RA, Dyakov MYu, Dueñas M, Dutta

- AK, Esteve-Raventós F, Fedosova AG, Fournier J, Gamboa P, Gouliamova DE, Grebenc T, Groenewald M, Hanse B, Hardy GESTJ, Held BW, Jurjević Ž, Kaewgrajang T, Latha KPD, Lombard L, Luangsa-ard JJ, Lysková P, Mallátová N, Manimohan P, Miller AN, Mirabolfathy M, Morozova OV, Obodai M, Oliveira NT, Ordóñez ME, Otto EC, Paloi S, Peterson SW, Phosri C, Roux J, Salazar WA, Sánchez A, Sarria GA, Shin H-D, Silva BDB, Silva GA, Smith MTh, Souza-Motta CM, Stchige AM, Stoilova-Disheva MM, Sulzbacher MA, Telleria MT, Toapanta C, Traba JM, Valenzuela-Lopez N, Watling R, Groenewald JZ (2016) Fungal planet description sheets: 400–468. *Persoonia* 36: 316–458. <https://doi.org/10.3767/003158516X692185>
- Crous PW, Wingfield MJ, Burgess TI, Hardy GESTJ, Barber PA, Alvarado P, Barnes CW, Buchanan PK, Heykoop M, Moreno G, Thangavel R, van der Spuy S, Barili A, Barrett S, Cacciola SO, Cano-Lira JF, Crane C, Decock C, Gibertoni TB, Guarro J, Guevara-Suarez M, Hubka V, Kolařík M, Lira CRS, Ordoñez ME, Padamsee M, Ryvarden L, Soares AM, Stchigel AM, Sutton DA, Vizzini A, Weir BS, Acharya K, Aloï F, Baseia IG, Blanchette RA, Bordallo JJ, Bratek Z, Butler T, Cano-Canals J, Carlavilla JR, Chander J, Cheewangkoon R, Cruz RHSE, da Silva M, Dutta AK, Ercole E, Escobio V, Esteve-Raventós F, Flores JA, Gené J, Góis JS, Haines L, Held BW, Jung MH, Hosaka K, Jung T, Jurjević Ž, Kautman V, Kautmanova I, Kiyashko AA, Kozanek M, Kubátová A, Lafourcade M, La Spada F, Latha KPD, Madrid H, Malysheva EF, Manimohan P, Manjón JL, Martín MP, Mata M, Merényi Z, Morte A, Nagy I, Normand AC, Paloi S, Pattison N, Pawłowska J, Pereira OL, Petterson ME, Picillo B, Raj KNA, Roberts A, Rodríguez A, Rodríguez-Campo FJ, Romański M, Ruszkiewicz-Michalska M, Scanu B, Schena L, Semelbauer M, Sharma R, Shouche YS, Silva V, Staniaszek-Kik M, Stielow JB, Tapia C, Taylor PWJ, Toome-Heller M, Vabeik-hokhei JMC, van Diepeningen AD, Van Hoa N, Van Tri M, Wiederhold NP, Wrzosek M, Zothanzama J, Groenewald JZ (2017) Fungal Planet description sheets: 558–624. *Persoonia* 38: 240–384. <https://doi.org/10.3767/003158517X698941>
- Cui BK, Li HJ, Ji X, Zhou JL, Song J, Si J, Yang ZL, Dai YC (2019) Species diversity, taxonomy and phylogeny of Polyporaceae (Basidiomycota) in China. *Fungal Diversity* 97: 137–392. <https://doi.org/10.1007/s13225-019-00427-4>
- Dai YC, Yang ZL, Cui BK, Yu CJ, Zhou LW (2009) Species diversity and utilization of medicinal mushrooms and fungi in China. *International Journal of Medicinal Mushrooms* 11: 287–302. <https://doi.org/10.1615/IntJMedMushr.v11i3.80>
- De Silva DD, Rapior S, Sudarman E, Stadler M, Xu J, Alias SA, Hyde KD (2013) Bioactive metabolites from macrofungi: ethnopharmacology, biological activities and chemistry. *Fungal Diversity* 62: 1–40. <https://doi.org/10.1007/s13225-012-0187-4>
- Donk MA (1948) Notes on Malesian fungi I. *Bulletin du Jardin Botanique de Buitenzorg Série* 317: 473–482.
- Douanla-Meli C, Langer E (2009) *Ganoderma carocalcareum* sp. nov., with crumbly-friable context parasite to saprobe on *Anthocleista nobilis* and its phylogenetic relationship in *G. resinaceum* group. *Mycological Progress* 8: 145–155. <https://doi.org/10.1007/s11557-009-0586-4>
- Doyle JJ, Doyle JL (1987) A rapid isolate procedure from small quantities of fresh leaf tissue. *Phytochemical Bulletin* 19: 11–15.

- Espinosa-García V, Mendoza G, Shnyreva VA, Padrón JM, Trigos Á (2021) Biological Activities of Different Strains of the Genus *Ganoderma* spp. (Agaricomycetes) from Mexico. *International Journal of Medicinal Mushrooms* 23:67–77. <https://doi.org/10.1615/IntJMedMushrooms.2021037451>
- Furtado JS (1981) Taxonomy of *Amauroderma* (Basidiomycetes, Polyporaceae). *Mem N Y Bot Gard* 34: 1–109.
- Glen M, Yuskianti V, Puspitasari D, Francis A, Agustini L, Rimbawanto A, Indrayadi H, Gafur A, Mohammed CL (2014) Identification of basidiomycete fungi in Indonesian hardwood plantations by DNA barcoding. *Forest Pathology* 44: 496–508. <https://doi.org/10.1111/efp.12146>
- Glez-Peña D, Gómez-Blanco D, Reboiro-Jato M, Fdez-Riverola F, Posada D (2010) ALTER: program-oriented conversion of DNA and protein alignments. *Nucleic Acids Research* 38: 14–18. <https://doi.org/10.1093/nar/gkq321>
- Hall TA (1999) BioEdit: a user-friendly biological sequence alignment editor and analysis program for Windows 95/98/NT. In: *Nucleic Acids Symposium Series* 41: 95–98.
- Hapuarachchi KK, Karunarathna SC, Phengsintham P, Yang HD, Kakumyan P, Hyde KD, Wen TC (2019) Ganodermataceae (Polyporales): Diversity in Greater Mekong Subregion countries (China, Laos, Myanmar, Thailand and Vietnam). *Mycosphere* 10: 221–309. <https://doi.org/10.5943/mycosphere/10/1/6>
- Hapuarachchi KK, Karunarathna SC, Raspé O, De Silva KHWL, Thawthong A, Wu XL, Kakumyan P, Hyde KD, Wen TC (2018) High diversity of *Ganoderma* and *Amauroderma* (Ganodermataceae, Polyporales) in Hainan Island, China. *Mycosphere* 9: 931–982. <https://doi.org/10.5943/mycosphere/9/5/1>
- He MQ, Zhao RL, Hyde KD, Begerow D, Kemler M, Yurkov A, McKenzie EHC, Raspé O, Kakishima M, Sánchez-Ramírez S, Vellinga EC, Halling R, Papp V, Zmitrovich IV, Buyck B, Ertz D, Wijayawardene NN, Cui BK, Schoutteten N, Liu XZ, Li TH, Yao YJ, Zhu XY, Liu AQ, Li GJ, Zhang MZ, Ling ZL, Cao B, Antonín V, Boekhout T, da Silva BDB, Crop ED, Decock C, Dima B, Dutta AK, Fell JW, Geml J, Ghobad-Nejhad M, Giachini AJ, Gibertoni TB, Gorjón SP, Haelewaters D, He SH, Hodkinson BP, Horak E, Hoshino T, Justo A, Lim YW, Menolli JN, Mešić A, Moncalvo JM, Mueller GM, Nagy LG, Nilsson RH, Noordeloos M, Nuytinck J, Orihara T, Ratchadawan C, Rajchenberg M, Silva-Filho AGS, Sulzbacher MA, Tkalčec Z, Valenzuela R, Verbeken A, Vizzini A, Wartchow F, Wei TZ, Weiß M, Zhao CL, Kirk PM (2019) Notes, outline and divergence times of Basidiomycota. *Fungal Diversity* 99: 105–367. <https://doi.org/10.1007/s13225-019-00435-4>
- Imazeki R (1939) Studies on *Ganoderma* of Nippon. *Bulletin of the Tokyo Science Museum* 1: 29–52.
- Justo A, Miettinen O, Floudas D, Ortiz-Santana B, Sjökvist E, Lindner DL, Nakasone K, Niemelä T, Larsson KH, Ryvarden L, Hibbett DS (2017) A revised family-level classification of the the Polyporales (Basidiomycota). *Fungal Biology* 121: 798–824. <https://doi.org/10.1016/j.funbio.2017.05.010>
- Karsten PA (1881) Enumeratio boletinearum et polyprocarum fennicarum, systemate novo dispositarum. *Revue de Mycologie* 3: 16–19.

- Katoh K, Standley DM (2013) MAFFT multiple sequence alignment software Version 7: Improvements in performance and usability. *Molecular Biology and Evolution* 30: 772–780. <https://doi.org/10.1093/molbev/mst010>
- Kinge TR, Mih AM (2011) *Ganoderma rywardense* sp. nov. associated with basal stem rot (BSR) disease of oil palm in Cameroon. *Mycosphere* 2: 179–188.
- Kornerup A, Wanscher JH (1978) *Methuen handbook of colour* (3rd edn.) Methuen. London, England. <https://doi.org/10.1079/9780851998268.0000>
- Li TH, Hu HP, Deng WQ, Wu SH, Wang DM, Tsering T (2015) *Ganoderma leucocontextum*, a new member of the *G. lucidum* complex from southwestern China. *Mycoscience* 56: 81–85. <https://doi.org/10.1016/j.myc.2014.03.005>
- Liu H, Guo LJ, Li SL, Fan L (2019) *Ganoderma shanxiense*, a new species from northern China based on morphological and molecular evidence. *Phytotaxa* 406: 129–136. <https://doi.org/10.11646/phytotaxa.406.2>
- Liu Yj, Whelen S, Hall BD (1999) Phylogenetic relationships among ascomycetes: evidence from an RNA polymerase II subunit. *Molecular Biology and Evolution* 16: 1799–1808. <https://doi.org/10.1093/oxfordjournals.molbev.a026092>
- Lloyd AL, Held BW, Barnes CW, Schink MJ, Smith ME, Smith JA, Blanchette RA (2018) Elucidating ‘*lucidum*’: distinguishing the diverse laccate *Ganoderma* species of the United States. *PLoS ONE* 13: e0199738. <https://doi.org/10.1371/journal.pone.0199738>
- Luangharn T, Karunarathna SC, Dutta AK, Paloi S, Lian CK, Huyen LT, Pham HND, Hyde KD, Xu JC, Mortimer PE (2021) *Ganoderma* (Ganodermataceae, Basidiomycota) species from the Greater Mekong Subregion. *Journal of Fungi* 7: 1–83. <https://doi.org/10.3390/jof7100819>
- Luangharn T, Karunarathna SC, Khan S, Xu JC, Mortimer PE, Hyde KD (2017) Antibacterial activity, optimal culture conditions and cultivation of the medicinal *Ganoderma austral*, new to Thailand. *Mycosphere* 8: 1108–1123. <https://doi.org/10.5943/myco-sphere/8/8/11>
- Luangharn T, Karunarathna SC, Mortimer PE, Kevin DH, Xu JC (2019) Additions to the knowledge of *Ganoderma* in Thailand: *Ganoderma casuarinicola*, a new record; and *Ganoderma thailandicum* sp. nov. *MycKeys* 59: 47–65. <https://doi.org/10.3897/mycokeys.59.36823>
- Matheny PB, Wang Z, Binder M, Curtis JM, Lim YW, Nilsson RH, Hughes KW, Petersen RH, Hofstetter V, Ammirati JF, Schoch C, Langer GE, McLaughlin DJ, Wilson AW, Crane PE, Frøslev T, Ge ZW, Kerrigan RW, Slot JC, Vellinga EC, Liang ZL, Aime MC, Baroni TJ, Fischer M, Hosaka K, Matsuura K, Seidl MT, Vaura J, Hibbett DS (2007) Contributions of *rpb2* and *tef1* to the phylogeny of mushrooms and allies (Basidiomycota, Fungi). *Molecular Phylogenetics and Evolution* 43: 430–451. <https://doi.org/10.1016/j.ympev.2006.08.024>
- Miller MA, Pfeiffer W, Schwartz T (2010) Creating the CIPRES Science Gateway for inference of large phylogenetic trees. *Proceedings of the Gateway Computing Environments Workshop (GCE)*, New Orleans, 8 pp. <https://doi.org/10.1109/GCE.2010.5676129>
- Moncalvo JM, Ryvarden L (1997) A nomenclatural study of the Ganodermataceae Donk. *Synopsis Fungorum* 11: 1–114.
- Moncalvo JM, Wang HF, Hseu RS (1995) Gene phylogeny of the *Ganoderma lucidum* complex based on ribosomal DNA sequences. Comparison with traditional taxonomic characters. *Mycological Research* 99: 1489–1499. [https://doi.org/10.1016/S0953-7562\(09\)80798-3](https://doi.org/10.1016/S0953-7562(09)80798-3)

- Murrill, WA (1902) The Polyporaceae of North America: I. The genus *Ganoderma*. Bull Torrey BotClub 29: 599–608. <https://doi.org/10.2307/2478682>
- Nylander JAA, Wilgenbusch JC, Warren DL, Swofford DL (2008) AWTY (are we there yet?): a system for graphical exploration of MCMC convergence in Bayesian phylogenetics. Bioinformatics 24: 581–583. <https://doi.org/10.1093/bioinformatics/btm388>
- Paterson RR (2006) *Ganoderma*– a therapeutic fungal biofactory. Phytochemistry 67: 1985–2001. <https://doi.org/10.1016/j.phytochem.2006.07.004>
- Patouillard N (1889) Le genre *Ganoderma*. Bulletin de la Société Mycologique de France 5: p64.
- Pilotti CA, Sanderson FR, Aitken AB, Armstrong W (2004) Morphological variation and hostrange of two *Ganoderma* species from Papua New Guinea. Mycopathologia 158: 251–265. <https://doi.org/10.1023/B:MYCO.0000041833.41085.6f>
- Rambaut A (2012) FigTree version 1.4.0. <http://tree.bio.ed.ac.uk/software/figtree/>
- Rannala B, Yang Z (1996) Probability distribution of molecular evolutionary trees: a new method of phylogenetic inference. Journal of molecular evolution 43: 304–311. <https://doi.org/10.1007/BF02338839>
- Richter C, Wittstein K, Kirk PM, Stadler M (2015) An assessment of the taxonomy and chemotaxonomy of *Ganoderma*. Fungal Diversity 71: 1–15. <https://doi.org/10.1007/s13225-014-0313-6>
- Ronquist F, Teslenko M, van der Mark P, Ayres DL, Darling A, Höhna S, Larget B, Liu L, SuchardMA, Huelsenbeck JP (2012) MrBayes 3.2: efficient Bayesian phylogenetic inference and model choice across a large model space. Systematic Biology 61: 539–542. <https://doi.org/10.1093/sysbio/sys029>
- Ryvarden L (2000) Studies in neotropical polypores 2: a preliminary key to neotropical species of *Ganoderma* with a laccate pileus. Mycologia 92: 180–191. <https://doi.org/10.2307/3761462>
- Ryvarden L (2004) Neotropical polypores part 1. Synop Fung 19: 1–227.
- Ryvarden L, Gilbertson RL (1993) European polypores. Part 1. *Abortiporus Lindtneria*. Synopsis Fungorum 6: 1–387.
- Song J, Xing JH, Decock C, He XL, Cui BK (2016) Molecular phylogeny and morphology reveal a new species of *Amauroderma* (Basidiomycota) from China. Phytotaxa 260: 47–56. <https://doi.org/10.11646/phytotaxa.260.1.5>
- Steyaert RL (1972) Species of *Ganoderma* and related genera mainly of the Bogor and Leiden Herbaria. Persoonia 7: 55–118.
- Sun YF, Costa-Rezende DH, Xing JH, Zhou JL, Zhang B, Gibertoni TB, Gates G, Glen M, Dai YC, Cui BK (2020) Multi-gene phylogeny and taxonomy of *Amauroderma* s. lat. (Ganodermataceae). Persoonia 44: 206–239. <https://doi.org/10.3767/persoonia.2020.44.08>
- Swofford DL (2003) PAUP*: phylogenetic analysis using parsimony (*and other methods). Sinauer Associates, Sunderland, Massachusetts. <http://ci.nii.ac.jp/naid/110002665463/>
- Tchoumi JMT, Coetzee MPA, Rajchenberg M, Roux J (2019) Taxonomy and species diversity of *Ganoderma* species in the Garden Route National Park of South Africa inferred from morphology and multilocus phylogenies. Mycologia 111: 730–747. <https://doi.org/10.1080/00275514.2019.1635387>
- Tchoumi JMT, Coetzee MPA, Rajchenberg M, Wingfield MJ, Roux J (2018) Three *Ganoderma* species, including *Ganoderma dunense* sp. nov., associated with dying *Acacia cyclops*

- trees in South Africa. *Australasian Plant Pathology* 47: 431–447. <https://doi.org/10.1007/s13313-018-0575-7>
- Tham LX, Hung NLQ, Duong PN, Hop DV, Dentinger BTM, Moncalvo J (2012) *Tomophagus cattienensis* sp.nov., an ew Ganodermataceae species from Vietnam: evidence from morphology and ITS DNA barcodes. *Mycological Progress* 11: 775–780. <https://doi.org/10.1007/s11557-011-0789-3>
- Wang DM, Wu SH (2007) Two species of *Ganoderma* new to Taiwan. *Mycotaxon* 102: 373–378.
- Wang DM, Wu SH, Su CH, Peng JT, Shih YH, Chen LC (2009) *Ganoderma multipileum*, the correct name for “*G. lucidum*” in tropical Asia. *Botanical Studies* 50: 451–458.
- Wang DM, Wu SH, Yao YJ (2014) Clarification of the concept of *Ganoderma orbiforme* with high morphological plasticity. *PLoS ONE* 9: e98733. <https://doi.org/10.1371/journal.pone.0098733>
- Wang DW, Wu SH (2010) *Ganoderma hoehnelianum* has priority over *G. shangsiense*, and *G. williamsianum* over *G. meijiangense*. *Mycotaxon* 113: 343–349. <https://doi.org/10.5248/113.343>
- Wang XH, Buyck B, Verbeken A, Hansen K (2015) Revisiting the morphology and phylogeny of *Lactifluus* with three new lineages from southern China. *Mycologia* 107: 941–958. <https://doi.org/10.3852/13-393>
- White TJ, Bruns T, Lee S, Taylor J (1990) Amplification and direct sequencing of fungal ribosomal RNA genes for phylogenetics. In: Innis MA, Gelfand DH, Sninsky JJ, White TJ (Eds) *PCR protocols: a guide to methods and applications*. Academic, San Diego, New York, pp 315–322. <https://doi.org/10.1016/B978-0-12-372180-8.50042-1>
- Wu SH, Chern CL, Wei CL, Chen YP, Akiba M, Hattori T (2020) *Ganoderma bambusicola* sp. nov. (Polyporales, Basidiomycota) from southern Asia. *Phytotaxa* 451: 75–85. <https://doi.org/10.11646/phytotaxa.456.1.5>
- Xing JH, Song J, Decock C, Cui BK (2016) Morphological characters and phylogenetic analysis reveal a new species within the *Ganoderma lucidum* complex from South Africa. *Phytotaxa* 266: 115–124. <https://doi.org/10.11646/phytotaxa.266.2.5>
- Xing JH, Sun YF, Han YL, Cui BK, Dai YC (2018) Morphological and molecular identification of two new *Ganoderma* species on *Casuarina equisetifolia* from China. *MycoKeys* 34: 93–108. <https://doi.org/10.3897/mycokeys.34.22593>
- Zhao JD (1989) Studies on the Taxonomy of Ganodermataceae in China XI. *Acta Mycologica Sinica* 8: 25–34. [In Chinese]
- Zhao JD, Hsu LW, Zhang XQ (1979) Taxonomic studies on the subfamily Ganodermoideae of China. *Acta Mycologica Sinica* 19: 265–279. [In Chinese]
- Zhao JD, Zhang XQ (2000) *Flora Fungorum Sinicorum* 18. Ganodermataceae. Science Press, Beijing. [In Chinese]
- Zhaxybayeva O, Gogarten JP (2002) Bootstrap, Bayesian probability and maximum likelihood mapping: exploring new tools for comparative genome analyses. *BMC Genomics* 3: e4. <https://doi.org/10.1186/1471-2164-3-4>
- Zhou LW, Cao Y, Wu SH, Vlasák J, Li DW, Li MJ, Dai YC (2015) Global diversity of the *Ganoderma lucidum* complex (Ganodermataceae, Polyporales) inferred from morphology and multilocus phylogeny. *Phytochemistry* 114: 7–15. <https://doi.org/10.1016/j.phytochem.2014.09.023>

Supplementary material I

Phylogenetic sequence dataset

Authors: Jun He

Data type: phylogenetic data

Explanation note: Sequence data of three partial loci internal transcribed spaces region (ITS), RNA polymerase II subunit 2 (RPB2), and translation elongation factor 1-alpha (TEF1- α) were used in the phylogenetic analyses.

Copyright notice: This dataset is made available under the Open Database License (<http://opendatacommons.org/licenses/odbl/1.0/>). The Open Database License (ODbL) is a license agreement intended to allow users to freely share, modify, and use this Dataset while maintaining this same freedom for others, provided that the original source and author(s) are credited.

Link: <https://doi.org/10.3897/mycokeys.84.69449.suppl1>

Two new lecanoroid lichen species from the forested wetlands of South Korea, with a key for Korean *Protoparmeliopsis* species

Beeyoung Gun Lee¹, Jae-Seoun Hur²

1 Baekdudaegan National Arboretum, Bonghwa 36209, South Korea **2** Korean Lichen Research Institute, Suncheon National University, Suncheon 57922, South Korea

Corresponding authors: Beeyoung Gun Lee (gitanoblue@koagi.or.kr), Jae-Seoun Hur (jshur1@scnu.ac.kr)

Academic editor: Xinli Wei | Received 29 June 2021 | Accepted 6 October 2021 | Published 12 November 2021

Citation: Lee BG, Hur J-S (2021) Two new lecanoroid lichen species from the forested wetlands of South Korea, with a key for Korean *Protoparmeliopsis* species. MycoKeys 84: 163–183. <https://doi.org/10.3897/mycokeys.84.70798>

Abstract

Lecanora parasymmicta Lee & Hur and *Protoparmeliopsis crystalliniformis* Lee & Hur are described as new lichen species to science from the forested wetlands in southern South Korea. Molecular analyses employing internal transcribed spacer (ITS) and mitochondrial small subunit (mtSSU) sequences strongly support the two lecanoroid species to be distinct in their genera. *Lecanora parasymmicta* is included in the *Lecanora symmicta* group. It is morphologically distinguished from *Lecanora symmicta* (Ach.) Ach., its most similar species, by areolate-rimose thallus, blackish hypothallus, larger apothecia, absence of thal-line excipulum from the beginning, narrower paraphyses, larger ascospores, smaller pycnoconidia, and the presence of placodiolic acid. The second new species *Protoparmeliopsis crystalliniformis* is included in a clade with *Protoparmeliopsis bipruinosa* (Fink) S.Y. Kondr. and *P. nashii* (B.D. Ryan) S.Y. Kondr., differs from *Protoparmeliopsis ertzii* Bungartz & Elix, its most morphologically similar species, by whitish thallus, flat to concave and paler disc, longer ascospores, thallus K+ yellow reaction, presence of atranorin and rhizocarpic acid, and the substrate preference to sandstone or basalt. A key is provided to assist in the identification of *Protoparmeliopsis* species in Korea.

Keywords

Biodiversity, hygrophyte, Lecanoraceae, phylogeny, taxonomy

Introduction

As the genus *Lecanora* has been considered one of the largest genera in lichens, several infrageneric groups have been specifically or comprehensively studied in diverse aspects in morphology, chemistry and molecular phylogeny (Eigler 1969; Brodo 1984; Lumbsch 1995; Motyka 1995, 1996; Printzen 2001; Pérez-Ortega et al. 2010; Zhao et al. 2016; Bungartz et al. 2020). Main groups have been traditionally but informally recognized such as the *Lecanora dispersa* group, the *L. polytropa* group, the *L. rupicola* group, the *L. subfusca* group, the *L. symmicta* group, the *L. varia* group and the subgenus *Placodium*. The genera *Lecanoropsis*, *Myriolecis* and *Protoparmeliopsis* are originated from the *L. saligna*-, the *L. dispersa*-, and the *L. muralis*- groups, respectively (Śliwa et al. 2012; Zhao et al. 2016). Even a new genus *Sedelnikovaea* is differentiated from *Protoparmeliopsis*, one of the recently described genera (Kondratyuk et al. 2014). Other more groups have been defined such as the *L. carpinea*-, the *L. filamentosa*-, the *L. intumescens*-, the *L. subcarnea*- groups (Pérez-Ortega et al. 2010; Zhao et al. 2016), and the *L. pallida* group including the *L. subcarnea* group, the *L. marginata* group, and the *L. pinguis* group including a section in *Placodium* for the lecanoroid lichens of the Galapagos Islands (Bungartz et al. 2020).

Although there have been many groups classified as above, a few groups are proved more natural and homogenous and other groups are represented heterogenous without clarity in taxonomy (Zhao et al. 2016). The *Lecanora varia* group s. lat. is one of the unclear groups, and some species in the group are classified into the *L. polytropa* group and other some species are nested into the *L. symmicta* group (Printzen and May 2002; Laundon 2003; Pérez-Ortega and Kantvilas 2018; Bungartz et al. 2020). The main difference between the latter two groups is that the *L. polytropa* group has the corticate apothecia becoming convex when mature and inhabits generally on well-lit acid rocks, but the *L. symmicta* group represents convex apothecia from the beginning and mainly inhabits barks or worked woods (Laundon 2003). Such an inconclusive group is in need of revision as other infrageneric groups have been revised (Śliwa and Flakus 2011).

Hue (1909) first reported the lecanoroid lichens from Korea by describing four new taxa in the genus *Lecanora*, *L. oreina* (Ach.) Ach., *L. hueana* Harm., *L. hueana* f. *microcarpa* Hue, and *L. membranifera* Hue, although all the taxa are classified in other genera at present. Hur et al. (2005) arranged twelve species of *Lecanora* with specific references for each species reported from Korea. Moon (2013) listed twenty four species of *Lecanora* if we discard *L. fusanii* Hue (syn. *Caloplaca fusanii* (Hue) Zahlbr.) and *L. vulnerata* Hue (syn. *Caloplaca vulnerata* (Hue) Zahlbr.). Overall fifty two taxa had been recorded in Korea toward 2020 (Jeon et al. 2009; Joshi et al. 2009; Kondratyuk et al. 2013, Aptroot and Moon 2014, 2015; Kondratyuk et al. 2015, 2016a, 2016b, 2017; Lee and Hur 2020). *Protoparmeliopsis*, the lobate lecanoroid genus, was first referenced for Korea in 2007 and represented by *Protoparmeliopsis muralis* M. Choisy (Wei et al. 2007, sub *Lecanora muralis* (Schreb.) Rabenh.). *Protoparmeliopsis chejuensis* S.Y. Kondr. & Hur, *P. kopachevskae* S.Y. Kondr., Lőkös & Hur, *P. pseudogyrophorica*

S.Y. Kondr., S.O. Oh & Hur, and *P. zerovii* S.Y. Kondr. were described or referenced from Korea during the 2010s (Kondratyuk et al. 2013, 2016a, 2017), and totally five species were recorded in the genus *Protoparmeliopsis* for the country, although *P. pseudogyrophorica* was later reclassified to *Sedelnikovaea pseudogyrophorica* (S. Y. Kondr., S.O. Oh & Hur) S. Y. Kondr. & Hur (Kondratyuk et al. 2019).

This study describes two new lichen-forming fungi species to science in the genera *Lecanora*, i.e., the *L. symmicta* group, and *Protoparmeliopsis*. Field surveys for the lichen biodiversity in the forested wetlands of southern South Korea were accomplished during the summer of 2020, and a few dozen specimens were collected in the wetland forests nearby seashore or in islands (Fig. 1). The collected specimens were comprehensively analyzed in ecology, morphology, chemistry and molecular phylogeny and did not correspond to any previously known species. We describe them as two new species, *Lecanora parasymmicta* and *Protoparmeliopsis crystalliniformis*, and these discoveries contributes to the taxonomy of the lecanoroid lichens of Korea by listing overall fifty three taxa of *Lecanora* and six taxa of *Protoparmeliopsis*. The specimens are deposited in the herbarium of the Baekdudaegan National Arboretum (KBA, the herbarium acronym in the Index Herbariorum), South Korea.

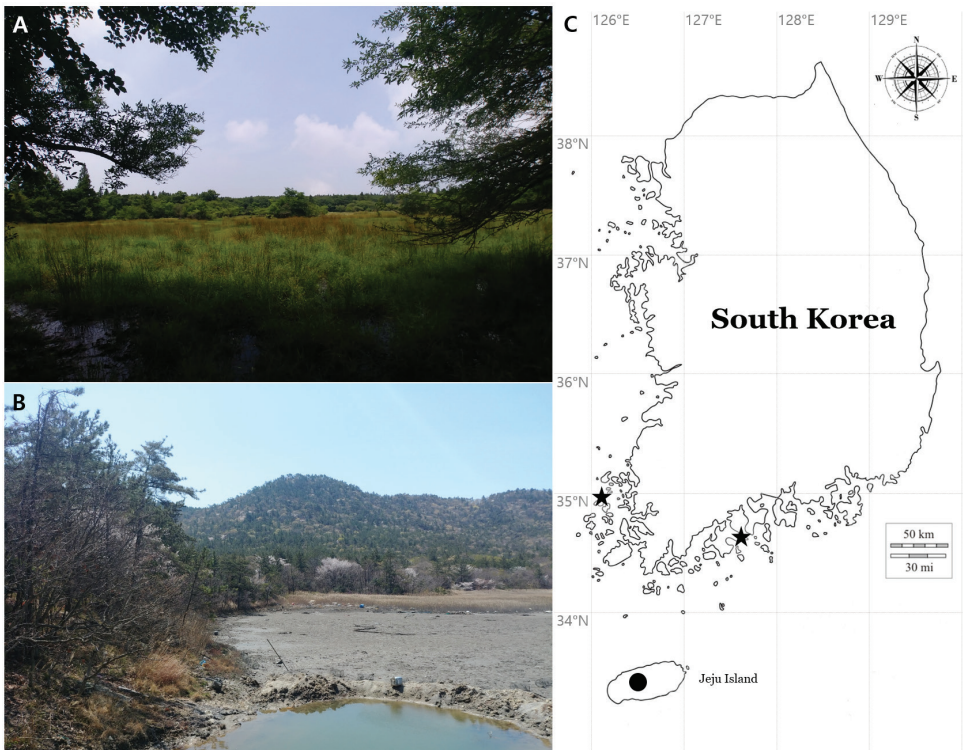


Figure 1. Specific collection sites for two new species **A** habitat/landscape of *Lecanora parasymmicta* **B** habitat/landscape of *Protoparmeliopsis crystalliniformis* **C** locations of *Lecanora parasymmicta* (black circle) and *Protoparmeliopsis crystalliniformis* (two black stars) on the map.

Materials and methods

Morphological and chemical analyses

Hand sections were prepared manually with a razor blade under a stereomicroscope (Olympus optical SZ51; Olympus, Tokyo, Japan), scrutinized under a compound microscope (Nikon Eclipse E400; Nikon, Tokyo, Japan) and pictured using a software program (NIS-Elements D; Nikon, Tokyo, Japan) and a DS-Fi3 camera (Nikon, Tokyo, Japan) mounted on a Nikon Eclipse Ni-U microscope (Nikon, Tokyo, Japan). The ascospores were examined at 1000× magnification in water. The length and width of the ascospores were measured and the range of spore sizes was shown with average, standard deviation (SD), length-to-width ratio, and number of measured spores. Thin-layer chromatography (TLC) was performed using solvent systems A and C according to standard methods (Orange et al. 2001).

Isolation, DNA extraction, amplification, and sequencing

Hand-cut sections of ten to twenty ascomata per collected specimen were prepared for DNA isolation and DNA was extracted with a NucleoSpin Plant II Kit in line with the manufacturer's instructions (Macherey-Nagel, Düren, Germany). PCR amplification for the internal transcribed spacer region (ITS1-5.8S-ITS2 rDNA), the mitochondrial small subunit, and the nuclear large subunit ribosomal RNA genes was achieved using Bioneer's AccuPower PCR Premix (Bioneer, Daejeon, Korea) in 20- μ l tubes with 16 μ l of distilled water, 2 μ l of DNA extracts and 2 μ l of primers ITS5 and ITS4 (White et al. 1990), mrSSU1 and mrSSU3R (Zoller et al. 1999) or LR0R and LR5 (Rehner and Samuels 1994). The PCR thermal cycling parameters used were 95 °C (15 sec), followed by 35 cycles of 95 °C (45 sec), 54 °C (45 sec), and 72 °C (1 min), and a final extension at 72 °C (7 min) based on Ekman (2001). The annealing temperature was occasionally altered by ± 1 degree in order to get a better result. PCR purification and DNA sequencing were accomplished by the genomic research company Macrogen (Seoul, Korea).

Phylogenetic analyses

All ITS and mtSSU sequences were aligned and edited manually using ClustalW in Bioedit V7.2.6.1 (Hall 1999). All missing and ambiguously aligned data and parsimony-uninformative positions were removed and only parsimony-informative regions were finally analyzed in MEGA X (Stecher et al. 2020). The final alignment comprised 1462 (ITS) and 1058 (mtSSU) columns for *Lecanora*. In them, variable regions were 171 (ITS) and 117 (mtSSU). The phylogenetically informative regions were 440 (ITS) and 152 (mtSSU). The final alignment for *Prototarmeliopsis* comprised 945 (ITS) and 985 (mtSSU) columns. In them, variable regions were 214 (ITS) and 53 (mtSSU). Finally, the phylogenetically informative regions were 268 (ITS) and 134 (mtSSU). Phylogenetic trees with bootstrap values were obtained in RAxML

GUI 2.0 beta (Edler et al. 2019) using the Maximum Likelihood method with a rapid bootstrap with 1000 bootstrap replications and GTR GAMMA for the substitution matrix. The posterior probabilities were obtained in BEAST 2.6.4 (Bouckaert et al. 2019) using the GTR 123141 (ITS for *Lecanora*), the GTR 121321 (mtSSU for *Lecanora*), the HKY (Hasegawa-Kishino-Yano) (ITS for *Protoparmeliopsis*), and the GTR 123123 (mtSSU for *Protoparmeliopsis*) models, as the appropriate models of nucleotide substitution produced by the Bayesian model averaging methods with bModelTest (Bouckaert and Drummond 2017), empirical base frequencies, gamma for the site heterogeneity model, four categories for gamma, and a 10,000,000 Markov chain Monte Carlo chain length with a 10,000-echo state screening and 1000 log parameters. Then, a consensus tree was constructed in TreeAnnotator 2.6.4 (Bouckaert et al. 2019) with no discard of burnin, no posterior probability limit, a maximum clade credibility tree for the target tree type, and median node heights. All trees were displayed in FigTree 1.4.2 (Rambaut 2014) and edited in Microsoft Paint. The bootstrapping and Bayesian analyses were repeated three times for the result consistency and no significant differences were shown for the tree shapes and branch values. The phylogenetic trees and DNA sequence alignments are deposited in TreeBASE under the study ID 28189. Overall analyses in the materials and methods were accomplished based on Lee and Hur (2020).

Results and discussion

Phylogenetic analyses

Four independent phylogenetic trees for the genera *Lecanora* and *Protoparmeliopsis* were produced from 117 sequences (71 for ITS, and 30 for mtSSU) from GenBank and, 16 new sequences (11 for ITS and 5 for mtSSU) from the new and compared species (Table 1). *Lecanora parasymmicta*, one of the new species, is positioned in the *L. symmicta* group in both ITS and mtSSU trees. The ITS tree illustrates that the new species is located in its own clade without any species close to it. *Lecanora symmicta*, the most similar species, is positioned in a clade with *L. confusa* Almb. and *L. compallens* Herk & Aptroot, situated far from the new species (Fig. 2). The mtSSU tree shows that the new species is located in a clade with *L. symmicta* and *L. strobilina* Ach., represented by a bootstrap value of 100 and a posterior probability of 1.0 for the branch (Fig. 3). The second new species, *Protoparmeliopsis crystalliniformis*, was positioned in *Protoparmeliopsis* in both ITS and mtSSU trees. The ITS tree explains that the new species is located in a clade with *P. bipruinosa* (Fink) S.Y. Kondr. and *P. nashii* (B.D. Ryan) S.Y. Kondr., represented by a bootstrap value of 92 and a posterior probability of 1.0 for the branch (Fig. 4). The mtSSU tree shows that *P. crystalliniformis* is located in its own clade (Fig. 5). The phylogenetic analyses, and according to the included taxa, did not indicate any such species to the two new proposed in *Lecanora* and *Protoparmeliopsis*.

Table 1. Species list and DNA sequence information employed for phylogenetic analysis.

No.	Species	ID (ITS)	ID (mtSSU)	Voucher
1	<i>Lecanora aitema</i>	GU480092		SPO1
2	<i>Lecanora atosulphurea</i>	KY266931		O-L-195558
3	<i>Lecanora austrocalifornica</i>	GU480103		SPO2
4	<i>Lecanora cinereofusca</i>	KP224470	KP224465	Lendemer 34944 (NY)
5	<i>Lecanora cinereofusca</i>	KP224471	KP224464	Lendemer 35007 (NY)
6	<i>Lecanora compallens</i>	KY586043		JM6948
7	<i>Lecanora confusa</i>	GU480093		SPO10
8	<i>Lecanora confusa</i>	GU480120		SPO9
9	<i>Lecanora conizaeoides</i>	AF189717		U229
10	<i>Lecanora conizaeoides</i>		KJ766418	AFTOL-ID 1858
11	<i>Lecanora expallens</i>	KY586040		UGDA-L17316
12	<i>Lecanora flavoleprosa</i>	GU480101		SPO18
13	<i>Lecanora</i> cf. <i>fulvastra</i>	GU480119		SPO8
14	<i>Lecanora helmutii</i>	MG973240		MA:Lichen:19506
15	<i>Lecanora orostbea</i>	AF070035		U244
16	<i>Lecanora parasymmicta</i>	MW832793	MW832799	BDNA-L-0001218
17	<i>Lecanora parasymmicta</i>	MW832794	MW832800	BDNA-L-0001220
18	<i>Lecanora parasymmicta</i>	MW832795	MW832801	BDNA-L-0001235
19	<i>Lecanora perpruinosa</i>	AF070025		U176
20	<i>Lecanora perpruinosa</i>		DQ787344	U506
21	<i>Lecanora polytropha</i>	DQ534470		Hur ANT050752
22	<i>Lecanora polytropha</i>	HQ650643	DQ986807	AFTOL-ID 1798
23	<i>Lecanora polytropha</i>	JN873881		U.C. Riverside 47815UCR1
24	<i>Lecanora polytropha</i>		DQ787348	U520
25	<i>Lecanora saxigena</i>	KP224467	KP224460	Lendemer 25832 (NY)
26	<i>Lecanora saxigena</i>	KP224468	KP224461	Lendemer 33186 (NY)
27	<i>Lecanora solaris</i>	MH512984		LYF14–69
28	<i>Lecanora solaris</i>		MH520111	ED (14336) & LY
29	<i>Lecanora stanislai</i>	KY586041		UGDA-L17244
30	<i>Lecanora stanislai</i>		MK778544	J. Malicek 10367
31	<i>Lecanora strobilina</i>	MG973235		MA:Lichen:19510
32	<i>Lecanora strobilina</i>	MG973236		MA:Lichen:19511
33	<i>Lecanora strobilina</i>	MG973237		MA:Lichen:19509
34	<i>Lecanora strobilina</i>		KJ766420	DUKE:M. Kukwa 4761
35	<i>Lecanora strobilinoidea</i>	MG973238		MA:Lichen:19507
36	<i>Lecanora subintricata</i>	GU480112		SPO28
37	<i>Lecanora sulphurea</i>	AF070030		U212
38	<i>Lecanora sulphurea</i>		DQ787356	U508
39	<i>Lecanora symmicta</i>	AF070024		U205
40	<i>Lecanora symmicta</i>	GU480113		SPO29
41	<i>Lecanora symmicta</i>	MH481912		O-L-209831
42	<i>Lecanora symmicta</i>	MW832788		BDNA-L-0000547
43	<i>Lecanora symmicta</i>	MW832789		BDNA-L-0000548(br)
44	<i>Lecanora symmicta</i>	MW832790		BDNA-L-0000548(yel)
45	<i>Lecanora symmicta</i>	MW832791		BDNA-L-0000551
46	<i>Lecanora symmicta</i>	MW832792		BDNA-L-0000642
47	<i>Lecanora symmicta</i>		KJ766421	EGR:K. Molnar 23-08-2005/B
48	<i>Lecanora symmicta</i>		KJ152466	C. Printzen 9999a (FR)
49	<i>Lecanora varia</i>	MK672852	MK693694	Kondratyuk S. 21325 (KW-L)
50	<i>Polyzozia contractula</i>	AF070032		U236

No.	Species	ID (ITS)	ID (mtSSU)	Voucher
51	<i>Polyzozia contractula</i>	HQ650604	DQ986898	AFTOL-ID 877
52	<i>Polyzozia poliophaea</i>	MG925981	MG925879	O:L 200460
53	<i>Polyzozia</i> sp.	MW832798		BDNA-L-0001105
54	<i>Protoparmeliopsis achariana</i>	AF070019		U155
55	<i>Protoparmeliopsis achariana</i>		DQ787342	U525
56	<i>Protoparmeliopsis bipruinosa</i>	AF159932		U354
57	<i>Protoparmeliopsis bolcana</i>	MK672838	MK693686	Kondratyuk S. 20309 (KW-L)
58	<i>Protoparmeliopsis chejuensis</i>	MK672839	MK693687	KoLRI 022622
59	<i>Protoparmeliopsis chejuensis</i>	MK672840	MK693688	KoLRI 022618
60	<i>Protoparmeliopsis crystalliniformis</i>	MW832796	MW832802	BDNA-L-0000298
61	<i>Protoparmeliopsis crystalliniformis</i>	MW832797	MW832803	BDNA-L-0000349
62	<i>Protoparmeliopsis garovaglii</i>	AF189718		M107
63	<i>Protoparmeliopsis garovaglii</i>	KT453728	KT453818	Leavitt 089 (BRY-C)
64	<i>Protoparmeliopsis garovaglii</i>	KU934537		Leavitt 199 (BRY-C)
65	<i>Protoparmeliopsis garovaglii</i>	MK084624		Szczepanska 1240
66	<i>Protoparmeliopsis garovaglii</i>	MK084626		Flakus 21175
67	<i>Protoparmeliopsis garovaglii</i>	MK672841	MK693689	M. Haji Moniri (KW-L)
68	<i>Protoparmeliopsis kopachevskae</i>	MK672845		KoLRI 040224
69	<i>Protoparmeliopsis kopachevskae</i>	MK672846		KoLRI 040267
70	<i>Protoparmeliopsis kopachevskae</i>	MK672847		KoLRI 040276
71	<i>Protoparmeliopsis laatokaensis</i>	MN912366		20132508
72	<i>Protoparmeliopsis macrocyclos</i>	AF159933		U273
73	<i>Protoparmeliopsis muralis</i>	KC791770		BGK247
74	<i>Protoparmeliopsis muralis</i>	KP059048	KP059054	SK 765
75	<i>Protoparmeliopsis muralis</i>	KT818623		DNA 9890 (F)
76	<i>Protoparmeliopsis muralis</i>	KU934555		Leavitt 146 (BRY-C)
77	<i>Protoparmeliopsis muralis</i>	KU934560		Vondrak 106b (PRA)
78	<i>Protoparmeliopsis muralis</i>	KY379232		BGK257
79	<i>Protoparmeliopsis muralis</i>	LC547497		CBM:FL-41434
80	<i>Protoparmeliopsis muralis</i>		KJ766466	EGR:K. Molnar U0501/AO
81	<i>Protoparmeliopsis nashii</i>	AF159931		U253
82	<i>Protoparmeliopsis peltata</i>	KT453722	KT453860	
83	<i>Protoparmeliopsis peltata</i>	KT453723		MS014622
84	<i>Protoparmeliopsis peltata</i>	KU934746		Kaz 13085pelt
85	<i>Protoparmeliopsis peltata</i>	KU934751		Vondrak V127 (PRA)
86	<i>Protoparmeliopsis pseudoglyphorica</i>	MK672851	MK693693	KoLRI 016651
87	<i>Protoparmeliopsis zareii</i>	KP059049	KP059055	SK 480
88	<i>Protoparmeliopsis zareii</i>		KP059056	SK 481
89	<i>Protoparmeliopsis</i> sp.	KU934865		Vondrak 9980 (PRA)
90	<i>Protoparmeliopsis</i> sp.	KU934866		Vondrak 10043 (PRA)
91	<i>Protoparmeliopsis</i> sp.	KU934867		Vondrak 10044 (PRA)
92	<i>Protoparmeliopsis</i> sp.	KU934868		Vondrak 10055 (PRA)
93	<i>Protoparmeliopsis</i> sp.	KU934869		Vondrak 9992 (PRA)
94	<i>Tephromela atra</i>	HQ650608	DQ986879	AFTOL-ID 1373
Overall		82	35	

DNA sequences which were generated in this study, in bold the new species *Lecanora parasymmicta* and *Protoparmeliopsis crystalliniformis* and newly generated sequences of *Lecanora symmicta* and *Polyzozia* sp. specimens. All others were obtained from GenBank. The species names are followed by GenBank accession numbers and voucher information. ITS, internal transcribed spacer; mtSSU, mitochondrial small subunit; Voucher, voucher information.

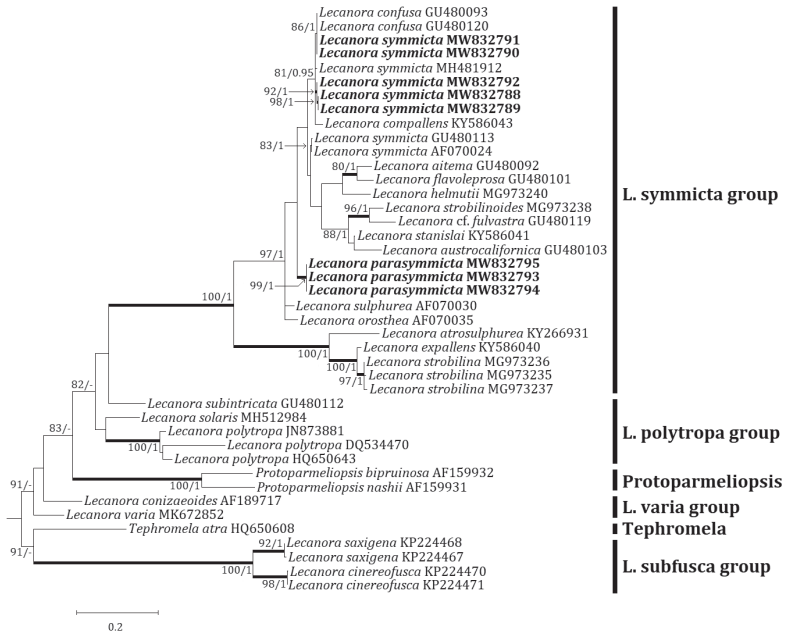


Figure 2. Phylogenetic relationships amongst available species in the *Lecanora symmicta* group based on a Maximum Likelihood analysis of the dataset of ITS sequences. The tree was rooted with five sequences of the *Lecanora subfusca* group and *Tephromela*. Maximum Likelihood bootstrap values $\geq 70\%$ and posterior probabilities $\geq 95\%$ are shown above internal branches. Branches with bootstrap values $\geq 90\%$ are shown in bold. The new sequences of *Lecanora parasymmicta* and *Lecanora symmicta* produced from this study are presented in bold, and all species names are followed by the GenBank accession numbers. Reference Table 1 provides the species related to the specific GenBank accession numbers and voucher information.

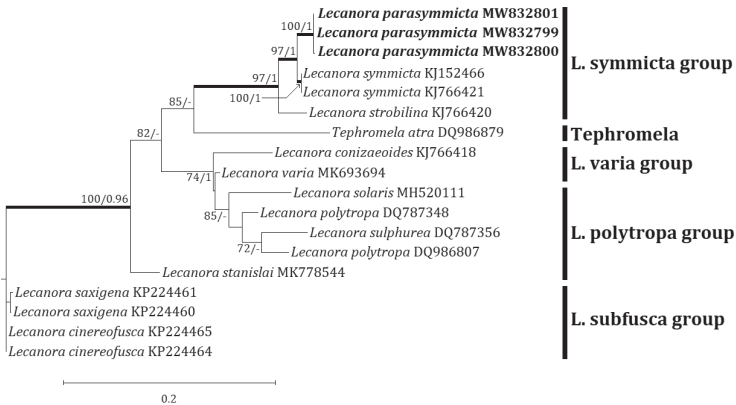


Figure 3. Phylogenetic relationships amongst available species in the *Lecanora symmicta* group based on a Maximum Likelihood analysis of the dataset of the mitochondrial small subunit (mtSSU) sequences. The tree was rooted with four sequences of the *Lecanora subfusca* group. Maximum Likelihood bootstrap values $\geq 70\%$ and posterior probabilities $\geq 95\%$ are shown above internal branches. Branches with bootstrap values $\geq 90\%$ are shown in bold. The new species *Lecanora parasymmicta* is presented in bold, and all species names are followed by the GenBank accession numbers. Reference Table 1 provides the species related to the specific GenBank accession numbers and voucher information.

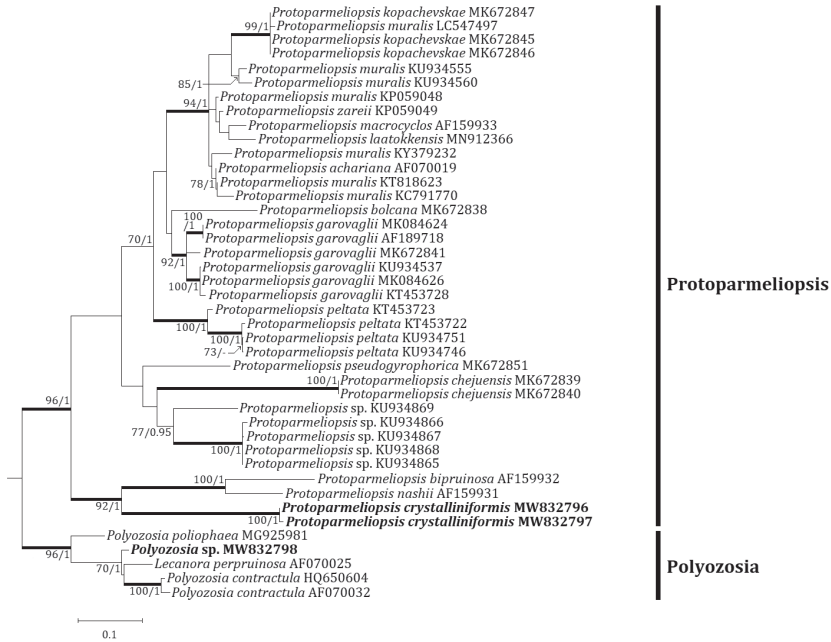


Figure 4. Phylogenetic relationships amongst available species in the genus *Protoparmeliopsis* based on a Maximum Likelihood analysis of the dataset of ITS sequences. The tree was rooted with five sequences of the genus *Polyzosia*. Maximum Likelihood bootstrap values $\geq 70\%$ and posterior probabilities $\geq 95\%$ are shown above internal branches. Branches with bootstrap values $\geq 90\%$ are shown in bold. The new species *Protoparmeliopsis crystalliniformis* is presented in bold, and all species names are followed by the GenBank accession numbers. Reference Table 1 provides the species related to the specific GenBank accession numbers and voucher information.



Figure 5. Phylogenetic relationships amongst available species in the genus *Protoparmeliopsis* based on a Maximum Likelihood analysis of the dataset of the mitochondrial small subunit (mtSSU) sequences. The tree was rooted with three sequences of the genus *Polyzosia*. Maximum Likelihood bootstrap values $\geq 70\%$ and posterior probabilities $\geq 95\%$ are shown above internal branches. Branches with bootstrap values $\geq 90\%$ are shown in bold. The new species *Protoparmeliopsis crystalliniformis* is presented in bold, and all species names are followed by the GenBank accession numbers. Reference Table 1 provides the species related to the specific GenBank accession numbers and voucher information.

Taxonomy

Lecanora parasymmicta B.G. Lee & J.-S. Hur sp. nov.

Mycobank No: 839182

Fig. 6

Diagnosis. *Lecanora parasymmicta* differs from *L. symmicta*, the most similar species, by its areolate-rimose thallus (vs. areolate to leprose thallus), blackish hypothallus (vs. hypothallus indistinct), larger apothecia (up to 1.7 mm diam. vs. up to 1 mm diam.), absence of thalline excipulum from the beginning (vs. presence of thalline excipulum when young at least), narrower paraphyses (1–1.5 μm vs. 2–2.5 μm), larger ascospores (11–18 \times 4–7 μm vs. 9–15.5 \times 4–5 μm), smaller pycnoconidia (12–21 \times 0.5–0.8 μm vs. 18–25 \times 0.5–1.0 μm), chemical reactions (thallus K \pm slightly yellow, C–, KC– and UV– vs. K–, C \pm orange, KC \pm slightly yellow, UV+ dull orange), and the presence of placodiolic acid (vs. presence of arthothelin and \pm thiophanic acid).

Type. SOUTH KOREA, Jeju Island, Aewol-eup, Gwangnyeongri/bongseongri, Mt. Halla, a forested wetland, 33°21.85'N, 126°26.91'E, 980 m alt., on bark of *Maackia fauriei* (H. Lév.) Takeda, 08 July 2020, B.G.Lee & H.J.Lee 2020-001020, with *Graphis scripta* (L.) Ach. (holotype: BDNA-L-0001220; GenBank MW832794 for ITS and MW832800 for mtSSU); same locality, on bark of *Malus sieboldii* (Regel) Rehder, 08 July 2020, B.G.Lee & H.J.Lee 2020-001018, (paratype: BDNA-L-0001218; GenBank MW832793 for ITS and MW832799 for mtSSU); same locality, on bark of *Malus sieboldii*, 08 July 2020, B.G.Lee & H.J.Lee 2020-001019, with *Phaeographis* aff. *inusta* (paratype: BDNA-L-0001219); same locality, on bark of *Maackia fauriei*, 08 July 2020, B.G.Lee & H.J.Lee 2020-001026, (paratype: BDNA-L-0001226); same locality, on bark of *Maackia fauriei*, 08 July 2020, B.G.Lee & H.J.Lee 2020-001035, with *Lecanora megalocheila* (Hue) H. Miyaw. (paratype: BDNA-L-0001235; GenBank MW832795 for ITS and MW832801 for mtSSU); same locality, on bark of *Ligustrum obtusifolium* Siebold & Zucc., 08 July 2020, B.G.Lee & H.J.Lee 2020-001036, with *Graphis scripta* (paratype: BDNA-L-0001236).

Description. Thallus corticolous, crustose, areolate to rimose but not leprose, light olivish gray to light gray, margin determinate, not pruinose, 60–200 μm thick; cortex hyaline, 5–10 μm thick; medulla often intermixed with algae and even with bark layer, small crystals in cortex or between algae, dissolving in K; photobiont coccoid, cells globose to ellipsoid, 5–15 μm . Hypothallus blackish.

Apothecia abundant, rounded, often contiguous or even coalescent, emerging on the surface of thallus and sessile when mature but margin generally attached to thallus surface, constricted at the base, 0.3–1.7 mm diam. Disc flat in the beginning and soon convex, smooth or becoming rugose by apothecia adjoining, not pruinose or slightly pruinose, pale yellow in the beginning and slightly darker when mature, sometimes with dark spots (algae), 180–400 μm thick; biatorine. Thalline excipulum absent from the beginning, proper excipulum present and sometimes slightly paler than disc, more distinctive when young, hyaline but yellowish brown to pale brown at periphery with granules which dissolving in K, periphery color same to epihyemium, ca. 90 μm wide



Figure 6. *Lecanora parasymmicta* morphology (BDNA-L-0001235, paratype in **A** BDNA-L-0001220, holotype in **B–M**) **A–C** habitus and apothecia, thalline margin of apothecia consistently absent from the beginning **D** blackish hypothallus (red arrows) **E** apothecia in vertical section **F** biatorine apothecia without thalline margin **G–J** clavate asci with eight spores **K** ascospores constantly simple but rarely 1-septate **L** immersed pycnidia **M** thread-like, curved pycnoconidia. Scale bars: 1 mm (**A–D**); 200 μm (**E**); 50 μm (**F**); 10 μm (**G–K**); 100 μm (**L**); 10 μm (**M**).

laterally and 70–80 μm wide at periphery, disappearing to the base. Epihymenium yellowish brown to pale brown, granular, dissolving in K, 10–20 μm high. Hymenium hyaline, 70–90 μm high. Subhymenium hyaline, 30–50 μm high. Hypothecium hyaline, prosoplectenchymatous (irregular), 50–60 μm high. Crystals and oil droplets absent in apothecial section. Paraphyses septate, anastomosing, 1–1.5 μm wide, simple or branched at tips, tips not swollen or slightly swollen, not pigmented, epihymenium pigmented by granules, not by paraphysial tips, ca. 1.5 μm wide. Asci clavate, 8-spored, 50–60 \times 13–21 μm ($n = 7$). Ascospores constantly simple but rarely 1-septate, coarsely biseriate or irregularly arranged, 11–18 \times 4–7 μm (mean = 13.8 \times 5.8 μm ; SD = 1.62(L), 0.63(W); L/W ratio 1.8–4.0, ratio mean = 2.4, ratio SD = 0.3; $n = 105$). Pycnidia immersed, ostiolar region slightly projected with a thalline excipulum, round to irregularly asymmetric, brown to black, 220 \times 180 μm . Pycnoconidia thread-like, generally curved, 12–21 \times 0.5–0.8 μm .

Chemistry. Thallus K– or K+ slightly yellowish, KC–, C–, Pd–. Hymenium, epihymenium and ascus tholus I+ blue. UV–. Usnic acid, zeorin, and placodiolic acid were detected by TLC.

Table 2. Comparison of the new species with close species in the *Lecanora symmetrica* group.

Species	<i>L. parasymmetrica</i>	<i>L. aitema</i>	<i>L. confusa</i>	<i>L. strobilina</i>	<i>L. symmetrica</i>
Thallus growth form	areolate-rimose	granular-areolate	granular-areolate	granular-subareolate	areolate-reprose
Thallus color	olive-gray to gray	cream-white	green gray to yellow gray	white to pale yellow-green	variable (pale yellow-green, white or green-gray)
Prunia	absent or slightly pruinose on disc	absent	absent	present	absent
Hypothallus	blackish	indistinct or pale brown	absent or indistinct	indistinct	indistinct
Apothecia (mm diam.)	0.3–1.7	0.2–0.5	0.4–0.7	0.4–1.0	0.3–1.0
Thalline excipulum	absent from beginning	present when young	present when young	present when young	present when young
Epithymenium	yellow-brown	yellow-brown	brown	colorless	colorless, yellow-brown to olive
Paraphyses (μm)	1–1.5	2–2.5	1–2	1–1.5	2–2.5
Asci (μm)	50–60 \times 13–21	35–45 \times 10–15	32–45 \times 11–15	35–45 \times 10–17	30–47 \times 8–12*
Ascospores (μm)	11–18 \times 4–7	12–17 \times 4.5–5.5	10–14 \times 4–5	10–15 \times 4–6	9–15.5 \times 4–5 8–12 \times 4–6*
Pycnoconidia (μm)	12–21 \times 0.5–0.8	not observed	not observed	25 \times 1.0	18–25 \times 0.5–1.0
Spot test	thallus K \pm slightly yellow, C-, KC-	thallus K-, KC \pm slightly yellow	thallus K-, C+, orange, KC+ orange	thallus K+ yellow to brown, KC \pm yellow	thallus K-, C \pm orange, KC \pm slightly yellow
UV	negative	pale orange	bright orange	pale orange	dull orange
Substance	usnic acid, zeorin, placodiolic acid	\pm usnic acid, \pm zeorin	usnic acid, \pm zeorin, thiophanic acid, \pm arthothelin	usnic acid, zeorin	usnic acid, zeorin, arthothelin, \pm thiophanic acid
Reference	BDNA-L-0001218 (paratype), BDNA-L-0001220 (holotype), and BDNA-L-0001235 (paratype)	Smith et al. 2009	Nath III et al. 2004; Smith et al. 2009	Brodo et al. 2001; Smith et al. 2009	Brodo et al. 2001; Nash III et al. 2004; Smith et al. 2009; BDNA-L-0000547, BDNA-L-0000548, and BDNA-L-0000551

The morphological and chemical characteristics for several species close to the new species are referenced mainly from the previous literature. All information on the new species is measured from type specimens (BDNA-L-0001218, BDNA-L-0001220, and BDNA-L-0001235) in this study. Particularly the asci of the closest species, *Lecanora symmetrica*, was not described from the previous literature and the asci and the ascospores for the species are measured from selected specimens (BDNA-L-0000547, BDNA-L-0000548, and BDNA-L-0000551) in this study, represented with asterisk marks(*).

Distribution and ecology. The species occurs on the bark of *Ligustrum obtusifolium*, *Maackia fauriei*, and *Malus sieboldii*. The species is currently known from the type collections.

Etymology. The species epithet indicates the lichen's morphological similarity to the close species *Lecanora symmicta*.

Notes. The new species is morphologically similar to *Lecanora symmicta* in its areolate and gray thallus, yellowish apothecia without developed thalline excipulum, yellowish brown epihymenium filled with pigmented granules which dissolving in K, and the presence of conidia. However, the new species differs from *L. symmicta* by its areolate-rimose thallus, blackish hypothallus, larger apothecia, absence of thalline excipulum from the beginning, narrower paraphyses, larger asci, larger ascospores, smaller pycnoconidia, chemical reaction, and the presence of placodiolic acid (Brodo et al. 2001; Nash III et al. 2004; Smith et al. 2009).

The new species is comparable to *Lecanora aitema* (Ach.) Hepp, *L. confusa*, and *L. strobilina* in the *L. symmicta* group as all those are corticolous without soredia or leprose thallus. However, the new species differs from *L. aitema* by olive-gray to gray thallus, blackish hypothallus, larger and paler apothecia, absence of thalline excipulum from the beginning, larger asci, wider ascospores, chemical reaction, presence of placodiolic acid, and the substrate preference to deciduous trees/shrubs (vs. conifers) (Smith et al. 2009).

The new species is different from *Lecanora confusa* by the absence of thalline excipulum from the beginning, larger asci, larger ascospores, chemical reaction, and the presence of placodiolic acid (Nash III et al. 2004; Smith et al. 2009).

The new species is distinguished from *Lecanora strobilina* by olive-gray to gray thallus without pruina, presence of black hypothallus, absence of thalline excipulum from the beginning, yellow-brown epihymenium, absence of crystals in apothecial section, larger asci, larger ascospores, smaller pycnoconidia, chemical reaction, and the presence of placodiolic acid (Brodo et al. 2001; Smith et al. 2009). Molecular phylogeny strongly supports that the new species is distinct in the *L. symmicta* group without any species close to it, illustrating the compared species above are located in different clades far from the new species (Figs 2 and 3). Reference Table 2 provides the key characteristics distinguishing *L. parasymmicta* from the closely related species in the *L. symmicta* group above.

All above compared species do not contain placodiolic acid and *Lecanora* species with placodiolic acid, such as *L. placodiolica* Lumbsch & Elix, *L. cinereofusca* H. Magn., *L. sarcopidoides* (A. Massal.) Hedl., *L. subravida* Nyl., *L. semitensis* (Tuck.) Zahlbr. and *L. opiniconensis* Brodo, are considered for discriminating the new species. *Lecanora placodiolica* differs from the new species by yellowish thallus, absence of hypothallus, presence of thalline excipulum, and darker (red-brown) discs (Lumbsch and Elix 1998). *Lecanora cinereofusca* belongs to the *L. subfusca* group with large crystals, and *L. sarcopidoides* and *L. subravida* are the members of the *L. saligna* group with presence of thalline excipulum and smaller ascospores (Van den Boom and Brand 2008). They are quite different from the new species in morphology although they produce

placodiolic acid. *Lecanora semitensis* differs from the new species by yellowish thallus, darker (dark grayish brown to yellow) discs, presence of thalline excipulum, smaller ascospores ($8\text{--}12 \times 4\text{--}5 \mu\text{m}$), and the substrate preference to rock other than bark of trees (Nash III et al. 2004). *Lecanora opiniconensis* represents yellowish thallus composed of lobate areoles, absence of hypothallus, presence of thalline excipulum, absence of zeorin, and the substrate preference to siliceous rock other than bark of trees (Brodo 1986).

***Lecanora symmicta* specimens examined.** SOUTH KOREA, Gangwon Province, Gangneung, Seongsan-myeon, Eoheul-ri, a forested wetland, $37^{\circ}43.61'N$, $128^{\circ}48.13'E$, 212 m alt., on bark of *Alnus sibirica* Fisch. ex Turcz., 02 June 2020, B.G.Lee & H.J.Lee 2020-000347, with *Lecanora strobilina*, *Lecidella euphorea* (Flörke) Kremp., *Traponora varians* (Ach.) J. Kalb & Kalb (BDNA-L-0000547; GenBank MW832788 for ITS); same locality, on bark of *Alnus sibirica*, 02 June 2020, B.G.Lee & H.J.Lee 2020-000348, two variants (one with pale brown discs and the other with yellow discs) of *Lecanora symmicta* with *Lecidella euphorea*, *Rinodina* sp., *Traponora varians* (BDNA-L-0000548; GenBank MW832789 for ITS of the former variant and GenBank MW832790 for ITS of the latter); same locality, on bark of *Alnus sibirica*, 02 June 2020, B.G.Lee & H.J.Lee 2020-000351, two above variants of *Lecanora symmicta* with *Traponora varians* (BDNA-L-0000551; GenBank MW832791 for ITS); Pyeongchang-gun, Daegwallyeong-myeon, Hoenggye-ri, a forested wetland, $37^{\circ}46.00'N$, $128^{\circ}42.33'E$, 1,047 m alt., on bark of *Maackia amurensis* Rupr. & Maxim., 03 June 2020, B.G.Lee & H.J.Lee 2020-000442, with *Buellia disciformis* (Fr.) Mudd, *Buellia* sp., *Catillaria nigroclavata* (Nyl.) J. Steiner, *Lecanora megalocheila*, *Lecidella euphorea*, *Rimularia* cf. *caeca*, *Rinodina* sp. (BDNA-L-0000642; GenBank MW832792 for ITS).

***Protoparmeliopsis crystalliniformis* B.G. Lee & J.-S. Hur sp. nov.**

Mycobank No: 839183

Fig. 7

Diagnosis. *Protoparmeliopsis crystalliniformis* differs from *P. ertzii* by thallus color (grayish white to white vs. pale beige to ochraceous), flat to concave disc (vs. flat to convex disc), paler disc color (pale brown to dark brown vs. deep reddish brown), longer ascospores ($8.5\text{--}17 \times 4.2\text{--}7 \mu\text{m}$ vs. $9.4\text{--}11.3 \times 5.3\text{--}6.6 \mu\text{m}$), chemistry (thallus K^+ yellow, and the presence of atranorin and rhizocarpic acid vs. all spot tests negative and no substance), and the substrate preference (sandstone or basalt vs. exposed lava).

Type. SOUTH KOREA, South Jeolla Province, Sinan, Ja-Eun Island, a wetland just nearby coast, $34^{\circ}55.96'N$, $126^{\circ}04.30'E$, 5 m alt., on rock (sandstone), 16 April 2020, B.G.Lee & D.Y.Kim 2020-000149, with *Ramalina yasudae* Räsänen, *Xanthoparmelia coreana* (Gyeln.) Hale (holotype: BDNA-L-0000349; GenBank MW832797 for ITS, MW832803 for mtSSU, and MW832822 for LSU); same locality, on rock (sandstone, not calcareous), 16 April 2020, B.G.Lee & D.Y.Kim 2020-000151, with *Buellia spuria* (Schaer.) Anzi, *Ramalina yasudae*, *Xanthoparmelia coreana* (paratype: BDNA-L-0000351).

Description. Thallus saxicolous, areolate to squamulose, linearly or web-like dispersed following furrows of substrate, not forming a rosette, pale grayish white to white,

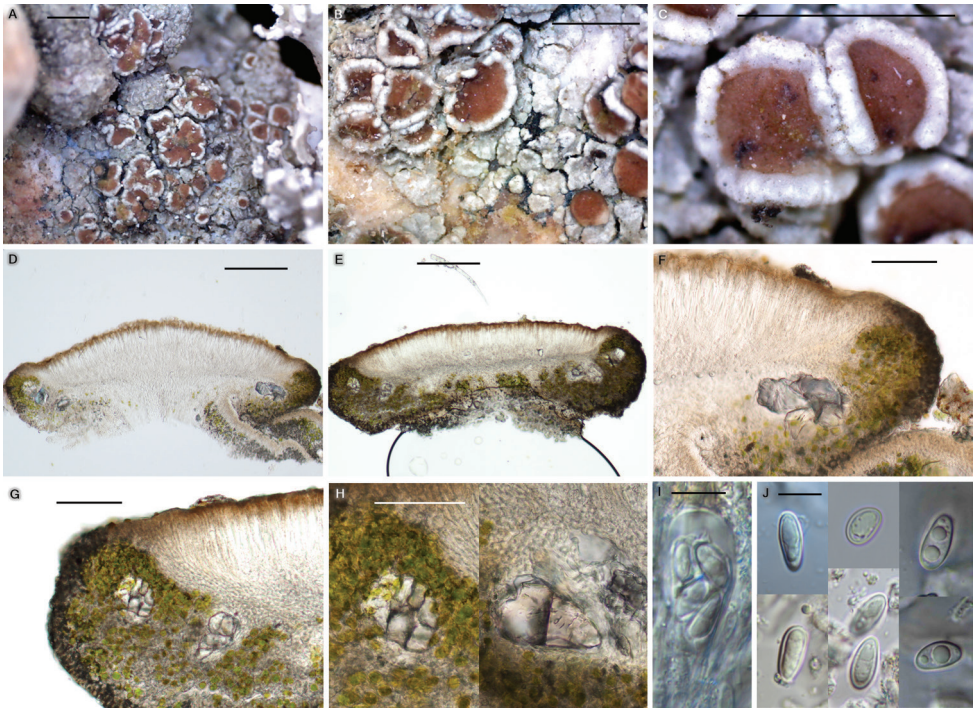


Figure 7. *Protoparmeliopsis crystalliniformis* morphology (BDNA-L-0000349, holotype) **A–C** habitus and apothecia, areolate to squamulose thallus in white to whitish gray color **D–E** apothecia in vertical section **F–G** well-developed thalline margin **H** large crystals present in the thalline margin, not dissolving in KOH **I** clavate ascus **J** ascospores constantly simple and ellipsoid, often biguttulate in the beginning. Scale bars: 1 mm (**A–C**); 200 µm (**D–E**); 100 µm (**F–G**); 50 µm (**H**); 10 µm (**I–J**).

margin indeterminate, not pruinose, 100–450 µm thick; cortex pale brown, 10–20 µm thick; medulla below algal layer, 30–50 µm (sometimes 150–200 µm) thick; algal layer 50–80 µm thick, small crystals in cortex or between algal cells, dissolving but remaining in K; photobiont coccoid, cells globose to ellipsoid, 5–15 µm. Hypothallus absent.

Apothecia abundant, rounded, often contiguous or even coalescent, emerging on the surface of thallus and sessile when mature, constricted at the base, 0.3–1.7 mm diam. Disc flat or slightly concave, crenulate or entire, smooth or becoming rugose by apothecia adjoining, not pruinose, pale brown to dark brown from the beginning, 250–350 µm thick; lecanorine. Thalline excipulum persistent or rarely excluded, concolorous to thallus, 125–160 µm laterally, 80–150 µm at periphery, cortex inconspicuous, concolorous to epihymenium or slightly paler, up to 5 µm, with small and large crystals, small crystals dissolving but remaining in K, large crystals not dissolving in K. Proper excipulum inconspicuous. Epihymenium brown to pale brown, with tiny granules, granules and pigments dissolving in K, 10–20 µm high. Hymenium hyaline, 80–100 µm high. Subhymenium hyaline, 30–50 µm high. Hypothecium hyaline, prosoplectenchymatous (irregular), 100–150 µm high. Oil droplets present in hymenium to upper hypothecium. Paraphyses septate, anastomosing, 1–1.5 µm wide, generally

Table 3. Comparison of the new species with close species in the genus *Protoparmeliopsis*.

Species	<i>P. crystalliniformis</i>	<i>P. bipruinosa</i>	<i>P. ertzii</i>	<i>P. nashii</i>
Thallus color	gray–white to white	pale yellow–green to gray–green–yellow, finally pale brown	pale beige to ochraceous	various shades of yellow to orange–brown cast
Pruina	not present	pruina on both thallus and disc	not present	not on thallus, but present on disc
Disc evenness	flat to slightly concave	flat to slightly convex	flat to convex	flat to slightly concave
Disc color	pale brown to dark brown	yellow–brown to pale orange or green	deep reddish brown	weakly yellow to strongly yellow
Crystals	large crystals, insoluble	not observed	large crystals, insoluble	not observed
Ascospores (µm)	8.5–17 × 4.2–7	10–14 × 4–7.5	8.8–12.7 × 4.9–6.9	8–14 × 4–9
Spot test	thallus K+ yellow, KC–, C–, Pd–	thallus K–, C–; cortex KC+ yellow, P–; medulla KC–, P+ yellow or P–	all negative	thallus K– or occasionally K+, C–; cortex KC+ yellow, P–; medulla KC–, P+ yellow or less often P–
Substance	atranorin, rhizocarpic acid	usnic acid, psoromic acid, or fatty acids	no substance	usnic acid, psoromic acid, or fatty acids
Substrate	sandstone or basalt on seashore	volcanic tuff, basalt, rhyolite, or sedimentary rocks from desert scrub to woodlands	exposed lava on island	siliceous rocks (conglomerate to volcanic rocks), rarely on limestone in woodlands, desert scrub or grassland
Reference	BDNA-L-0000298, BDNA-L-0000349 (holotype), and BDNA-L-0000351 (paratype)	Nash III et al. 2004	Bungartz et al. 2020	Nash III et al. 2004

The morphological, chemical and ecological characteristics for several species close to the new species are referenced mainly from the previous literature. All information on the new species is measured from selected specimens (BDNA-L-0000298, BDNA-L-0000349, and BDNA-L-0000351) in this study.

simple or occasionally branched at tips, tips not swollen or slightly swollen, not pigmented, 1.5–2 µm wide. Asci narrowly clavate, 8-spored, 40–65 × 10–12 µm (n = 6). Ascospores simple and often biguttulate in the beginning then having an oval-shaped oil drop by assembly of guttules when mature, ellipsoid to narrowly ellipsoid, rarely globose, 8.5–17 × 4.2–7 µm (mean = 11.8 × 5.5 µm; SD = 1.9(L), 0.6(W); L/W ratio 1.4–3.1, ratio mean = 2.2, ratio SD = 0.4; n = 102). Pycnidia not detected.

Chemistry. Thallus K+ yellow, KC–, C–, Pd–. Hymenium I+ blue. UV–. Atranorin and rhizocarpic acid were detected by TLC.

Distribution and ecology. The species occurs on the rock (sandstone or basalt) nearby coast. The species is currently known from two localities in the southern coast of South Korea.

Etymology. The species epithet indicates the insoluble large crystals present in the thalline excipulum of the lichen.

Notes. The new species is morphologically similar to *Protoparmeliopsis ertzii* in having insoluble large crystals in the thalline excipulum and the absence of usnic acid, which are the key characteristics distinguishing them from all other species in the genus *Protoparmeliopsis*. However, the new species differs from *P. ertzii* by whitish thallus, flat to concave disc, paler disc color, longer ascospores, chemical reaction, presence of atranorin and rhizocarpic acid, and the substrate preference (Bungartz et al. 2020).

The new species is compared with *P. bipruinosa* and *P. nashii* as those are closest to the new species in molecular results (Figs 4 and 5). However, the new species differs from *P. bipruinosa* by whitish thallus, absence of pruina, presence of large crystals, and the presence of atranorin and rhizocarpic acid (Nash III et al. 2004).

The new species is different from *P. nashii* by whitish thallus, absence of pruina, presence of large crystals, and the presence of atranorin and rhizocarpic acid (Nash III et al. 2004). Reference Table 3 provides specific characteristics distinguishing *P. parasymplicita* from closely related species above in *Protoparmeliopsis*.

Additional specimens examined. SOUTH KOREA, South Jeolla Province, Goheung, Yeongnam-myeon, Ucheon-ri, a coastal area, 34°37.02'N, 127°29.82'E, 31 m alt., on rock (basalt), 14 April 2020, B.G.Lee 2020-000098, with *Caloplaca bogilana* Y. Joshi & Hur, *Circinaria caesiocinerea* (Nyl. ex Malbr.) A. Nordin, Savić & Tibell, *Pertusaria flavicans* Lamy (BDNA-L-0000298; GenBank MW832796 for ITS, MW832802 for mtSSU, and MW832821 for LSU); same locality, on rock (basalt), 14 April 2020, B.G.Lee 2020-000099, with *Buellia* sp., *Circinaria caesiocinerea* (BDNA-L-0000299); same locality, on rock (basalt), 14 April 2020, B.G.Lee 2020-000100, with *Buellia* aff. *nashii* (BDNA-L-0000300); same locality, on rock (basalt), 14 April 2020, B.G.Lee 2020-000102, with *Buellia* sp., *Caloplaca bogilana*, *Circinaria caesiocinerea*, *Endocarpon maritimum* Y. Joshi & Hur, *Parmotrema grayanum* (Hue) Hale (BDNA-L-0000302); same locality, on rock (basalt), 14 April 2020, B.G.Lee 2020-000103, with *Circinaria caesiocinerea*, *Endocarpon maritimum*, *Pertusaria flavicans* (BDNA-L-0000303); same locality, on rock (basalt), 14 April 2020, B.G.Lee 2020-000105, with *Buellia* aff. *nashii*, *Circinaria caesiocinerea*, *Pertusaria flavicans* (BDNA-L-0000305); same locality, on rock (basalt), 14 April 2020, B.G.Lee 2020-000107, with *Xanthoparmelia mexicana*

(Gyeln.) Hale (BDNA-L-0000307); same locality, on rock (basalt), 14 April 2020, B.G.Lee 2020-000108, with *Caloplaca bogilana*, *Endocarpon maritimum*, *Pertusaria flavicans* (BDNA-L-0000308); same locality, on rock (basalt), 14 April 2020, B.G.Lee 2020-000110, with *Buellia* aff. *nashii*, *Buellia* sp., *Lecanora oreinoides* (Körb.) Hertel & Rambold (BDNA-L-0000310).

Key to *Protoparmeliopsis* and *Sedelnikovaea* species in Korea (6 taxa)

- 1 Thalline margin with large crystals, containing atranorin and rhizocarpic acid..... *P. crystalliniformis*
- Thalline margin without large crystals..... 2
- 2 Thallus whitish..... 3
- Thallus yellowish, brownish, or greenish 4
- 3 Apothecia 0.4–0.7 mm diam., disc with white pruina, epihymenium brownish, hymenium 30–40 µm high, hypothecium 70–100 µm high, ascospores wider 6–7 µm *P. chejuensis*
- Apothecia 0.5–1.5 mm diam., disc without pruina but thalline margin with pruina, epihymenium dull yellowish, hymenium 45–55 µm high, hypothecium 60–70 µm high, ascospores narrower 4.5–5.5 µm *P. kopachevskae*
- 4 Soralia developed on thallus, apothecia absent *P. zerovii*
- Soralia absent, apothecia present 5
- 5 Thallus greenish gray, disc light yellow to pale brown, ascospores 8–13 × 4.5–7 µm, medulla KC– (not containing gyrophoric acid)..... *P. muralis*
- Thallus yellowish, green to grayish yellow, disc dull brown to dark brown, ascospores 17–21 × 5.5–6.5 µm, medulla KC+ yellow (containing gyrophoric acid)..... *Sedelnikovaea pseudogyrophorica* (*P. pseudogyrophorica*)

Acknowledgements

This work was supported by a grant from the Korean National Research Resource Center Program (NRF-2017M3A9B8069471) and the Korean Forest Service Program through the Korea National Arboretum (KNA-202003127AF-00) for the forested wetland conservation of Korea.

References

- Aptroot A, Moon KH (2014) 114 new reports of microlichens from Korea, including the description of five new species, show that the microlichen flora is predominantly Eurasian. *Herzogia* 27(2): 347–365. <https://doi.org/10.13158/heaia.27.2.2014.347>
- Aptroot A, Moon KH (2015) New lichen records from Korea, with the description of the lichenicolous *Halecania parasitica*. *Herzogia* 28(1): 193–203. <https://doi.org/10.13158/heaia.28.1.2015.193>

- Bouckaert RR, Drummond AJ (2017) bModelTest: Bayesian phylogenetic site model averaging and model comparison. *BMC Evolutionary Biology* 17(1): e42. <https://doi.org/10.1186/s12862-017-0890-6>
- Bouckaert R, Vaughan TG, Barido-Sottani J, Duchêne S, Fourment M, Gavryushkina A, Heled J, Jones G, Kühnert D, De Maio N, Matschiner M, Mendes FK, Müller NE, Ogilvie HA, du Plessis L, Poppinga A, Rambaut A, Rasmussen D, Siveroni I, Suchard MA, Wu CH, Xie D, Zhang C, Stadler T, Drummond AJ (2019) BEAST 2.5: An advanced software platform for Bayesian evolutionary analysis. *PLoS Computational Biology* 15(4): e1006650. <https://doi.org/10.1371/journal.pcbi.1006650>
- Brodo IM (1984) The North American species of the *Lecanora subfusca* group. *Beihefte zur Nova Hedwigia* 79: 63–185.
- Brodo IM (1986) A new lobate species of the lichen genus *Lecanora* (Ascomycotina, Lecanoraceae). *Mycotaxon* 26: 309–317.
- Brodo IM, Sharnoff SD, Sharnoff S (2001) *Lichens of North America*. Yale University Press, U.S.A. <https://doi.org/10.29173/bluejay5827>
- Bungartz F, Elix JA, Printzen C (2020) Lecanoroid lichens in the Galapagos Islands: the genera *Lecanora*, *Protoparmeliopsis*, and *Vainionora* (Lecanoraceae, Lecanoromycetes). *Phytotaxa* 431(1): 1–85. <https://doi.org/10.11646/phytotaxa.431.1.1>
- Eidler D, Klein J, Antonelli A, Silvestro D (2019) raxmlGUI 2.0 beta: a graphical interface and toolkit for phylogenetic analyses using RAxML. *bioRxiv*. <https://doi.org/10.1101/800912>
- Eigler G (1969) Studien zur Gliederung der Flechtengattung *Lecanora*. *Dissertationes Botanicae* 4: 1–195.
- Ekman S (2001) Molecular phylogeny of the Bacidiaceae (Lecanorales, lichenized Ascomycota). *Mycological Research* 105: 783–797. <https://doi.org/10.1017/S0953756201004269>
- Hall TA (1999) BioEdit: A User-Friendly Biological Sequence Alignment Editor and Analysis Program for Windows 95/98/NT. *Nucleic Acids Symposium Series* 41: 95–98.
- Hue A (1909) *Le Lecanora oreina* Ach. et quelques lichens Coréens. *Journal de Botanique, sér. 22*: 77–85.
- Hur JS, Koh YJ, Harada H (2005) A checklist of Korean lichens. *Lichenology* 4: 65–95.
- Jeon HS, Koh YJ, Lőkös L, Lee YM, Byun BK, Hur JS (2009) Report on the lichen list of North Korea. *The Korean Journal of Mycology* 37(1): 1–10. <https://doi.org/10.4489/KJM.2009.37.1.001>
- Joshi Y, Wang XY, Lee YM, Byun BK, Koh YJ, Hur JS (2009) Notes on some new records of macro-and micro-lichens from Korea. *Mycobiology* 37(3): 197–202. <https://doi.org/10.4489/MYCO.2009.37.3.197>
- Kondratyuk S, Lőkös L, Tschabanenko S, Haji Moniri M, Farkas E, Wang X, Oh SO, Hur JS (2013) New and noteworthy lichen-forming and lichenicolous fungi. *Acta Botanica Hungarica* 55(3–4): 275–349. <https://doi.org/10.1556/abot.55.2013.3-4.9>
- Kondratyuk SY, Jeong MH, Galanina IA, Yakovchenko LS, Yatsyna AP, Hur JS (2014) Molecular phylogeny of placodioid lichen-forming fungi reveal a new genus, *Sedelnikovaea*. *Mycotaxon* 129(2): 269–282. <https://doi.org/10.5248/129.269>
- Kondratyuk SY, Lőkös L, Farkas E, Oh SO, Hur JS (2015) New and noteworthy lichen-forming and lichenicolous fungi 3. *Acta Botanica Hungarica* 57(3–4): 345–382. <https://doi.org/10.1556/034.57.2015.3-4.7>

- Kondratyuk SY, Lőkös L, Halda JP, Haji Moniri M, Farkas E, Park JS, Lee BG, Oh SO, Hur JS (2016a) New and noteworthy lichen-forming and lichenicolous fungi 4. *Acta Botanica Hungarica* 58(1–2): 75–136. <https://doi.org/10.1556/034.58.2016.1-2.4>
- Kondratyuk SY, Lőkös L, Halda JP, Upreti DK, Mishra GK, Haji Moniri M, Farkas E, Park JS, Lee BG, Liu D, Woo JJ, Jayalal RGU, Oh SO, Hur JS (2016b) New and noteworthy lichen-forming and lichenicolous fungi 5. *Acta Botanica Hungarica* 58(3–4): 319–396. <https://doi.org/10.1556/abot.58.2016.3-4.7>
- Kondratyuk SY, Lőkös L, Halda JP, Roux C, Upreti DK, Schumm F, Mishra GK, Nayaka S, Farkas E, Park JS, Lee BG, Liu D, Woo JJ, Hur JS (2017) New and noteworthy lichen-forming and lichenicolous fungi 6. *Acta Botanica Hungarica* 59(1–2): 137–260. <https://doi.org/10.1556/034.59.2017.1-2.7>
- Kondratyuk SY, Lőkös L, Jang SH, Hur JS, Farkas E (2019) Phylogeny and taxonomy of *Polyzozia*, *Sedelnikovaea* and *Verseghya* of the Lecanoraceae (Lecanorales, lichen-forming Ascomycota). *Acta Botanica Hungarica* 61(1–2): 137–184. <https://doi.org/10.1556/034.61.2019.1-2.9>
- Lee BG, Hur JS (2020) A new lichenized fungus, *Lecanora baekdudaeganensis*, from South Korea, with a taxonomic key for Korean *Lecanora* species. *MycoKeys* 70: 39–58. <https://doi.org/10.3897/mycokeys.70.51569>
- Laundon J (2003) Six lichens of the *Lecanora varia* group. *Nova Hedwigia* 76(1–2): 83–111. <https://doi.org/10.1127/0029-5035/2003/0076-0083>
- Lumbsch HT (1995) A new species in the *Lecanora subfusca* group containing usnic acid in addition to atranorin. *The Lichenologist* 27(3): 161–167. [https://doi.org/10.1016/S0024-2829\(05\)80015-5](https://doi.org/10.1016/S0024-2829(05)80015-5)
- Lumbsch HT, Elix JA (1998) Five new species of *Lecanora* from Australia (lichenized Ascomycotina; Lecanoraceae). *Mycotaxon* 67: 391–403.
- Moon KH (2013) Lichen-forming and lichenicolous fungi of Korea. National Institute of Biological Resources, Incheon.
- Motyka J (1995) Porosty (Lichenes). 1. Rodzina Lecanoraceae. Lubelskie Towarzystwo Naukowe, Lublin.
- Motyka J (1996) Porosty (Lichenes). 2–4. Rodzina Lecanoraceae. Lubelskie Towarzystwo Naukowe, Lublin.
- Nash III TH, Ryan BD, Diederich P, Gries C, Bungartz F (2004) Lichen flora of the Greater Sonoran Desert Region, Vol. II. Lichens Unlimited/Arizona State University, Tempe.
- Orange A, James PW, White FJ (2001) Microchemical Methods for the Identification of Lichens. The British Lichen Society, London.
- Pérez-Ortega S, Kantvilas G (2018) *Lecanora helmetii*, a new species from the *Lecanora symmetrica* group from Tasmania. *Herzogia* 31(1): 639–649. <https://doi.org/10.13158/heia.31.1.2018.639>
- Printzen C (2001) Corticolous and lignicolous species of *Lecanora* (Lecanoraceae, Lecanorales) with usnic or isousnic acid in the Sonoran Desert Region. *The Bryologist* 104(3): 382–409. [https://doi.org/10.1639/0007-2745\(2001\)104\[0382:CALSOL\]2.0.CO;2](https://doi.org/10.1639/0007-2745(2001)104[0382:CALSOL]2.0.CO;2)

- Printzen C, May P (2002) *Lecanora ramulicola* (Lecanoraceae, Lecanorales), an overlooked lichen species from the *Lecanora symmicta* group. *The Bryologist* 105(1): 63–69. [https://doi.org/10.1639/0007-2745\(2002\)105\[0063:LRLLAO\]2.0.CO;2](https://doi.org/10.1639/0007-2745(2002)105[0063:LRLLAO]2.0.CO;2)
- Rambaut A (2014) FigTree v1.4.2. Edinburgh: University of Edinburgh. <http://tree.bio.ed.ac.uk/software/figtree>
- Rehner SA, Samuels GJ (1994) Taxonomy and phylogeny of *Gliocladium* analysed from nuclear large subunit ribosomal DNA sequences. *Mycological Research* 98: 625–634. [https://doi.org/10.1016/S0953-7562\(09\)80409-7](https://doi.org/10.1016/S0953-7562(09)80409-7)
- Śliwa L, Flakus A (2011) *Lecanora microloba*, a new saxicolous species from Poland. *The Lichenologist* 43(1): 1–6. <https://doi.org/10.1017/S0024282910000551>
- Śliwa L, Miadlikowska J, Redelings BD, Molnar K, Lutzoni F (2012) Are widespread morphospecies from the *Lecanora dispersa* group (lichen-forming Ascomycota) monophyletic?. *The Bryologist* 115(2): 265–277. <https://doi.org/10.2307/23321028>
- Smith CW, Aptroot A, Coppins BJ, Fletcher A, Gilbert OL, James PW, Wolseley PA (2009) *The lichens of Great Britain and Ireland*. The British Lichen Society, London.
- Stecher G, Tamura K, Kumar S (2020) Molecular Evolutionary Genetics Analysis (MEGA) for macOS. *Molecular Biology and Evolution* 37(4): 1237–1239. <https://doi.org/10.1093/molbev/msz312>
- Van den Boom PPG, Brand AM (2008) Some new *Lecanora* species from western and central Europe, belonging to the *L. saligna* group, with notes on related species. *The Lichenologist* 40(6): 465–497. <https://doi.org/10.1017/S0024282908007299>
- Wei XL, Han KS, Lee YM, Koh YJ, Hur JS (2007) New Record of *Lecanora muralis* (Lichenized Fungus) in South Korea. *Mycobiology* 35(2): 45–46. <https://doi.org/10.4489/MYCO.2007.35.2.045>
- White TJ, Bruns T, Lee S, Taylor JW (1990) Amplification and direct sequencing of fungal ribosomal RNA genes for phylogenetics. *PCR protocols: a guide to methods and applications* 18(1): 315–322. <https://doi.org/10.1016/B978-0-12-372180-8.50042-1>
- Zhao X, Leavitt SD, Zhao ZT, Zhang LL, Arup U, Grube M, Pérez-Ortega S, Printzen C, Śliwa L, Kraichak E, Divakar PK, Crespo A, Lumbsch HT (2016) Towards a revised generic classification of lecanoroid lichens (Lecanoraceae, Ascomycota) based on molecular, morphological and chemical evidence. *Fungal Diversity* 78(1): 293–304. <https://doi.org/10.1007/s13225-015-0354-5>
- Zoller S, Scheidegger C, Sperisen C (1999) PCR primers for the amplification of mitochondrial small subunit ribosomal DNA of lichen-forming ascomycetes. *The Lichenologist* 31(5): 511–516. <https://doi.org/10.1006/lich.1999.0220>

Morphological and phylogenetic analyses reveal a new genus and two new species of Tubakiaceae from China

Zhaoxue Zhang¹, Taichang Mu¹, Shubin Liu¹, Rongyu Liu¹,
Xiuguo Zhang¹, Jiwen Xia¹

¹ Shandong Provincial Key Laboratory for Biology of Vegetable Diseases and Insect Pests, College of Plant Protection, Shandong Agricultural University, Taian, 271018, China

Corresponding author: Jiwen Xia (xiajiwen1@126.com)

Academic editor: Pedro Crous | Received 4 September 2021 | Accepted 3 November 2021 | Published 22 November 2021

Citation: Zhang Z, Mu T, Liu S, Liu R, Zhang X, Xia J (2021) Morphological and phylogenetic analyses reveal a new genus and two new species of Tubakiaceae from China. MycoKeys 84: 185–201. <https://doi.org/10.3897/mycokeys.84.73940>

Abstract

Species of Tubakiaceae have often been reported as plant pathogens or endophytes, commonly isolated from a wide range of plant hosts. The isolated fungi were studied through a complete examination, based on multilocus phylogenies from combined datasets of ITS/LSU/*rpb2* and ITS/*tef1/tub2*, in conjunction with morphological characteristics. Five strains isolated from *Lithocarpus fohaiensis* and *Quercus palustris* in China represented a new genus of Tubakiaceae, *Obovoideisporodochium* and three species, viz. *Obovoideisporodochium lithocarpi* sp. nov., *Tubakia lushanensis* sp. nov. and *T. dryinoides*.

Keywords

multigene phylogeny, new genus, new species, taxonomy, *Tubakia*

Introduction

Diaporthales represents an important order in Sordariomycetes containing taxa that are mainly isolated as endophytes, saprobes or plant pathogens on various hosts (Fan et al. 2018). Tubakiaceae is a family in Diaporthales, which has been

studied in recent years by Braun et al. (2018) by incorporating morphological and molecular data with appropriate genes to resolve species limitations in the family. Tubakiaceae currently comprises eight genera including *Apiognomonioides* U. Braun et al., *Involutiscutellula* U. Braun & C. Nakash., *Oblongisporothyrium* U. Braun & C. Nakash., *Paratubakia* U. Braun & C. Nakash., *Racheliella* Crous & U. Braun, *Saprothyrium* U. Braun et al., *Sphaerosporothyrium* U. Braun et al. and *Tubakia* B. Sutton (Braun et al. 2018).

Tubakia, the type genus of Tubakiaceae, was introduced by Sutton (1973). Species of *Tubakia* are endophytes in leaves and twigs of many tree species, but can also cause conspicuous leaf symptoms as plant pathogens (Harrington et al. 2012; Harrington & McNew 2016, 2018; Braun et al. 2018). The genus is characterised by unique pycnothyria, consisting of pigmented, radiating, seta-like cells (scutellum) on top of a columella, with small phialides on the underside of the scutellum producing ellipsoid, hyaline to brown conidia that are forced out from under the pycnothyrium for rain dispersal (Harrington & McNew 2018). Some species produce a second type of much smaller conidia (microconidia), either in “normal” pycnothyria or in separate, mostly smaller pycnothyria (Braun et al. 2018).

Saccardo (1913) introduced the genus *Actinopelte* for *A. japonica*, a scutellate fungus found in Japan on *Castanea crenata* (= *C. pubinervis*). Saccardo (1913) confused the large conidia of this species with asci, which was clarified and corrected by Theissen (1913) who provided a detailed discussion, description and illustration (Theissen 1913) of *A. japonica*. Von Höhnelt (1925) revisited *Actinopelte*, added a new species, *A. americana* and introduced the new combination *A. dryina*, based on *Leptothyrium dryinum*. Yokoyama & Tubaki (1971) discussed the history of this genus in detail, published results of comprehensive examinations of Japanese collections *in vivo* and *in vitro* and described *A. castanopsidis*, *A. rubra* and *A. subglobosa*, based on Japanese collections. Since Saccardo's *Actinopelte* turned out to be illegitimate (later homonym of *Actinopelte* Stitzenb. 1861), Sutton (1973) introduced the replacement name *Tubakia* and reallocated all species recognised and treated in Yokoyama & Tubaki (1971) to this genus. Twenty-one additional *Tubakia* species have subsequently been described including fifteen new *Tubakia* species and six combinations in *Tubakia* species (Yun & Rossman 2011; Harrington et al. 2012; Braun et al. 2014; Harrington & McNew 2018; Senanayake et al. 2017; Braun et al. 2018; Yun & Kim 2020).

During field trips to collect plant pathogens causing leaf spots symptoms in China, several specimens associated with typical diaporthean symptoms were collected from various tree hosts, i.e. *Betula dahurica* (Betulaceae), *Juglans regia* (Juglandaceae), *Prunus davidiana* (Rosaceae), *Lithocarpus fohaiensis*, *Quercus mongolica* and *Q. palustris* (Fagaceae). Based on morphological analyses as well as phylogenetic data, this study presents a new genus of Tubakiaceae, *Obovoideisporodochium* and three species, viz. *Obovoideisporodochium lithocarpi* sp. nov., *Tubakia lushanensis* sp. nov. and *T. dryinoides* from diseased leaves of *L. fohaiensis* or *Q. palustris*.

Materials and methods

Isolation and morphological studies

The samples were collected from the Shandong and Yunnan Provinces, China. The strains were isolated from diseased leaves of *Lithocarpus fohaiensis* and *Quercus palustris* using tissue isolation methods. Tissue fragments (5 mm × 5 mm) were taken from the margin of leaf lesions and surface-sterilised by consecutively immersing in 75% ethanol solution for 1 min, 5% sodium hypochlorite solution for 30 s and then rinsing in sterile distilled water for 1 min. The pieces were dried with sterilised paper towels and placed on potato dextrose agar (PDA). All the PDA plates were incubated in a biochemical incubator at 25°C for 2–4 days. The colonies from the periphery were picked out and inoculated on to new PDA plates. Colony photos after 7 days and 15 days were taken by a digital camera (Canon Powershot G7X). Micromorphological characters were observed using an Olympus SZX10 stereomicroscope and Olympus BX53 microscope, all fitted with Olympus DP80 high definition colour digital cameras to photo-document fungal structures. All fungal strains were stored in 10% sterilised glycerine at 4°C for further studies. The holotype specimens are deposited in the Herbarium of Plant Pathology, Shandong Agricultural University (HSAUP). Ex-type cultures are deposited in the Shandong Agricultural University Culture Collection (SAUCC). Taxonomic information of the new taxa was submitted to MycoBank (<http://www.mycobank.org>).

DNA extraction and amplification

Genomic DNA was extracted from fungal mycelia grown on PDA, using a modified cetyltrimethylammonium bromide (CTAB) protocol as described in Guo et al. (2000). The internal transcribed spacer regions with intervening 5.8S nrRNA gene (ITS), the partial large subunit (LSU) nrRNA gene, part of the beta-tubulin gene region (*tub2*), partial translation elongation factor 1-alpha (*tef1*) and partial RNA polymerase II second largest subunit (*rpb2*) genes were amplified and sequenced by using the primer pairs ITS5/ITS4 (White et al. 1990), LR0R/LR5 (Rehner & Samuels 1994; Vilgalys & Hester 1990), Bt2a/Bt2b (Glass & Donaldson 1995), EF1-728F/EF-2 (O'Donnell et al. 1998; Carbone & Kohn 1999) and *frpb2-5F/frpb2-7cR* (Liu et al. 1999; Sung et al. 2007).

The PCR was performed using an Eppendorf Master Thermocycler (Hamburg, Germany). Amplification reactions were performed in a 25 µl reaction volume, which contained 12.5 µl Green Taq Mix (Vazyme, Nanjing, China), 1 µl of each forward and reverse primer (10 µM stock) (Biosune, Shanghai, China) and 1 µl template genomic DNA in amplifier, adjusted with distilled deionised water to a total volume of 25 µl. The PCR parameters were as follows: 94°C for 5 min, followed by 35 cycles of denaturation at 94°C for 30 s, annealing at a suitable temperature for 50 s, extension at 72°C for 1 min and a final elongation step at 72°C for 10 min. The annealing temperatures for the genes were 55°C for ITS, 52°C for LSU, 53°C for *tub2*, 48°C for *tef1*

and 56°C for *rpb2*. The PCR products were separated with the 1% agarose gel, with added GelRed and UV light used to visualise the fragments. Sequencing was done bi-directionally, conducted by the Biosune Company Limited (Shanghai, China). Consensus sequences were obtained using MEGA v. 7.0 (Kumar et al. 2016). All sequences generated in this study were deposited in GenBank (Table 1).

Phylogeny

The generated consensus sequences for each gene were subjected to megablast searches to identify closely-related sequences in the NCBI's GenBank nucleotide database (Zhang et al. 2000). For the ITS-LSU-*rpb2* and ITS-*tef1-tub2* analyses, subsets of sequences from the alignments of Braun et al. (2018) were used as backbones. Newly-generated sequences in this study were aligned with additional related sequences downloaded from GenBank (Table 1) using MAFFT 7 online service with the Auto strategy (Kato et al. 2019, <http://mafft.cbrc.jp/alignment/server/>). To establish the identity of the isolates at species level, phylogenetic analyses were conducted, first individually for each locus and then as combined analyses (ITS-LSU-*rpb2* and ITS-*tef1-tub2*).

Phylogenetic analyses were based on Maximum Likelihood (ML) and Bayesian Inference (BI) for the multilocus analyses. For BI, the best evolutionary model for each partition was determined using MrModelTest v. 2.3 (Nylander 2004) and incorporated into the analyses. ML and BI were run on the CIPRES Science Gateway portal (<https://www.phylo.org/>) (Miller et al. 2012) using RAxML-HPC2 on XSEDE v. 8.2.12 (Stamatakis 2014) and MrBayes on XSEDE v. 3.2.7a (Huelsenbeck & Ronquist 2001; Ronquist & Huelsenbeck 2003; Ronquist et al. 2012), respectively. For the ML analyses, the default parameters were used and BI was carried out using the rapid bootstrapping algorithm with the automatic halt option. Bayesian analyses included four parallel runs of 5,000,000 generations, with the stop rule option and a sampling frequency of 50 generations. The burn-in fraction was set to 0.25 and posterior probabilities (PP) were determined from the remaining trees. All resulting trees were plotted using FigTree v. 1.4.4 (<http://tree.bio.ed.ac.uk/software/figtree>) and the layout of the trees was done in Adobe Illustrator CC 2019.

Result

Phylogenetic analyses

ITS/LSU/*rpb2* phylogeny

The alignment contained 37 isolates representing *Tubakia* and allied taxa and a strain of *Greeneria uvicola* (FI12007) was used as outgroup. The final alignment contained a total of 2459 characters used for the phylogenetic analyses, including alignment gaps, viz. ITS: 1–676, LSU: 677–1545, *rpb2*: 1546–2459. Of these characters, 1858 were constant, 115 were variable and parsimony-uninformative and 486 were parsimony-

Table 1. Species and GenBank accession numbers of DNA sequences used in this study. New sequences in bold.

Species	Voucher ¹	Host/Substrate	Country	ITS	LSU	GenBank accession number	<i>mtb2</i>	<i>rpb2</i>
<i>Greeneria nivola</i>	FI12007	—	Uruguay	HQ586009	GQ870619	—	—	—
<i>Involucriscutellula rubra</i>	CBS 192.71*	<i>Quercus phillyraoides</i>	Japan	MG591899	MG591993	MG592086	MG592180	MG976476
	MUCC 2303	<i>Quercus phillyraoides</i>	Japan	MG591900	MG591994	MG592087	MG592181	MG976477
	ATCC 22473	<i>Quercus phillyraoides</i>	Japan	MG591901	MG591995	MG592088	—	MG976478
<i>Oblongisporobryum castanopsidis</i>	CBS 124732	<i>Castanopsis cuspidata</i>	Japan	MG591849	MG591942	MG592037	MG592131	MG976453
	CBS 189.71*	<i>Castanopsis cuspidata</i>	Japan	MG591850	MG591943	MG592038	MG592132	MG976454
<i>Obovoldisporodochium lithocarpis</i>	SAUCC 0748*	<i>Lithocarpus jibaitensis</i>	China	MW820279	MW821346	MZ996876	MZ962157	MZ962155
	SAUCC 0745	<i>Quercus glauca</i>	Japan	MW820280	MW821347	MZ996877	MZ962158	MZ962156
<i>Paratubakia subglobosa</i>	CBS 124733	<i>Quercus glauca</i>	Japan	MG591913	MG592008	MG592102	MG592194	MG976489
	CBS 193.71*	<i>Quercus glauca</i>	Japan	MG591914	MG592009	MG592103	MG592195	MG976490
<i>Paratubakia subglobosoides</i>	MUCC 2293*	<i>Quercus glauca</i>	Japan	MG591915	MG592010	MG592104	MG592196	MG976491
<i>Rachicella wingfieldiana</i>	CBS 143669*	<i>Syzgium guineense</i>	Africa	MG591911	MG592006	MG592100	MG592192	MG976487
<i>Sphaerosporibryum mexicanum</i>	CPC 32258	<i>Quercus eduardi</i>	Mexico	MG591895	MG591989	MG592082	MG592176	—
	CPC 33021*	<i>Quercus eduardi</i>	Mexico	MG591896	MG591990	MG592083	MG592177	MG976473
<i>Tubakia americana</i>	CBS 129014	<i>Quercus macrocarpa</i>	USA	MG591873	MG591966	MG592058	MG592152	MG976449
<i>Tubakia californica</i>	CPC 31505*	<i>Quercus kelloggii</i>	USA	MG591835	MG591928	MG592023	MG592117	MG976451
<i>Tubakia dryina</i>	CBS 112097*	<i>Quercus nobis</i>	Italy	MG591851	MG591944	MG592039	MG592133	MG976455
<i>Tubakia dryinoides</i>	SAUCC 1924	<i>Quercus pulustris</i>	China	MW784842	MW784852	MW842260	MW842263	MW842266
	CBS 1397.75	<i>Quercus</i> sp.	France	MG591874	MG591967	MG592059	MG592153	MG976458
	MUCC2290	<i>Catanea crenata</i>	Japan	MG591876	MG591968	MG592061	MG592155	MG976459
	MUCC2291	<i>Catanea crenata</i>	Japan	MG591877	MG591969	MG592062	MG592156	MG976460
	MUCC2292*	<i>Quercus phillyraoides</i>	Japan	MG591878	MG591970	MG592063	MG592157	MG976461
<i>Tubakia hallii</i>	CBS 129013	<i>Quercus stellata</i>	USA	MG591880	MG591972	MG592065	MG592159	MG976462
<i>Tubakia tovensis</i>	CBS 129012*	<i>Quercus macrocarpa</i>	USA	MG591879	MG591971	MG592064	MG592158	—
<i>Tubakia japonica</i>	ATCC 22472*	<i>Catanea crenata</i>	Japan	MG591886	MG591978	MG592071	MG592165	MG976465
<i>Tubakia koreana</i>	KCTC46072	<i>Quercus mongolica</i>	South Korea	KP886837	—	—	—	—
<i>Tubakia liquidambaris</i>	CBS 1397.44	<i>Liquidambar styraciflua</i>	USA	MG605068	MG605077	MG605578	—	—
<i>Tubakia lushanensis</i>	SAUCC 1921	<i>Quercus pulustris</i>	China	MW784677	MW784850	MW842262	MW842265	MW842268
	SAUCC 1923*	<i>Quercus canbyi</i>	China	MW784678	MW784851	MW842261	MW842264	MW842267
<i>Tubakia melukiana</i>	CPC 32255*	<i>Quercus serrata</i>	Mexico	MG591893	MG591987	MG592080	MG592174	MG976472
<i>Tubakia oblongispora</i>	MUCC 2295*	<i>Quercus acutissima</i>	Japan	MG591897	MG591991	MG592084	MG592178	MG976474
<i>Tubakia paradyrjoides</i>	MUCC 2294*	<i>Quercus acutissima</i>	Japan	MG591898	MG591992	MG592085	MG592179	MG976475
<i>Tubakia seoulensis</i>	CBS 127490*	<i>Quercus mongolica</i>	South Korea	MG591907	KP260499	MG592094	MG592186	—
	CBS 127491	<i>Quercus mongolica</i>	South Korea	HM991735	KP260500	MG592095	MG592187	MG976484
<i>Tubakia sierraffiensis</i>	CPC 33020	<i>Quercus eduardi</i>	Mexico	MG591910	MG592005	MG592099	MG592191	MG976486
<i>Tubakia</i> sp.	CBS 115011	<i>Quercus nobis</i>	Netherlands	MG591912	MG592007	MG592101	MG592193	MG976488
<i>Tubakia suttoniana</i>	CBS 639.93	<i>Quercus</i> sp.	Italy	MG591921	MG592016	MG592110	MG592202	MG976493

¹ Isolates marked with “*” are ex-type or ex-epitype strains.

informative. MrModelTest recommended that the Bayesian analysis should use Dirichlet base frequencies for the ITS, LSU and *rpb2*. The GTR+I+G model was proposed for ITS, LSU and *rpb2*. The MCMC analysis of the three concatenated genes, run for 700,000 generations, resulted in 14,001 trees. The initial 3500 trees, representative of the analysis burn-in phase, were discarded, while the remaining trees were used to calculate posterior probabilities in the majority rule consensus trees (Fig. 1; first value: PP > 0.74 shown). The alignment contained a total of 744 unique site patterns (ITS: 266, LSU: 128, *rpb2*: 350). The topology of the ML tree confirmed the tree topology obtained from the Bayes analyses and, therefore, only the ML tree is presented (Fig. 1). Bayesian posterior probability (> 0.74) and ML bootstrap support values (> 74%) are shown as first and second position above nodes, respectively. The 37 strains were assigned to 25 species clades, based on the three-gene phylogeny (Fig. 1).

ITS/*tef1*/*tub2* phylogeny

The alignment contained 37 isolates representing *Tubakia* and allied taxa and a strain of *Greeneria uvicola* (FI12007) was used as outgroup. The final alignment contained a total of 1939 characters used for the phylogenetic analyses, including alignment gaps, viz. ITS: 1–676, *tef1*: 677–1358, *tub2*: 1359–1939. Of these characters, 1077 were constant, 136 were variable and parsimony-uninformative and 726 were parsimony-informative. MrModelTest recommended that the Bayesian analysis should use Dirichlet base frequencies for the ITS, *tef1* and *tub2* data partitions. The GTR+I+G model was proposed for ITS and HKY+I+G for *tef1* and *tub2*. The MCMC analysis of the three concatenated genes, run for 170,000 generations resulted in 3401 trees. The initial 850 trees, representative of the analysis burn-in phase, were discarded, while the remaining trees were used to calculate posterior probabilities in the majority rule consensus trees (Fig. 2; first value: PP > 0.74 shown). The alignment contained a total of 997 unique site patterns (ITS: 266, *tef1*: 416, *tub2*: 315). The topology of the ML tree confirmed the tree topology obtained from the Bayes analyses and, therefore, only the ML tree is presented (Fig. 2). Bayesian posterior probability (> 0.74) and ML bootstrap support values (> 74%) are shown as first and second position above nodes, respectively. The 37 strains were assigned to 25 species clades, based on the three-gene phylogeny (Fig. 2).

Based on phylogenetic data (Figs. 1 and 2) and morphological analyses, the present study revealed a new genus of Tubakiaceae, *Obovoideisporodochium* and three species, viz. *Obovoideisporodochium lithocarpi* sp. nov., *Tubakia lushanensis* sp. nov. and *T. dryinoides*.

Taxonomy

***Obovoideisporodochium* Z. X. Zhang, J. W. Xia & X. G. Zhang, gen. nov.**

MycoBank No: 841103

Type species. *Obovoideisporodochium lithocarpi* Z. X. Zhang, J. W. Xia & X. G. Zhang

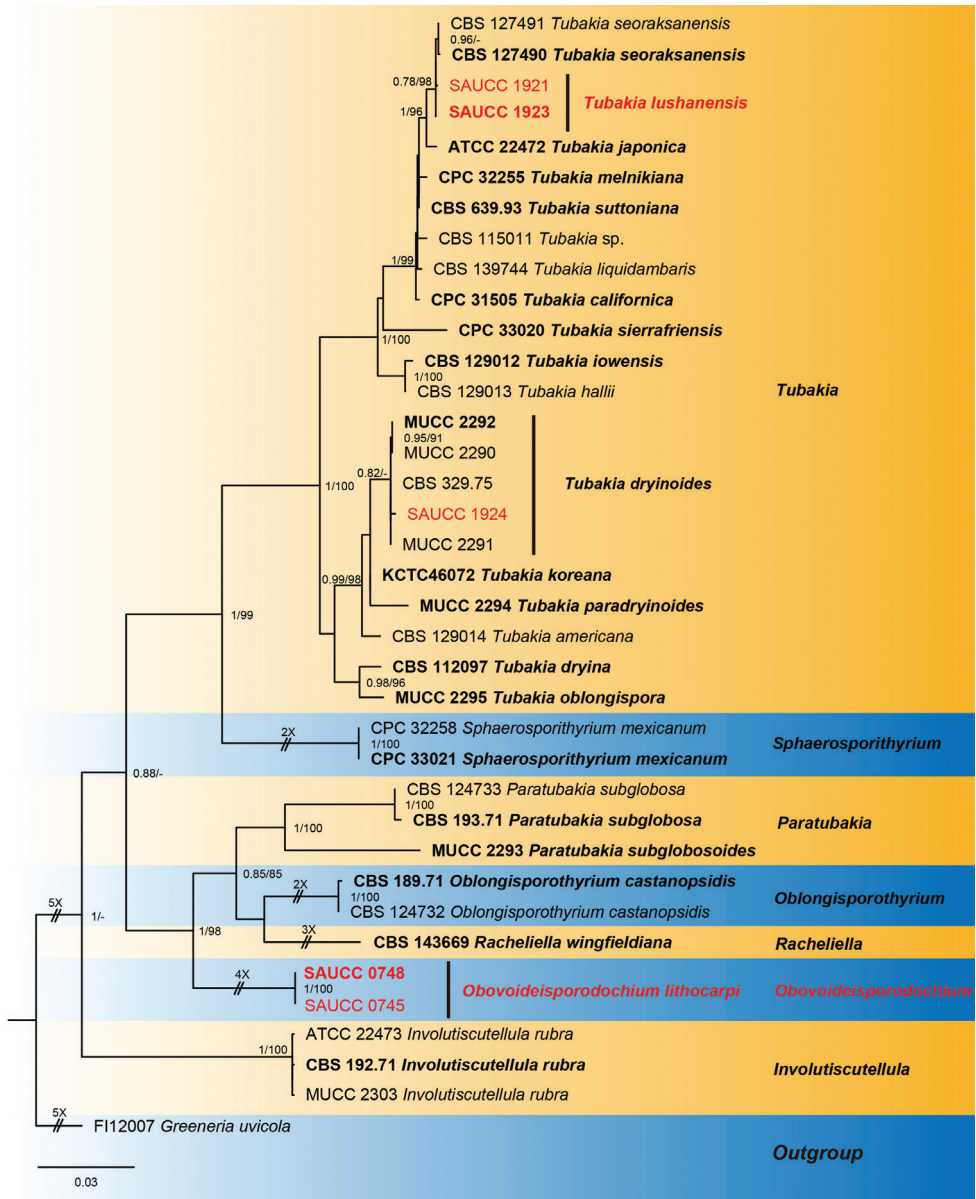


Figure 1. Phylogram of Tubakiaceae, based on the concatenated ITS, LSU and *rpb2* sequence alignment. The BI and ML bootstrap support values above 0.74 and 74% are shown at the first and second position, respectively. The tree is rooted to *Greeneria uvicola* (culture FI12007) and ex-type cultures are indicated in bold face. Strains from the current study are in red. Some branches were shortened for layout purposes – these are indicated by two diagonal lines with the number of times a branch was shortened indicated next to the lines.

Etymology. Composed of “obovoideisporo-” (obovoid spores) and “-dochium” (referring to the conidioma, i.e. sporodochium).

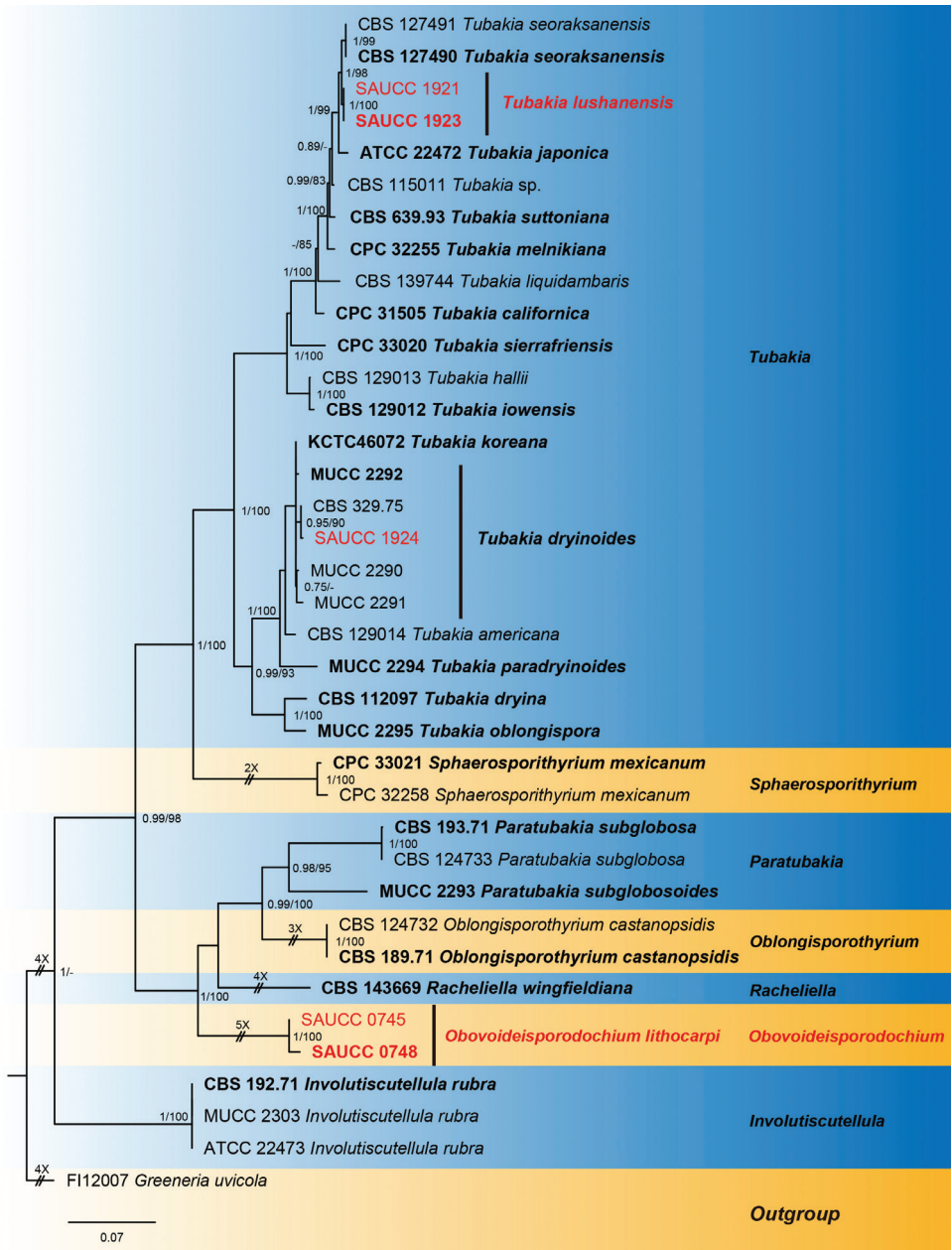


Figure 2. Phylogram of Tubakiaceae, based on the concatenated ITS, *tef1* and *tub2* sequence alignment. The BI and ML bootstrap support values above 0.74 and 74% are shown at the first and second position, respectively. The tree is rooted to *Greeneria uvicola* (culture FI12007) and ex-type cultures are indicated in bold face. Strains from the current study are in red. Some branches were shortened for layout purposes – these are indicated by two diagonal lines with the number of times a branch was shortened indicated next to the lines.

Description. Genus of Tubakiaceae. Living as endophyte in leaves and causing leaf spots. Asexual morph: mycelium consisting of septate, smooth and hyaline hyphae, thin-walled. Conidiomata sporodochial, appeared within 20 days or longer, formed on agar surface, slimy, pale bluish-green, semi-submerged. Sporodochial conidiophores densely and irregularly branched, bearing apical whorls of 2–3 phialides; sporodochial phialides monophialidic, subulate to subcylindrical, smooth, thin-walled, tapering towards apex, swelling at base. Conidia formed singly, obovoid to ellipsoid, smooth, thin walled, apex obtuse, base with inconspicuous to conspicuous hilum. Sexual morph: unknown.

Notes. In the two phylogenetic trees (Figs.1 and 2), *Obovoideisporodochium* is allied to *Racheliella*, *Oblongisporothyrium* and *Paratubakia*, but forms a separate lineage with full support (PP = 1, ML-BS = 100%), suggesting a genus of its own.

***Obovoideisporodochium lithocarpi* Z. X. Zhang, J. W. Xia & X. G. Zhang, sp. nov.**

Mycobank No: 841104

Fig. 3

Type. China, Yunnan Province: Xishuangbanna Tropical Botanical Garden, Chinese Academy of Sciences, on diseased leaves of *Lithocarpus fohaiensis* (Fagaceae), 11 Sep 2020, Z. X. Zhang, (holotype HSAUP0748, ex-type living culture SAUCC 0748).

Etymology. Name refers to the genus of the host plant *Lithocarpus fohaiensis*.

Description. Asexual morph: mycelium consisting of septate, smooth and hyaline hyphae, thin-walled, 1.0–2.0 μm . Colonies on PDA incubated at 25°C in the dark with an average radial growth rate of 5–6 mm/d and reaching 75–80 mm diam. in 14 d, formed some conspicuous concentric circles, aerial mycelium cottony, white initially, then becoming greyish-sepia. Conidiomata sporodochial, appeared within 20 days or longer, formed on agar surface, slimy, pale bluish-green, semi-submerged. Sporodochial conidiophores densely and irregularly branched, 12.0–26.5 \times 1.5–3.0 μm , bearing apical whorls of 2–3 phialides; sporodochial phialides monophialidic, subulate to subcylindrical, 9.5–20.0 \times 1.5–3.0 μm , smooth, thin-walled, tapering towards apex, swelling at base. Conidia formed singly, obovoid to ellipsoid, 5.5–8.0 \times 2.5–4.0 μm , length/width ratio 1.7–3.1, hyaline, smooth, thin walled, apex obtuse, base with inconspicuous to conspicuous hilum, 0.4–0.9 μm diam. Sexual morph: unknown.

Culture characteristics. Cultures incubated on MEA at 25°C in darkness, attaining 52.0–58.0 mm diam. after 14 d (growth rate 3.5–4.0 mm diam./d), grey-white to creamy white with irregular margin, spread like petals from the inside and outside, reverse dark to light brown, distributed in an irregular circle. Conidial formation not observed.

Additional specimen examined. China, Yunnan Province: Xishuangbanna Tropical Botanical Garden, Chinese Academy of Sciences, on diseased leaves of *Lithocarpus fohaiensis* (Fagaceae), 11 Sep 2020, Z. X. Zhang, HSAUP0745; living culture SAUCC 0745.

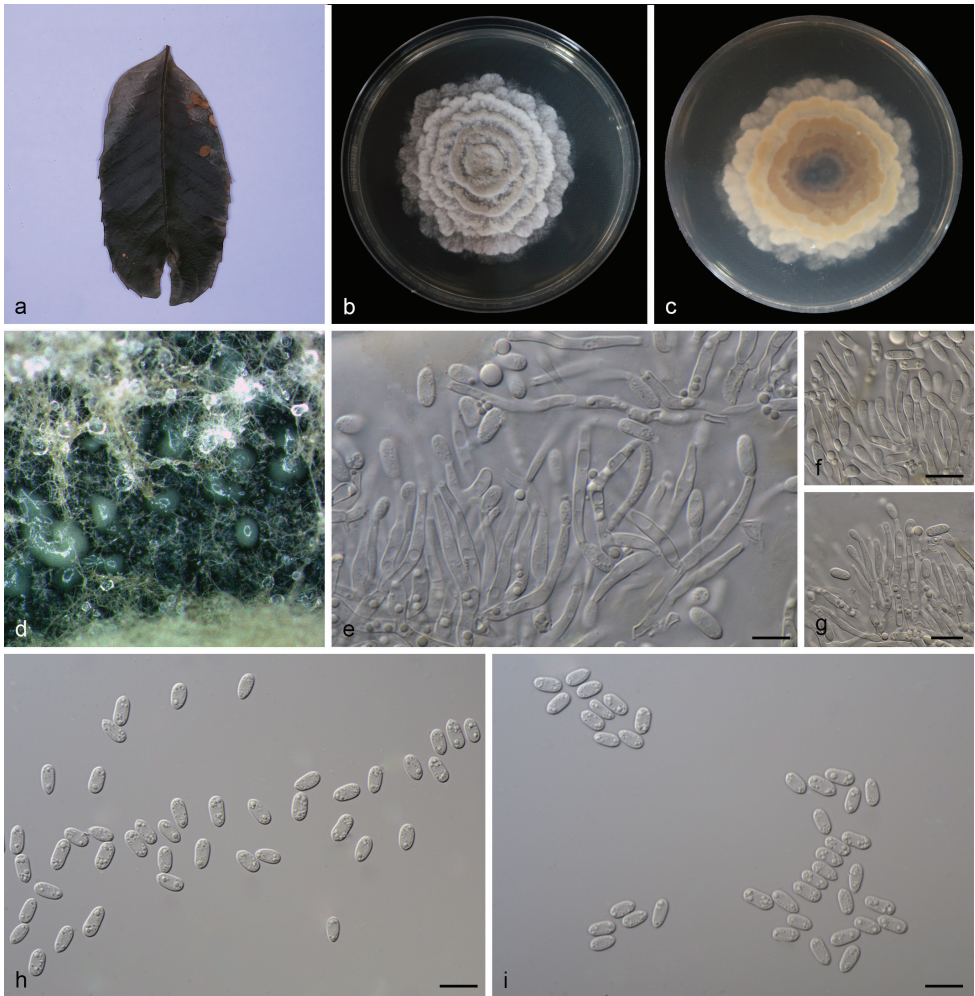


Figure 3. *Obovoideisporodochium lithocarpi* (SAUCC 0748). **a** infected leaf of *Lithocarpus fohaiensis*; **b** surface of colony after 15 days on MEA; **c** reverse of colony after 15 days on MEA; **d** conidiomata; **e–g** conidiophores, conidiogenous cells and conidia; **h–i** conidia. Scale bars: 10 μm (**e–i**).

Notes. In the two phylogenetic trees (Figs. 1 and 2), *Obovoideisporodochium lithocarpi* is related to *Racheliella wingfieldiana*, *Oblongisporothyrium castanopsidis*, *Paratubakia subglobosa* and *P. subglobosoides*, but forms a separate single species lineage with full support (PP = 1, ML-BS = 100%). Furthermore, the conidia of *O. lithocarpi* (5.5–8.0 μm \times 2.5–4.0 μm) are smaller than those of *R. wingfieldiana* (11.0–15.0 μm \times 6.5–7.5 μm), *Ob. castanopsidis* (14.0–17.0 μm \times 7.0–9.5 μm), *P. subglobosa* (10.0–13.0 μm \times 8.0–11.0 μm) and *P. subglobosoides* (10.0–12.5 μm \times 5.5–10.0 μm) and *Racheliella*, *Oblongisporothyrium* and *Paratubakia* spp. form crustose conidiomata and true pycnothyria.

***Tubakia lushanensis* Z. X. Zhang, J. W. Xia & X. G. Zhang, sp. nov.**

Mycobank No: 841105

Fig. 4

Type. China, Shandong Province: Zibo Lushan National Forest Park, on diseased leaves of *Quercus palustris* Münchh (Fagaceae), 20 Sep 2020, Z. X. Zhang, (holotype HSAUP1923, ex-type living culture SAUCC 1923).

Etymology. Named after the type locality, Lushan National Forest Park.

Description. Asexual morph: Leaf spots irregular, occurring on leaf veins and at leaf edges. Colonies on PDA incubated at 25°C in the dark with an average radial growth rate of 5–7 mm/d and occupying an entire 90 mm Petri dish in 14 d, forming some conspicuous concentric circles, aerial mycelium cottony, white initially, then becoming greyish-sepia. Conidiomata pycnidial, usually globose or subglobose when viewed from above, formed on agar surface, black, semi-submerged, up to 200 µm diam. Pycnidial wall composed of an outer layer of yellow-brown, thick-walled *textura angularis* and an inner layer with hyaline, thin-walled cells. Conidiophores reduced to conidiogenous cells lining the inner cavity, ampulliform or flask-shaped, smooth, hyaline, 9.0–15.0 µm × 2.0–4.0 µm. Conidia solitary, globose to irregular globose, ellipsoid to broad ellipsoid, 10.0–18.0 µm × 7.5–16.0 µm, length/width ratio 1.0–1.7, slightly lighter and wall thin when immature, slightly darker and wall thickened when ripening, smooth, apex rounded, base with peg-like hila, 1.3–2.3 µm diam. Microconidia not observed. Sexual morph not observed.

Culture characteristics. Cultures incubated on MEA at 25°C in darkness, attaining 52.0–56.0 mm diam. after 14 d (growth rate 3.7–4.0 mm diam./d), creamy white to pale brown with regular margin, grey near the centre and hyphae clusters, reverse brown to dark brown rings, heterogeneous colour, with creamy-white edge. Conidial formation not observed.

Additional specimen examined. China, Shandong Province: Zibo Lushan National Forest Park, on diseased leaves of *Quercus palustris* Münchh. (Fagaceae), 20 Sep 2020, Z. X. Zhang, HSAUP1921; living culture SAUCC 1921.

Notes. The phylogenetic analysis of a combined three-gene alignment (ITS, *tef1* and *tub2*) showed that *T. lushanensis* formed an independent clade and is phylogenetically distinct from its closest sister species *T. seoraksanensis*. This species can be distinguished from *T. seoraksanensis* by 65 different nucleotides in the concatenated alignment (21/628 in the ITS, 31/581 in the *tef1* and 13/521 in the *tub2*). Morphologically, *T. lushanensis* differs from *T. seoraksanensis* in having smaller conidia (10.0–18.0 µm × 7.5–16.0 µm vs. 13.0–25.0 µm × 10.0–15.0 µm) (Yun & Rossman 2011). Furthermore, the MEA's colony colour of *T. lushanensis* is different from *T. seoraksanensis* (surface: creamy white, pale brown to grey vs. whitish to pale yellow; reverse: creamy white, brown to dark brown vs. olive brown, light olive brown to yellow; Yun & Rossman 2011). Therefore, we describe this fungus as a novel species.

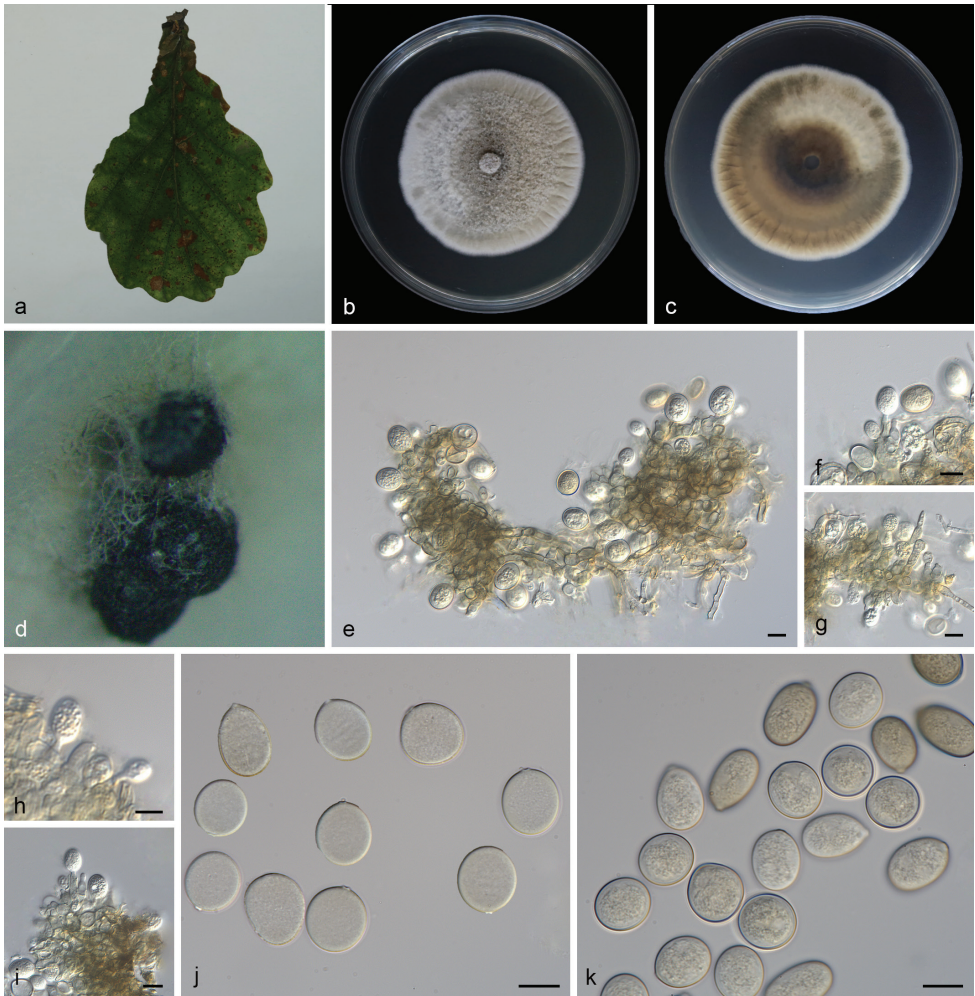


Figure 4. *Tubakia lushanensis* (SAUCC 1923). **a** diseased leaf of *Quercus palustris*; **b** surface of colony after 15 days on MEA; **c** reverse of colony after 15 days on MEA; **d** conidiomata; **e–i** conidiogenous cells with conidia; **j–k** conidia. Scale bars: 10 µm (**e–k**).

***Tubakia dryinoides* C. Nakash., Fungal Systematics and Evolution 1: 80 (2018)**

Fig. 5

Description. Asexual morph: Living as endophyte in leaves, forming distinct leaf lesions, shape and size variable, subcircular to angular-irregular, pale brown to brown. Colonies on PDA incubated at 25°C in the dark with an average radial growth rate of 5–7 mm/d and occupying an entire 90 mm Petri dish in 14 d, forming some conspicuous concentric circles, aerial mycelium cottony, white initially, then becoming greyish-sepia. Conidiomata sporodochial, appeared within 14 days or longer, formed on agar surface, slimy, black, semi-submerged. Sporodochial conidiophores densely

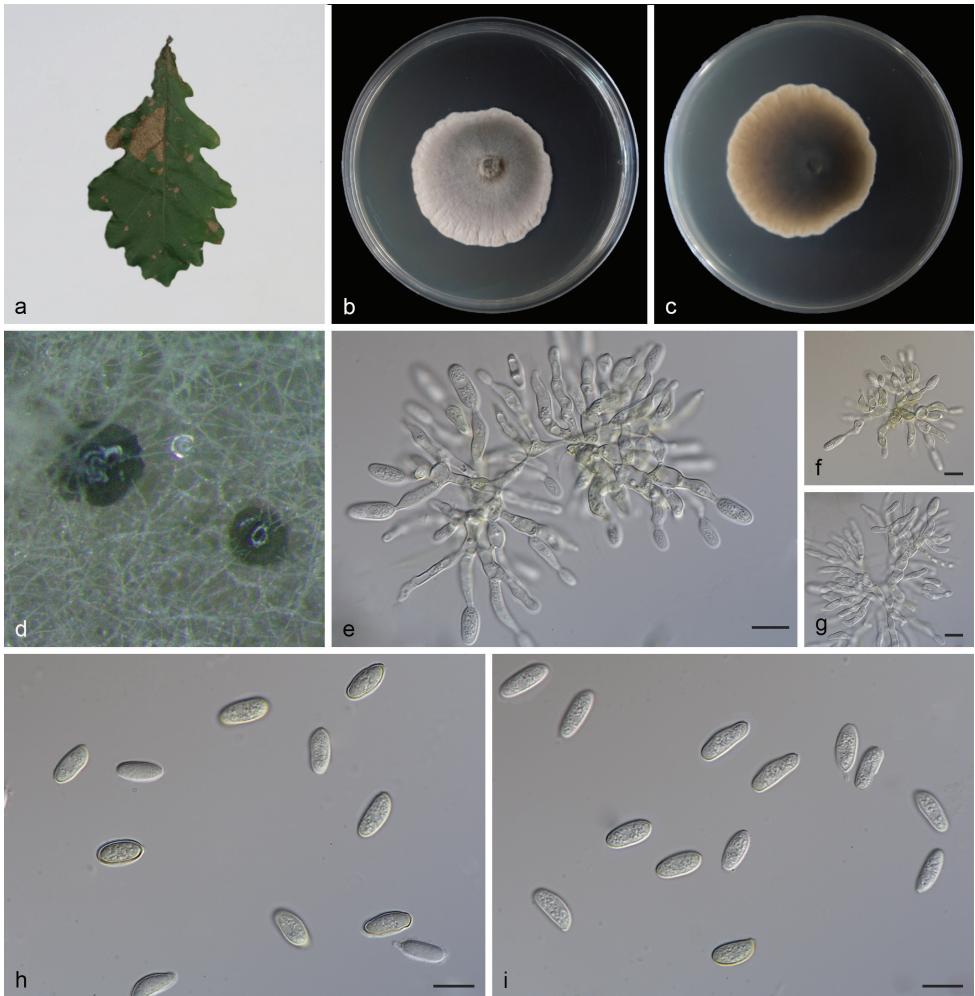


Figure 5. *Tubakia dryinoides* (SAUCC 1924). **a** diseased leaf of *Quercus palustris*; **b** surface of colony after 15 days on MEA; **c** reverse of colony after 15 days on MEA; **d** conidiomata; **e–g** conidiophores, conidigenous cells with conidia; **h–i** conidia. Scale bars: 10 μm (**e–i**).

and irregularly branched, 11.0–24.0 $\mu\text{m} \times 1.5$ –5.0 μm , bearing apical whorls of 2–3 phialides; sporodochial phialides monophialidic, subulate to subcylindrical, 9.0–16.0 $\mu\text{m} \times 1.5$ –5.0 μm , smooth, thin-walled, apex obtuse to truncate, sometimes forming indistinct periclinal thickenings. Conidia solitary, ellipsoid to obovoid, 6.5–14.0 $\mu\text{m} \times 4.0$ –6.0 μm , wall thin, up to 1.0 μm , hyaline to subhyaline, smooth, apex and base broadly rounded, with inconspicuous to conspicuous basal hilum (frill), occasionally somewhat peg-like and truncate when conspicuous. Microconidia not observed. Sexual morph not observed.

Culture characteristics. Cultures incubated on MEA at 25°C in darkness, attaining 38.0–42.0 mm diam. after 14 d (growth rate 2.7–3.0 mm diam./d), margin scal-

loped, at first creamy white, grey near the centre, reverse light brown to dark, with olivaceous edge. Conidial formation not observed.

Specimen examined. China, Shandong Province: Zibo Lushan National Forest Park, on diseased leaves of *Quercus palustris* (Fagaceae), 20 Sep 2020, Z. X. Zhang, HSAUP1924, living culture SAUCC 1924.

Notes. Braun et al. (2018) described *Tubakia dryinoides*, based on morphological and molecular data. The holotype of *T. dryinoides* (NBRC H-11618) was collected from *Quercus phillyraeoides* A. Gray (Braun et al. 2018). In our current research, isolate (SAUCC 1924) collected from diseased leaves of *Quercus palustris* clustered in the *Tubakia dryinoides* clade by strong support (Figs. 1 and 2). We, therefore, consider the isolated strain (SAUCC 1924) as *T. dryinoides*. The conidiomata of *T. dryinoides* is only known from true pycnothyria and the sporodochial conidiomata of the isolated strain (SAUCC 1924) is new for *T. dryinoides* (Braun et al. 2018). Additionally, the conidia of our isolate (SAUCC 1924) is narrower than the original description of *T. dryinoides* (4.0–6.0 µm vs. 5.5–10.0 µm; Braun et al. 2018).

Discussion

In the study of the phylogenetic affinity and position of *Tubakia* in the Ascomycota hierarchical system, Senanayake et al. (2017) placed this genus in the newly-introduced family Melanconiellaceae. However, the recently-published phylogenetic analyses, including sequence data of the type species of *Tubakia*, confirmed that *Tubakia* warranted a family of its own, Tubakiaceae (Braun et al. 2018) and the description of eight genera including *Apiognomonoides* U. Braun et al., *Involutiscutellula* U. Braun & C. Nakash., *Oblongisporothyrium* U. Braun & C. Nakash., *Paratubakia* U. Braun & C. Nakash., *Racheliella* Crous & U. Braun, *Saprothyrium* U. Braun et al., *Sphaerosporothyrium* U. Braun et al. and *Tubakia* B. Sutton (Braun et al. 2018). The family comprises genera and species with sporodochia, crustose to pustulate pycnidoid stromatic conidiomata and superficial scutellate pycnothyria, monophialidic, colourless, conidiogenous cells, often with collarettes and conidia formed singly, mostly globose to broad ellipsoid-obovoid, aseptate, hyaline to pigmented, often with basal frill or truncate peg-like hilum.

The present study found two new species, one of which represents a novel genus in Tubakiaceae. In order to support the validity of the new species, we followed the guidelines of Braun et al. (2018). Based on ITS/LSU/*rpb2* and ITS/*tef1/tub2* molecular data, phylogenetic analyses revealed that two of the obtained isolates (SAUCC 0745 and SAUCC 0748) cluster in a separate lineage, fully supported at genus-level and related to the genera *Racheliella*, *Oblongisporothyrium* and *Paratubakia*. The new genus is named *Obovoideisporodochium* gen. nov. (type species: *Obovoideisporodochium lithocarpi* sp. nov.). The phylogenetic analyses also revealed that three isolates (SAUCC 1921, SAUCC 1923 and SAUCC 1924) pertain to the genus *Tubakia*. Owing to different nucleotides in the concatenated alignment and morphology, two isolates (SAUCC

1921 and SAUCC 1923) of *Tubakia* were identified as a new species, namely *T. lushanensis* sp. nov, whereas the third isolate (SAUCC 1924) was identified as *T. dryinoides*.

The centre of genetic diversity of *Tubakia* appears to be in East Asia, where *Quercus* and other genera of Fagaceae are the most common hosts (Harrington & McNew 2018). Our study supports this phenomenon well. *Tubakia lushanensis* (SAUCC 1921 and SAUCC 1923) and *T. dryinoides* (SAUCC 1924) were isolated from *Quercus palustris* (Fagaceae), thereby increasing the genetic diversity of *Tubakia* in East Asia.

Acknowledgements

This work was supported by the National Natural Science Foundation of China (no. 31900014, 31750001 and 31770016).

References

- Braun U, Bien S, Hantsch L, Heuchert B (2014) *Tubakia chinensis* sp. nov. and a key to the species of the genus *Tubakia*. *Schlechtendalia* 28: 23–28.
- Braun U, Nakashima C, Crous PW, Groenewald JZ, Moreno-Rico O, Rooney-Latham S, Blomquist CL, Haas J, Marmolejo J (2018) Phylogeny and taxonomy of the genus *Tubakia* s. lat. *Fungal Systematics and Evolution* 1: 41–99. <https://doi.org/10.3114/fuse.2018.01.04>
- Carbone I, Kohn LM (1999) A method for designing primer sets for speciation studies in filamentous ascomycetes. *Mycologia* 91(3): 553–556. <https://doi.org/10.1080/00275514.1999.12061051>
- Fan XL, Bezerra JDP, Tian CM, Crous PW (2018) Families and genera of diaporthalean fungi associated with canker and dieback of tree hosts. *Persoonia* 40: 119–134. <https://doi.org/10.3767/persoonia.2018.40.05>
- Glass NL, Donaldson GC (1995) Development of primer sets designed for use with the PCR to amplify conserved genes from filamentous ascomycetes. *Applied and Environmental Microbiology* 61(4): 1323–1330. <https://doi.org/10.1128/AEM.61.4.1323-1330.1995>
- Guo LD, Hyde KD, Liew ECY (2000) Identification of endophytic fungi from *Livistona chinensis* based on morphology and rDNA sequences. *New Phytologist* 147(3): 617–630. <https://doi.org/10.1046/j.1469-8137.2000.00716.x>
- Harrington TC, McNew DL (2016) Distribution and intensification of bur oak blight in Iowa and the Midwest. In: Porter KM and Conkling BL (eds): *Forest health monitoring: national status, trends, and analysis 2015*. Forest Service & Research Station, Southern Research Station, General Technical Report SRS-213: 105–110.
- Harrington TC, McNew DL (2018) A re-evaluation of *Tubakia*, including three new species on *Quercus* and six new combinations. *Antonie van Leeuwenhoek* 111(7): 1003–1022. <https://doi.org/10.1007/s10482-017-1001-9>

- Harrington TC, McNew DL, Yun HY (2012) Bur oak blight, a new disease on *Quercus macrocarpa* caused by *Tubakia iowensis* sp. nov.. *Mycologia* 104: 79–92. <https://doi.org/10.3852/11-112>
- Huelsenbeck JP, Ronquist F (2001) MrBayes: Bayesian inference of phylogeny. *Bioinformatics* 17(17): 754–755. <https://doi.org/10.1093/bioinformatics/17.8.754>
- Katoh K, Rozewicki J, Yamada KD (2019) MAFFT online service: multiple sequence alignment, interactive sequence choice and visualization. *Briefings in Bioinformatics* 20: 1160–1166. <https://doi.org/10.1093/bib/bbx108>
- Kumar S, Stecher G, Tamura K (2016) MEGA7: Molecular Evolutionary Genetics Analysis Version 7.0 for Bigger Datasets. *Molecular Biology and Evolution* 33(7): 1870–1874. <https://doi.org/10.1093/molbev/msw054>
- Liu YJ, Whelen S, Hall BD (1999) Phylogenetic Relationships among Ascomycetes: evidence from an RNA polymerase II subunit. *Molecular Biology and Evolution* 16(12): 1799–1808. <https://doi.org/10.1093/oxfordjournals.molbev.a026092>
- Miller MA, Pfeiffer W, Schwartz T (2012) The CIPRES Science Gateway: enabling high-impact science for phylogenetics researchers with limited resources. In: *Proceedings of the 1st Conference of the Extreme Science and Engineering Discovery Environment. Bridging from the extreme to the campus and beyond*. Association for Computing Machinery, USA, 1–8. <https://doi.org/10.1145/2335755.2335836>
- Nylander JAA (2004) MrModelTest v. 2. Program distributed by the author. Evolutionary Biology Centre, Uppsala University.
- O'Donnell K, Kistler HC, Cigelnik E, Ploetz RC (1998) Multiple evolutionary origins of the fungus causing Panama Disease of banana: Concordant evidence from nuclear and mitochondrial gene genealogies. *Proceedings of the National Academy of Sciences of the United States of America* 95(5): 2044–2049. <https://doi.org/10.1073/pnas.95.5.2044>
- Rehner SA, Samuels GJ (1994) Taxonomy and phylogeny of *Gliocladium* analysed from nuclear large subunit ribosomal DNA sequences. *Mycological Research* 98(6): 625–634. [https://doi.org/10.1016/S0953-7562\(09\)80409-7](https://doi.org/10.1016/S0953-7562(09)80409-7)
- Ronquist F, Huelsenbeck JP (2003) MrBayes 3: Bayesian Phylogenetic Inference under Mixed Models. *Bioinformatics* 19(12): 1572–1574. <https://doi.org/10.1093/bioinformatics/btg180>
- Ronquist F, Teslenko M, van der Mark P, Ayres DL, Darling A, Höhna S, Larget B, Liu L, Suchard MA, Huelsenbeck JP (2012) MrBayes 3.2: efficient Bayesian phylogenetic inference and model choice across a large model space. *Systematic Biology* 61(3): 539–542. <https://doi.org/10.1093/sysbio/sys029>
- Saccardo PA (1913) *Notae mycologicae*. Series XVI. *Annales Mycologici* 11: 493–511.
- Senanayake IC, Crous PW, Groenewald JZ, Maharachchikumbura SSN, Jeewon R, Phillips AJL, Bhat JD, Perera RH, Li QR, Li WJ, Tangthirasunun N, Norphanphou C, Karunarathna SC, Camporesi E, Manawasinghe IS, Al-Sadi AM, Hyde KD (2017) Families of Diaporthales based on morphological and phylogenetic evidence. *Studies in Mycology* 86: 217–296. <https://doi.org/10.1016/j.simyco.2017.07.003>

- Stamatakis A (2014) RAxML Version 8: a tool for phylogenetic analysis and post-analysis of large phylogenies. *Bioinformatics* 30(9): 1312–1313. <https://doi.org/10.1093/bioinformatics/btu033>
- Sutton BC (1973) *Tubakia* nom. nov. *Transactions of the British Mycological Society* 60: 164–165. [https://doi.org/10.1016/S0007-1536\(73\)80077-4](https://doi.org/10.1016/S0007-1536(73)80077-4)
- Sung GH, Sung JM, Hywel-Jones NL, Spatafora JW (2007) A multi-gene phylogeny of Clavicipitaceae (Ascomycota, Fungi): identification of localized incongruence using a combinatorial bootstrap approach. *Molecular Phylogenetics and Evolution* 44(3): 1204–1223. <https://doi.org/10.1016/j.ympev.2007.03.011>
- Theissen F (1913) Ueber einige Mikrothyriaceen. *Annales Mycologici* 11: 493–511.
- Vilgalys R, Hester M (1990) Rapid genetic identification and mapping of enzymatically amplified ribosomal DNA from several *Cryptococcus* species. *Journal of Bacteriology* 172(8): 4238–4246. <https://doi.org/10.1128/JB.172.8.4238-4246.1990>
- Von Höhnelt F (1925) Neue Fungi imperfecti. 5. Mitteilung. *Mitteilungen des Botanischen Instituts der Technischen Hochschule Wien* 2: 65–73.
- White T, Burns T, Lee S, Taylor J (1990) Amplification and direct sequencing of ribosomal RNA genes for phylogenetics. In: Innis MA (Ed.) *PCR Protocols: A Guide to Methods and Applications*. Academic Press, New York, 315–322. <https://doi.org/10.1016/B978-0-12-372180-8.50042-1>
- Yokoyama T, Tubaki K (1971) Cultural and taxonomical studies on the genus *Actinopelte*. Institute of Fermentation, Osaka, Research Communication 5: 43–77. <https://doi.org/10.1007/BF02051502>
- Yun HY, Kim YH (2020) *Tubakia koreana* sp. nov. causing *Quercus* leaf blight. *Mycotaxon* 135(1): 223–229. <https://doi.org/10.5248/135.223>
- Yun HY, Rossman AY (2011) *Tubakia seoraksanensis*, a new species from Korea. *Mycotaxon* 115: 369–373. <https://doi.org/10.5248/115.369>
- Zhang Z, Schwartz S, Wagner L, Miller W (2000) A greedy algorithm for aligning DNA sequences. *Journal of Computational Biology* 7: 203–214. <https://doi.org/10.1089/10665270050081478>

